U.S. DEPARTMENT OF COMMERCE
National Technical Information Service

PB-254 167

BURNER DESIGN CRITERIA FOR CONTROL OF NOx FROM NATURAL GAS COMBUSTION

VOLUME I. DATA ANALYSIS AND SUMMARY OF CONCLUSIONS

INSTITUTE OF GAS TECHNOLOGY

PREPARED FOR
INDUSTRIAL ENVIRONMENTAL RESEARCH LABORATORY

APRIL 1976

182192

PB 254 167

EPA-600/2-76-098a
April 1976

Environmental Protection Technology Series

BURNER DESIGN CRITERIA FOR CONTROL OF NO_x FROM NATURAL GAS COMBUSTION

Volume I

Data Analysis and Summary of Conclusions

Industrial Environmental Research Laboratory
Office of Research and Development
U.S. Environmental Protection Agency
Research Triangle Park, North Carolina

REPRODUCED BY
NATIONAL TECHNICAL
INFORMATION SERVICE
U. S. DEPARTMENT OF COMMERCE
SPRINGFIELD, VA. 22161

RESEARCH REPORTING SERIES

Research reports of the Office of Research and Development, U.S. Environmental Protection Agency, have been grouped into five series. These five broad categories were established to facilitate further development and application of environmental technology. Elimination of traditional grouping was consciously planned to foster technology transfer and a maximum interface in related fields. The five series are:

1. Environmental Health Effects Research
2. Environmental Protection Technology
3. Ecological Research
4. Environmental Monitoring
5. Socioeconomic Environmental Studies

This report has been assigned to the ENVIRONMENTAL PROTECTION TECHNOLOGY series. This series describes research performed to develop and demonstrate instrumentation, equipment, and methodology to repair or prevent environmental degradation from point and non-point sources of pollution. This work provides the new or improved technology required for the control and treatment of pollution sources to meet environmental quality standards.

EPA REVIEW NOTICE

This report has been reviewed by the U.S. Environmental Protection Agency, and approved for publication. Approval does not signify that the contents necessarily reflect the views and policy of the Agency, nor does mention of trade names or commercial products constitute endorsement or recommendation for use.

This document is available to the public through the National Technical Information Service, Springfield, Virginia 22161.

TECHNICAL REPORT DATA

(Please read Instructions on the reverse before completing)

1. REPORT NO. EPA-600/2-76-098a	2.	3. RECIPIENT'S ACCESSION NO.
4. TITLE AND SUBTITLE Burner Design Criteria for Control of NOx from Natural Gas Combustion; Volume I. Data Analysis and Summary of Conclusions		5. REPORT DATE April 1976 6. PERFORMING ORGANIZATION CODE
7. AUTHOR(S) D. R. Shoffstall		8. PERFORMING ORGANIZATION REPORT NO.
9. PERFORMING ORGANIZATION NAME AND ADDRESS Institute of Gas Technology IIT Center, 3424 South State Street Chicago, Illinois 60616		10. PROGRAM ELEMENT NO. 1AB014; 21BCC-029 11. CONTRACT/GRANT NO. 68-02-1360
12. SPONSORING AGENCY NAME AND ADDRESS EPA, Office of Research and Development Industrial Environmental Research Laboratory Research Triangle Park, NC 27711		13. TYPE OF REPORT AND PERIOD COVERED Final; 6/73-9/75 14. SPONSORING AGENCY CODE EPA-ORD

15. SUPPLEMENTARY NOTES Project officer for this report is D. G. Lachapelle, Mail Drop 65, Ext 2236.

16. ABSTRACT Volume I of the report gives details of, and analyzes, trials conducted with natural gas to determine the relationship between combustion aerodynamics and pollution emission characteristics of industrial burners. Three burner types were studied (kiln, ported baffle, and movable vane boiler), based on relative gas load and estimated total industrial emissions. Experimental measurements on a pilot-scale furnace included baseline characterization of each burner and variation of primary operating parameters (air preheat, air/fuel ratio, firing rate, heat release rate, position of gas nozzle in burner block, and air swirl intensity). Additional emissions data were gathered for suspected control conditions (fuel injector design, flue gas recirculation, fuel/air momentum ratio, and burner block angle). It also describes in detail the experimental facility and sampling probes used to collect the data. Volume II discusses completely the procedure used to select the test burners. It includes detailed flame characterizations of baseline operations assembled from in-the-flame temperature, gas species, and flow direction data analysis. Similar in-the-flame studies were made for control conditions which minimized emissions for each burner type. It also includes all raw data collected from the input/output trials.

17. KEY WORDS AND DOCUMENT ANALYSIS

a. DESCRIPTORS		b. IDENTIFIERS/OPEN ENDED TERMS	c. COSATI Field/Group	
Air Pollution	Flames	Air Pollution Control	13B	
Nitrogen Oxides	Swirling	Stationary Sources	07B	13H, 07A
Aerodynamics		Axial Injection	20D	
Natural Gas		Radial Injection	21D	
Combustion Control		Swirl	21B	
Burners		Industrial Burners	13A	

18. DISTRIBUTION STATEMENT Unlimited	19. SECURITY CLASS *(This Report)* Unclassified	21. NO. OF PAGES 204
	20. SECURITY CLASS *(This page)* Unclassified	22. PRICE $7.75 / 2.25

EPA Form 2220-1 (9-73)

EPA-600/2-76-098a
April 1976

BURNER DESIGN CRITERIA FOR CONTROL OF NO_X FROM NATURAL GAS COMBUSTION

VOLUME I. DATA ANALYSIS AND SUMMARY OF CONCLUSIONS

by

D.R. Shoffstall

Applied Combustion Research
Institute of Gas Technology
IIT Center--3424 South State Street
Chicago, Illinois 60616

Contract No. 68-02-1360
ROAP No. 21BCC-029
Program Element No. 1AB014

EPA Project Officer: David G. Lachapelle

Industrial Environmental Research Laboratory
Office of Energy, Minerals, and Industry
Research Triangle Park, NC 27711

Prepared for

U.S. ENVIRONMENTAL PROTECTION AGENCY
Office of Research and Development
Washington, DC 20460

ABSTRACT

Volume I of this final report gives a detailed presentation and analysis of trials conducted with natural gas to determine the relationship between combustion aerodynamics and pollution emission characteristics of industrial burners. Three types of burners were studied (kiln, ported baffle, and movable-vane boiler) based on their relative gas load and estimated total industrial emissions. Experimental measurements carried out on a pilot-scale furnace included a baseline characterization of each burner and variation of primary operating parameters (air preheat, air/fuel ratio, firing rate, heat-release rate, position of gas nozzle in burner block, and air swirl intensity). Additional emissions data were gathered for suspected control conditions (fuel injector design, flue gas recirculation, fuel/air momentum ratio and burner block angle). This volume also contains a detailed description of the experimental facility and sampling probes used to collect the data.

A companion publication, Volume II, gives a complete discussion of the procedure used to select the test burners. Included also are detailed flame characterizations of base-line operations assembled from in-the-flame temperature, gas species, and flow direction data analysis. Similar in-the-flame studies were made for control conditions which minimized emissions for each burner type. All raw data collected from the input-output trials are also included.

TABLE OF CONTENTS

ABSTRACT iii

LIST OF FIGURES vii

LIST OF TABLES xvii

ACKNOWLEDGMENT xix

INTRODUCTION 1

BURNER SELECTION RATIONALE 3

DESCRIPTION OF EXPERIMENTAL BURNERS 6

- KILN BURNER 6
- SWIRL BAFFLE BURNER 10
- UTILITY BOILER BURNER 10

DESCRIPTION OF FURNACE TEST FACILITY 14

EXPERIMENTAL PLAN 29

GENERAL FLAME CHARACTERISTICS 31

KILN BURNER 34

BAFFLE BURNER 70

UTILITY BOILER BURNER 110

APPENDIX. DATA CORRELATION 167

Preceding page blank

LIST OF FIGURES

Figure No.		Page
1	Cutaway view of experimental kiln burner	7
2	Divergent gas nozzle	8
3	Combination gas nozzle	9
4	Assembly drawing of baffle burner	11
5	Boiler burner	12
6	Boiler burner air register vanes	13
6a	Rectangular test furnace	15
7	Removable sidewall furnace panels for interior flame probing	16
8	Overall system schematic diagram of rectangular test furnace system	17
9	Radiant tube preheater for main furnace combustion air	18
10	Flue-gas cooler	20
11	Control room facility and analytical instrumentation	22
12	Gas-sampling probe head for nonparticulate flue gases	25
13	Modified IFRF temperature probe	26
14	General probe holder	28
15	Flame types tested	32
16	Flame geometry and luminosity of kiln burner	36
17	Flame geometry and luminosity typical of kiln burner	37
18	In-the-flame profiles of kiln burner using combination nozzle with 30% axial and 70% radial injection; 3.2% primary air	38
19	Normalized NO concentration as a function of percent O_2 in the flue (excess air) for the combination nozzle kiln burner using 30% axial and 70% radial injection and 3.2% primary air	39

Preceding page blank

LIST OF FIGURES, Cont.

Figure No.		Page
20	In-the-flame profiles for combination nozzle kiln burner with 30% axial and 70% radial injection, with 13% EFGR	43
21	Normalized NO concentration as a function of O_2 in the flue (excess air) for combination nozzle kiln burner with 30% axial and 70% radial injection using EFGR (13%)	44
22	Normalized NO concentration as a function of O_2 in the flue (excess air) for the combination nozzle kiln burner with 30% axial and 70% radial injection with a 1130°C wall temperature	46
23	Normalized NO concentration as a function of O_2 in the flue (excess air) for combination nozzle kiln burner with 30% axial and 70% radial injection using 13% EFGR with reduced wall temperature, 1150°C	47
24	Normalized NO concentration as a function of O_2 in the flue for combination nozzle kiln burner with 30% axial-70% radial injection with 6% primary air and a 1310°C wall temperature	48
25	Normalized NO concentration as a function of O_2 in the flue for combination nozzle kiln burner with 30% axial and 70% radial injection with 6% primary air and a 1150°C wall temperature	49
26	Comparison of NO formation for 6% and 3% primary air on the combination nozzle kiln burner using 30% axial and 70% radial injection	51
27	Normalized NO concentration as a function of O_2 in the flue (excess air) for combination nozzle kiln burner with the nozzle in the exit position using 3.5% primary air and 30% axial-70% radial injection	52
28	Normalized NO concentration as a function of O_2 in the flue (excess air) for combination nozzle kiln burner using 14% axial and 86% radial injection, 3.5% primary air and 1345°C walls	54
29	Normalized NO concentration as a function of O_2 in the flue (excess air) for combination nozzle kiln burner using 6.6% primary air; 14% axial-86% radial injection and 1345°C walls	55

LIST OF FIGURES, Cont.

Figure No.		Page
30	Normalized NO concentration as a function of O_2 in the flue (excess air) for combination nozzle kiln burner using 3.5% primary air; 14% axial-86% radial injection and 1320°C walls; with nozzle in exit position	56
31	Normalized NO concentration as a function of O_2 in the flue (excess air) for combination nozzle kiln burner using 3.2% primary air and 0.0% axial gas injection	57
32	Normalized NO concentration as a function of O_2 in the flue (excess air) for combination nozzle kiln burner in the exit position and using 0.0% axial gas injection	58
33	Normalized NO concentration as a function of O_2 in the flue (excess air) for combination nozzle kiln burner with reduced gas input (1900 CFH) and 30% axial gas injection	60
34	Normalized NO concentration as a function of O_2 in the flue (excess air) for combination nozzle kiln burner fired with 1800 SCFH of gas and 0.0% axial injection	61
35	Normalized NO concentration as a function of O_2 in the flue (excess air) for divergent nozzle kiln burner using 3.5% primary air; 2700 SCFH gas input and 1320°C walls	63
36	Normalized NO concentration as a function of O_2 in the flue (excess air) for divergent nozzle kiln burner using 3.5% primary air; 2700 SCFH gas and (cooled) 1145°C walls	65
37	Normalized NO concentration as a function of O_2 in the flue (excess air) for divergent nozzle kiln burner operated with (cooled) 1150°C walls and 9.5% primary air	66
38	Normalized NO concentration as a function of O_2 for the IFLB burner with a standard gas nozzle at gas inputs of 3070 and 2005 SCFH	71
39	IFLB burner with standard fuel nozzle	72
40	IFLB burner with divergent nozzle	72

LIST OF FIGURES, Cont.

Figure No.		Page
41	Nozzle positions tested for the baffle burner	73
42	In-the-flame profiles along the axis of a baffle burner for typical operating conditions	75
43	Normalized NO concentration as a function of flue O_2 for the IFLB burner with a standard gas nozzle and 15% and 30% FGR	76
44	Normalized NO concentration as a function of flue O_2 for the IFLB burner with a standard gas nozzle at a wall temperature of 965°C	78
45	Normalized NO concentration as a function of flue O_2 for the IFLB burner with a combination gas nozzle and radial injection	79
46	Normalized NO concentration as a function of flue O_2 for the IFLB burner with a combination gas nozzle and axial and radial injection	81
47	Normalized NO concentration as a function of flue O_2 for the IFLB burner with the various gas nozzles in different positions	82
48	In-the-flame profiles for the axial fired baffle burner in the controlled operating condition	84
49	Normalized NO concentration as a function of flue O_2 for the IFLB burner with standard, divergent, and axial gas nozzles	86
50	Normalized NO concentration as a function of flue O_2 for the SFLB burner with a standard gas nozzle	88
51	Normalized NO concentration as a function of flue O_2 for the SFLB burner with a standard gas nozzle at wall temperatures of 1450° and 1050°C	89
52	Normalized NO concentration as a function of flue O_2 for the SFLB burner with a standard gas nozzle and 15% and 25% FGR	91
53	Normalized NO concentration as a function of flue O_2 for the SFLB burner with the various gas nozzles	92
54	Normalized NO concentration as a function of flue O_2 for the SFLB burner with standard, divergent, and axial gas nozzles	94

LIST OF FIGURES, Cont.

Figure No.		Page
55	Normalized NO concentration as a function of wall temperature for the SFLB burner with a standard gas nozzle	97
56	Normalized NO concentration as a function of flue O_2 for the IFLB burner with a low-velocity gas nozzle	98
57	Normalized NO concentration as a function of flue O_2 for the IFLB burner with low-velocity, high-velocity and divergent gas nozzles	100
58	Normalized NO concentration as a function of flue O_2 for the IFLB burner with standard, divergent, and axial gas nozzles	101
59	Normalized NO concentration as a function of flue O_2 with 25% primary air	103
60	Normalized NO concentration as a function of flue O_2 for the LNO-I burner under luminous-flame operating conditions	105
61	Normalized NO concentration as a function of flue O_2 for the LNO-I burner with 15% primary air	106
62	Ring fuel injector	112
63	Nozzle heads for fuel gun injector	114
64	Nozzle positions tested for the movable-vane boiler burner	115
65	Secondary combustion air deflector plate	117
65a	60-degree gun nozzle in exit position	118
65b	30-degree ring nozzle flame in deflector position	118
66	In-the-flame profiles of boiler burner operated under typical conditions	119
67	Normalized NO concentration as a function of flue O_2 for the movable-vane boiler burner with a 60-degree gun nozzle	120

LIST OF FIGURES, Cont.

Figure No.		Page
68	Normalized NO concentration as a function of flue O_2 for the movable-vane boiler burner with a 60-degree gun nozzle, 1.5% and 2.5% FGR	122
69	Normalized NO concentration as a function of flue O_2 for the movable-vane boiler burner with a 60-degree gun nozzle in different positions	123
70	Normalized NO concentration as a function of flue O_2 for the movable-vane boiler burner with a composite plot of gas nozzles	125
71	Normalized NO concentration as a function of flue O_2 for the movable-vane boiler burner with a 60-degree gun nozzle in different positions and a 15-degree vane angle	127
72	Normalized NO concentration as a function of flue O_2 for the movable-vane boiler burner with a 60-degree gun nozzle in different positions and a 45-degree vane angle	128
73	Normalized NO concentration as a function of flue O_2 for the movable-vane boiler burner with a composite plot of gas nozzles at a 45-degree vane angle	129
74	Normalized NO concentration as a function of flue O_2 for the movable-vane boiler burner with a 60-degree gun nozzle in different positions and a 60-degree vane angle	130
75	Normalized NO concentration as a function of flue O_2 for the movable-vane boiler burner with a composite plot of gas nozzles at a 60-degree vane angle	131
76	Tangential/radial velocity ratio as a function of vane angle	132
77	Normalized NO concentration as a function of tangential/radial velocity ratio for the movable-vane boiler burner with a 60-degree gun nozzle	134
78	In-the-flame profiles of boiler burner using 60-degree gun nozzle	136
79	Normalized NO concentration as a function of wall temperature for the movable-vane boiler burner with a 60-degree gun nozzle	138

LIST OF FIGURES, Cont.

Figure No.		Page
80	Normalized NO concentration as a function of secondary air temperature for the movable-vane boiler burner with a 60-degree gun nozzle	139
81	Normalized NO concentration as a function of flue O_2 for the movable-vane boiler burner with a 30-degree ring nozzle in different positions	141
82	Normalized NO concentration as a function of flue O_2 for the movable-vane boiler burner with a 30-degree ring nozzle in different positions and a 15-degree vane angle	142
83	Normalized NO concentration as a function of flue O_2 for the movable-vane boiler burner with a 30-degree ring nozzle in different positions and a 45-degree vane angle	143
84	Normalized NO concentration as a function of flue O_2 for the movable-vane boiler burner with a 30-degree ring nozzle in different positions and a 60-degree vane angle	144
85	Normalized NO concentration as a function of tangential/radial velocity ratio for the movable-vane boiler burner with a composite plot of nozzles	146
86	Normalized NO concentration as a function of wall temperature for the movable-vane boiler burner with a 30-degree ring nozzle	148
87	Normalized NO concentration as a function of secondary air temperature for the movable-vane boiler burner with a 30-degree ring nozzle	149
88	Normalized NO concentration as a function of flue gas recirculation percentage for the movable-vane boiler burner with a 30-degree ring nozzle	151
89	Normalized NO concentration as a function of flue O_2 for the movable-vane boiler burner with a 30-degree gun nozzle	152
90	Normalized NO concentration as a function of flue O_2 for the movable-vane boiler burner with a composite nozzle plot and a 15-degree burner block angle	154

LIST OF FIGURES, Cont.

Figure No.		Page
91	Normalized NO concentration as a function of flue O_2 for the movable-vane boiler burner with a composite nozzle plot, a 15-degree burner block angle and a 15-degree vane angle	155
92	Normalized NO concentration as a function of flue O_2 for the movable-vane boiler burner with a composite nozzle plot, a 15-degree burner block angle and a 45-degree vane angle	156
93	Normalized NO concentration as a function of flue O_2 for the movable-vane boiler burner with a composite nozzle plot, a 15-degree burner block angle and a 60-degree vane angle	157
94	Normalized NO concentration as a function of tangential/radial velocity ratio for the movable-vane boiler burner with a composite nozzle plot	158
95	Normalized NO concentration as a function of flue O_2 and vane angle for the movable-vane boiler burner with a 30-degree ring nozzle	159
96	Normalized NO concentration as a function of burner block angle for the movable-vane boiler burner with a 30-degree ring nozzle	161
97	Normalized NO concentration as a function of tangential/radial velocity ratio and burner block angle for the movable-vane boiler burner with a 30-degree ring nozzle	162
98	Normalized NO concentration as a function of flue O_2 for the movable-vane boiler burner with a composite nozzle plot, 60-degree vane angle and 45-degree burner block	163
99	Normalized NO concentration as a function of adiabatic flame temperature for the kiln burner	173
100	Normalized NO concentration as a function of $[1000/T_{ADB}(°K)]$ for the kiln burner	174
101	Logarithmic ratio of $NO/[O_2]$ as a function of $[1000/T_{ADB}(°K)]$ for the kiln burner	175
102	Normalized NO concentration as a function of adiabatic flame temperature for the intermediate flame length ported baffle burner	176

LIST OF FIGURES, Cont.

Figure No. Page

103 Normalized NO concentration as a function of $[1000/T_{ADB}(°K)]$ for the intermediate flame length ported baffle burner 177

104 Logarithmic ratio of $NO/[O_2]$ as a function of $[1000/T_{ADB}(°K)]$ for the intermediate flame length ported baffle burner 178

105 Normalized NO concentration as a function of adiabatic flame temperature for the short flame ported baffle burner 179

106 Normalized NO concentration as a function of $[1000/T_{ADB}(°K)]$ for the short flame ported baffle burner 180

107 Logarithmic ratio of $NO/[O_2]$ as a function of $[1000/T_{ADB}(°K)]$ for the short flame ported baffle burner 181

108 Normalized NO concentration as a function of adiabatic flame temperature for the movable-vane boiler burner 183

109 Normalized NO concentration as a function of $[1000/T_{ADB}(°K)]$ for the movable-vane boiler burner 184

110 Logarithmic ratio of $NO/[O_2]$ as a function of $[1000/T_{ADB}(°K)]$ for the movable-vane boiler burner 185

LIST OF TABLES

Table No. Page

1 Basic Burner Types and National NO_x Emissions Levels 5

2 Linear Equations for NO_x Formation as a Function of Oxygen Concentration, % 40

3 Synopsis of Data Collected for the Kiln Burner 68

4 Normalized NO as a Function of Nozzle Type, Block Angle, and Excess O_2 for the IFLB Burner With an Air Preheat Temperature of 460°C 85

5 Normalized NO Concentration at 1% Excess O_2 With an Air Preheat Temperature of 460°C as a Function of Baffle Type, Gas Nozzle Type, and Burner-Block Angle 95

6 Synopsis of Data Collected for the Baffle Burner 108

7 Listing of Burner Operating Conditions as a Function of Vane Angle for the 60-Degree Gun Nozzle (Gas Input, 2996 SCFH; Exit and Deflector Positions; 1340°C Wall Temperature; 30-Degree Burner-Block Angle; 460°C Secondary Air Preheat Temperature) 133

8 Listing of Burner Operating Conditions as a Function of Vane Angle for the 30-Degree Ring Nozzle With a 30-Degree Burner Block (Gas Input, 2907 SCFH; Exit and Deflector Nozzle Positions; 1369°C Wall Temperature; 460°C Secondary Air Preheat; 2% Excess Oxygen) 145

9 Synopsis of Data Collected for the Boiler Burner 164

10 Burner Operating Conditions Used in Data Correlation 171

11 Conversion Table, English to Metric Units 186

Preceding page blank

ACKNOWLEDGMENT

The author would like to acknowledge the help of Mike Kerna, Lloyd McHie, David Orchowski and Mike Peer who all contributed to the successful completion of this research. Thanks also goes to David W. Pershing and Dr. J.O.L. Wendt, of the University of Arizona, and David Lachapelle, the EPA Project Officer, for their many helpful discussions and contributions made in the data analyses. The assistance extended by Cheryl Zrna and Dennis Larson in preparation of this report is also appreciated.

Preceding page blank

INTRODUCTION

There is a current and vital need for significant reductions in the pollutant emissions from stationary fuel combustion sources. The Second Annual Report of the Council on Environmental Quality (in 1971) stated that stationary fuel combustion, which includes electric power generation, is the second largest combustion-related NO_x emission source, contributing nearly 50% of the total national NO_x emissions. Only transportation ranked higher, contributing 51.4% of the nation's total NO_x emissions.

The use of fuels for stationary combustion can be broken down into household, commercial, and industrial, including the generation of electricity. Within this breakdown, the industrial sector uses over 70% of the annual consumption of fossil fuel. Consequently, industry must be considered the major source of pollutant emissions. Any development effort for reducing these emissions will most certainly have a significant national impact. Judging from the predictions of increased energy demand by industry, the need for pollution control methods in industry will be even more critical within the next 10 years.

There are two basic methods for reducing industrial combustion-related emissions. The first method for decreasing pollution is to decrease the amount of fuel consumed per unit of product or service. In this way, emissions can be reduced in direct proportion to the decrease in fuel usage. Both industry and energy suppliers are already actively engaged in developing process technology which will improve fuel utilization. There is a substantial inducement to develop the means for better fuel utilization because of both the pollution factor and reduced costs. However, considering the rapid growth in the demand for products and services, the national consumption of fossil fuels will still continue to grow and with it the total emissions of pollutants. Better fuel utilization only helps to retard an increase in total emissions.

The second method for decreasing atmospheric pollution from the industrial combustion of fuels is to reduce the pollutant emissions per unit of fuel burned. This method of solving the problem is completely compatible with the first approach of reducing the amount of fuel burned per unit of product produced. This solution also is being actively pursued by a) switching fuels (for example, by substituting low-sulfur oils or natural gas for high-sulfur oil or coal), b) by developing and applying stack-gas cleanup processes, and c) by modifying combustion systems. Of these three methods to reduce pollution emissions, combustion modification is the least developed technologically and is not yet widely available for commercial use by industry. Only the utility power boiler segment of industry has implemented combustion changes to significantly reduce emissions. Yet, new burner designs and combustion systems specifically designed for low NO_x emissions offer the most promising long-range solution.

The overall objective of this program is to develop technology so that optimum low-emission (NO_x, CO, and HC) combustion systems can be designed and widely used by industry. The work will establish the relative controls available through the various burner designs and classical modification techniques for major burner classes. The specific result of this study will be alternative control strategies for gas-fired systems.

To ensure that the results of this program have the most immediate and greatest impact on the industrial emissions problem, three burner types were selected for experimental study which represented a weighted combination of the largest total gas usage and emission rates.

BURNER SELECTION RATIONALE

In order to select three distinctly different types of burners to be investigated, a classification system was developed which would categorize a burner type by its combustion and heat-release characteristics. The relative gas loads for each of these burner types were determined from gas consumption statistics by industrial process and by an assessment of the dominant burner type used for each process. The assessment of the predominant burner type by industrial process came from industrial burner manufacturers. The gas load statistics by industrial process were available in American Gas Association publications and from nonproprietary gas supply and utilization studies conducted by IGT.

Obtaining relative NO_x emission rates by burner type was extremely difficult because of the lack of published data over the broad range of industries covered. Therefore, each of the industry processes was assigned into one of three categories of NO_x emission levels. It was assumed that the high emission processes emitted 0.5 lb/million Btu;* intermediate emission processes, 0.25 lb/million Btu; and low emission processes, only 0.05 lb of NO_x/million Btu of fuel consumed. Obviously, very few processes and burner types produce exactly the quantity of NO_x of the group into which they were placed. However, for the purposes of this program evaluation, this method provides a sufficiently good relative measure of the contribution of each burner type to the national NO_x emission problem.

Each industry process and burner type was placed in the appropriate category based on available literature data or based on our expertise in the area of NO_x emissions developed by the field testing of burners and the testing of scaled industrial burners in our laboratory. This latter method was coupled with our knowledge of the firing rate, heat-release pattern, percent excess air, and average temperature of the industrial process. We therefore have data on the total gas load/yr and on the NO_x emission rate in lb/million Btu for each type of burner.

---

* It is EPA policy to use Metric units; however, in this report English units are occasionally used for convenience. See attached conversion table.

The selection of the three burners to be investigated was based on the total pounds of emissions for each burner type on a national basis. Total emissions for each burner type were determined by multiplying the gas load/yr in Btu's by the NO_x emission rate in lb/million Btu.

The results of this evaluation are presented as the identification of the predominate burner type associated with each of the many fuel-consuming industrial processes, a relative measure of the total national NO_x emissions by burner type, and the selection of three burners for study in this program based on the highest national NO_x emission levels.

There are seven burner types identified by combustion characteristics. These are shown in Table 1, along with the total national (estimated) NO_x emission levels established by this study. The three burners selected for further experimental study were the 1) register burner, 2) the non-premix gas-momemtum-controlled burner, and 3) the non-premix swirl burner. These burners contribute significantly more NO_x to the national environment than any of the others shown. The nozzle mix, nozzle premix, and fuel premix burners were grouped together because they are very often used interchangeably by industry and therefore are difficult to evaluate separately in terms of their NO_x emmisions.

The last category in Table 1, shown as "other," is made up of many burner types, usually of a very specialized design or application. Any one of these burners contributes very little NO_x.

The three burners selected for further study may be more easily recognized by their trade descriptions and applications. The register burner is the typical design used on utility power boilers and large industrial boilers. The non-premix gas-momemtum-controlled burner is more commonly called a kiln burner and is used in open hearth steel furnaces, glass melting, cement kilns, lime kilns, aluminum ore drying, and nonferrous smelting furnaces. The non-premix swirl burner is sometimes called a "baffle" burner or "large capacity" burner. It is the typical design used in steel soaking pits, steel reheat furnaces, and other material heating processes requiring temperatures up to about 2500°F.

A detailed classification by industrial burner type and their relative NO_x emissions is presented in Volume II.

Table 1. BASIC BURNER TYPES AND NATIONAL NO_x EMISSION LEVELS

	Burner Type	NO_x Emissions, 10^6 lb/yr
1.	Nozzle Mix Nozzle Premix Full Premix	84.3
2.	Register Burner	831.2*
3.	Flat Flame	7.6
4.	Delayed Mixing	1.4
5.	Non-Premix Gas Momentum-Controlled	441.0*
6.	Non-Premix Swirl	92.4*
7.	Other	11.9

*Burners selected for further study in this research program.

DESCRIPTION OF EXPERIMENTAL BURNERS

This program was conducted using three experimental burners simulating a kiln burner, a swirl-type burner, and a utility boiler burner. Each of the burners was designed for natural gas firing at a rate of 3.5 million Btu/hr. The swirl-type baffle burner was full scale. The kiln and boiler burners were aerodynamically scaled down by a factor of about 10. Each of the burners was designed so that operating conditions could be readily changed over a wider than normal range. Therefore, the burners can be used to study "off-normal" conditions.

KILN BURNER

Figure 1 shows a cutaway view of the experimental kiln burner. The combination of the burner block and housing simulate the firing end and air duct entrance of a kiln aerodynamically scaled down from a 35 million Btu/hr unit. The housing and block were velocity-scaled around a typical kiln velocity of 10 ft/s and calculated for our input of 3500 SCFH of natural gas and 10% excess air.

The actual burner was designed with two different tip configurations. An adjustable divergent gas orifice (Figure 2) can replace the radial flow tip (Figure 3). Both tip designs have provisions for a purely axial flow or any rate of axial-to-radial gas flow. An air flow at a velocity of 150-200 ft/s around the gas nozzles is sized at about 20% of the air put through the housing.

The gas nozzle tip opening is variable on both tip designs. It is designed around a gas velocity of about 500 ft/s. However, the variable opening feature allows variations in gas velocity from about 1000 ft/s (at maximum gas pressure available at test site) to about 40 ft/s at the maximum-open setting.

The kiln burner (gas nozzle and secondary air annulus) is constructed so it can be positioned flush with the inside wall of the furnace or pulled back into the air housing up to 18 inches. Positioning the burner flush with the inner furnace wall would be considered typical for most kiln designs.

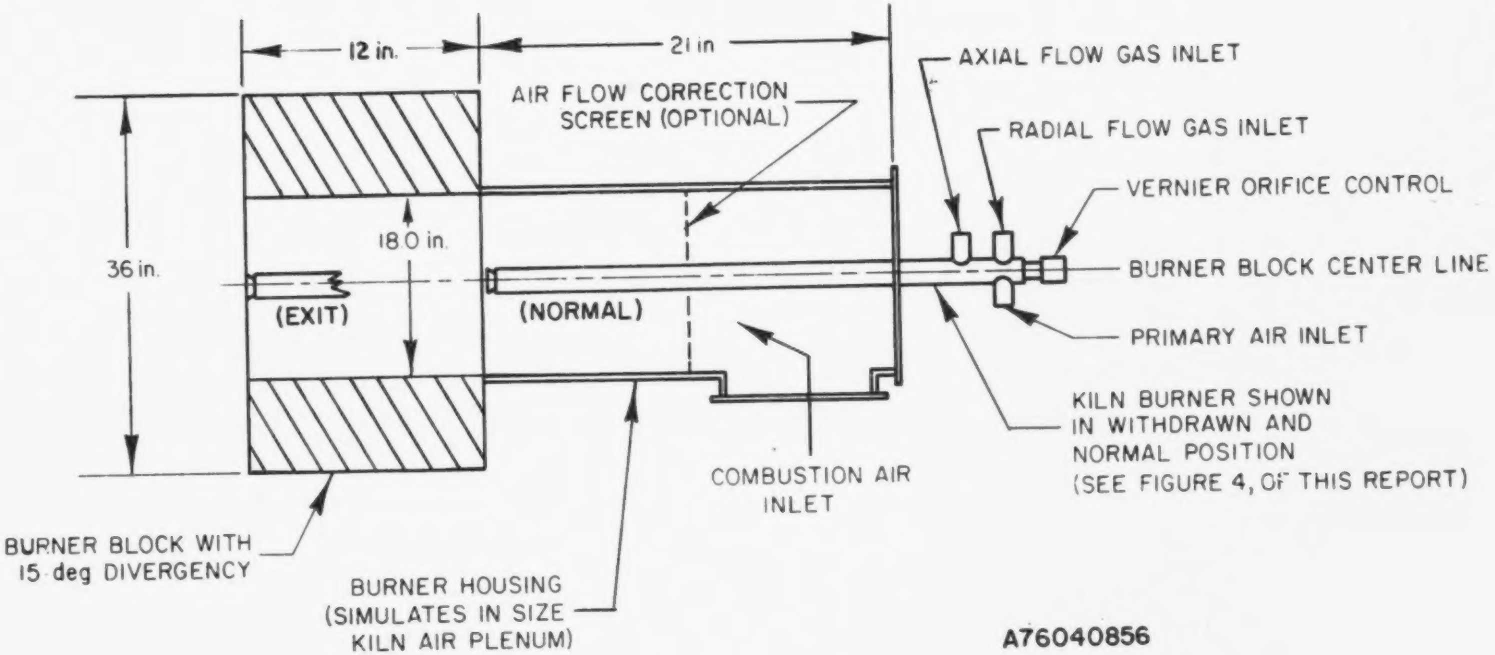
12 in.
21 in
AIR FLOW CORRECTION SCREEN (OPTIONAL)
AXIAL FLOW GAS INLET
RADIAL FLOW GAS INLET
VERNIER ORIFICE CONTROL
36 in.
18.0 in.
BURNER BLOCK CENTER LINE
(EXIT)
(NORMAL)
PRIMARY AIR INLET
KILN BURNER SHOWN IN WITHDRAWN AND NORMAL POSITION (SEE FIGURE 4, OF THIS REPORT)
COMBUSTION AIR INLET
BURNER BLOCK WITH 15 deg DIVERGENCY
BURNER HOUSING (SIMULATES IN SIZE KILN AIR PLENUM)
A76040856

Figure 1. Cutaway view of experimental kiln burner

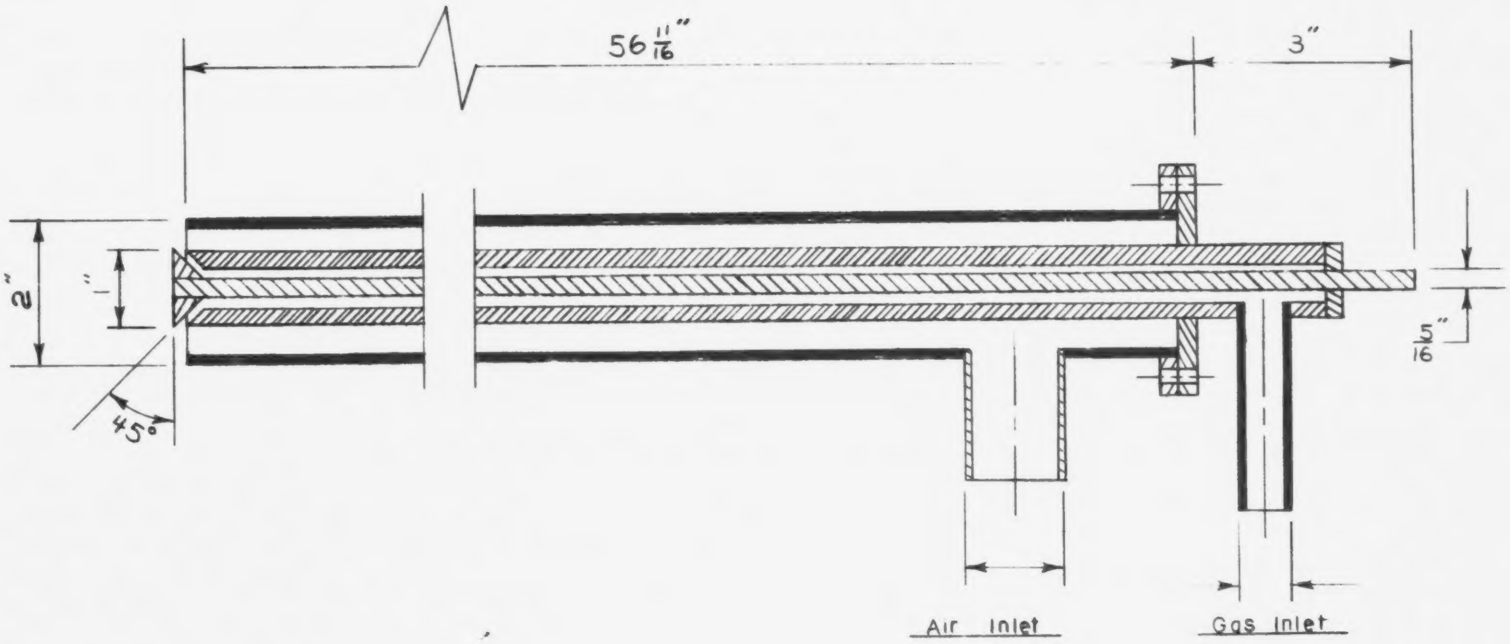
56 11/16"
3"
2"
1"
45°
5/16"
Air Inlet
Gas Inlet

Figure 2. Divergent gas nozzle

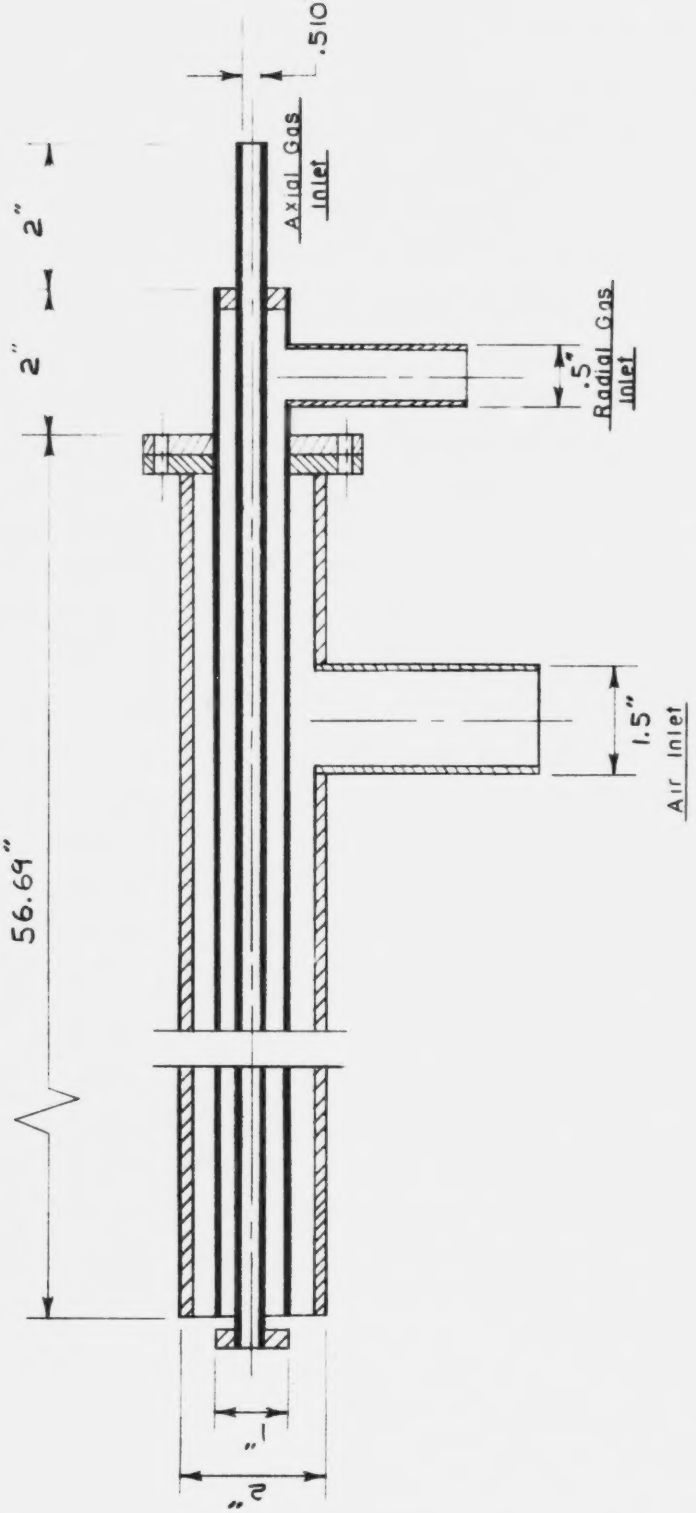
.510"
Axial Gas Inlet
2"
2"
Radial Gas Inlet
.5"
1.5"
Air Inlet
56.69"
1"
2"

Figure 3. Combination gas nozzle

SWIRL BAFFLE BURNER

The swirl baffle burner used for experimental work was full scale. This type of burner is found on many large process heating furnaces such as steel reheating, batch glass melting, and tunnel kilns. It normally consists of a centrally located gas nozzle surrounded by a baffle which has holes cast into it for air flow (Figure 4). The burner is similar to the baffle burner used by IGT in previous work for the EPA under Contract No. 68-02-0216.

The gas nozzle is designed for either radial flow, axial flow, or a combination of both in any desired ratio. In addition, nozzles of various diameters are available in order to vary axial gas velocity for a fixed gas flow rate. The radial gas ports are designed for a velocity of about 600 ft/s at a 3500 SCFH gas input. The axial nozzle is designed for a range of velocities from about 230 to 1000 ft/s at a 3500 SCFH gas input, depending on the diameter of the nozzle which is installed in the burner housing. Varying the velocity of the radial or axial gas flow and/or the axial/radial gas flow ratios will vary the flame characteristics.

The flame patterns of this burner can also be varied by changing the air flow pattern and velocity. The air enters the burner block through six equally spaced holes or ports in the ceramic air baffle. Baffles are available with holes from 2.5 inches to 1.0 inches in diameter, which will vary air velocity from about 50 ft/s to 330 ft/s. A swirl can also be imparted to the air flow with baffles having the holes cast in at an angle. Three baffles with this capability are available.

UTILITY BOILER BURNER (REGISTER TYPE)

Figure 5 shows a cross-sectional view of the experimental boiler burner with a coal-firing attachment installed along with the conventional gas burner. A vane register is used to impart swirl to the airstream as it enters the combustion region. The vanes can be adjusted (Figure 6) from full open to 90 degrees closed. The full-open position causes fully radial air flow and the longest flame.

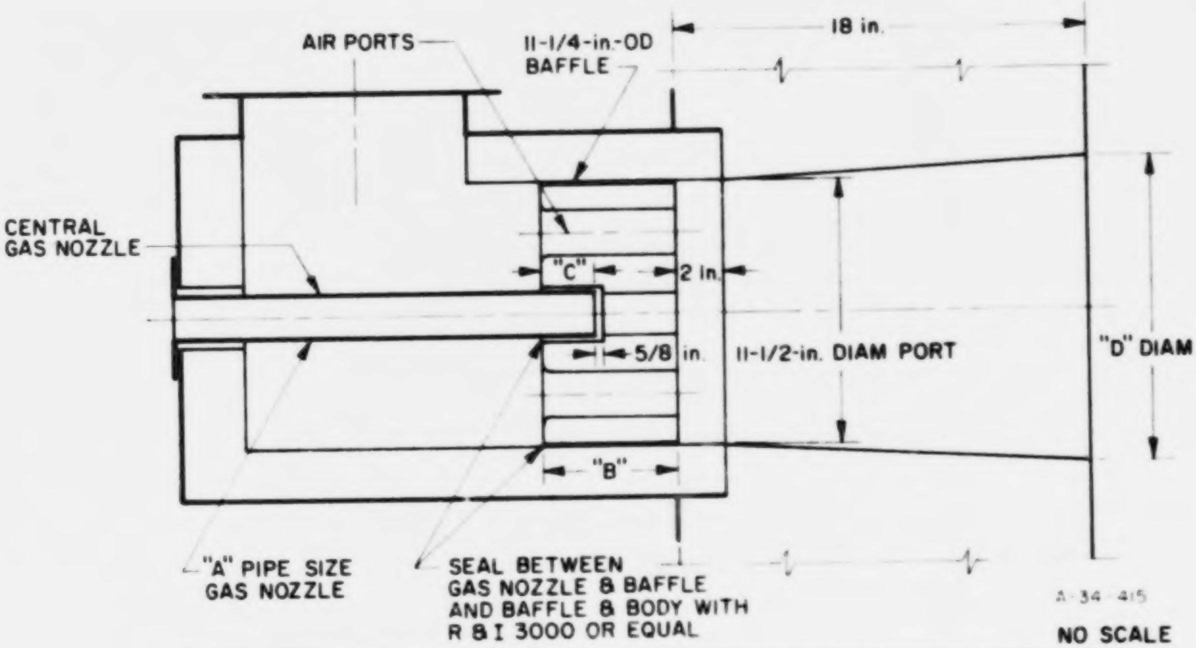
18 in.
AIR PORTS
11-1/4-in.-OD BAFFLE
CENTRAL GAS NOZZLE
"C"
2 in.
5/8 in.
11-1/2-in. DIAM PORT
"D" DIAM
"B"
"A" PIPE SIZE GAS NOZZLE
SEAL BETWEEN GAS NOZZLE & BAFFLE AND BAFFLE & BODY WITH R & I 3000 OR EQUAL
A-34-415
NO SCALE

BAFFLE	AIR PRESSURE FOR 40,000 SCF/hr at 850 °F	"A"	"B"	"C"	"D"
a. LONG FLAME	3.25 in. wc	1-1/4 in.	6 in.	2-3/8 in.	13 in.
b. SHORT FLAME	18 in. wc	3/4 in.	5 in.	2-3/8 in.	16-1/2 in.
c. INTER. FLAME	14 in. wc	1 in.	8 in.	3-7/8 in.	13 in.

Figure 4. Assembly drawing of baffle burner

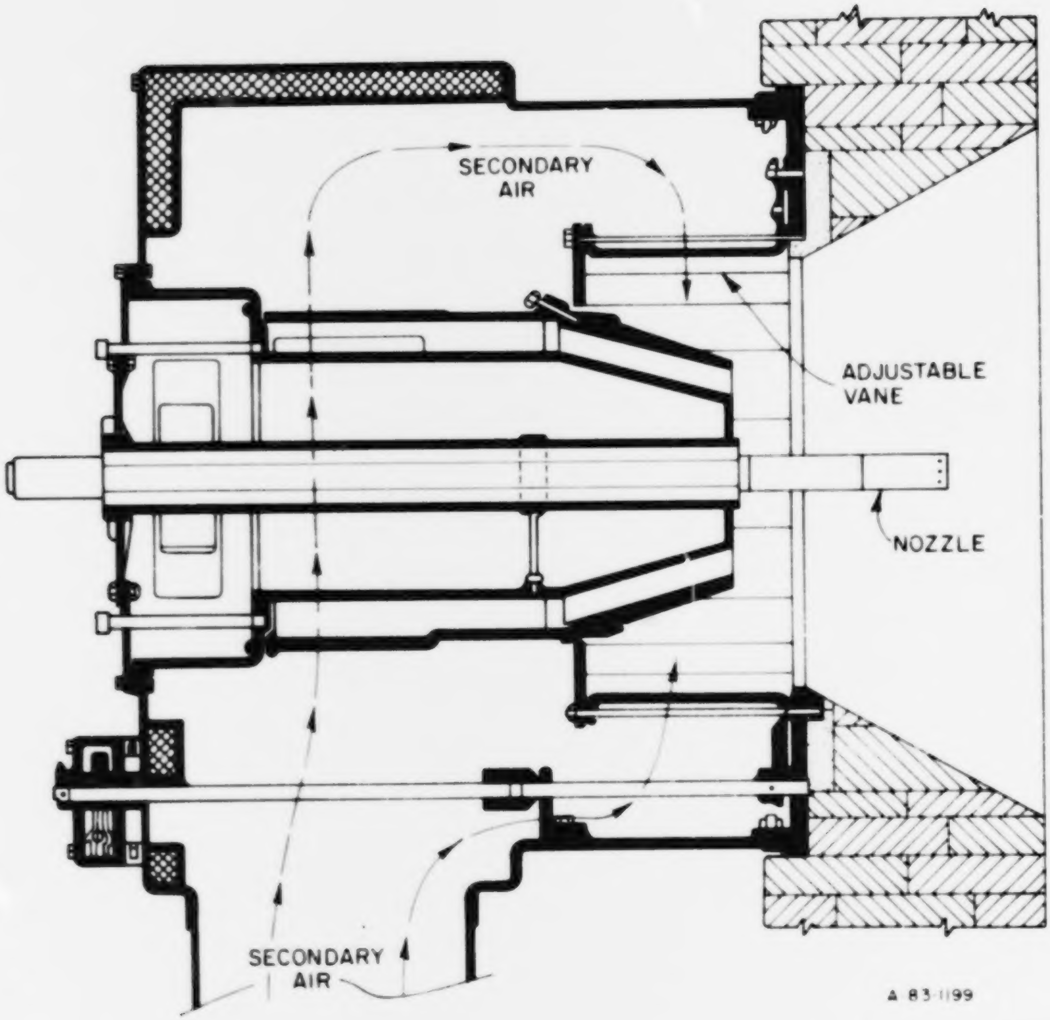
SECONDARY AIR
ADJUSTABLE VANE
NOZZLE
SECONDARY AIR
A 83-1199

Figure 5. Boiler burner

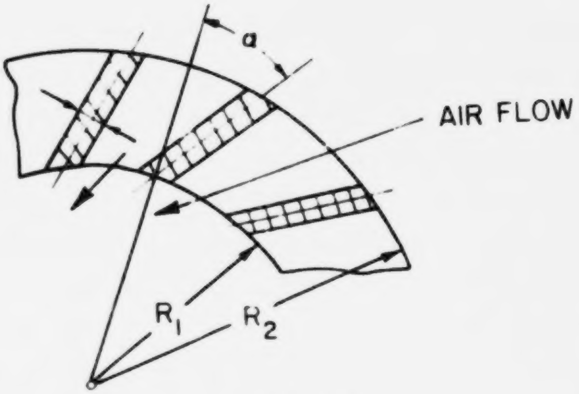

A-34-414

Figure 6. Boiler burner air register vanes

The gas nozzle can be either of pure axial-flow or partial radial-flow design. The radial design consists of an end-plugged pipe with six equally spaced holes drilled around the circumference of the pipe and about 1/4 inch from the end. The orifices or ports are sized for a gas velocity of about 300 to 600 ft/s at a 3500 SCFH gas flow. The burner block is only 6 inches thick, which allows much of the combustion to occur within the actual furnace enclosure.

DESCRIPTION OF FURNACE TEST FACILITY

The experimental work was conducted on a rectangular furnace with a 25-sq-ft cross-sectional area and a 15-foot length. This furnace can be end- or sidewall-fired at a rate of 4 million Btu/hr. The furnace is equipped for in-the-flame sampling, preheated air, and flue-gas recirculation. (See Figure 6a.) This furnace is capable of operating at temperatures up to 3000°F or as low as 1600°F at constant (maximum) gas input of 4 million Btu/hr and up to 40% excess air. Cooling is achieved with cooling coils embedded in the refractory walls. The furnace is constructed completely of 9-inch-thick cast refractories, with removable panels in one sidewall to permit insertion of sampling probes (Figure 7). The overall furnace system is shown schematically in Figure 8. The system is flexible enough that the following operating parameters can be independently varied:

- Heat input, up to 4 million Btu/hr (8.0 million for certain burners)
- Air input, up to 40% excess
- Heat losses to the furnace walls by changing flow in water-cooling tubes cast into the refractories
- Combustion air temperature, up to 1000°F
- Flue gas recirculation capability, up to 35% of combustion air
- Furnace pressure, up to +0.05 inch of water.

The combustion air for the main furnace can be preheated up to a temperature of 1000°F with a separately fired radiant tube air preheater. The radiant tube furnace (Figure 9) consists of an insulated airtight steel chamber 4 feet high, 4 feet wide, and 16 feet long. As the combustion air to be preheated passes through this chamber, it is heated by convection from three 6-inch-diameter "hairpin" gas-fired radiant tubes.

The radiant tubes and refractory flow passages inside the preheater are arranged to provide an S-shaped flow pattern, which maximizes residence time for heating at the maximum allowable pressure drop (20 ounces) for which the flow pattern will provide the necessary air flow of 75,000 SCFH.

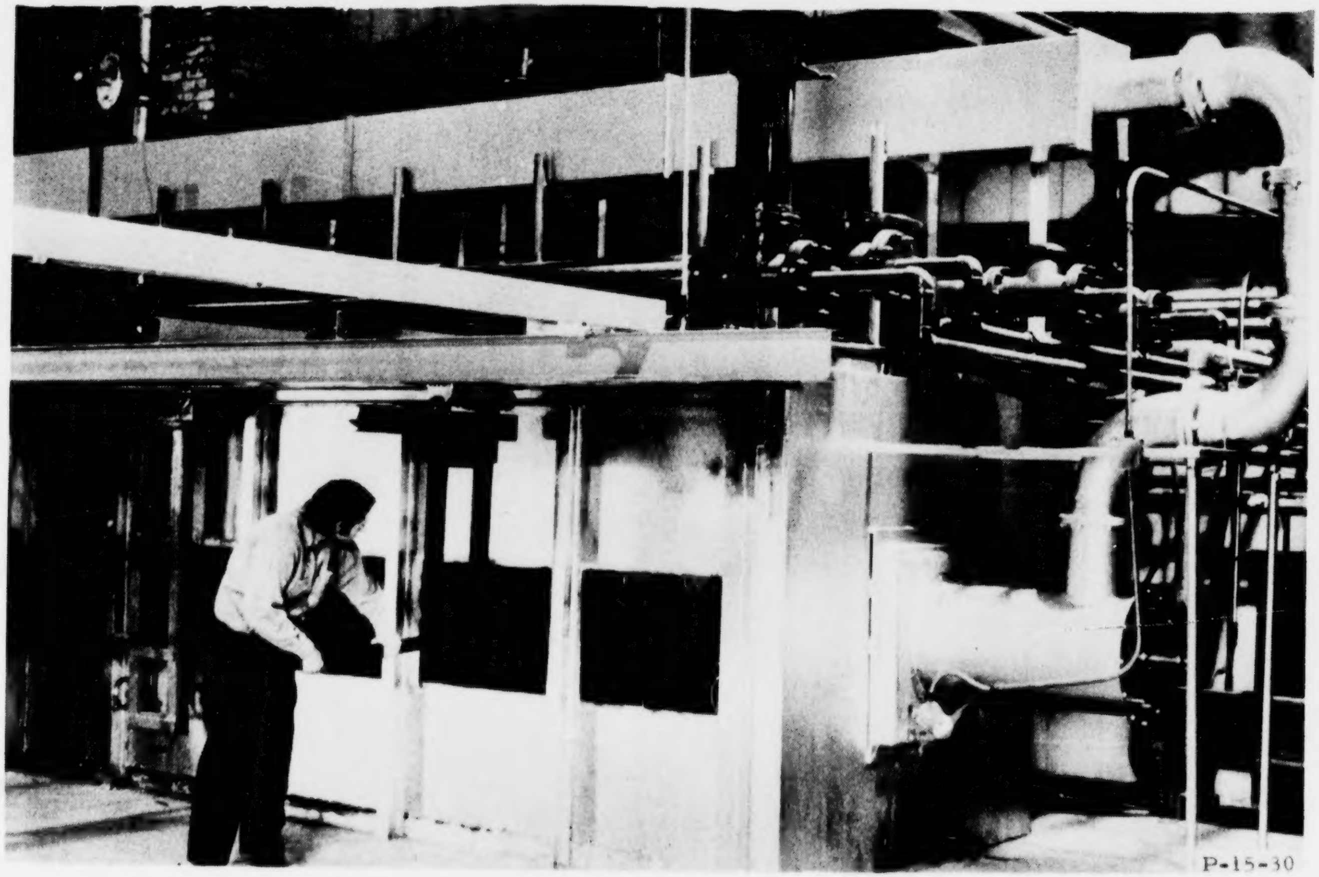

Figure 6a. Rectangular test furnace

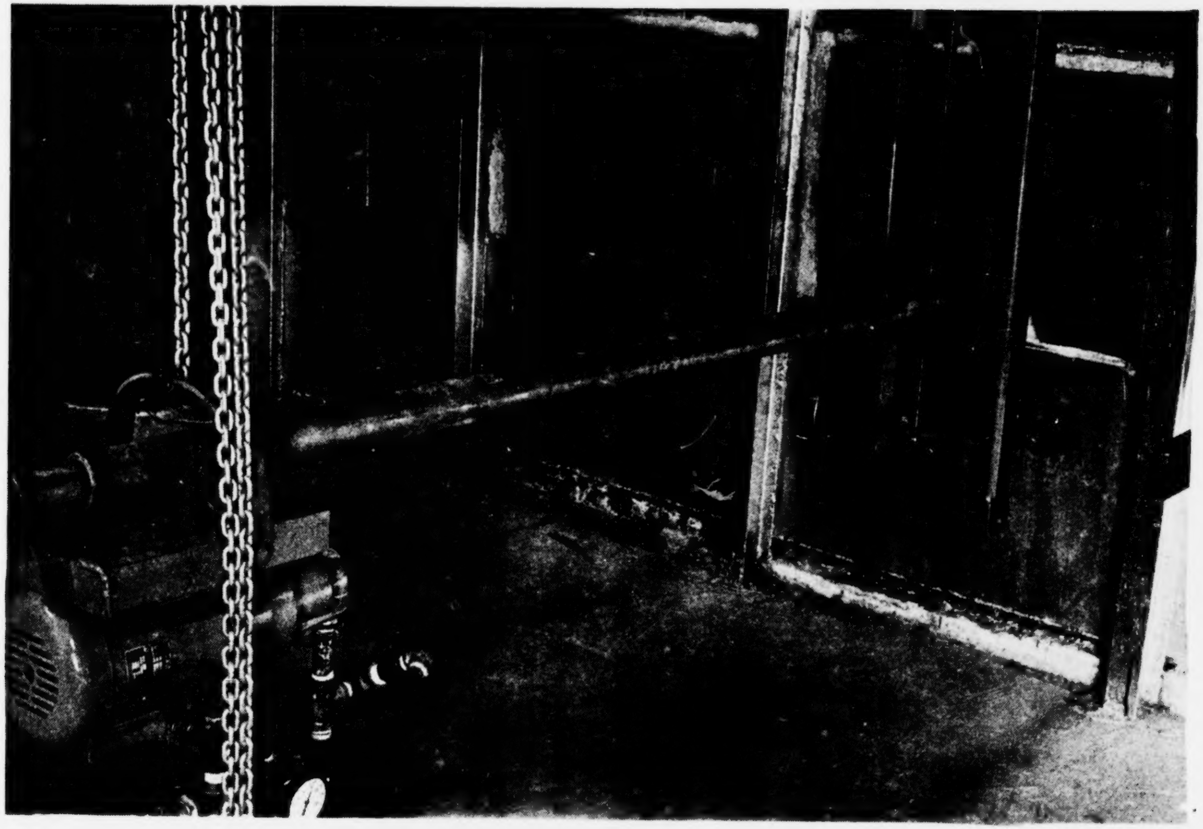

Figure 7. Removable sidewall furnace panels for interior flame probing

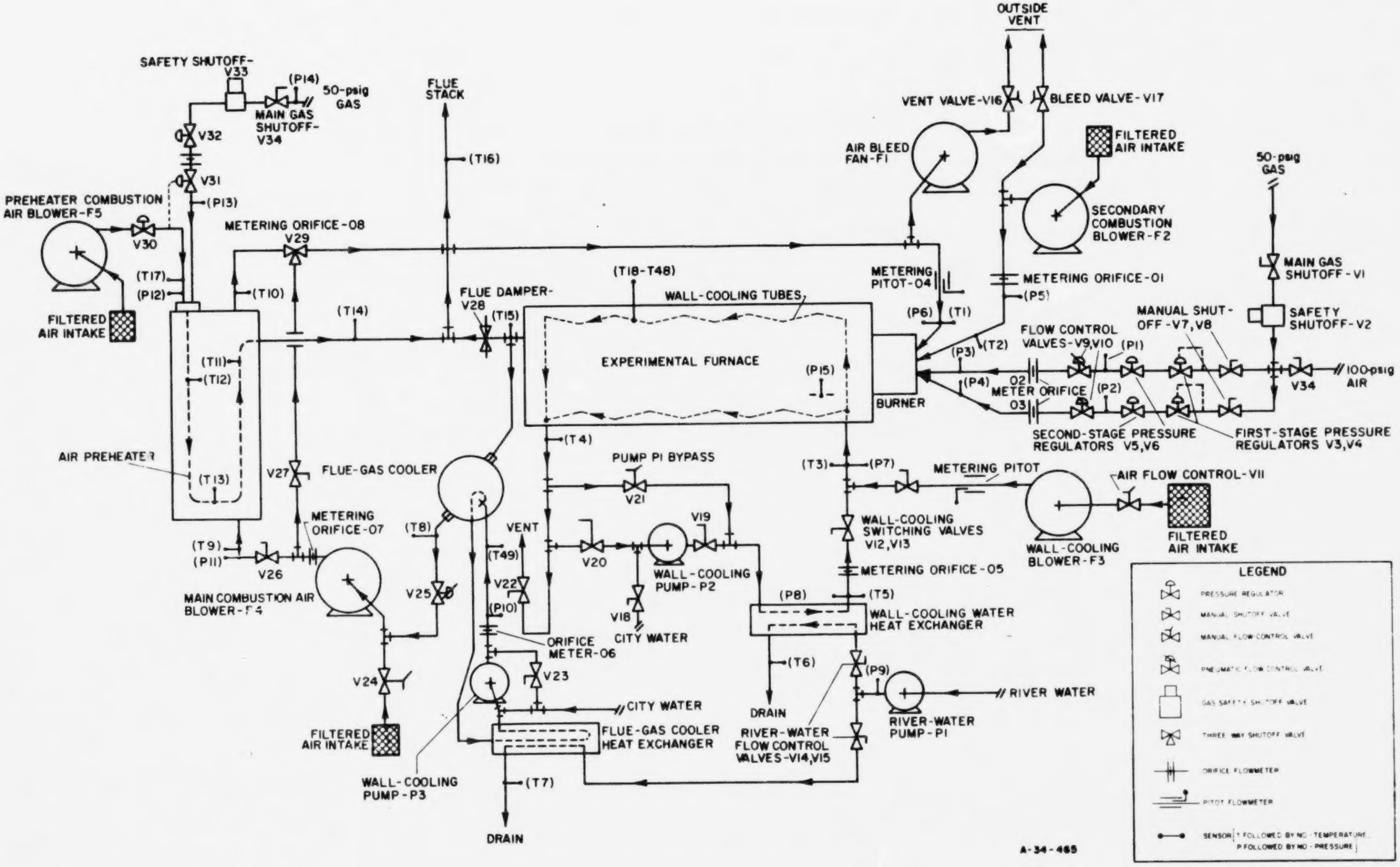
OUTSIDE VENT
VENT VALVE-V16
BLEED VALVE-V17
AIR BLEED FAN-F1
FILTERED AIR INTAKE
SECONDARY COMBUSTION BLOWER-F2
50-psig GAS
MAIN GAS SHUTOFF-V1
SAFETY SHUTOFF-V2
METERING ORIFICE-O1
(P5)
METERING PITOT-O4
(P6)
(T1)
(P3)
(T2)
(P4)
FLOW CONTROL VALVES-V9,V10
(P1)
(P2)
MANUAL SHUT-OFF-V7,V8
O2
METER ORIFICE
O3
SECOND-STAGE PRESSURE REGULATORS V5,V6
FIRST-STAGE PRESSURE REGULATORS V3,V4
V34
100-psig AIR
BURNER
EXPERIMENTAL FURNACE
WALL-COOLING TUBES
(T18-T48)
(P15)
SAFETY SHUTOFF-V33
(P14)
50-psig GAS
MAIN GAS SHUTOFF-V34
V32
V31
(P13)
PREHEATER COMBUSTION AIR BLOWER-F5
V30
(T17)
(P12)
FILTERED AIR INTAKE
METERING ORIFICE-O8
V29
(T10)
(T14)
FLUE STACK
(T16)
FLUE DAMPER-V28
(T15)
(T11)
(T12)
AIR PREHEATER
(T13)
V27
FLUE-GAS COOLER
METERING ORIFICE-O7
(T9)
(P11)
V26
MAIN COMBUSTION AIR BLOWER-F4
(T8)
V25
V24
FILTERED AIR INTAKE
VENT
(T49)
V22
(P10)
ORIFICE METER-O6
V23
CITY WATER
FLUE-GAS COOLER HEAT EXCHANGER
WALL-COOLING PUMP-P3
(T7)
DRAIN
(T4)
PUMP P1 BYPASS
V21
V19
V20
WALL-COOLING PUMP-P2
V18
CITY WATER
(P8)
WALL-COOLING WATER HEAT EXCHANGER
(T6)
DRAIN
(T3)
(P7)
METERING PITOT
AIR FLOW CONTROL-V11
WALL-COOLING SWITCHING VALVES V12,V13
WALL-COOLING BLOWER-F3
FILTERED AIR INTAKE
METERING ORIFICE-O5
(T5)
(P9)
RIVER WATER
RIVER-WATER PUMP-P1
RIVER-WATER FLOW CONTROL VALVES-V14,V15
LEGEND
PRESSURE REGULATOR
MANUAL SHUTOFF VALVE
MANUAL FLOW CONTROL VALVE
PNEUMATIC FLOW CONTROL VALVE
GAS SAFETY SHUTOFF VALVE
THREE WAY SHUTOFF VALVE
ORIFICE FLOWMETER
PITOT FLOWMETER
SENSOR (T FOLLOWED BY NO. - TEMPERATURE, P FOLLOWED BY NO. - PRESSURE)
A-34-465

Figure 8. Overall system schematic diagram of rectangular test furnace system

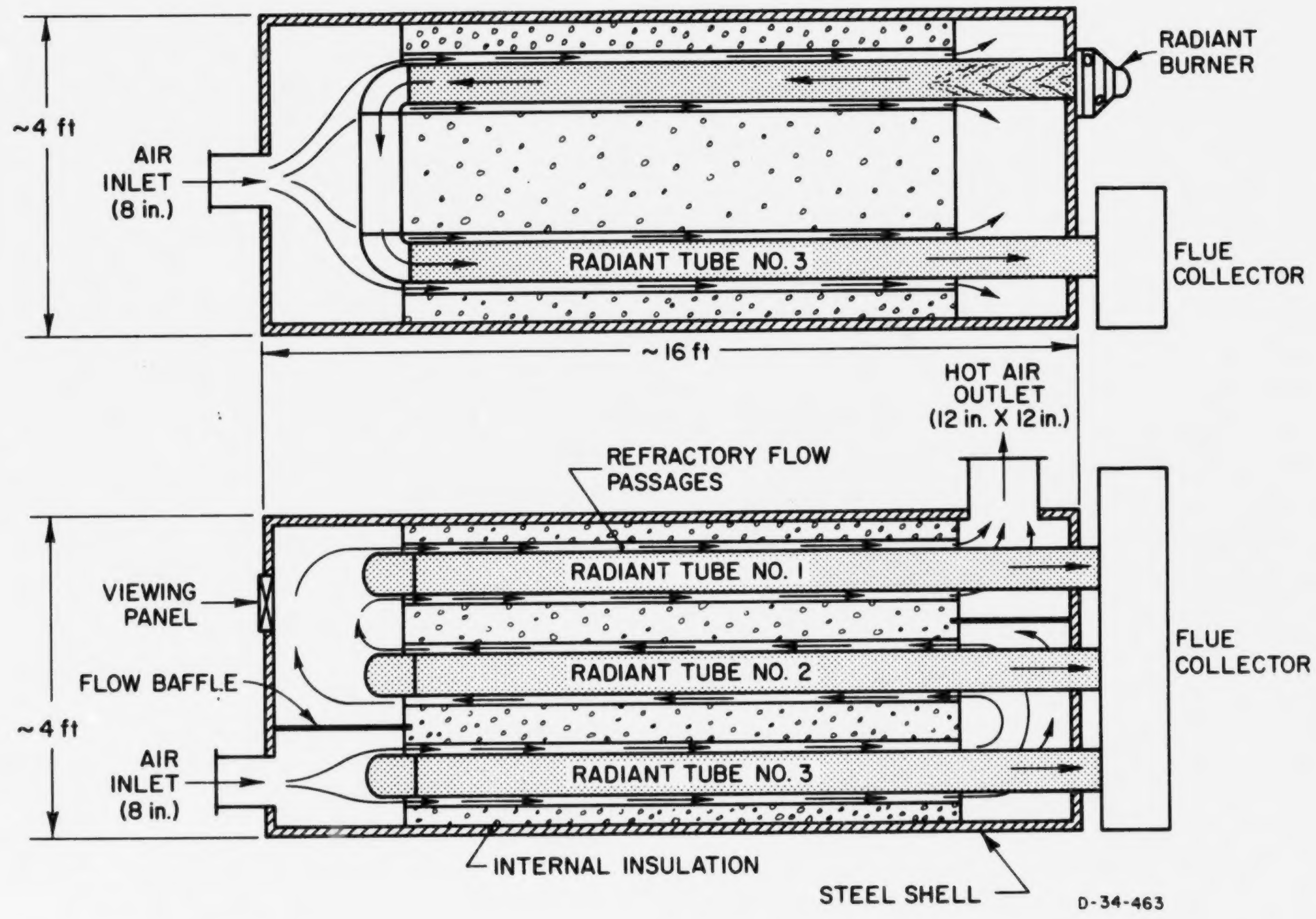
RADIANT BURNER
~4 ft
AIR INLET (8 in.)
RADIANT TUBE NO. 3
FLUE COLLECTOR
~16 ft
HOT AIR OUTLET (12 in. X 12 in.)
REFRACTORY FLOW PASSAGES
VIEWING PANEL
RADIANT TUBE NO. 1
FLOW BAFFLE
RADIANT TUBE NO. 2
FLUE COLLECTOR
~4 ft
AIR INLET (8 in.)
RADIANT TUBE NO. 3
INTERNAL INSULATION
STEEL SHELL
D-34-463

Figure 9. Radiant tube preheater for main furnace combustion air

The temperature of the air can be regulated by changing the heat input to the radiant tubes. Ambient temperature air can be supplied by completely shutting down the preheater or by directing the air through the preheater bypass pipe. The bypass pipe was installed to allow working on the preheater without shutting down the air supply to the main furnace. Air bypass is achieved by selective switching of valves.

Flue products for recirculation back to the burner and main furnace are obtained from the furnace itself. Flue products can be withdrawn from the furnace flue passage just prior to the main furnace flue damper. Up to 14,000 SCFH of flue products can be withdrawn from the flue, which provides a 30% recirculation factor when the furnace is fired at 3.5 million Btu/hr with 20% excess air.

The main furnace flue products are actually pulled from the flue (Figure 8) by the suction in the inlet side of the main furnace combustion air fan (F4). The flue products enter the recirculation withdrawal and treatment system, at about 2800°F, through a short length of internally insulated steel duct. These hot gases are cooled to about 125°F in a packed-bed water cooler (Figure 10). Cooled city water (about 70°F) is sprayed down on a bed of refractory packings as the hot gases pass up through the packed bed. This cooling system lowers the water content of the flue gas from about 0.008 to about 0.007 lb/cu ft, which is the dew point of the gases at about 125°F. (The lost water content can be readded later in the system if experimental conditions require this treatment.) The cooled gases then pass through a flow-control shutoff valve (V25 in Figure 8). This valve controls the flue-gas flow rate, which regulates the percentage of recirculated products. This valve is interlocked to an outlet temperature sensor on the gas cooler. If the outlet temperature of the gases exceeds 150°F, which would damage the combustion air fan, the control valve (V25) shuts down. This stops the flow of flue gases. Beyond the flue-gas control valve, the flue gases are mixed with the required amount of air for combustion. A control valve (V24) regulates the amount of air pulled in by the fan. The total amount of air for combustion and flue products is metered with an orifice plate (O7) at the outlet of the fan. The flue products and air then pass into the air preheater or preheater bypass pipe.

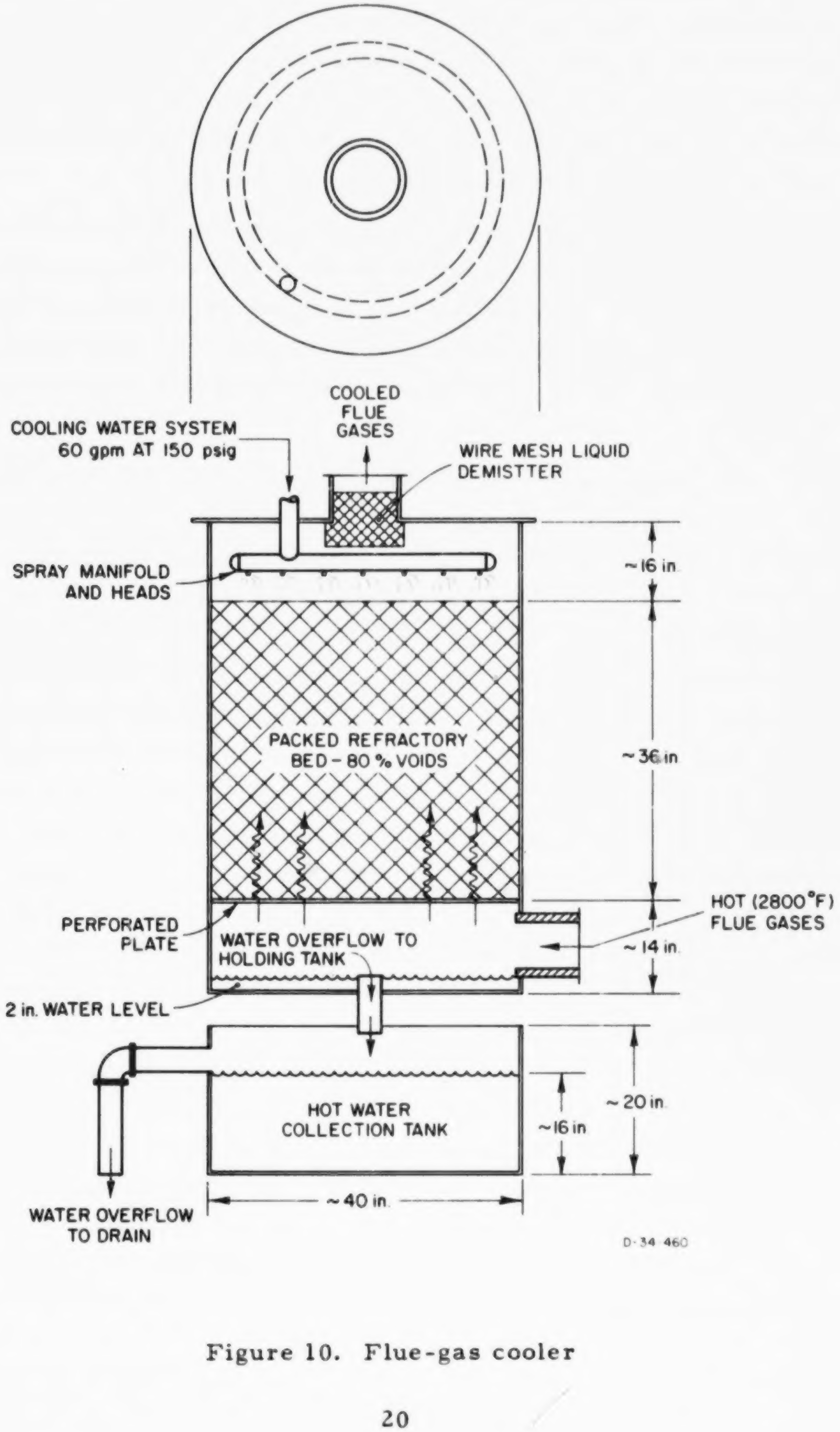
COOLED FLUE GASES
COOLING WATER SYSTEM 60 gpm AT 150 psig
WIRE MESH LIQUID DEMISTTER
SPRAY MANIFOLD AND HEADS
~16 in.
PACKED REFRACTORY BED - 80 % VOIDS
~36 in
PERFORATED PLATE
WATER OVERFLOW TO HOLDING TANK
HOT (2800°F) FLUE GASES
~14 in.
2 in. WATER LEVEL
HOT WATER COLLECTION TANK
~16 in
~20 in.
~40 in.
WATER OVERFLOW TO DRAIN
D-34 460

Figure 10. Flue-gas cooler

The water used in the flue-gas cooler is clean city water, which is continuously recycled. A water flow of 60 gpm is supplied at 150 psig, by a turbine pump, to a series of spray heads in the gas cooler. The hot (200°F) spent water flows out of the cooler into an atmospheric holding tank. This tank is equipped with a constant-level overflow to the building drain. In this way, any condensed water from the combustion is removed and disposed of in the sewer. The water in the holding tank is periodically treated with sodium hydroxide to prevent acid buildup in the water due to condensing flue-gas components. One such component removed by the flue-gas cooler is NO_2. The hot water from the water holding tank is cycled through an American Standard heat exchanger capable of removing 1.5 million Btu/hr of heat from the water. Cooling in the heat exchanger is provided by a flow of river water at a rate of about 150 gpm at 80 psig. The river water is supplied by a river adjacent to the test facility through a service pump (P1) maintained by IGT.

Figure 11 is an overall view of furnace controls and the analytical instrumentation package. The equipment used for concentration measurements of chemical species during this program are listed below; these analyzers included a;

Beckman 742 Polarographic Oxygen (O_2)
Beckman Paramagnetic Oxygen (O_2)
Beckman NDIR Methane (CH_4)
Beckman NDIR Carbon Monixide (CO)
Beckman NDIR Carbon Dioxide (CO_2)
Varian 1200 Flame Ionization Chromatograph (Total HC and C_1 to C_9)
Beckman NDIR Nitric Oxide (NO)
Beckman UV-NO_2
Hewlett-Packard Thermoconductivity Chromatography, Hydrogen (H), Nitrogen (N_2), Argon (A_2), CO, CO_2, C_1 to C_5, Oxygen (O_2)
Beckman Chemiluminescent NO-NO_2
Data Integration System

This instrumentation package allowed concentration measurements of the following major components: a) measurement of hydrocarbon compounds C_1 to C_9; b) independent check of NO-NO_2 chemiluminescent with NDIR-NO and NDUV-NO_2; c) independent check of paramagnetic O_2, polarographic O_2, NDIR-CH_4, NDIR-CO and NDIR-CO_2 with the respective chromatographic species concentration; and d) measurement of hydrogen (H_2), argon (A_2), and nitrogen (N_2).

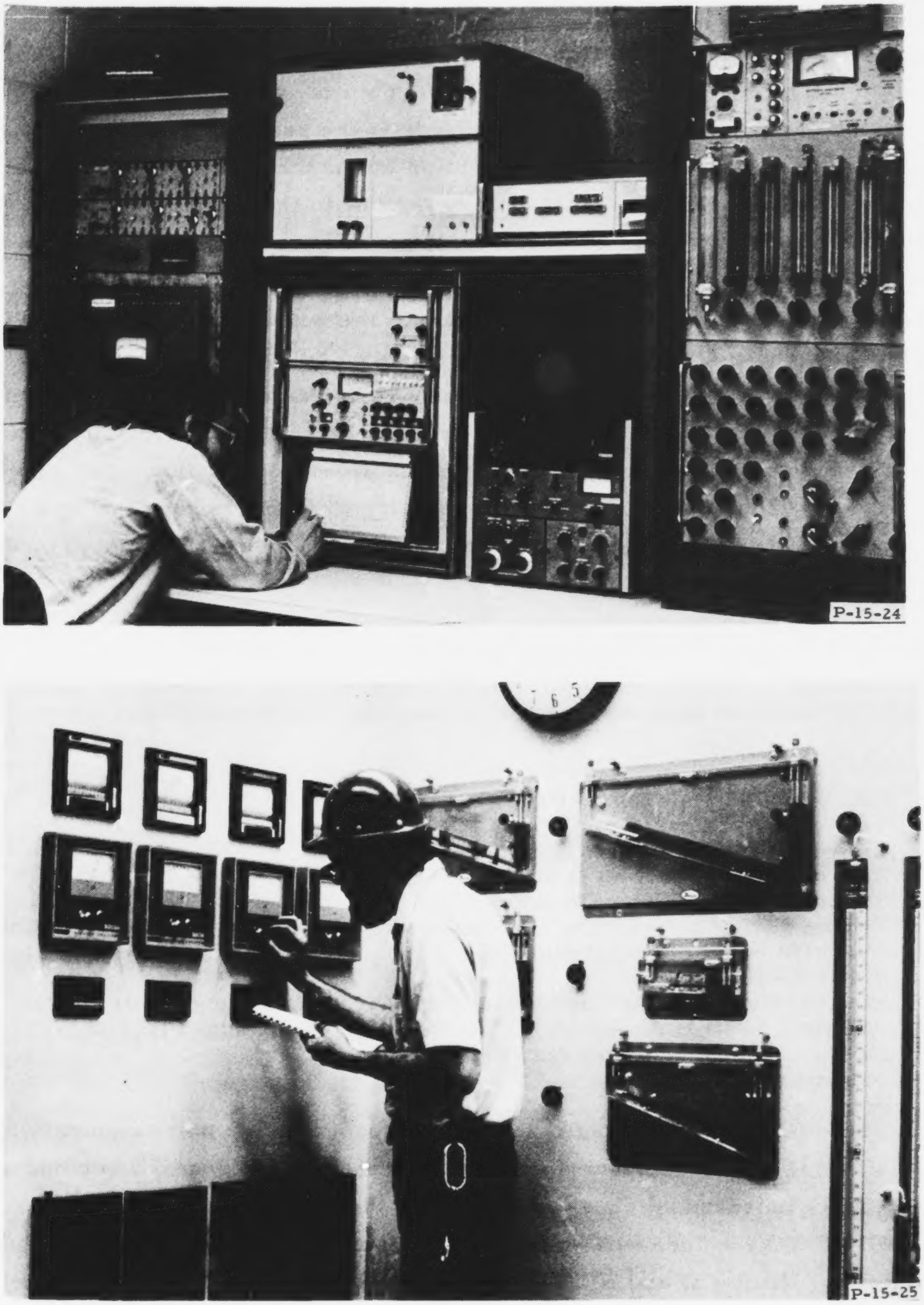
P-15-24
P-15-25

Figure 11. Control room facility and analytical instrumentation

The following is a general description of the measurement system used for this program.

1. NO and NO_2 Instrumentation

The chemiluminescent NO_x and NDUV-NO_2 system was mounted in a roll-around cabinet that could be placed out at the furnace. This was important in minimizing sampling distances, which can affect accuracy. The chemiluminescent unit was equipped with a carbon converter. Test work by IGT and others has demonstrated that in a reducing environment the carbon converter maintains a better conversion efficiency than converters made of stainless steel, quartz or molybdenum.

The instrumentation was calibrated by using both a permeation tube with a controlled known release of NO_x and certified prepared cylinders of NO and NO_2 gases.

The sample gas was drawn from the furnace through a special alumina probe by a Dia-Pump Model 08-800-73 all stainless steel and Teflon pump delivering approximately 0.4 CFM. (This sample delivery rate was dictated by the requirements of the measuring instruments.) The sample is immediately passed through a stainless steel large-particle filter. Both the pump and filter were kept above 100°C to prevent condensation of the water vapor inherent to combustion products.

2. CO, CH_4, and CO_2 Measurements

Nondispersive infrared analyzers were used for carbon monoxide, methane, and carbon dioxide measurements. These analyzers do not affect the sample gas and can be operated in series. They were calibrated by using certified gases with known concentrations of the species being determined. The infrared analyzers require a completely dry sample. Therefore, the sample was first passed through a water trap and a 3 Å molecular drying sieve. A small in-line filter was placed immediately after the drying tube to trap particles of sieve that may be carried over by the gas stream.

3. Oxygen Measurements

A portion of the "conditioned" sample gas is diverted from the NDIR units to a Beckman Model 600 paramagnetic analyzer. A second oxygen analyzer, a Beckman Model 742 polarographic, was used as a cross-check on the oxygen concentration. The Model 742 analyzer has an advantage over the paramagnetic in time response.

4. Chromatographic Measurements

As a detailed gas analysis was required, the sample is fed to a Hewlett-Packard 7620-A thermal conductivity chromatograph which permitted concentration evaluations of hydrogen, nitrogen, argon, oxygen, carbon monoxide, carbon dioxide and hydrocarbons C_1 to C_5. To achieve separation of these species a helium carrier gas was used in conjunction with a Porapak Q column. Three temperature program rates were also required ranging from –100°C to 300°C. A sample loop volume of 100 ml was used to insure linearity in the hydrogen response for concentrations up to 60%.

For total hydrocarbon analysis a Beckman hydrocarbon analyzer was used. A detailed hydrocarbon analysis could be made using a Varian 1200 flame ionization chromatograph. All chromatographic readings were electronically integrated and printed out as a function of resolution time.

In addition to flue gas analysis, a major task of this program was to map profiles of temperature, chemical species and flow direction for each burner type. Modified designs of the International Flame Research Foundation were used to construct probes which enabled this type of data collection.

Figure 12 shows the assembly drawing of the gas sampling probe used both in the flame and flue. To minimize NO_2 reduction in the probe, an alumina tube was inserted for the first 18 inches and was joined to Teflon tubing to carry the gas sample to the analyzers.

Temperature data was collected using a suction pyrometer whose design is illustrated in Figure 13. A Pt-Pt Rh 10% thermocouple was used. The efficiency of the pyrometer was measured at 96% with a 25 second response time.

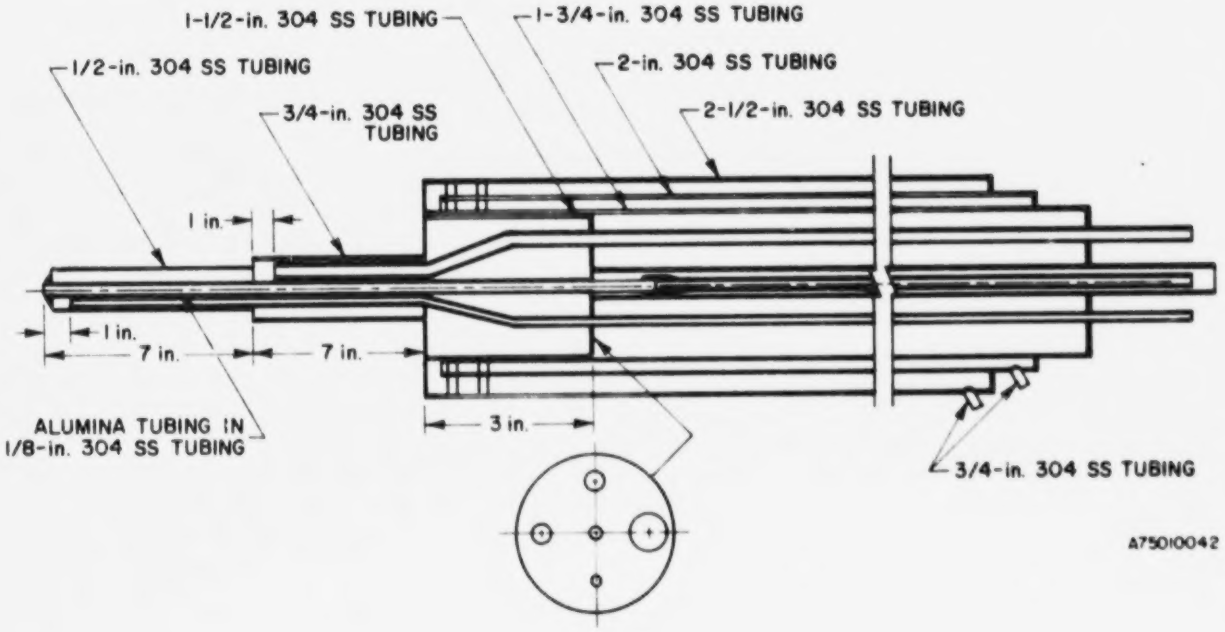
1-1/2-in. 304 SS TUBING
1-3/4-in. 304 SS TUBING
1/2-in. 304 SS TUBING
2-in. 304 SS TUBING
3/4-in. 304 SS TUBING
2-1/2-in. 304 SS TUBING
1 in.
1 in.
7 in.
7 in.
3 in.
ALUMINA TUBING IN 1/8-in. 304 SS TUBING
3/4-in. 304 SS TUBING
A75010042

Figure 12. Gas-sampling probe head
for nonparticulate flue gases

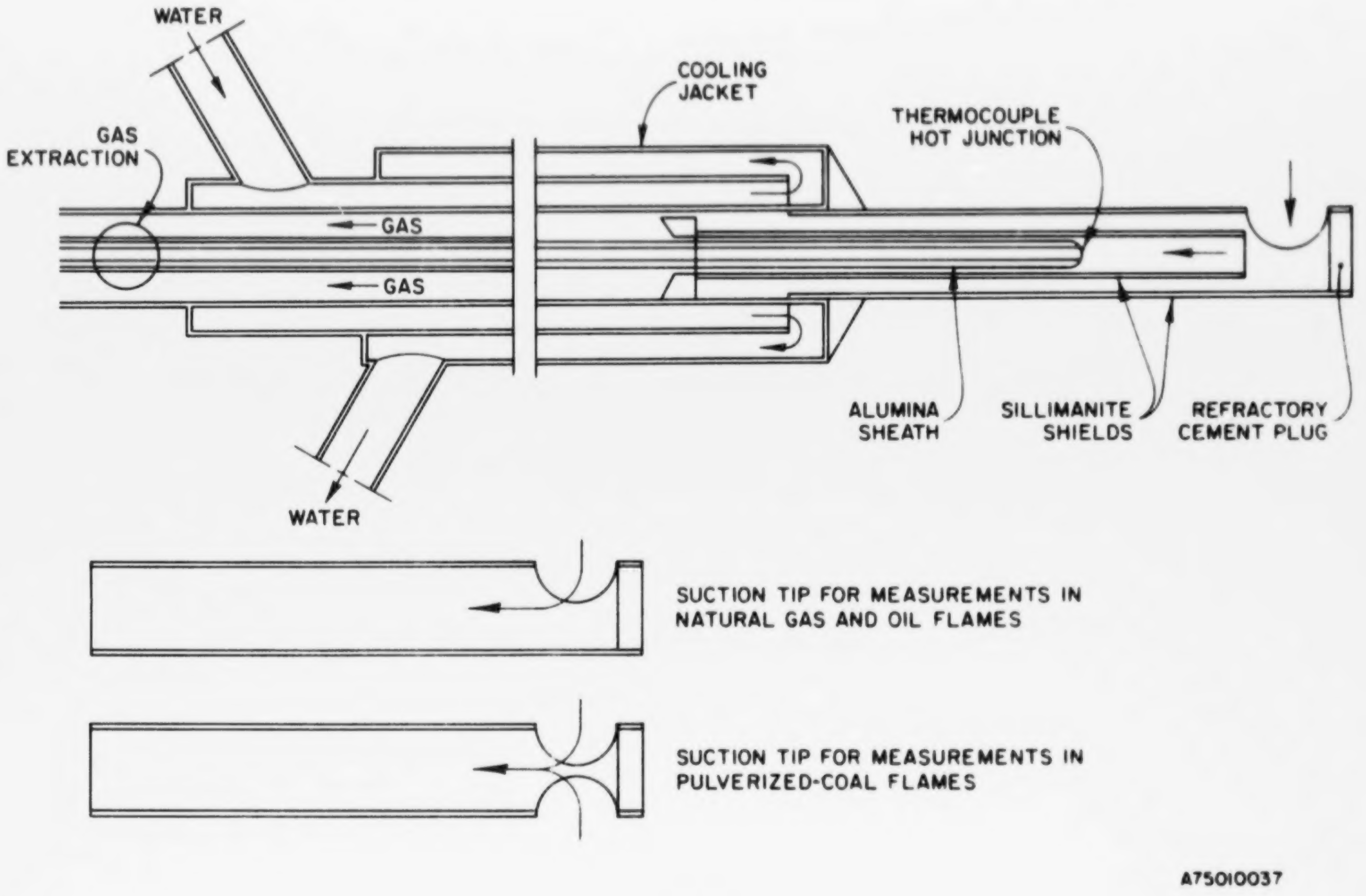
WATER
COOLING JACKET
GAS EXTRACTION
THERMOCOUPLE HOT JUNCTION
GAS
GAS
ALUMINA SHEATH
SILLIMANITE SHIELDS
REFRACTORY CEMENT PLUG
WATER
SUCTION TIP FOR MEASUREMENTS IN NATURAL GAS AND OIL FLAMES
SUCTION TIP FOR MEASUREMENTS IN PULVERIZED-COAL FLAMES
A75010037

Figure 13. Modified IFRF temperature probe

The gas sampling probe, suction pyrometer and direction flow probe were all designed to be installed in the general probe holder shown in Figure 14.

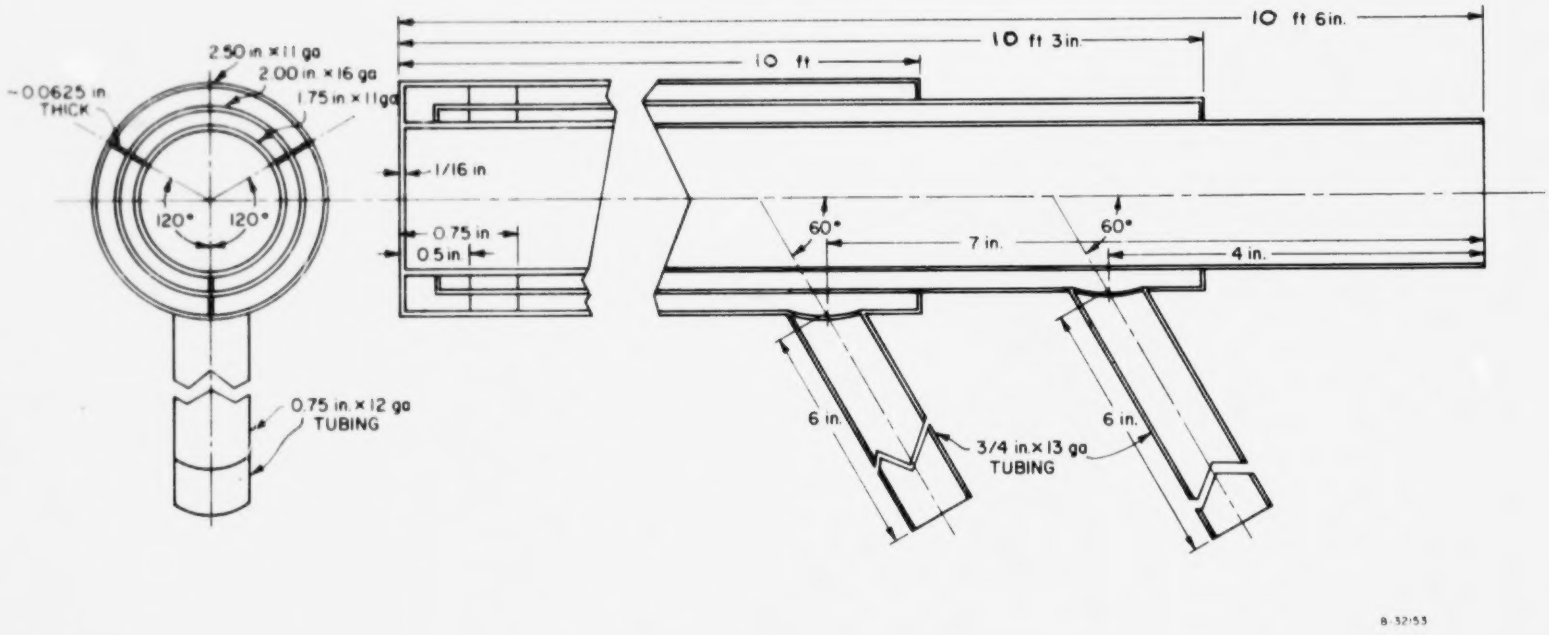
10 ft 6in.
10 ft 3in.
10 ft
2.50 in × 11 ga
2.00 in. × 16 ga
1.75 in. × 11 ga
~0.0625 in THICK
120°
120°
1/16 in
0.75 in
0.5 in
60°
60°
7 in.
4 in.
0.75 in. × 12 ga TUBING
6 in.
6 in.
3/4 in × 13 ga TUBING
8-32153

Figure 14. General probe holder

EXPERIMENTAL PLAN

The experimental measurements involved — a base-line characterization of flue gas as a function of primary operating variables, a detailed in-the-flame investigation at selected base-line conditions, a characterization of emissions as a function of various emission control techniques and/or combination of techniques, and, finally, an in-the-flame investigation for those control techniques found to be most effective for NO_x control.

For each of the burners studied, base-line operation of that burner was characterized by conducting input/output measurements at the flue. This characterization included the effects of changing the following operating variables:

a. Three (3) air preheat temperatures (ambient, 400°, and 800°F)

b. Five (5) air/fuel ratios (excess air between stoichiometric and 25%, in 5% increments)

c. Two (2) firing rates (1.5 and 3.0 million Btu/hr)

d. Two (2) heat-release rates (as controlled by wall cooling with air, with one-half of the water load and with the full water load)

e. Fuel injector design (radial, axial, and a combination of both, or in the boiler-burner case, convergent radial, ring injector and divergent radial, and gun injector)

Each operating variable was evaluated independently, while holding all others constant. Thus, there were 300 different sets of conditions investigated for base-line operation of each burner type. In addition to the quantitative flue measurements, flame characteristics were documented photographically.

Upon completion of the base-line characterization with input-output tests at the furnace flue, an intensive flame analysis was conducted for each of the burners studied. These investigations were made at a preselected set of operating conditions. These detailed studies included the following:

a. Directional flow analysis (Approximately 10 radial scans were made in order to precisely define the configuration of the interval recirculating regions.)

b. Chemical species concentrations (Five radial profiles were conducted with the gas samples being analyzed for N_2, O_2, H_2, CO, CO_2, NO, NO_2, and individual hydrocarbons).

c. Temperature profile (A suction pyrometer was used for five radial scans to get time-averaged temperatures).

Once the base-line characterization was completed, this information was combined with known and potential emission control methods. The specific objective was to develop operating criteria for minimum emissions for each burner type. The following parameters were investigated:

a. Two (2) flue gas recirculation quantities (added to combustion air at 15% and 30% concentrations).

b. Two (2) combustion air swirl intensities (if applicable, studied at two intensities differing from the base-line condition).

c. Fuel/air momentum ratio (vary the gas and air velocities by a factor of 2 independently and also decrease the velocity of the gas by a factor of 2).

d. Three (3) burner-block analyses (using three different burner-block angles which differed from each other by 15 degrees).

e. Two (2) fuel injector positions (vary location of fuel injection to plane which is even with the front wall of the furnace).

There were 270 different sets of low-emission operating parameters investigated. As in the base-line characterization investigation, flame characteristics were documented photographically.

In order to develop an understanding of how the control techniques are limiting the formation of pollutants, a detailed flame analysis was conducted for one set of operating parameters which had minimized the pollutant concentration at the flue. The experimental investigation was carried out in a manner similar to that previously discussed.

GENERAL FLAME CHARACTERISTICS

A general aerodynamic characterization of a flame can be made by determining the different types of flow patterns that exist within a combustion chamber. A detailed flow analysis of a confined flame reveals that the front section of a combustion chamber can be divided into four zones: primary jet, primary recirculation, secondary jet, and secondary recirculation. The primary and secondary jets contain only particles with a forward flow direction (away from the burner), whereas the recirculation zones contain gas particles moving in the reverse flow direction (back toward the burner). The size, shape, and particle density of the recirculation zones are determined by the velocity, the ratio of gas to air, the spin intensity of the secondary jet, the burner-block angle, and, for the secondary recirculation zone, the size and shape of the combustion chamber. Figure 15 shows the three types of flow patterns that were observed during the pollution control trials.

A type I flow pattern is observed when the secondary jet has no tangential velocity component (no spin) and the primary jet velocity is much larger than the secondary jet velocity. Depending on the initial jet exit velocity from the fuel injector, the flame can be either attached to or detached from the injector. A type I flow pattern also can be generated with a secondary jet with a tangential velocity component (spin) if the burner-block divergent angle is equal to or less than the angle of the secondary jet relative to the burner axis. As a result, the burner block restricts the expansion of the secondary jet and inhibits the formation of a primary recirculation zone.

A type II flow pattern is generated when the secondary jet has a tangential velocity component large enough to cause the particles to adhere to and pack tightly against the burner block. This packing creates a low or negative pressure region in the center of the burner block. The pressure differential between the furnace and the central region of the burner block causes gas molecules to be pulled into this region and back toward the burner, thus creating the primary recirculation zone. When the velocity of the primary jet is greater than the velocity of the recirculating gases in the primary recirculation zone, the primary jet penetrates this reverse flow region and a recirculation lobe occurs on each side of the burner axis. This flow pattern is labeled type II.

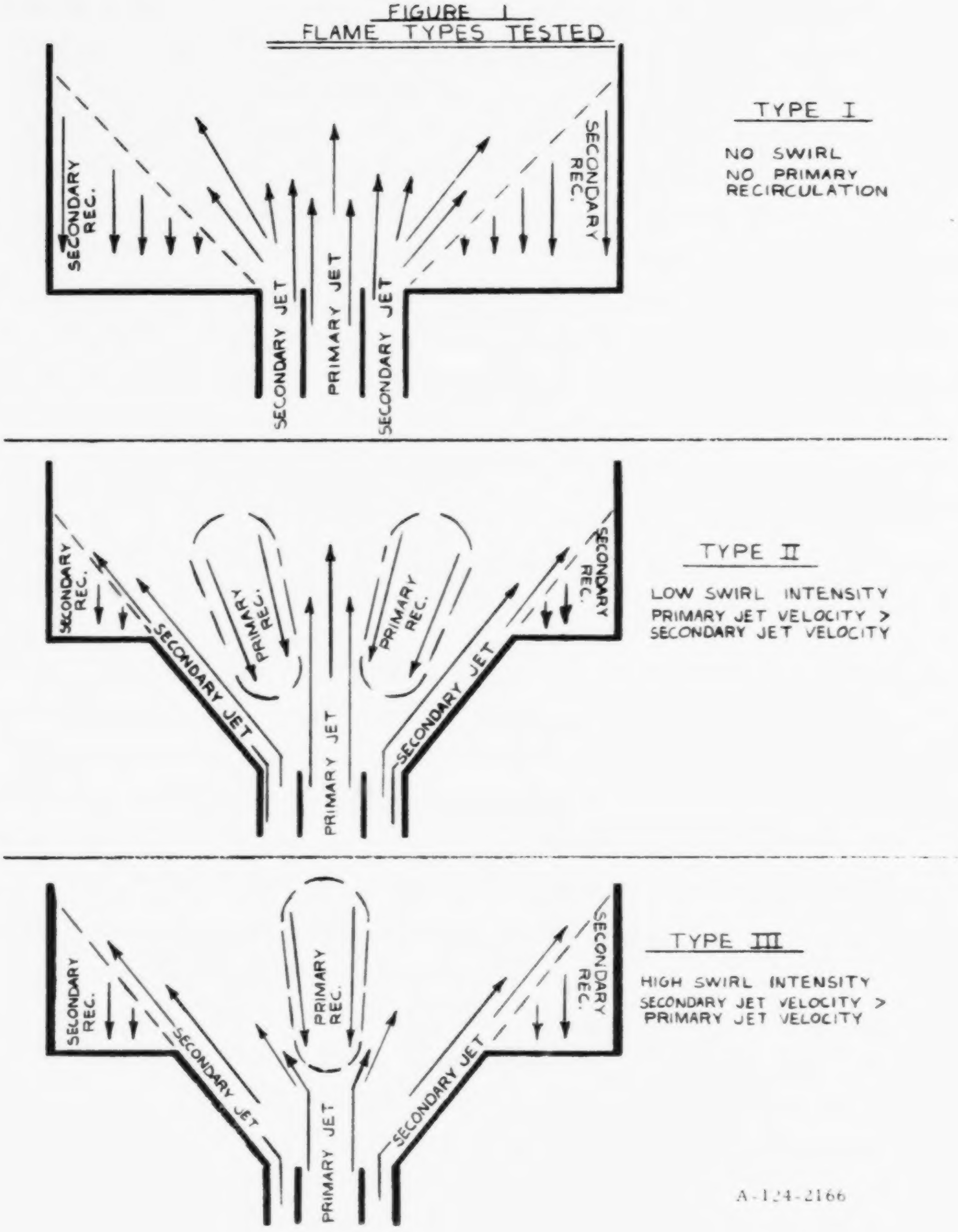
FIGURE I
FLAME TYPES TESTED
SECONDARY REC.
SECONDARY REC.
SECONDARY JET
PRIMARY JET
SECONDARY JET
TYPE I
NO SWIRL
NO PRIMARY RECIRCULATION
SECONDARY REC.
PRIMARY REC.
PRIMARY REC.
SECONDARY REC.
SECONDARY JET
PRIMARY JET
SECONDARY JET
TYPE II
LOW SWIRL INTENSITY
PRIMARY JET VELOCITY > SECONDARY JET VELOCITY
SECONDARY REC.
PRIMARY REC.
SECONDARY REC.
SECONDARY JET
PRIMARY JET
SECONDARY JET
TYPE III
HIGH SWIRL INTENSITY
SECONDARY JET VELOCITY > PRIMARY JET VELOCITY
A-124-2166

Figure 15. Flames types tested

If the central region of the burner block has a large enough negative pressure differential relative to the furnace, such that the velocity of the recirculating gases is greater than the velocity of the primary jet, penetration of the primary recirculation zone is not possible and a type III flow pattern results. A type III flow pattern also can be generated mechanically by introducing the fuel with only a radial velocity relative to the axis of the burner.

KILN BURNER

An assembly drawing of the kiln burner which was tested was shown in Figure 1. The air plenum, burner block combination were momentum scaled to simulate the firing end and air duct entrance of a 35 million Btu/hr kiln. For a natural gas firing rate of 3000 SCFH, standard trial input volume, a 10% level of excess air would have a velocity of 13 ft/s when preheated to 450°C. Two types of fuel injectors were designed to fit the experimental kiln burner. Figure 2 illustrates the divergent nozzle which has a 45-degree cone, whose base faces the furnace, surrounded by a 45-degree angle divergent orifice. The position of the cone is adjustable relative to the divergent orifice permitting control of the gas injection velocity. The combination nozzle is shown in Figure 3. This design includes an adjustable radial orifice and a fixed diameter axial orifice. The fuel input can either be totally axial, totally radial, or any desired ratio of axial to radial. The normal operating gas velocity during the trials was 500 ft/s; however, the variable orifice feature permitted variations in the gas velocity for a 3000 SCFH input from 40 ft/s to 1000 ft/s. Both the divergent and combination gas nozzles are surrounded by an annular duct for primary air which is used to help shape the flame. The injection velocity of the primary air is 6200 ft/s when its volume is 5% of the total combustion in volume.

The kiln burner was constructed so that the gas nozzle can be positioned flush with the inside wall of the furnace or pulled back into the burner block up to 13 inches. Positioning the nozzle withdrawn 13 inches into the burner block will be referred to as the normal operating position since both jets, primary and secondary, are momentum scaled during the initial stages of mass exchange. Positioning the nozzle flush with the inner furnace wall will be labeled the exit position and permits an expansion of the secondary jet into the larger diameter combustion chamber.

Detailed flame surveys were conducted during the kiln burner trials. These surveys included flow direction, temperature and gas analysis. The details of this survey work along with complete in-the-flame data and a comprehensive listing of the input-output data are presented in Volume II of this report. However, it is beneficial in understanding the interpretation of the input-output data to take a level look at some in-the-flame results.

BASELINE CONDITIONS

The baseline characterization of the kiln burner was made using the combination gas nozzle with 30% of the total gas input being injected axially (810 SCFH) and 70% of the gas being injected in the radial direction (1890 SCFH). The primary air was determined to be 3.2% using the relationship –

$$\% \text{ Primary Air} = \frac{\text{primary air (SCFH)}}{\text{secondary air (SCFH)} + \text{primary air (SCFH)}} \times 100$$

The wall temperature was 1330°C. Photographs illustrating flame geometry and luminosity with these and other operating conditions are shown in Figures 16 and 17.

For the baseline operating conditions, the in-the-flame data revealed a type I flow profile. The gas species and temperature data collected along the burner axis are presented in Figure 18. The high methane concentration (27.2%) and low flame temperature (825°C) at the burner block indicates a very flow rate of mass exchange between the fuel and combustion air. The NO concentration at the burner block exit is 17 ppm or only 6.4% of the flue concentration. Thus the major formation of NO (93.6%) occurs within the combustion chamber.

Figure 19 presents normalized nitrogen oxide (NO) versus excess oxygen (O_2) as a function of secondary air preheat for the baseline operating conditions. Measured CO levels greater than 500 ppm are listed by concentration next to their corresponding data point. These graphs show a linear relationship between the normalized NO and the excess oxygen. Straight line equations representing the dependence of normalized NO on excess oxygen for these and other operating conditions are presented in Table 2. This type of relationship in the range of excess oxygen being tested is characteristic of laminar diffusion flames. The rate of mixing between the fuel and combustion air helps determine the slope of the line. This linear relationship will break down at a stoichiometric fuel-air ratio, however extrapolating the test data to zero excess oxygen gives a normalized NO flue concentration referred to in this report as "stoichiometric." Although stoichiometric operation of industrial burners is not practical due to incomplete combustion and this calculated "stoichiometric" concentration is not exact, it does provide a basis for comparing the relative effectiveness of changes in burner and furnace

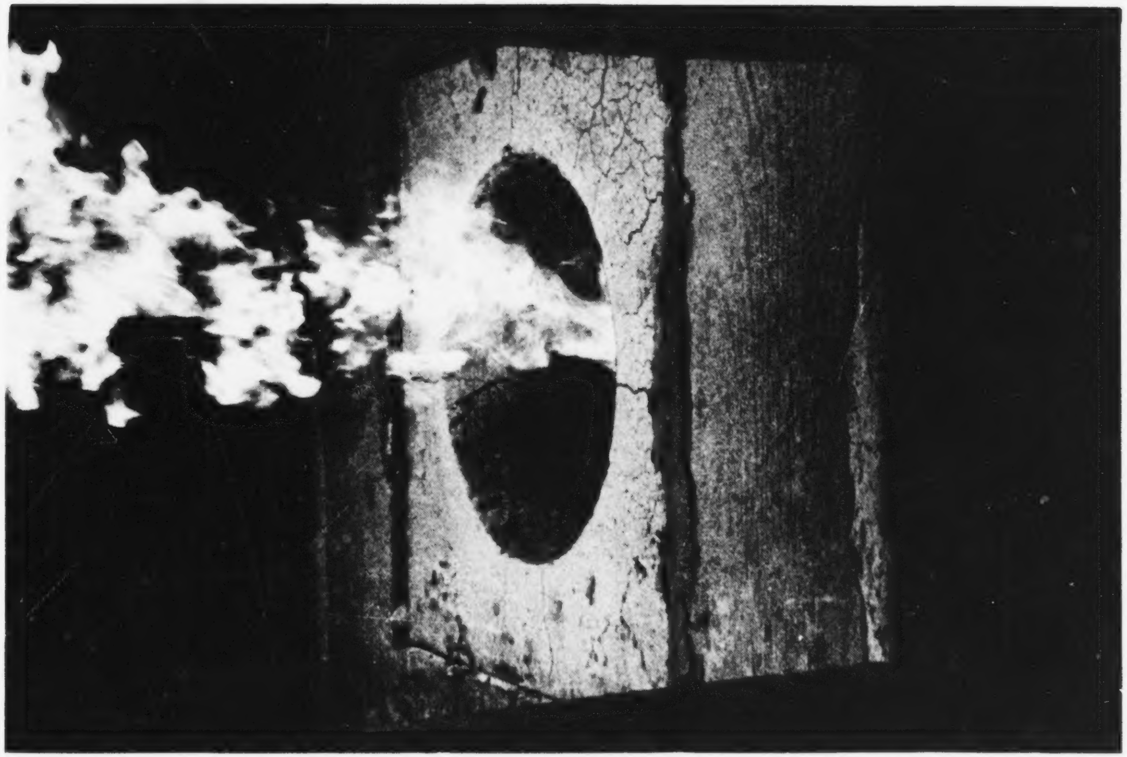

Figure 16. Flame geometry and luminosity of kiln burner

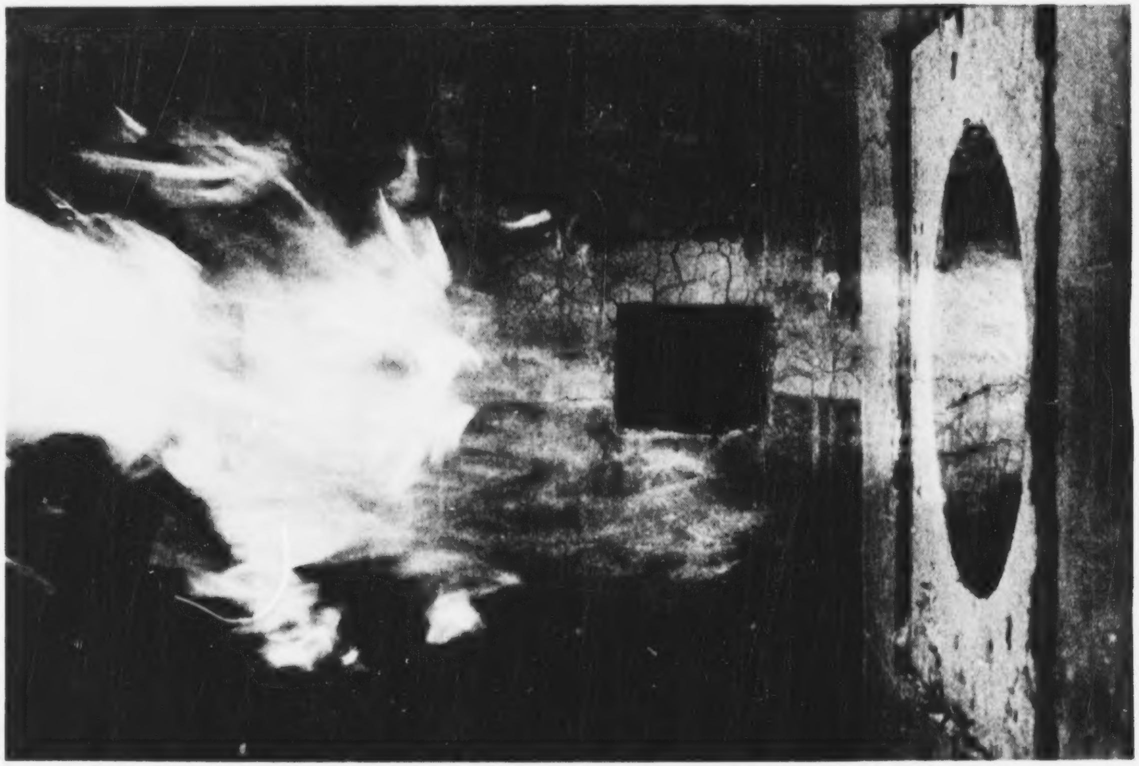

Figure 17. Flame geometry and luminosity typical of kiln burner

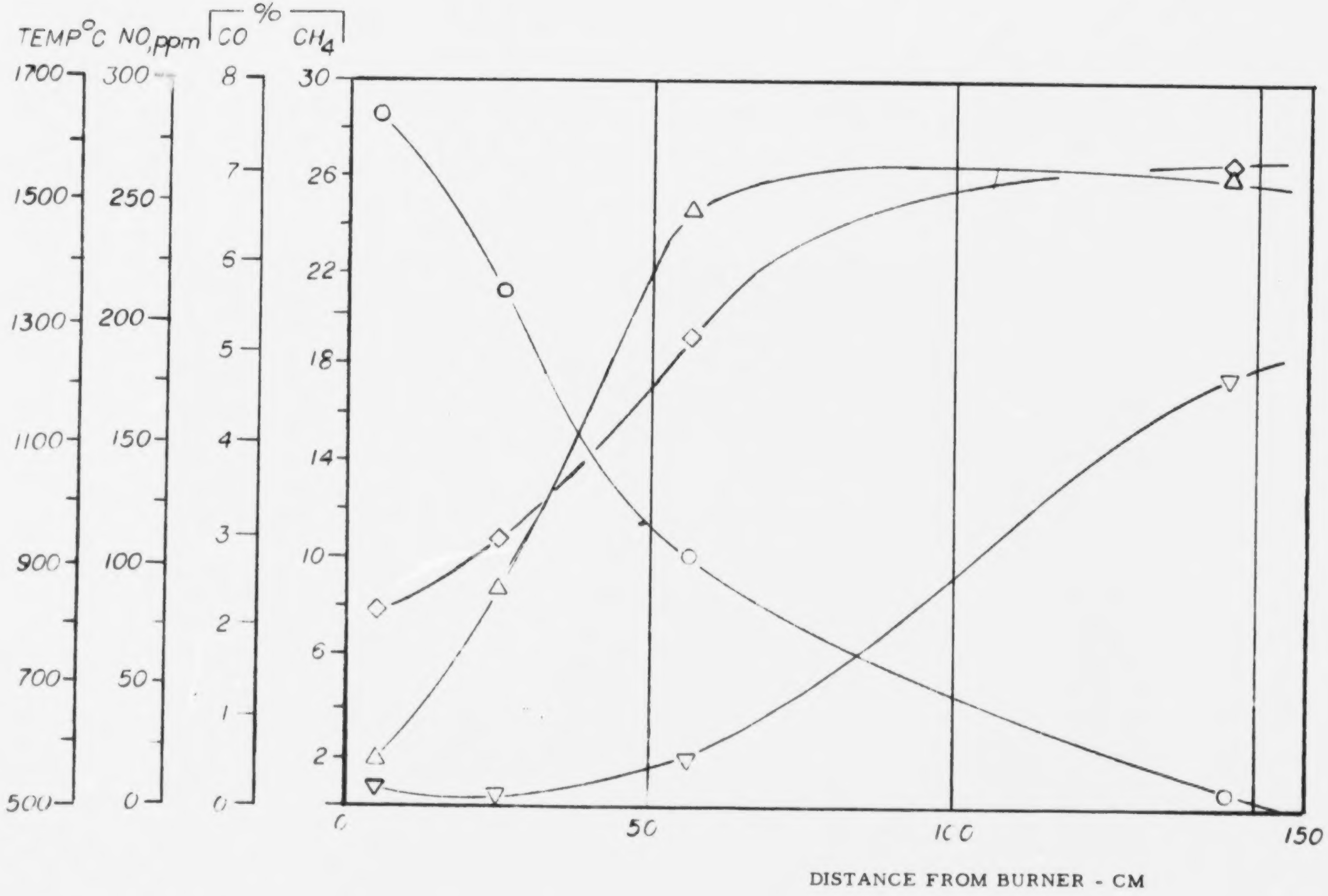

Figure 18. In-the-flame profiles of kiln burner using combination nozzle with 30% axial and 70% radial injection; 3.2% primary air

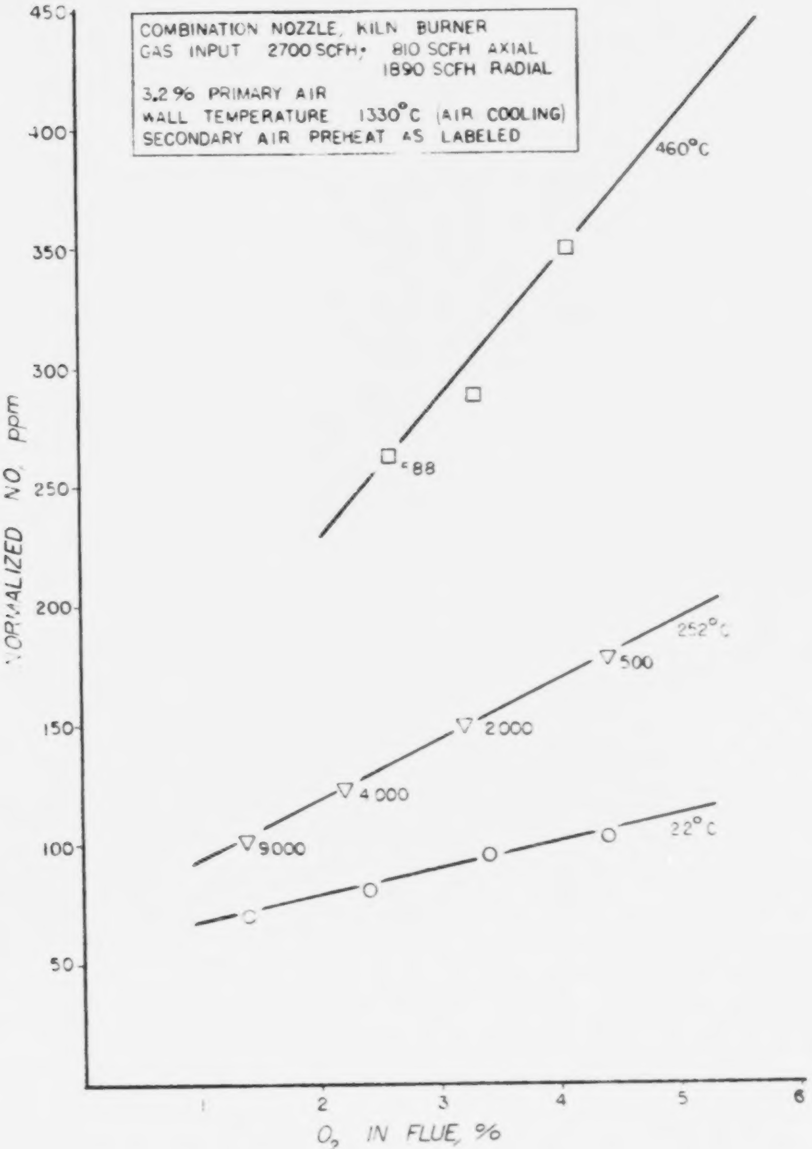

Figure 19. Normalized NO concentrations as a function of percent O_2 in the flue (excess air) for the combination nozzle kiln burner using 30% axial and 70% radial injection and 3.2% primary air

Table 2. LINEAR EQUATIONS FOR NO_x FORMATION AS A FUNCTION OF OXYGEN CONCENTRATION, X

*	Equation	Preheat Temperature, °C
19	$NO = 59X + 111$	460
	$NO = 25X + 68$	252
	$NO = 11.5X + 57$	22
21	$NO = 24.7X + 72$	463
	$NO = 7X + 24$	235
	$NO = 4.4X + 15$	22
22	$NO = 30.5X + 112$	465
	$NO = 13X + 55$	254
	$NO = 3X + 43$	22
23	$NO = 9.75X + 63$	460
	$NO = 3.5X + 36$	242
	$NO = 3.0X + 13$	22
24	$NO = 51.7X + 78$	438
	$NO = 17.7X + 52$	220
	$NO = 6.6X + 48$	22
25	$NO = 33.6X + 118$	466
	$NO = 24.1X + 53$	272
	$NO = 11.4X + 31$	22
27	$NO = 69.0X + 132$	445
	$NO = 23.4X + 65$	220
	$NO = 8.2X + 37$	22
28	$NO = 70.3X + 92$	457
	$NO = 32.8X + 75$	247
	$NO = 9.2X + 72$	22
29	$NO = 63.7X + 93$	466
	$NO = 19.4X + 67$	288
	$NO = 9.7X + 43$	22
30	$NO = 57.7X + 150$	457
	$NO = 27.8X + 53$	237
	$NO = 8.4X + 48$	22
31	$NO = 44.2X + 158$	447
	$NO = 26.6X + 53$	220
	$NO = 16.2X + 59$	22
32	$NO = 70.3X + 142$	459
	$NO = 21.8X + 71$	249
	$NO = 13.0X + 48$	22
33	$NO = 17.8X + 36$	456
	$NO = 6.9X + 23$	248
	$NO = 7.2X + 7$	22
34	$NO = 23X + 53$	460
	$NO = 13.4X + 43$	242
	$NO = 10X + 32$	22

Table 2, Cont. LINEAR EQUATIONS FOR NO_x FORMATION AS A FUNCTION OF OXYGEN CONCENTRATION, X

*	Equation	Preheat Temperature, °C
35	$NO = 31.0X + 303$	477
	$NO = 17.8X + 178$	243
	$NO = 14.5X + 60$	22
36	$NO = 23.6X + 63$	456
	$NO = 18.7X + 59$	250
	$NO = 8.7X + 41$	22
37	$NO = 17.0X + 58$	452
	$NO = 10.0X + 70$	244
	$NO = 6.4X + 50$	22

*Refers to corresponding Figure No. in this report.

X = Percentage oxygen (O_2) in the flue, %.

operating conditions controlling NO emissions. As an example, the "stoichiometric" concentration of normalized NO for baseline operating conditions at 460°C secondary air preheat is a factor of two larger than the concentration at ambient temperature. In addition, the normalized NO concentration increases at a rate five times greater for a 460°C secondary air temperature than for ambient temperature air.

EXTERNAL FLUE GAS RECIRCULATION (EFGR)

As a baseline control case, the effect of external flue gas recirculation was tested. The percentage of EFGR is determined using the relationship —

$$\%\ \text{EFGR} = \frac{\text{EFGR (SCFH)}}{\text{secondary air (SCFH)} + \text{primary air (SCFH)} + \text{fuel (SCFH)}} \times 100$$

Figure 20 illustrates in-the-flame data collected along the burner axis for baseline operating conditions with the addition of 13% EFGR to the secondary air. The temperature at the burner block exit is 1130°C or 305°C higher than the baseline temperature. This, in addition to the reduction in methane concentration from 28.6% for baseline conditions to 17.5% for 13% EFGR indicates that more of the total combustion was occurring within the burner block. The total combustibles have been reduced by 32% when the EFGR control flame at the burner block exit on the burner axis is compared to the baseline flame. The flame length is 106 cm or is 43% shorter than the baseline flame. The flow profile indicates that the flame is a type I. The NO concentration is 7 ppm or 5.8% of the flue concentration. This percentage of NO formation within the burner block is almost identical to the 6.4% measured for the baseline operating conditions. Thus in the furnace the EFGR flame has formed 113 ppm while the baseline flame produced 248 ppm. This factor of two suppression in NO concentration occurs due to lower flame temperatures produced by the EFGR dilution effect. The flue gas temperature for the EFGR flame is 1415°C compared with 1560°C for the baseline flame.

Figure 21 presents the NO concentrations measured as a function of excess oxygen and secondary preheat with the addition of 13% EFGR to the secondary air. During preheat both the flue gas and secondary air were blended and reached the same final preheat. The EFGR effect on "stoichiometric" NO was a reduction of approximately 40 ppm independent of secondary

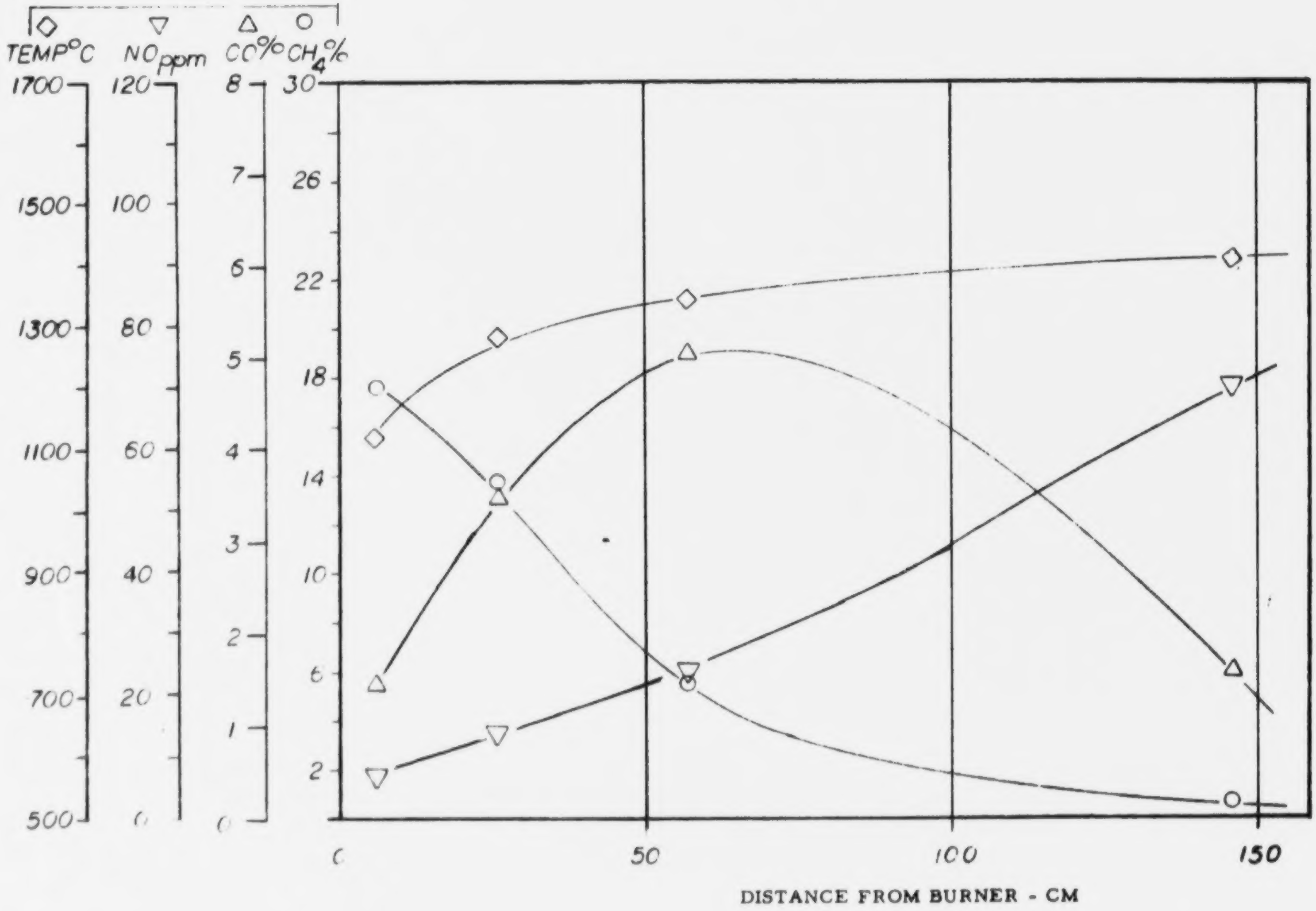

Figure 20. In-the-flame profiles for combination nozzle kiln burner with 30% axial and 70% radial injection, with 13% EFGR

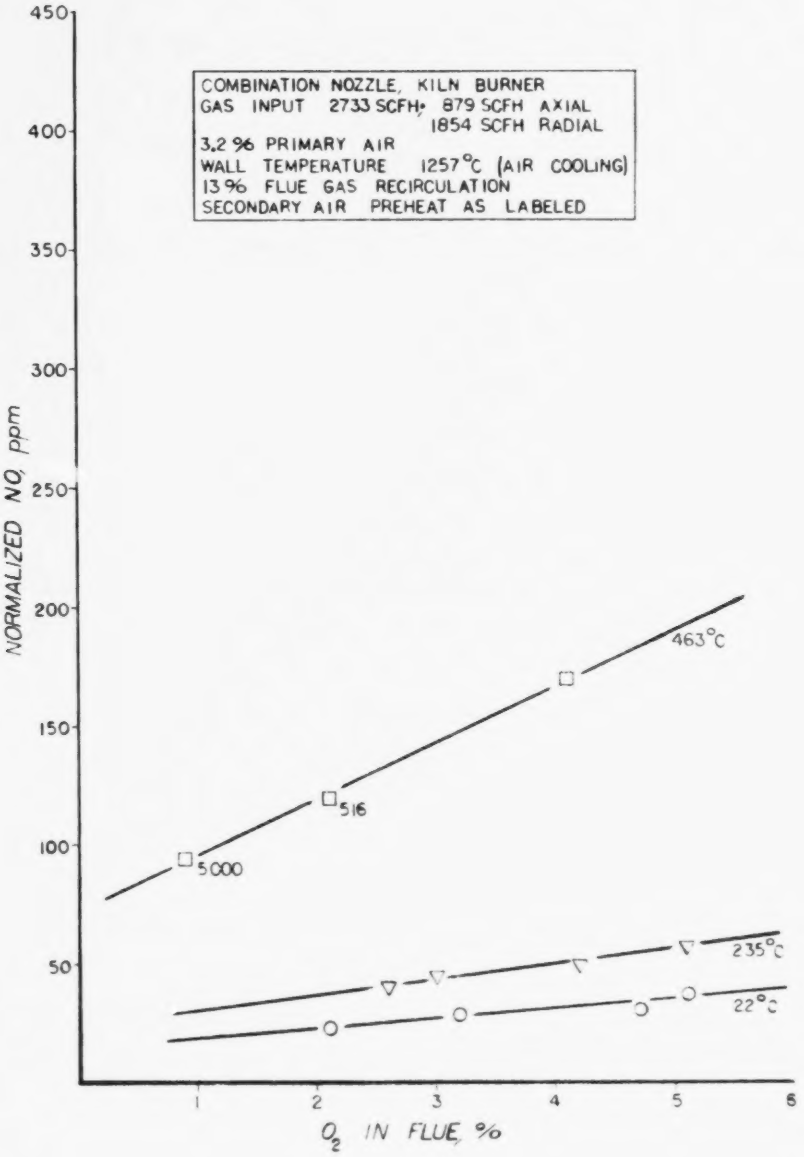

Figure 21. Normalized NO concentration as a function of O_2 in the flue (excess air) for combination nozzle kiln burner with 30% axial and 70% radial injection using EFGR (13%)

air preheat (Figure 19 vs Figure 21). Although there was a variation in the slope reduction as a function of preheat, the average reduction factor was 2.7 ± 0.4.

Comparing the baseline case (Figure 19) with the 13% EFGR curve (Figure 21) at 460°C shows a 52% reduction in the flue concentration of NO (at 3% O_2) as a result of 13% EFGR.

WALL TEMPERATURE

The data for Figure 22 were collected with the kiln burner operating in the baseline conditions with the exception of wall temperature. By water cooling tubes mounted in the furnace sidewalls, the temperature was decreased from 1330° to 1130°C. The flue concentrations of NO were decreased by approximately 30% (from the baseline case) due to the lower wall temperature at 3% excess oxygen.

Using the equations of Table 2 to compare NO emission levels from baseline operation to emissions with water-cooled walls reveals a 43% reduction using ambient temperature combustion air. While the intermediate (254°C) and high (465°C) preheat levels of combustion air resulted in respective reductions in NO emissions of 34% and 30%.

Combining the NO reduction techniques of EFGR and water cooling of the furnace sidewalls results in the emission curves plotted in Figure 23. This combined control technique results in "stoichiometric" reduction of 43% for the 460°C preheat temperature and a 77% reduction for ambient air temperature. Likewise, the magnitude of the slopes are reduced by approximately 80%. Translated directly into concentration reduction at the 3% excess oxygen level with a 460°C preheat, the combination control techniques resulted in an emission level of 92 ppm compared to 288 ppm for baseline operating conditions. This represents a 67% reduction in normalized flue NO concentrations.

PRIMARY AIR

To test the effect of primary air on the flue NO concentrations the primary air was roughly increased by a factor of 2, from 3.2% to 6%. The data for 6% primary air are presented in Figure 24 for air cooling of the furnace sidewalls and Figure 25 for water sidewall cooling.

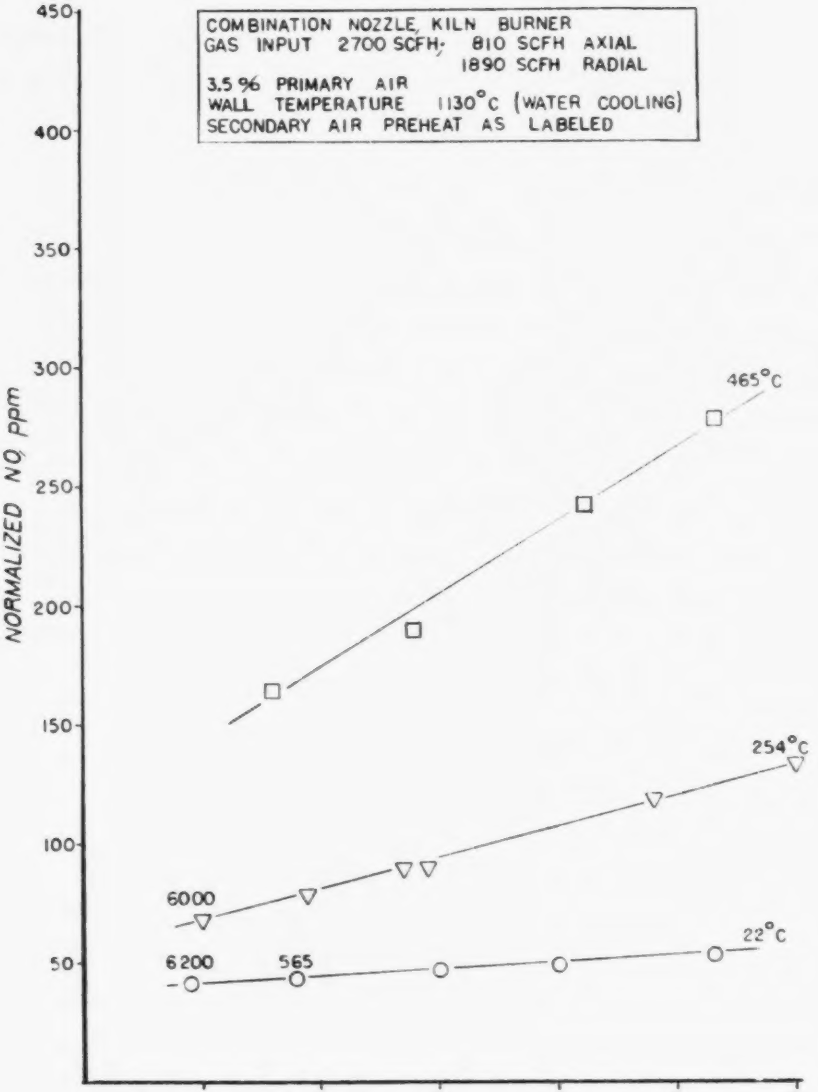

Figure 22. Normalized NO concentration as a function of O_2 in the flue (excess air) for the combination nozzle kiln burner with 30% axial and 70% radial injection with a 1130°C wall temperature

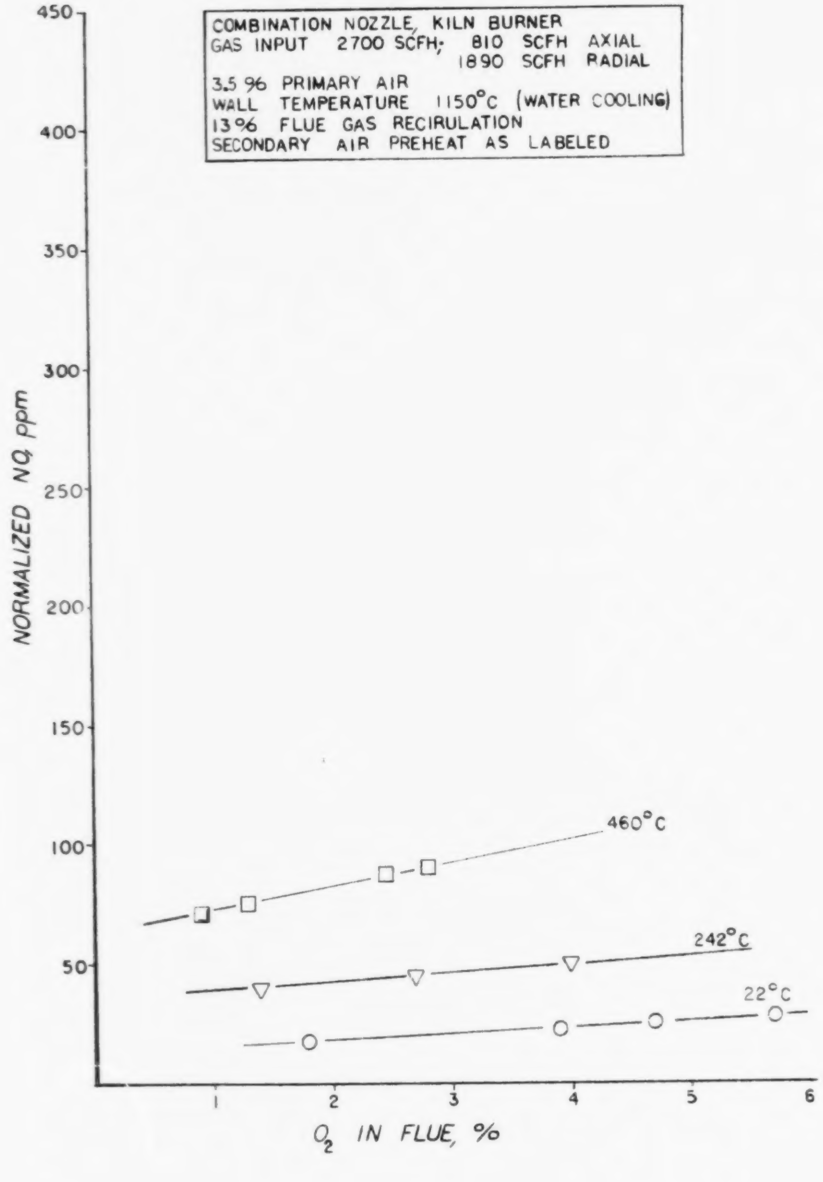

Figure 23. Normalized NO concentration as a function of O_2 in the flue (excess air) for the combination nozzle kiln burner with 30% axial and 70% radial injection using 13% EFGR with a reduced wall temperature, 1150°C

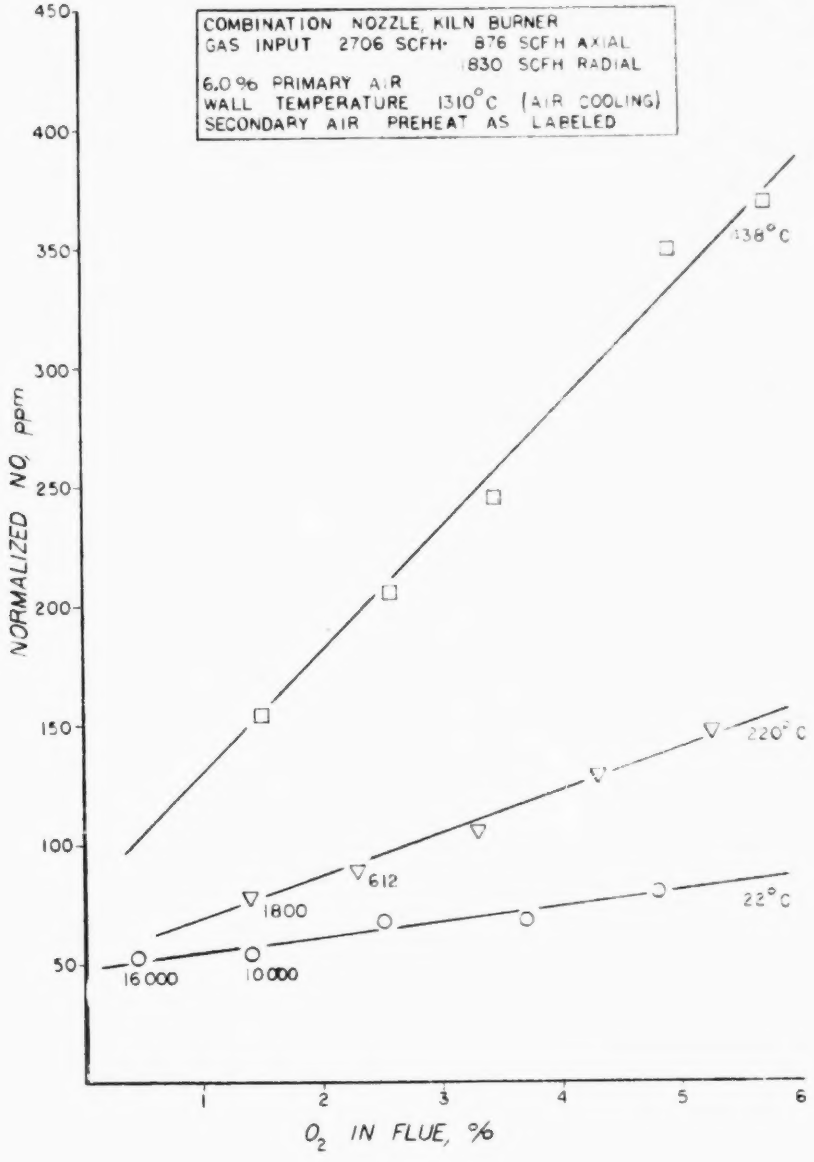

Figure 24. Normalized NO concentration as a function of O_2 in the flue for combination nozzle kiln burner with 30% axial-70% radial injection with 6% primary air and a 1310°C wall temperature

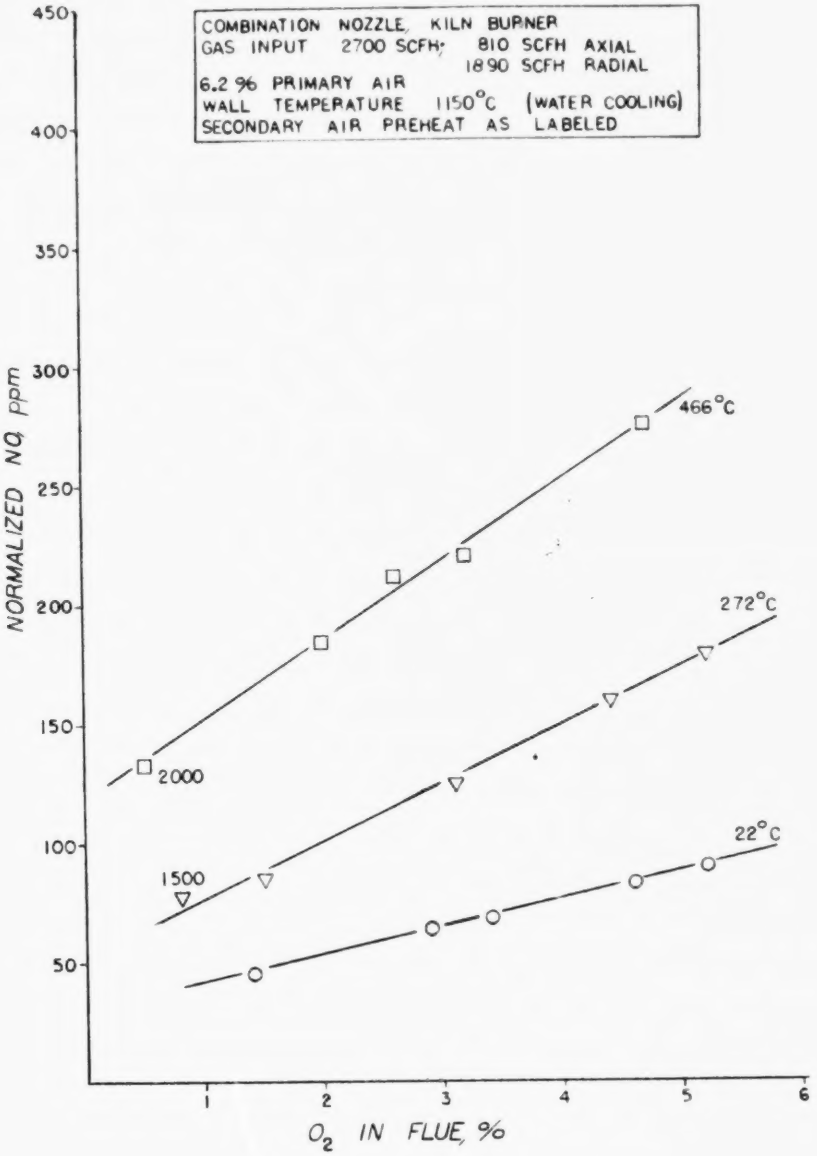

Figure 25. Normalized NO concentration as a function of O_2 in the flue for combination nozzle kiln burner with 30% axial and 70% radial injection with 6% primary air and a 1150°C wall temperature

A comparison of these data and baseline data at 3% excess oxygen are made in Figure 26. Wall temperature has little effect on NO emission levels with 6% primary air until the secondary combustion air temperature exceeds 200°C. The lower wall temperature then results in a gradual reduction in the NO emission level which reaches 17% at a secondary air preheat temperature of 470°C. Increasing the primary air percentage from 3.2% (baseline operation) to 6% while maintaining a 1330°C wall temperature results in a 9% reduction in NO emissions at a 470°C secondary air preheat temperature which gradually increases with decreasing secondary air preheat temperature until it reaches a maximum of 18% at ambient operation.

NOZZLE POSITION

Figure 27 presents NO concentrations measured under baseline conditions, but with the gas nozzle in the exit position (refer to Figure 1). For an excess oxygen level of 3%, the NO concentrations arising from baseline operation are similar to those with the nozzle in the exit position at combustion preheat temperatures below about 220°C. The deviation between the measured NO concentrations then begin to increase as a function of combustion air temperature until at about 450°C the nozzle in the exit position produced 27% more NO than the baseline conditions. This could result from the combustion air scrubbing additional heat off the walls of the furnace. For the lower secondary air preheats, this additional temperature increase is compensated by entrainment of secondary recirculation products. For the higher secondary air preheats, the additional temperature is sufficient to aid in raising the average flame temperature and increasing NO concentrations. Although this behavior is only exhibited by the kiln burner, the input-output nozzle position data plus the in-the-flame data presented earlier indicate that there is an optimum flame length or distance for fuel burn-out producing minimum NO emission levels.

AXIAL/RADIAL RATIOS

To determine the dependence of NO formation on the direction of gas injection and combustion intensity within the burner block, the ratio of axial to total fuel injection volumes was decreased from the 30% used in the baseline measurements to 14% and 0%. Ratios above 30% were not studied because of excessive flame length. Due to the slow fuel-air mixing rate, the flame for ratios above 30% extended into the furnace flue.

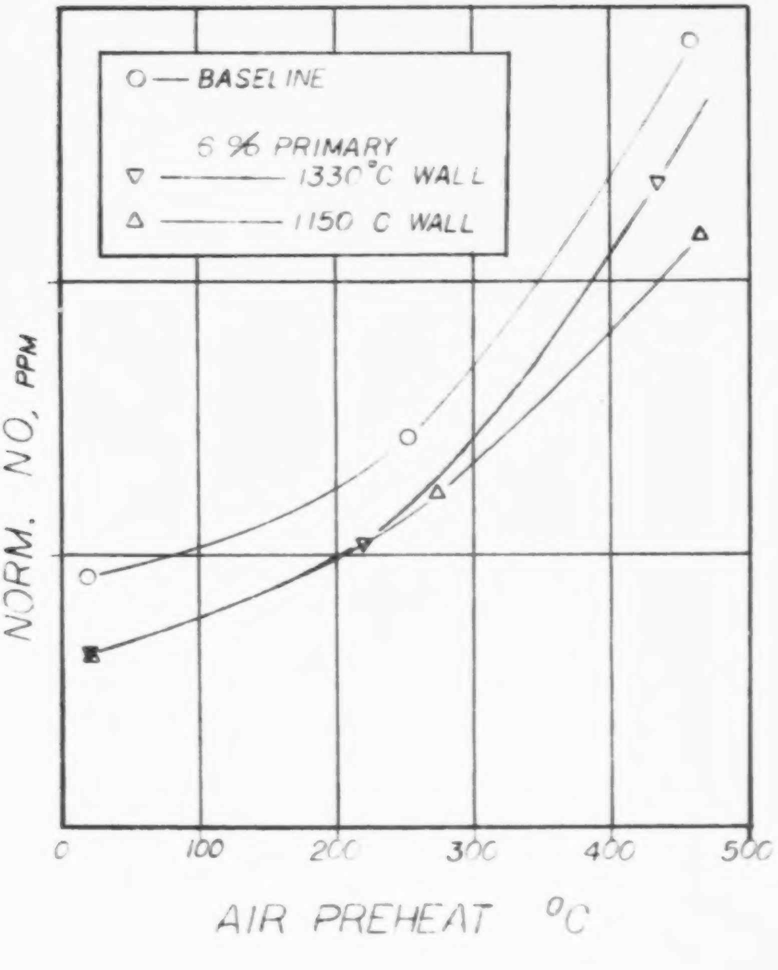

Figure 26. Comparison of NO formation for 6% and 3% primary air on the combination nozzle kiln burner using 30% axial and 70% radial injection

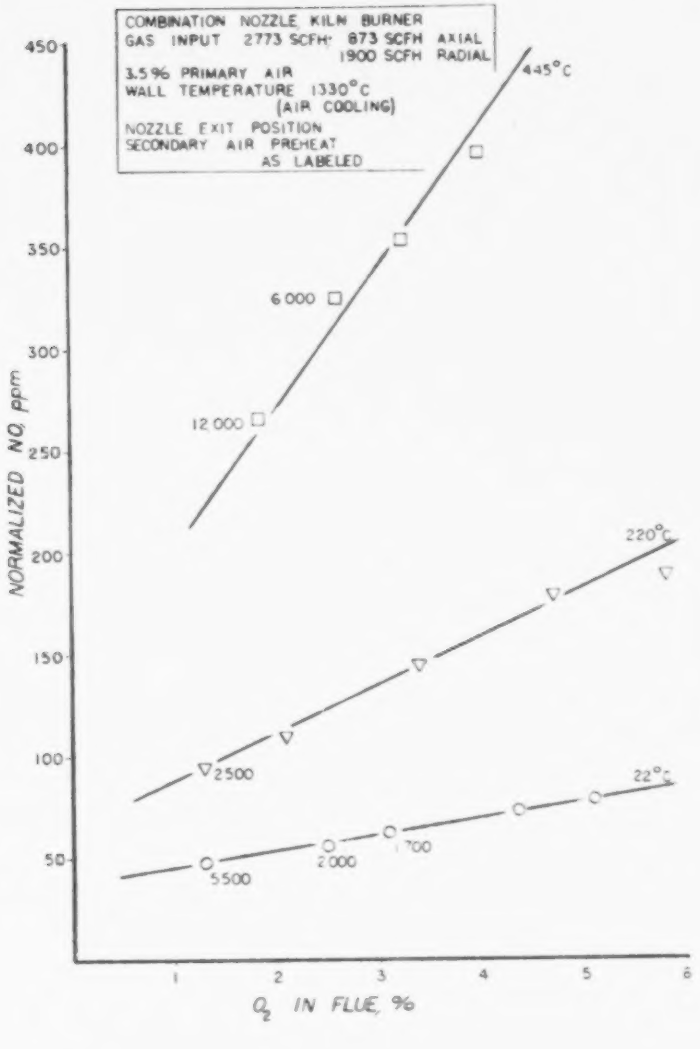

Figure 27. Normalized NO concentration as a function of O_2 in the flue (excess air) for the combination nozzle kiln burner with the nozzle in the exit position using 3.5% primary air and 30% axial-70% radial injection

Data collected for 14% axial to total fuel input are illustrated in Figures 28 through 30. Figure 28 shows operating conditions similar to baseline conditions with the exception of the 14% fuel injection ratio. The larger radial volume gas input resulted in higher levels of NO emissions. This is due to higher combustion intensity within the burner block producing higher flame temperatures. Comparing the baseline case (Figure 19) with the 14% axial gas input (Figure 28), straight line equations reveal that an increase in slope as well as "stoichiometric" NO occurs only for the intermediate preheat level. At 3% excess oxygen, this is reflected as a 22% increase in NO emissions compared with 9% and 5% increases at ambient and 460°C secondary air temperatures, respectively.

Increasing the primary air from 3.5% to 6.6% of the total air input resulted in the NO emissions presented in Figure 29. The increased volume of primary air brought the emission levels back in line with those measured for baseline conditions.

Figure 30 illustrates the NO concentrations measured as a function of excess oxygen for the 14% by volume gas axial input with the nozzle in the exit position. The exit nozzle position provides for a reduction in the flue concentration measured for 3% excess oxygen and air preheat levels up to about 380°C. The reduction at 250°C was approximately 25% with a resulting concentration of 132 ppm. Above 380°C, the exit nozzle position leads to increased concentrations of NO with a level of 325 ppm, or a 7% increase above the baseline conditions at a 460°C secondary air preheat. The explanation for the increase in NO emissions is due to the "scrubbing" heat transfer to the combustion air postulated earlier in the nozzle position section.

Figure 31 shows the data for total radial gas injection. In general, the NO concentrations measured were less than those with 14% axial injection. Compared with the baseline operating conditions, with no preheat, the total radial gas injection results in 18% higher emission at a level of 108 ppm; however, for preheats above 125°C, the total radial injection produces slightly lower (~5 ppm) levels of emissions. Data were collected for NO flue concentrations as a function of excess oxygen, with total radial injection and the nozzle in the exit position. These results are illustrated in Figure 32.

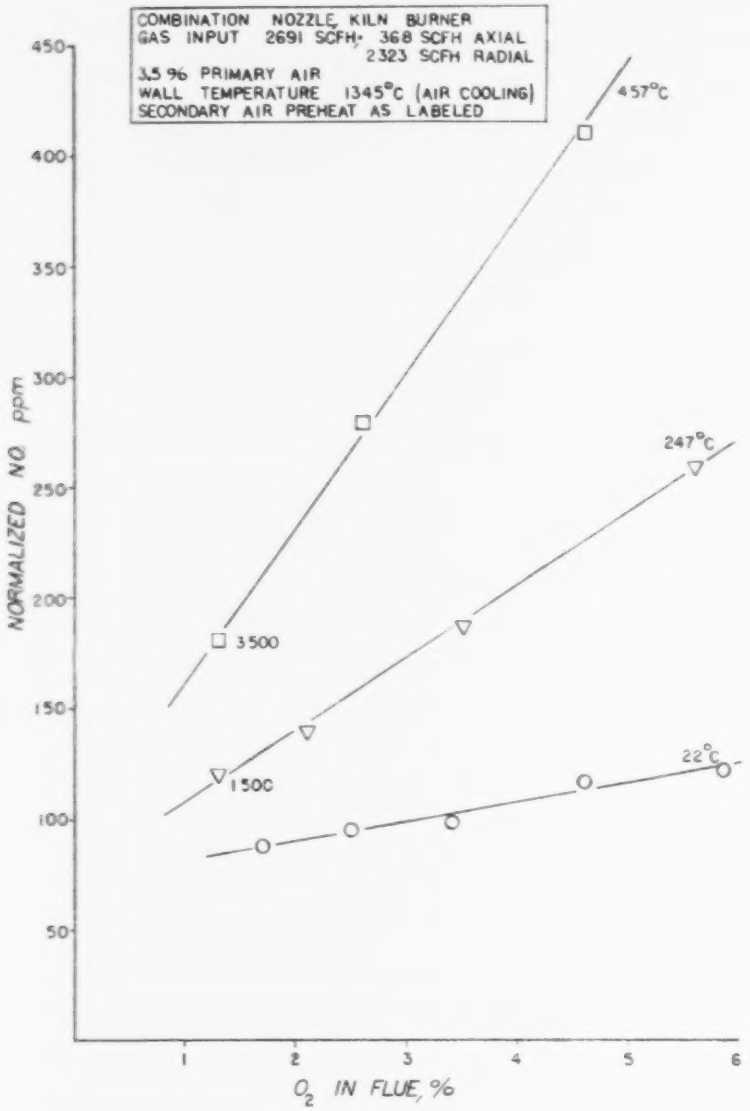

Figure 28. Normalized NO concentration as a function of O_2 in the flue (excess air) for the combination nozzle kiln burner using 14% axial and 86% radial injection, 3.5% primary air and 1345°C walls

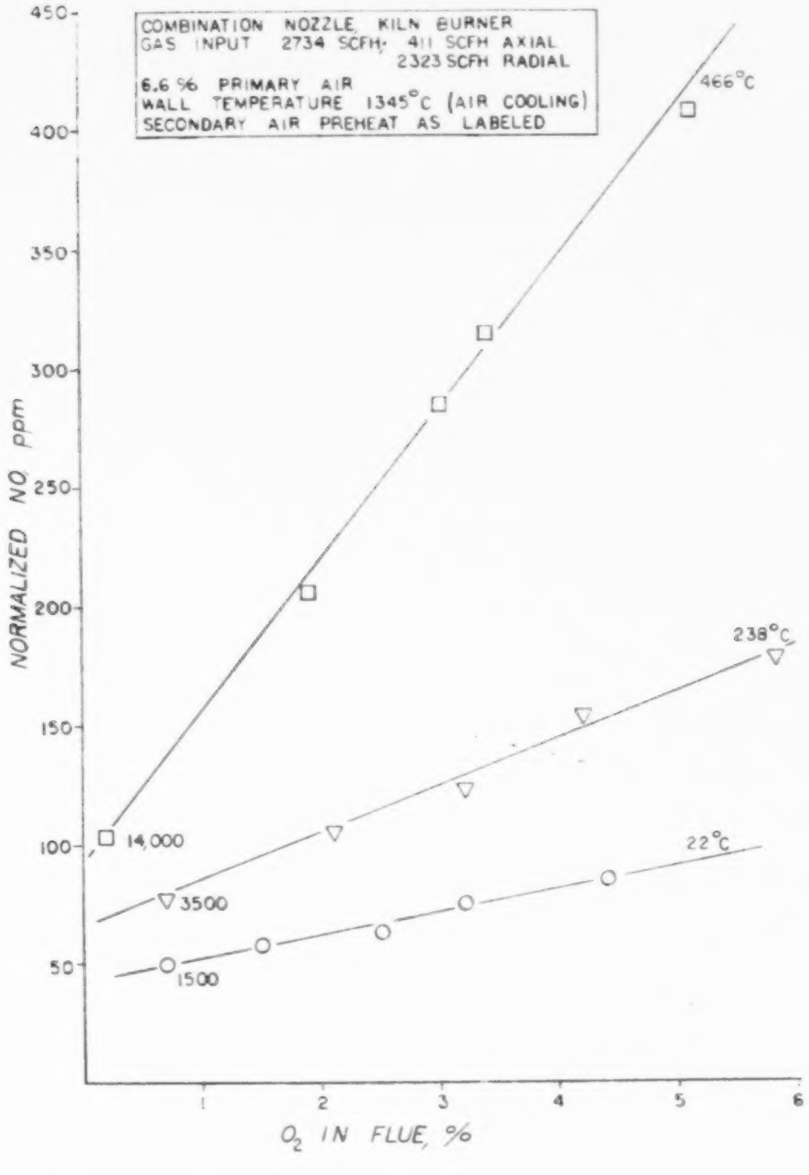

Figure 29. Normalized NO concentration as a function of O_2 in the flue (excess air) for combination nozzle kiln burner using 6.6% primary air; 14% axial-86% radial injection and 1345°C walls

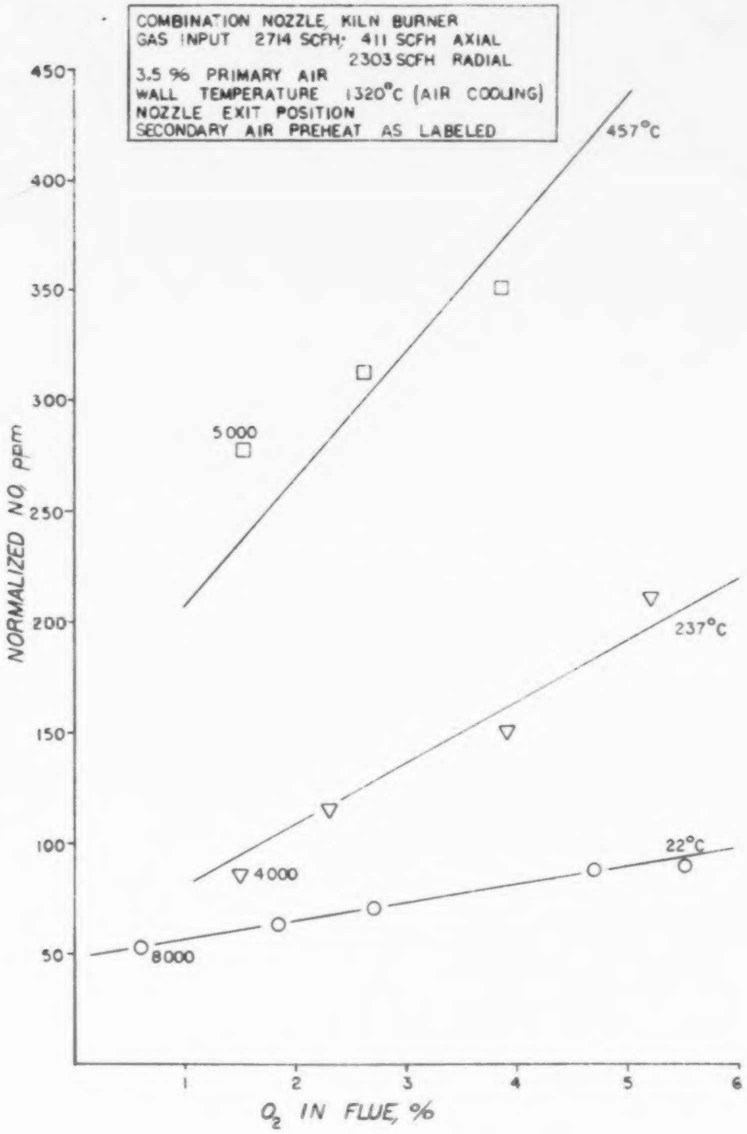

Figure 30. Normalized NO concentration as a function of O_2 in the flue (excess air) for the combination nozzle kiln burner using 3.5% primary air; 14% axial-86% radial injection and 1320°C walls; with nozzle in exit position

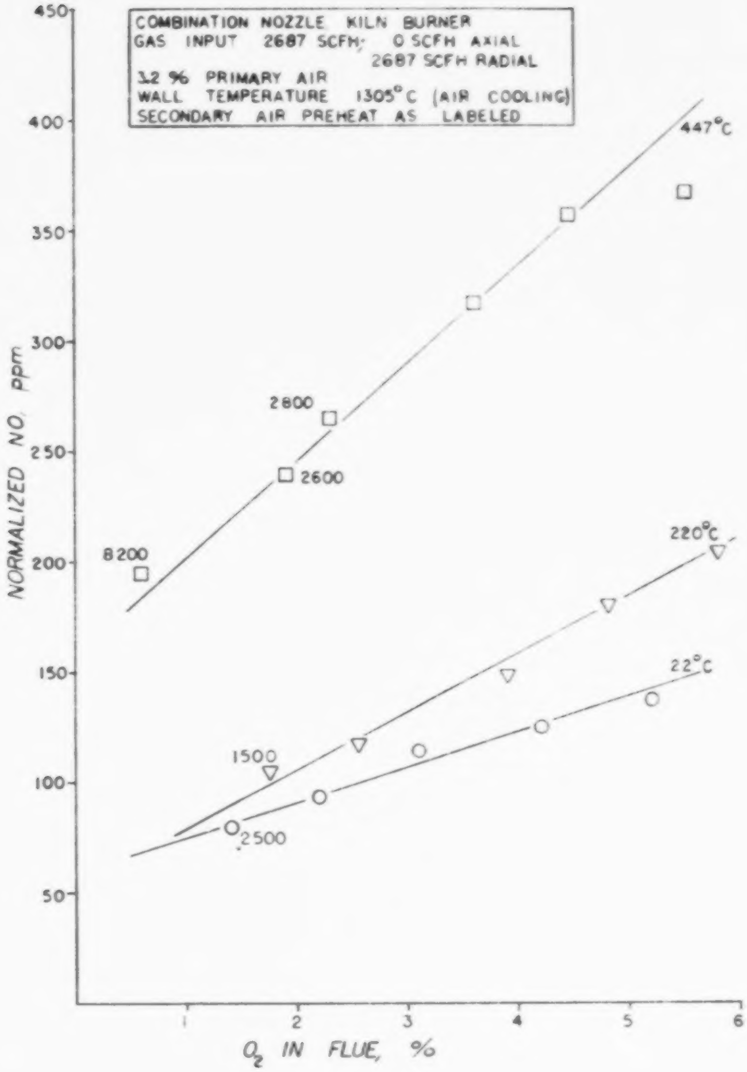

Figure 31. Normalized NO concentration as a function of O_2 in the flue (excess air) for the combination nozzle kiln burner using 3.2% primary air and 0.0% axial gas injection

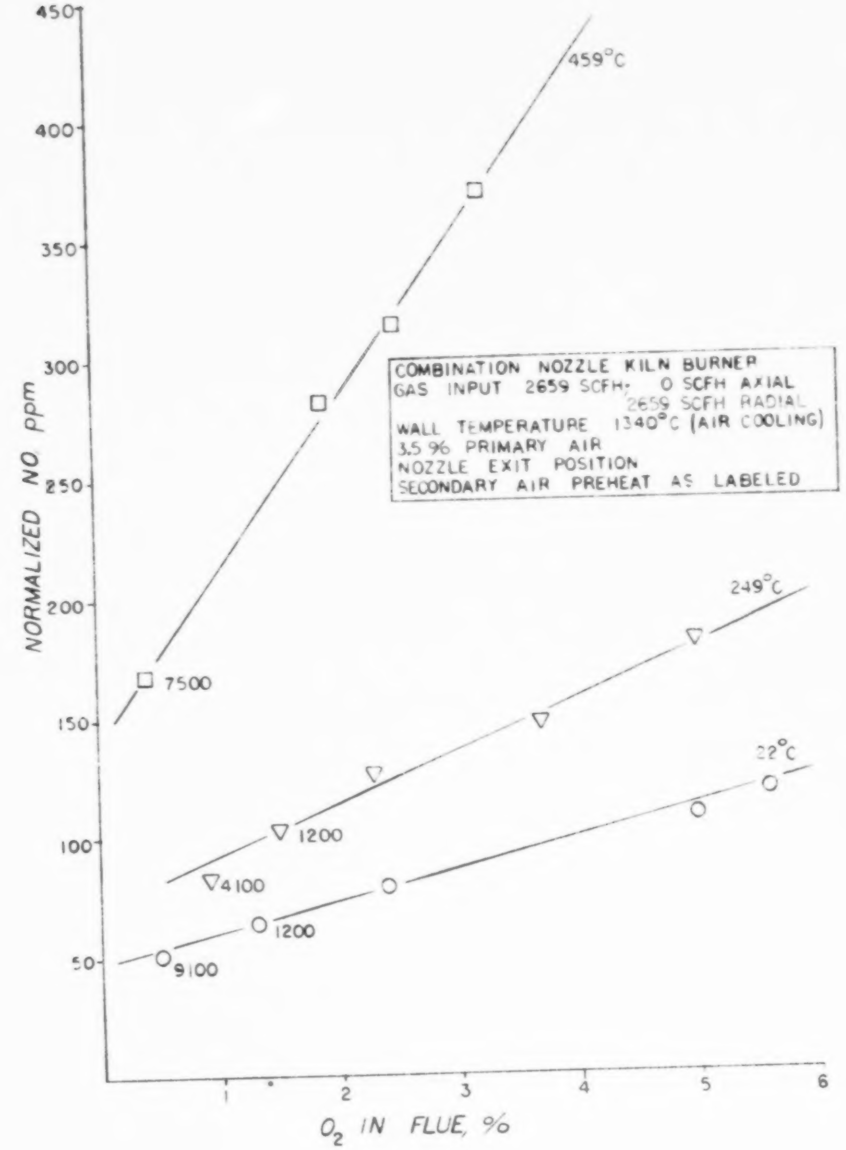

Figure 32. Normalized NO concentration as a function of O_2 in the flue (excess air) for combination nozzle kiln burner in the exit position and using 0.0% axial gas injection

Similar results to those previously presented were found. At no preheat the levels were about 90 ppm with a 5% reduction when compared with baseline operation and a 19% reduction when compared with radial injection in the normal position. At the intermediate preheat (~250°C) level, baseline operating conditions, total radial injection, and total radial injection in the exit position produce approximately the same levels of concentration (~135 ppm). At high preheat (~450°C), the NO concentration of 350 ppm was 21% higher than concentrations measured for the normal nozzle position or baseline operating conditions.

REDUCED FIRING RATE

Figure 33 shows data gathered with the gas input reduced to 1900 SCFH and 30% axial gas volume injection. To stabilize the flame, the primary air had to be increased to 6.2%. As a result of sidewall water cooling, the average wall temperature decreased to 1023°C. For the 460°C preheat, the "stoichiometric" NO concentration was less (by approximately a factor of 2) than that measured for the 2700 SCFH gas input, 1150°C wall temperature, and 13% EFGR. The slope of the line for the 1900 SCFH is only 72% that for 2700 SCFH and EFGR. Consequently, lower emissions are achieved for a kiln burner operating in a turndown condition than is achieved with a higher gas input and EFGR. For intermediate and no preheat, the emission levels are equivalent for the two operating conditions.

For a gas volume input of 1800 SCFH with only a radial component, the NO emission levels as a function of excess air are shown in Figure 34. The slopes of the NO concentration lines for the 1800 SCFH input was one-half the slope for the 2700 SCFH input baseline conditions at elevated secondary air temperature. The ratio of "stoichiometric" NO concentration as a function of secondary air temperature varied from a low of 1.23 for 245°C to 1.84 for 22°C and 2.98 for 460°C with all temperature cases having the largest NO levels for the 2700 SCFH firing rate. Thus, a reduction in firing rate to 70% of the total input resulted in a 58% reduction in NO emissions or a level of 122 ppm for 3% excess oxygen and a 460°C secondary air temperature.

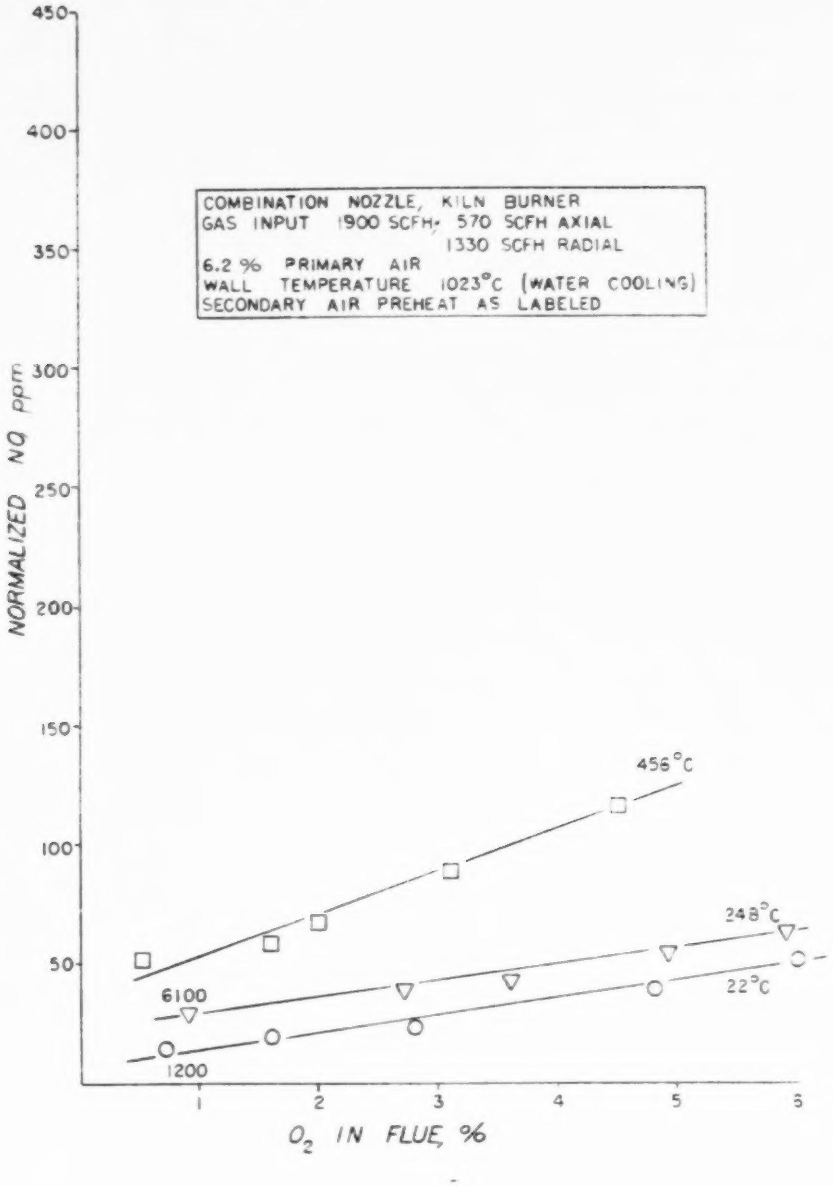

Figure 33. Normalized NO concentration as a function of O_2 in the flue (excess air) for the combination nozzle kiln burner with reduced gas input (1900 CFH) and 30% axial gas injection

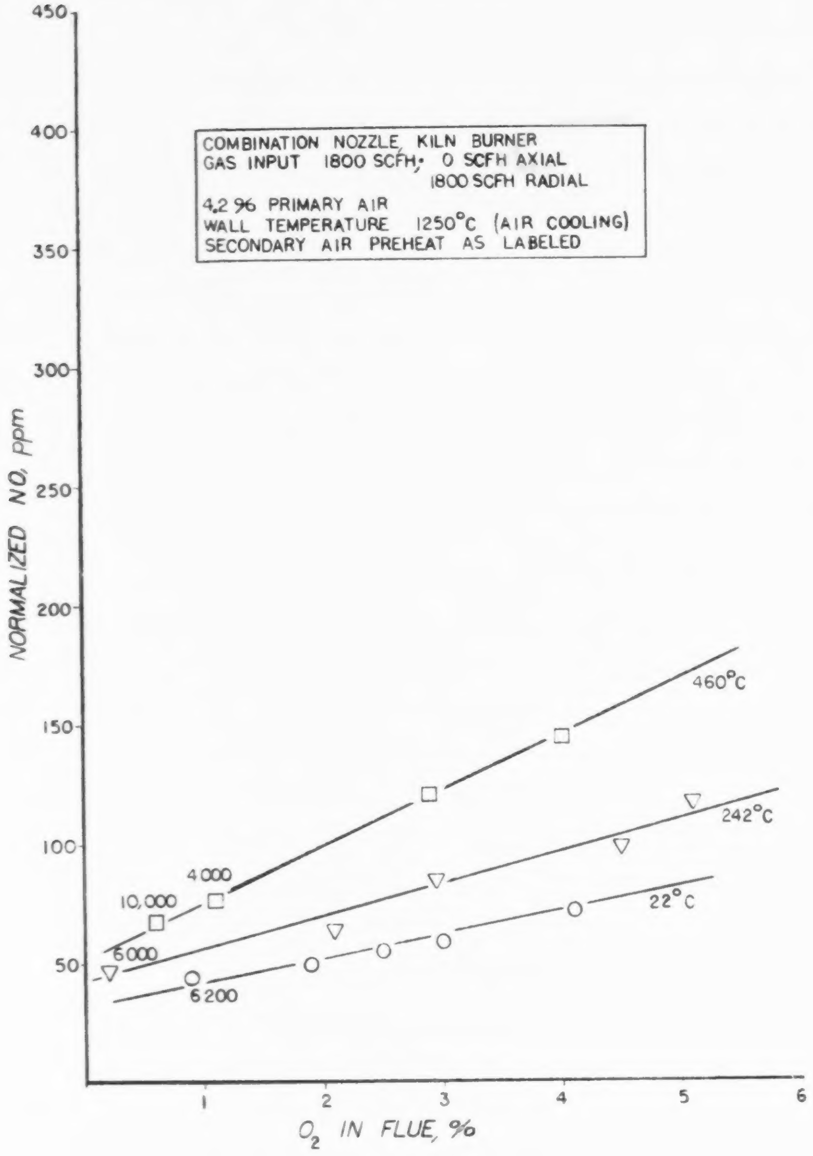

Figure 34. Normalized NO concentration as a function of O_2 in the flue (excess air) for the combination nozzle kiln burner fired with 1800 SCFH of gas and 0.0% axial injection

Since the operating conditions for the data in Figure 34 were similar to the baseline conditions (except for the 30% axial injection), a comparison of Figures 19 and 34 may yield a rough approximate of the total NO concentration from combustion of axially injected gas and an approximation of the contribution from the radially injected gas.

A comparison of "stoichiometric" NO concentrations would indicate half of the NO concentration was due to axial gas injection at high preheat (~460°C), 37% at 250°C and 44% at ambient. At ambient the major contribution is radially with the slopes being approximately identical only the stoichiometric difference of 25 ppm separates the 2700 SCFH, 30% axial fuel injection from the 1800 total radial injection. However, at elevated temperatures, the axially gas contribution increases significantly such that at 3% excess oxygen for a 250°C secondary air preheat 42% of the total NO could have its origin from the axial gas and for 460°C 58%. Some of the contribution could arise from effective additional secondary air preheat due to scrubbing of heat off the furnace walls, resulting in a higher flame temperature.

DIVERGENT FUEL NOZZLE

After the conbination nozzle trials were completed, the kiln burner was modified to accept the divergent gas nozzle (Figure 2) which permitted injection of the gas at an approximate 45-degree angle relative to the burner axis. This would simulate a fuel velocity vector similar to the combination nozzle when operated with 50% of the total fuel volume being injected radially and 50% axially. The advantage that the divergent nozzle has is that it projects all the gas out into the furnace for combustion rather than having a large radial portion burned within the burner block. The nozzle is able to maintain a flame length suitable for the pilot test furnace.

Figure 35 presents NO emissions data versus excess oxygen for baseline operating conditions with the divergent nozzle. At ambient temperature secondary air, the 30% axial injection with the combination nozzle and the divergent nozzle have nearly identical emission characteristics. At the intermediate and high secondary air preheat temperatures (250°C and 460°C, respectively) the NO slope lines for the divergent nozzle are about half those for the 30% axial combination nozzle. However, the significant factor is that the "stoichiometric" NO concentration for the divergent nozzle is

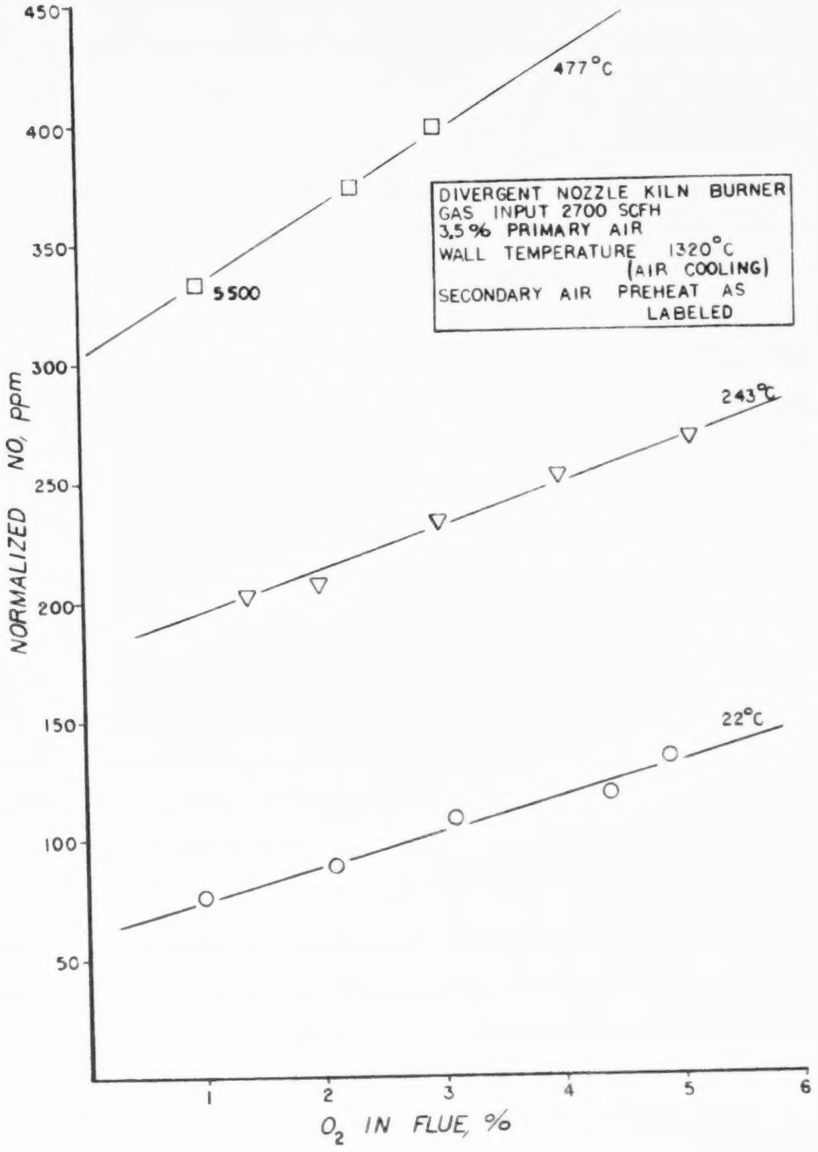

Figure 35. Normalized NO concentration as a function of O_2 in the flue (excess air) for the divergent nozzle kiln burner using 3.5% primary air; 2700 SCFH gas input and 1320°C walls

three times that of the 30% axial combination nozzle or 303 ppm compared with 111 ppm. Thus, at 3% excess oxygen, with a 460°C secondary air preheat, the NO emission level for the divergent nozzle is 396 ppm, while for the 30% axial combination nozzle it is 288 ppm. Consequently, it is again demonstrated that projecting the flame too far into the furnace, and delaying burnout beyond an optimum point, is an open invitation to increased levels of NO emissions.

To test the secondary air preheat scrubbing theory, the above tests were rerun with the walls water-cooled (Figure 36). This resulted in a sidewall temperature of 1145°C compared to that in the previous trials of 1320°C. The biggest significant factor was the reduction in the "stoichiometric" NO concentrations from baseline conditions. For the 460°C preheat there was a 79% reduction to 63 ppm; for the 250°C preheat a reduction of 67%, to a concentration of 59 ppm was observed; and for ambient temperature, a 41 ppm NO level was determined representing a 32% reduction. Comparing the data of Figure 36 to the baseline operating data with the 30% axial combination nozzle shown in Figure 35 indicates that for 460°C preheat and a 3% level of excess oxygen there is a 54% reduction in the NO to a level of 134 ppm by using the divergent nozzle with the 1145°C wall temperature.

Thus, if the furnace is maintained below a certain critical temperature, projecting the flame into the furnace has the desired effect. The combustion is delayed and products of combustion mix with the fuel and air, localized combustion intensity is reduced which both help to reduce peak flame temperatures and lower NO.

As a final reduction measure, the water cooling of the sidewalls was maintained but the primary air percentage of the total combustion air was increased to 9.5%. This increase in primary air should result in a larger volume of cold air (primary air not being preheated) available for combustion and consequently result in shielding and delaying the mixing of the preheated secondary air with the fuel. The trial results are presented in Figure 37. The "stoichiometric" NO concentrations, although slightly higher (~5 ppm), show no significant change with the additional primary air. The slopes of the NO concentration lines have decreased by about 25%. Thus, the divergent

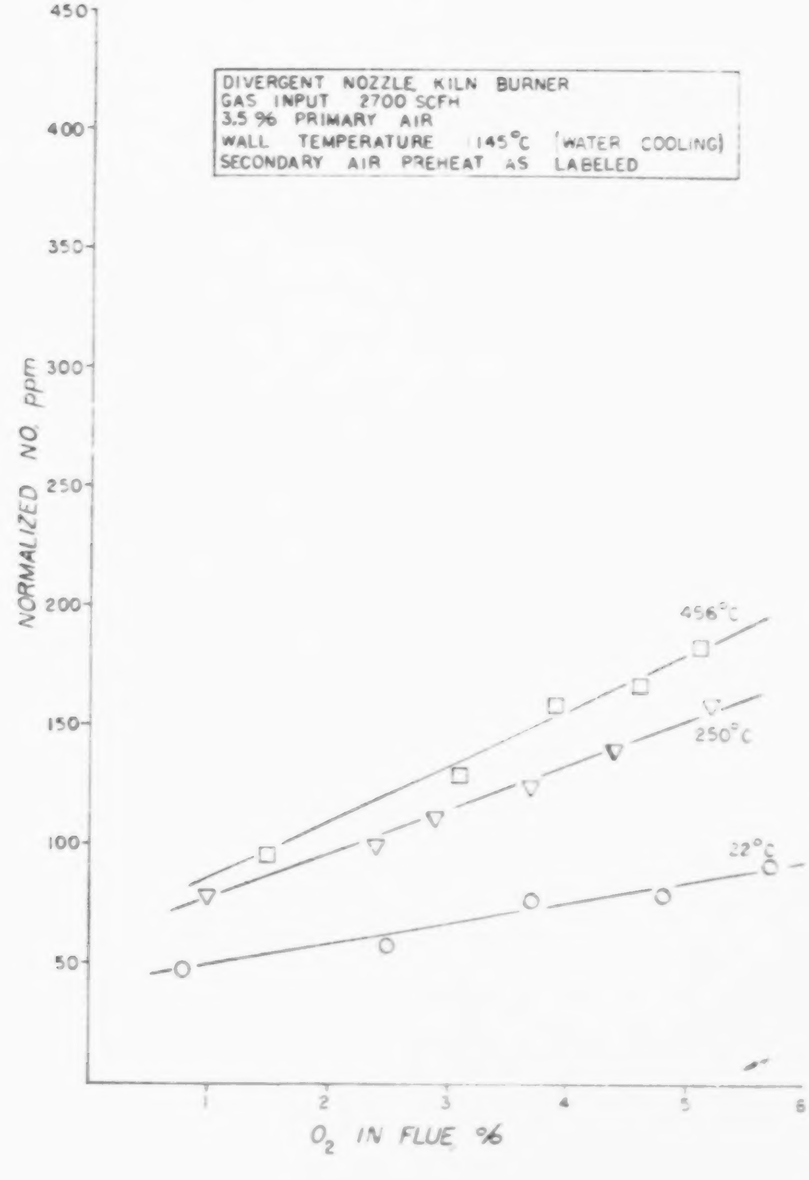

Figure 36. Normalized NO concentration as a function of O_2 in the flue (excess air) for the divergent nozzle kiln burner using 3.5% primary air; 2700 SCFH gas and (cooled) 1145°C walls

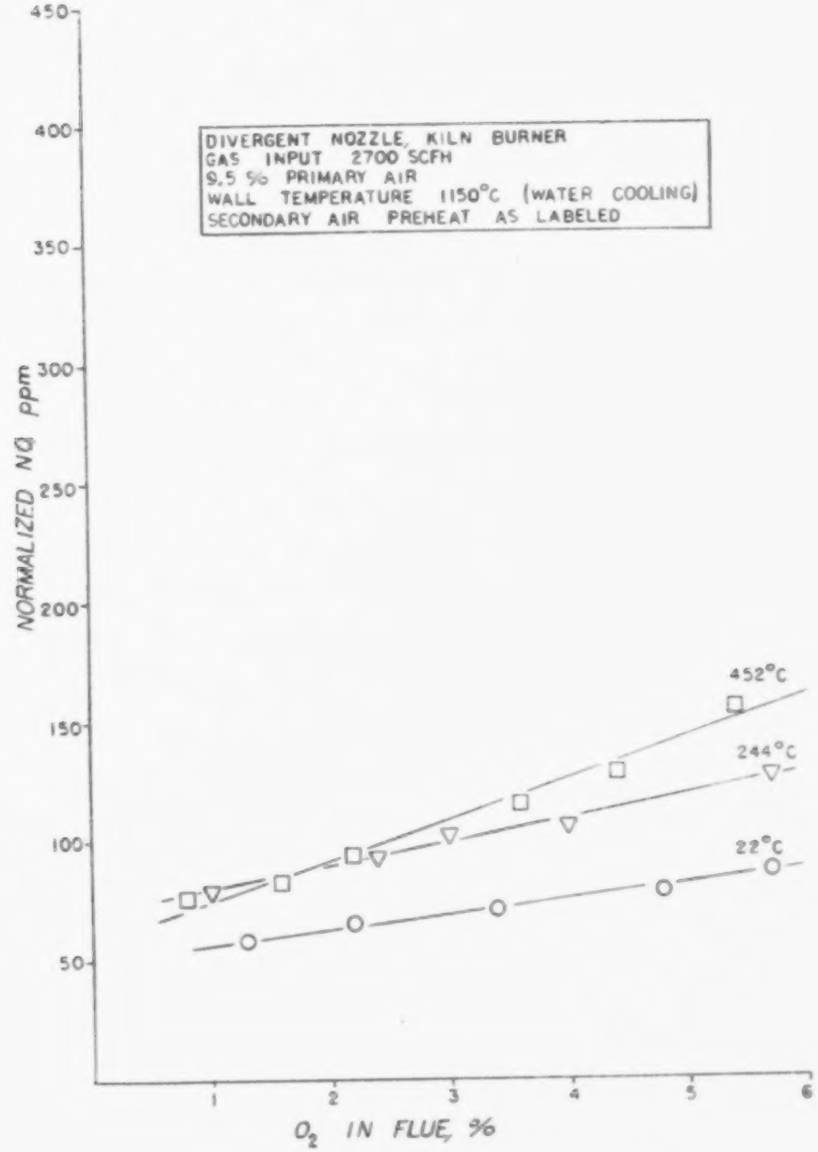

Figure 37. Normalized NO concentration as a function of O_2 in the flue (excess air) for the divergent nozzle kiln burner operated with (cooled) 1150°C walls and 9.5% primary air

nozzle with water wall cooling and 9.5% primary air has an NO emission level of 109 ppm for 3% excess oxygen and 460°C secondary air preheat or a 62% reduction when compared to baseline operating conditions.

SUMMARY OF KILN BURNER RESULTS

A synopsis of the operational variables studied for the kiln burner and their test results is presented in Table 3. The technique producing the most dramatic reductions in NO emission levels was wall temperature, which for the divergent nozzle resulted in a 66% decrease in the flue concentration. With hot furnace walls, external flue gas recirculation produced the largest reductions in NO with a 49% decrease. The use of combustion aerodynamics to recirculate combustion products to the base of the flame (internal flue gas recirculation) is difficult with the kiln burner since the secondary air has no control over flame characteristics.

Although variations in NO emissions occur because of changes in the amount of excess air, NO reduction levels can be established in addition to their relative effectiveness, by comparing the emission levels at a fixed level of excess air. The conclusions reached below are based on an excess air level equivalent to 3% oxygen in the flue and a combustion air preheat temperature of 460°C. For the combination nozzle:

a. 13% external flue-gas recirculation reduced NO emissions by 49%.

b. Cooling the walls from 1330°C to 1130°C reduced NO emissions by 29%. However, it is acknowledged that reduced wall temperature may not be a practical technique for some types of processes or furnaces.

c. Reducing the combustion air preheat from 460°C to 250°C led to a 50% reduction in NO emissions. No preheat gave a 68% reduction.

d. Combining the 1130°C wall temperature with the 13% external flue gas recirculation resulted in a 68% reduction, or an emission level equivalent to operating with ambient secondary air temperature.

e. Increasing the primary air to 6% of the total air input yielded a 19% decrease in NO emissions.

f. Combining the 6% level of primary air with the 1130°C wall temperature reduced the flue NO concentration by 24%.

g. Moving the injector to the exit position resulted in an increase in the NO level of 18%.

Table 3. SYNOPSIS OF DATA COLLECTED FOR THE KILN BURNER

Excess Oxygen, % 3*

Normalized NO, ppm

(Baseline operating conditions; gas input 2700 SCFH; 460°C secondary air preheat; combination gas nozzle, 810 SCFH axial, 1890 SCFH radial; normal nozzle position; 1330°C wall temperature; 3.2% primary air)

	Secondary Air Preheat, °C		
	460	250	22
Baseline Operation	288	143	92
EFGR, 13%	146	45	28
Wall Temperature, 1130°C	204	94	52
Wall Temperature, 1130°C and EFGR, 13%	92	47	22
Primary Air, 6%	233	125	42
Primary Air, 6% and Wall Temperature, 1130°C	219	105	68
Exit Nozzle Position	339	135	62
Axial Gas, 14%	303	173	100
Axial Gas, 14% and Exit Nozzle Position	323	136	73
Axial Gas, 14% and Primary Air, 6%			
Radial Gas, 100%	291	133	108
Radial Gas, 100% and Exit Nozzle Position	352	136	87
Gas Input, 1900 SCFH	89	44	29
Gas Input, SCFH and Radial Gas 100%	122	83	62
Divergent Nozzle	396	231	104
Divergent Nozzle and Wall Temperature, 1100°C	134	115	67
Divergent Nozzle, Wall Temperature, 1100°C and Primary Air, 9.5%	109	100	69

---

*NO concentrations at 1% excess oxygen have been omitted. Many operating conditions produced CO concentrations above 500 ppm making these conditions undesirable despite a low NO level.

h. Changing the ratio of axial gas to total gas to 14% (from 30%) resulted in a 5% increase in NO emissions. By increasing the primary air to 6% (from 3.5%), the level was brought back to that of baseline operation conditions.

i. With 100% of the gas being injected radially the emission levels were equivalent to baseline. Moving the nozzle into the exit position, however, resulted in a 22% increase in emissions.

j. Reducing the firing rate from 2700 SCFH to 1900 SCFH resulted in a 69% reduction in NO emissions.

For the divergent nozzle:

a. The divergent nozzle increased NO emissions by 38% compared to the combination nozzle. However, reducing the wall temperature resulted in a 53% reduction of NO emissions relative to baseline operations. Using the reduced wall temperature and 6% primary air produced an overall reduction of 62%.

It can be concluded for the kiln burner that there is an optimum flame shape and length that will produce minimum NO emissions. Too short a flame will produce high combustion intensity within the burner block thus causing high NO emissions. Projecting the flame to far down the furnace will result in additional preheating of the secondary combustion air by "scrubbing" heat from the furnace walls resulting in both higher flame temperatures and increased NO emissions. An effective procedure is to minimize wall temperature where practical (from data this should be below 1100°C) and maximize the volume and velocity of axial fuel (staying within limits of stable combustion and low flue CO). Short of this, increasing the volume of "cold" primary air is the easiest technique to follow.

BAFFLE BURNER

Figure 4 illustrates the design of the baffle burner. The gas nozzle lies parallel to and along the axis of the burner. It is inserted into the ceramic baffle, thus ensuring that the gas enters parallel to the axis of the baffle burner. Combustion air enters perpendicular to the axis and passes through the six ports in the baffle, which impart a swirl to the air in some designs. Two of these baffle ports are shown in Figure 4 with their axes parallel to the axis of the burner. Air exiting from the ports (as illustrated) would have only an axial velocity component, resulting in a "long" flame. To shorten the flame length, a tangential-flow component must be added to the combustion air velocity. This is accomplished by using a baffle where the combustion-air ports are rotated relative to the axis of the burner. For the "intermediate" flame length baffle (IFLB), the rotation orientation of the ports is 15 degrees and for the "short" flame length (SFLB) it is 25 degrees.

IFLB BURNER

Standard Conditions (IFLB)

Figure 38 presents normalized nitrogen oxide (NO) versus excess oxygen (O_2) test data for burner conditions typical of an industrial situation (standard gas nozzle, baffle nozzle position, and 4 degree burner-block angle). Measured CO levels greater than 500 ppm are listed by concentration next to their corresponding data point. Photographs illustrating flame geometry and flame luminosity under these industrial conditions are shown in Figures 39 and 40.

The standard gas nozzle is a 2-inch pipe that rests within a centering tube mounted between the baffle and the burner housing. Gas nozzle positions are illustrated in Figure 41. The gas nozzle position is denoted as the baffle position when the nozzle is even with the burner-block side of the baffle. Other nozzle positions investigated were the throat position (gas nozzle midway between the baffle and the front wall of the furnace) and the exit position (gas nozzle even with the front wall of the furnace). For the IFLB, the exit gas nozzle position produced unstable combustion and therefore is not included in the test results.

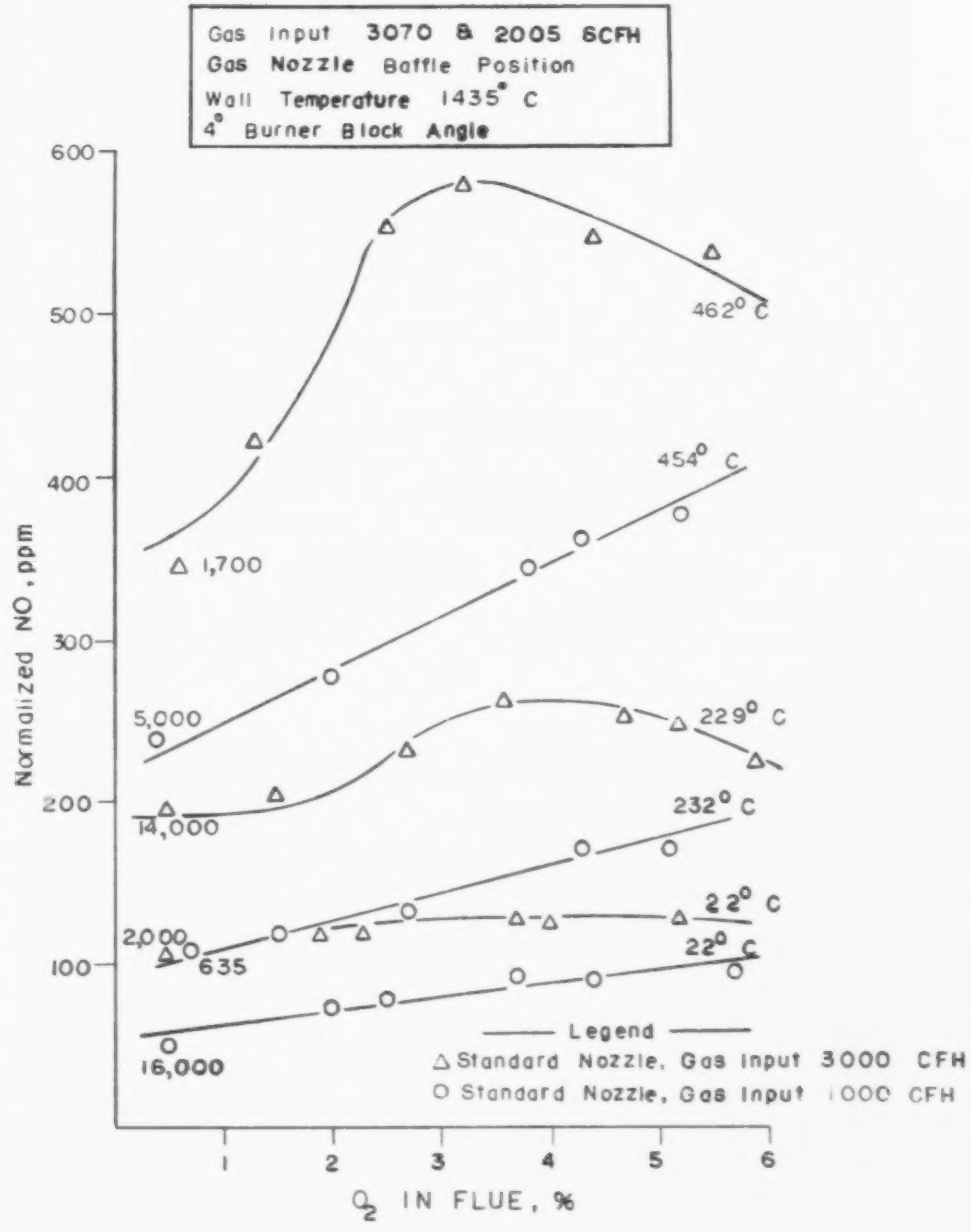

Figure 38. Normalized NO concentration as a function of flue O_2 for the IFLB burner with a standard gas nozzle at gas inputs of 3070 and 2005 SCFH

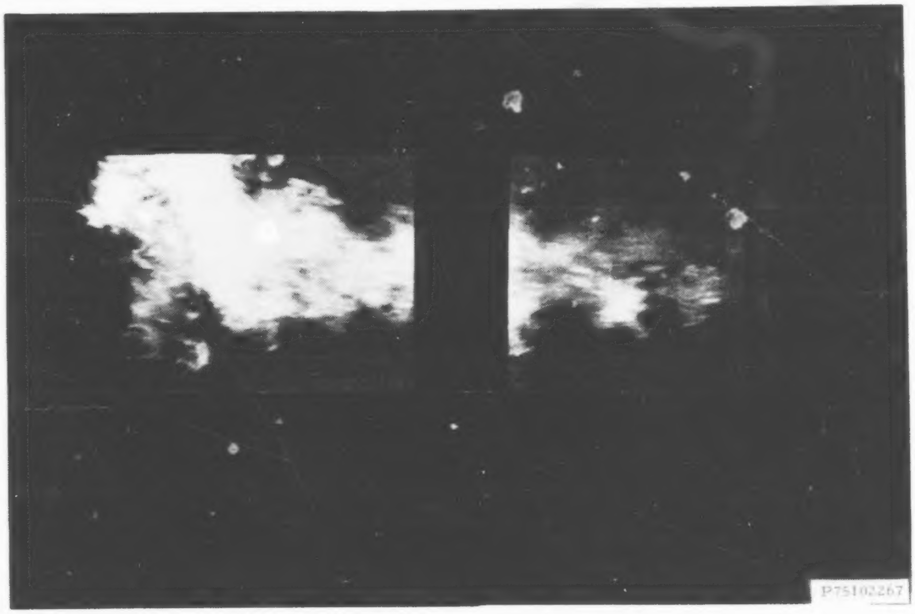

Figure 39. IFLB burner with standard fuel nozzle

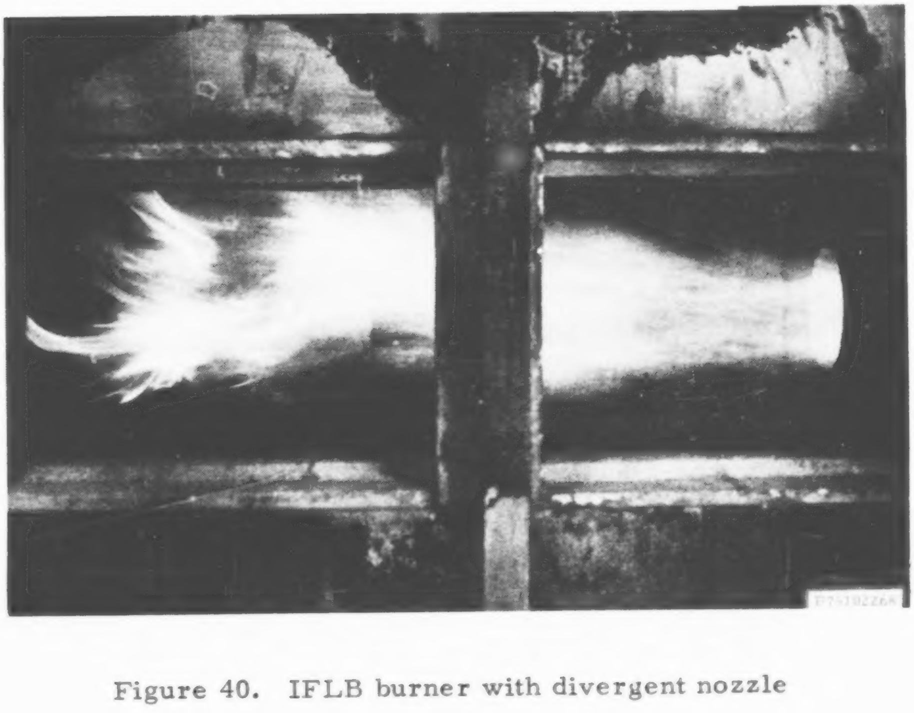

Figure 40. IFLB burner with divergent nozzle

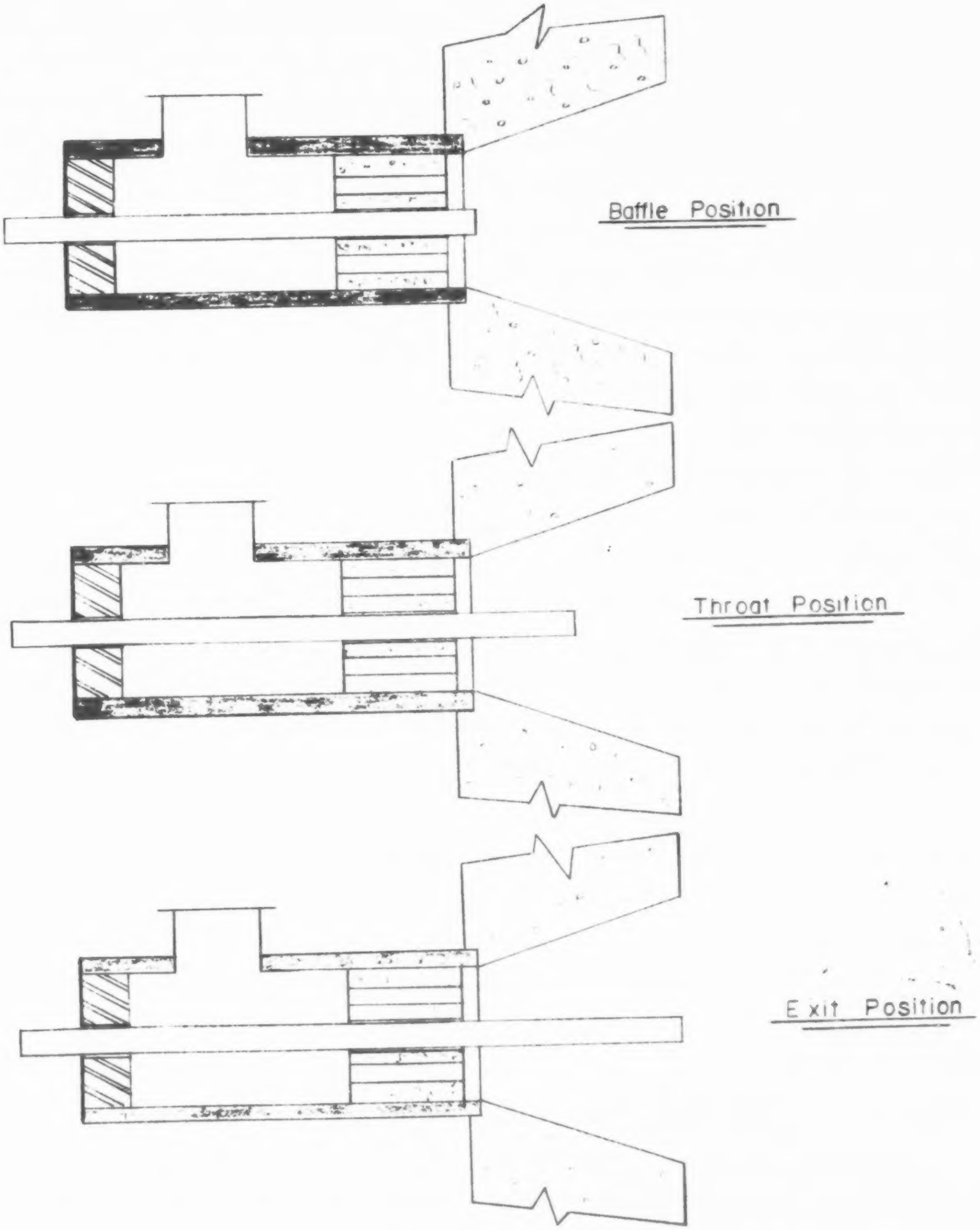
Baffle Position
Throat Position
Exit Position

Figure 41. Nozzle positions tested for the baffle burner

In-the-flame surveys were conducted during the baffle burner trials. These surveys included flow direction, temperature and gas analysis. The details of this survey work along with complete in-the-flame data and a comprehensive listing of the input/output data are presented in Volume II. However, it is beneficial in understanding the interpretation of the input/output data to take a brief look at some in-the-flame data.

Figure 42 presents some gas species and temperature data collected along the baffle burner axis for standard operating conditions. The flow direction data shows the profile of a type I flame. The axial momentum of the fuel jet is less than that of the combustion air. At the burner block exit there is a methane concentration of less than 2%. The CO concentration decreases from the burner block exit to the end of the furnace, with the maximum measured concentration being 9.2%. The temperature at the burner block is quite high at 1610°C. The NO concentration is 120 ppm or 24% of the 493 ppm flue concentration.

At a gas input of 3000 SCFH, the relationship between NO and excess O_2 became increasingly nonlinear as a function of temperature, as shown in Figure 43. This indicates that in the range of excess O_2 investigated, the higher the preheat, the more closely the NO-versus-O_2 relationship characterizes that of a premix flame.

For the second set of curves in Figure 43, burner conditions were the same, but the gas input was reduced to 2000 SCFH. In an attempt to maintain the same level of bulk NO formation, the wall temperature was held at 1420°C, compared with 1435°C for a gas input of 3000 SCFH. These curves show the same linear relationship between NO and excess O_2 that was observed for the kiln burner. This linear relationship is characteristic of a diffusion flame.

External Flue Gas Recirculation (EFGR) for IFLB

As a base-line control case, the effect of external flue gas recirculation was tested. The percentage of FGR is determined by using the relationship —

$$\% \text{ EFGR} = \frac{\text{EFGR (SCFH)}}{\text{Secondary air (SCFH)} + \text{Fuel (SCFH)}} \times 100$$

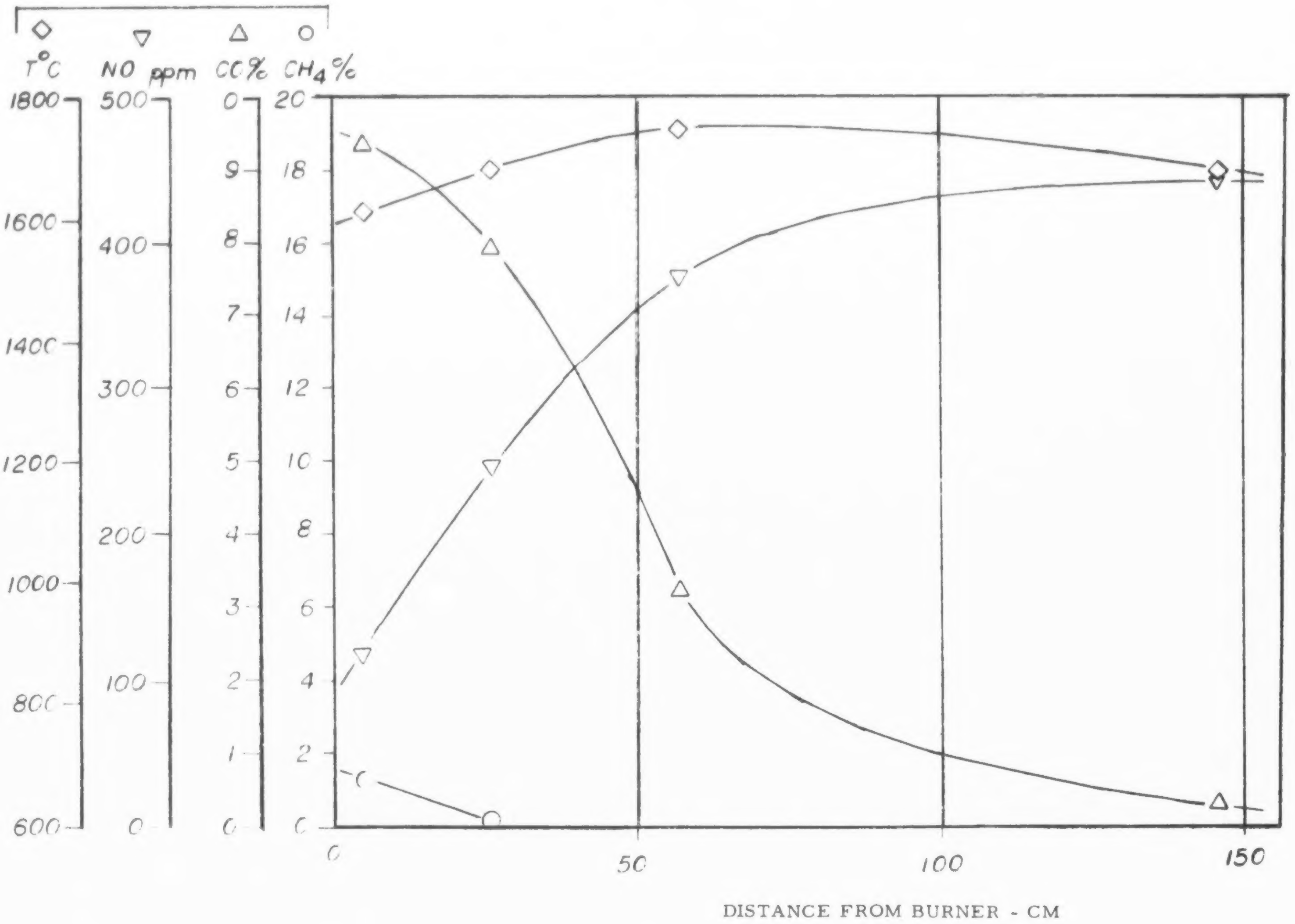

Figure 42. In-the-flame profiles along the axis of a baffle burner for typical operating conditions

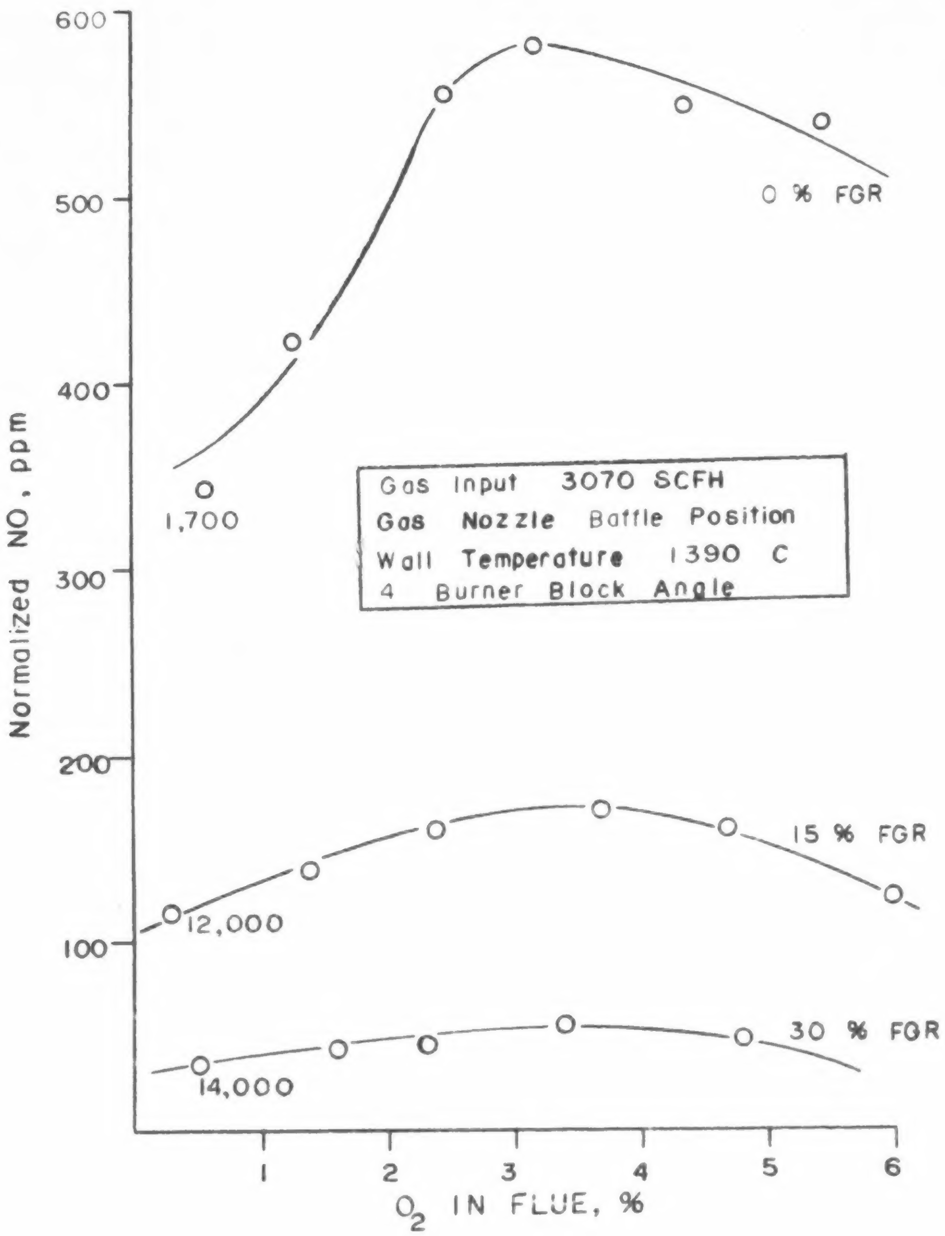

Figure 43. Normalized NO concentration as a function of flue O_2 for the IFLB burner with a standard gas nozzle and 15% and 30% FGR

By using the data presented in Figure 43, the NO concentration measured for standard burner operating conditions with 462°C secondary air preheat can be compared with the concentration at similar burner conditions but with the addition of 15% and 30% EFGR to the secondary air. During preheat, both the flue gas and secondary air were blended and reached the same final preheat temperature, which in this particular test was 460°C. At 3% excess O_2, a 15% FGR level reduced the normalized NO from 575 to 150 ppm, whereas 30% FGR reduced the measured NO concentration to 50 ppm.

Wall Temperature (IFLB)

The data for Figure 44 were collected with the burner operating in the normal industrial mode; however, the wall temperature was decreased from 1435° to 965°C by using water-cooling tubes within the furnace sidewalls.

This reduction in wall temperature resulted in approximately a factor of two decrease in the level of NO emissions. It is not possible to determine from the data what the magnitude in reduction of the prompt or bulk NO levels was. This in bulk NO formation occurs because of the increased heat removal in the post flame region and secondary recirculation zones. When these cooler recirculation zone products are entrained by the combustion air jet, the peak flame temperature is lowered resulting in a decrease in the prompt NO level.

Although it is not possible to operate with reduced wall temperatures (below 1200°C) in all industrial applications, these data demonstrate its effectiveness as an NO control technique. Suggestions for achieving lower operating wall temperature are monitoring fuel input, increased product load and/or secondary furnace cooling system.

Nozzle Type and Position (IFLB)

Figure 45 presents NO concentrations measured under standard burner conditions but with a radial gas injector. This injector forces the gas to enter the burner block radially to the axis of the burner, which causes a flame flow pattern categorized as type III. The combination gas nozzle shown in Figure 3, operating with radial injection only, was used.

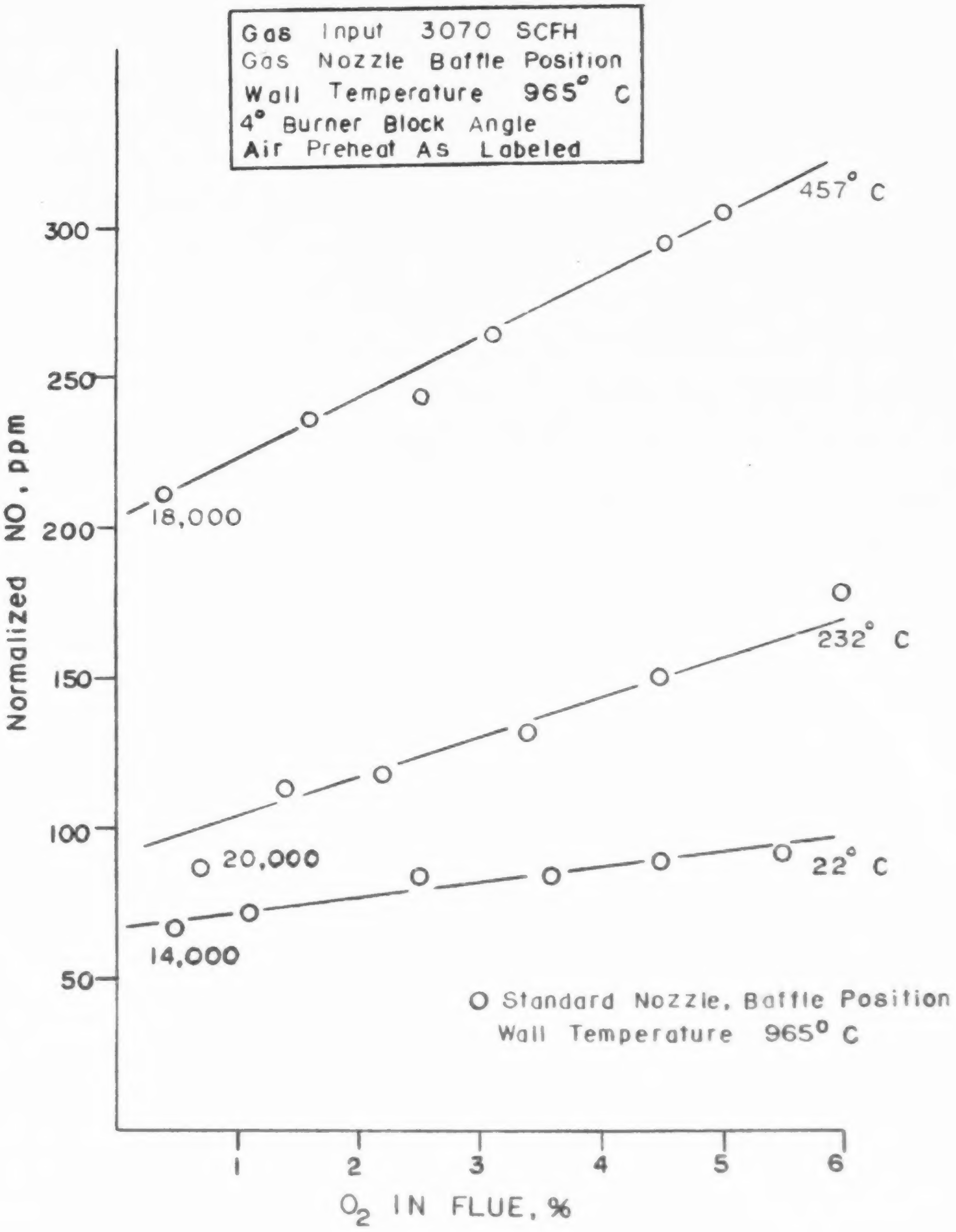

Figure 44. Normalized NO concentration as a function of flue O_2 for the IFLB burner with a standard gas nozzle at a wall temperature of 965°C

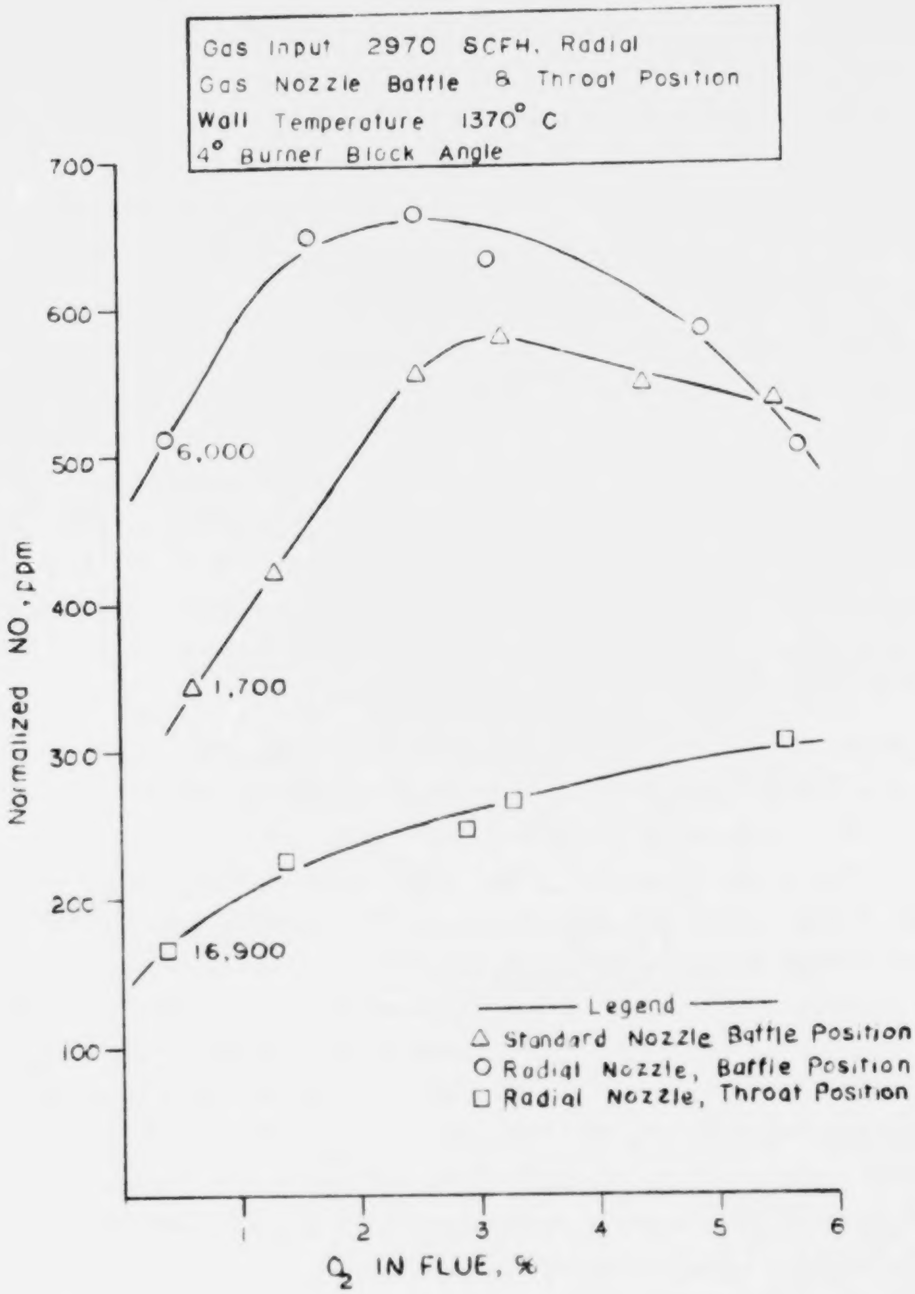

Figure 45. Normalized NO concentration as a function of flue O_2 for the IFLB burner with a combination gas nozzle and radial injection

The radial nozzle in the baffle position produced more NO than the standard nozzle because of the increased rate of heat release, coupled with the inability of the burner block to be used as a heat sink. However, when the radial nozzle was moved into the throat position, there was a dramatic drop in the measured NO concentration (approximately a factor of 2-1/2). This decrease could be due to the combustion occurring outside the burner block, which allows a larger mass exchange to occur among the fuel, the internal recirculation zone, the secondary air, and the external recirculation zone, thus lowering the flame temperature.

In an attempt to further slow the rate of heat release, half the gas was introduced radially while the other half was introduced axially (at a high velocity of approximately 300 ft/s). Again, data were collected for the half axial-half radial injection in both the baffle and throat positions. These results are presented in Figure 46. The axial gas injection had the desired effect: it decreased the NO concentration relative to all-radial injection by projecting the flame further into the furnace and slowing the rate of heat release. Again, moving the nozzle position into the throat of the burner block further reduced the NO concentrations.

Figure 47 is a composite plot showing all significant reductions in NO as a function of nozzle type and/or nozzle position. All these data were collected with a secondary air preheat at 460°C. The base-line conditions were those of the standard nozzle in the baffle position; this burner configuration produced the highest NO concentrations. Moving the standard nozzle into the throat position did not change the shape of the NO-versus-O_2 relationship, indicating that the basic mixing patterns were not dramatically altered. However, it did decrease the NO concentration to approximately 125 ppm. With a divergent gas nozzle (Figure 2) similar to the one used in the kiln burner, an additional decrease to 100 ppm NO resulted. The differences in NO concentration produced with the divergent nozzle and the standard nozzle in the throat position decreased as a function of excess O_2, until at 6% excess O_2, the NO concentrations were equal. The divergent nozzle produced a type III flame. The decrease in NO occurred because of the additional entrainment of combustion products from the primary and secondary recirculation zones. Although the data are not plotted, test results with the divergent nozzle in

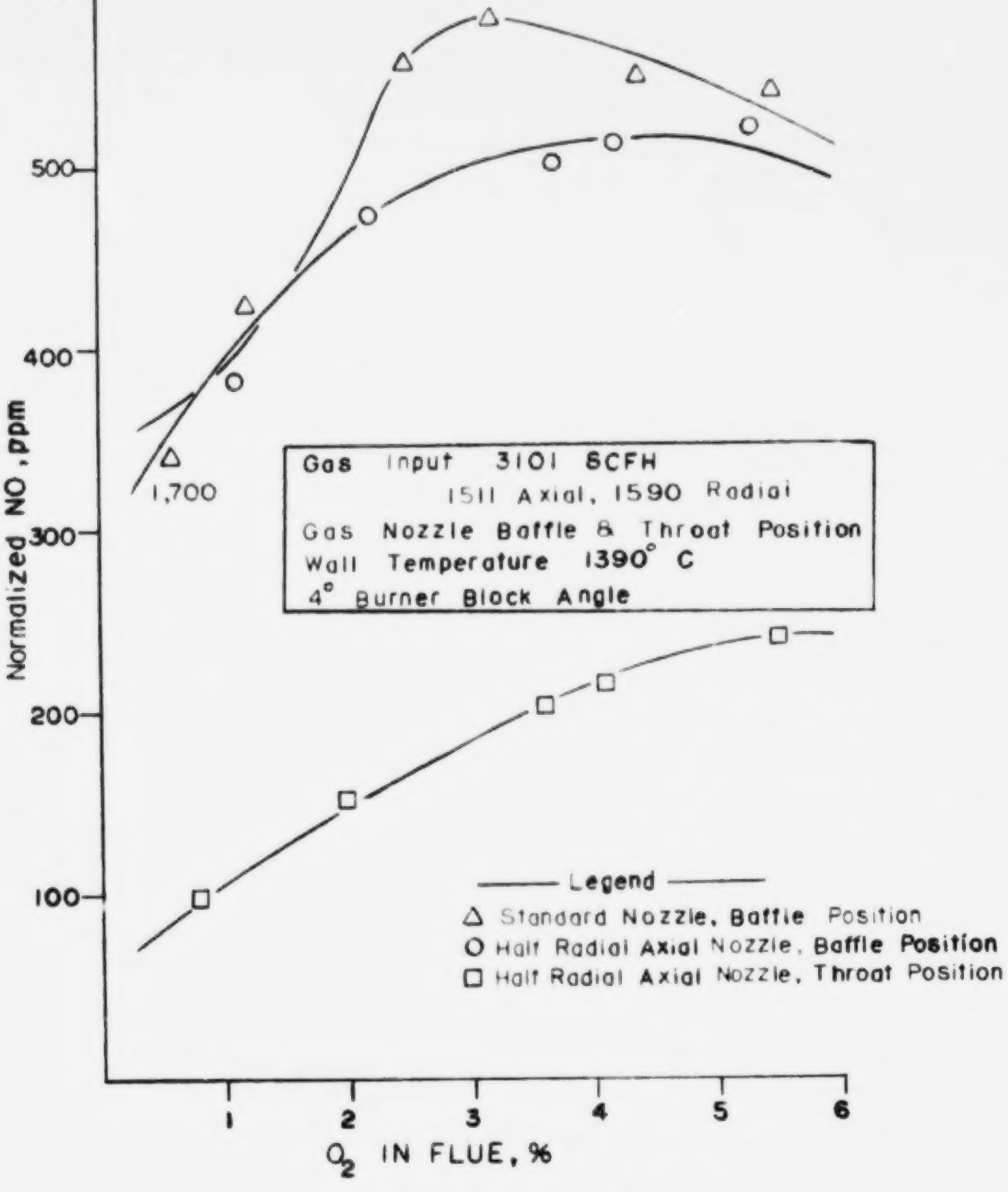

Figure 46. Normalized NO concentration as a function of flue O_2 for the IFLB burner with a combination gas nozzle and axial and radial injection

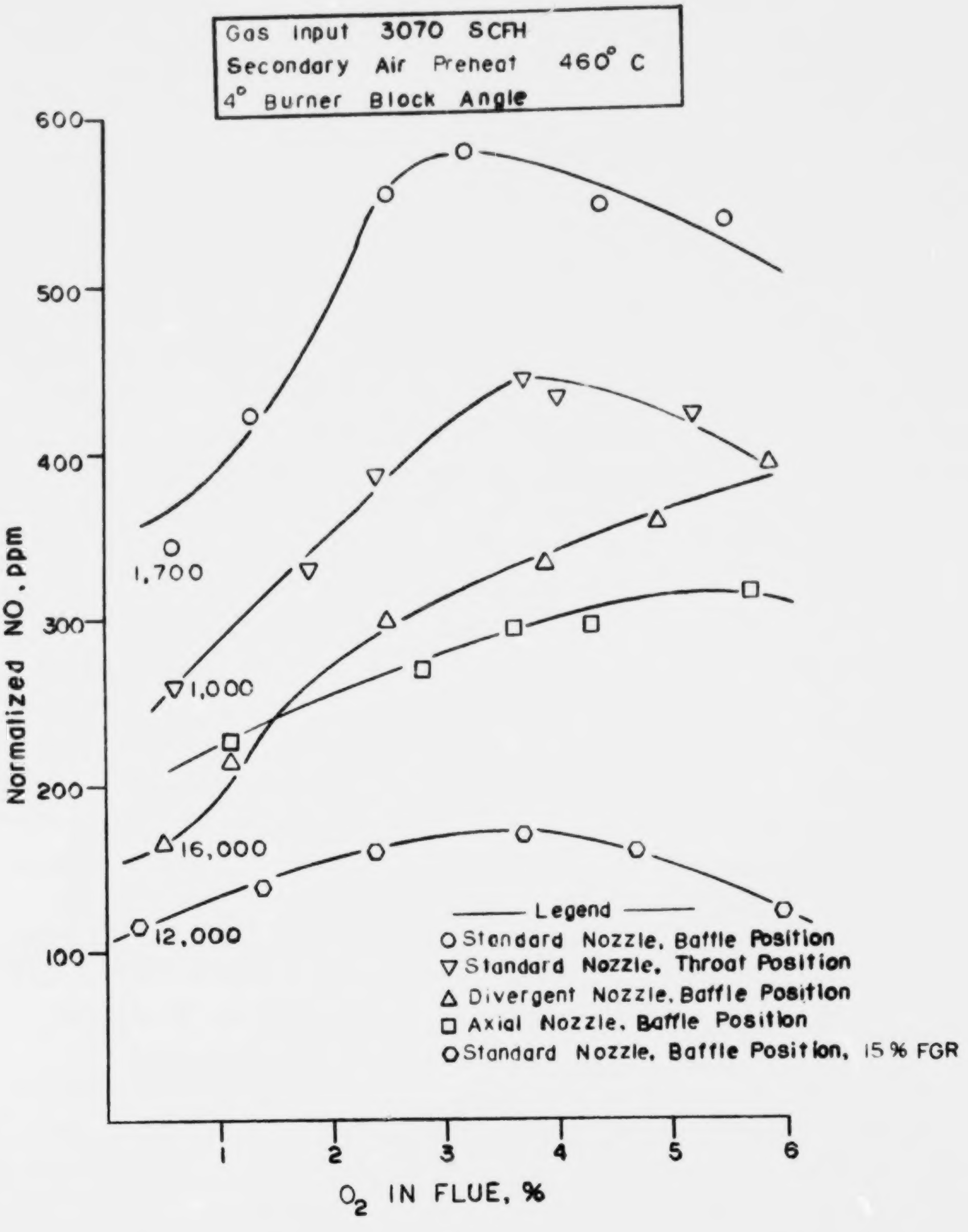

Figure 47. Normalized NO concentration as a function of flue O_2 for the IFLB burner with the various gas nozzles in different positions

the throat position paralleled those with the kiln burner; i.e., the NO was increased by moving the gas injector toward the combustion chamber. The difference in NO concentration as a function of nozzle position, however, is very small.

The most dramatic decrease in NO with burner alterations occurred when the gas velocity was increased by a factor of 16. This was accomplished by using all-axial gas injection, but decreasing the injector opening from the standard 2 inch to 0.5 inch. As shown in Figure 47, at less than 2% excess O_2, the divergent nozzle produced the lowest NO emissions; however, above that level of excess O_2, the high-velocity axial nozzle produced the lowest NO emissions. At 3% excess O_2 (11.4% excess air, a typical industrial level), comparing the normal burner output of 515 ppm with the high-velocity gas-injection burner output of 250 ppm, NO emissions were decreased by 325 ppm through a simple, low-cost alteration of the gas injector. Note that external FGR still remains the best depressant of NO formation that was tested. At 15% FGR, the NO level is 150 ppm with the standard baffle-and-nozzle configuration, which represents a total decrease of 425 ppm.

The control condition in-the-flame data was collected for the high momentum axial nozzle. Figure 48 presents some of the gas species and temperatures measured along the burner axis. As with the standard operating conditions the flow profile is a type I. The difference between the profiles is that now the primary jet axial momentum is greater than the axial momentum of the combustion air. This is reflected in the high concentration of methane (15%), measured at the burner block exit. The temperature at the burner block exit is only 1265°C or about 350°C cooler than that from standard operating conditions. The NO concentration at the burner block exit is 21 ppm or 8% of the 254 ppm flue concentration.

Burner-Block Angle (IFLB)

To test the influence of the primary recirculation zones on the level of NO emissions, the burner-block angle was increased from 4 to 8 degrees. The primary recirculation zones contain not only combustion products but also fuel and air. The entrainment of these gases by the primary and secondary jets should help to depress the flame temperature; however, they

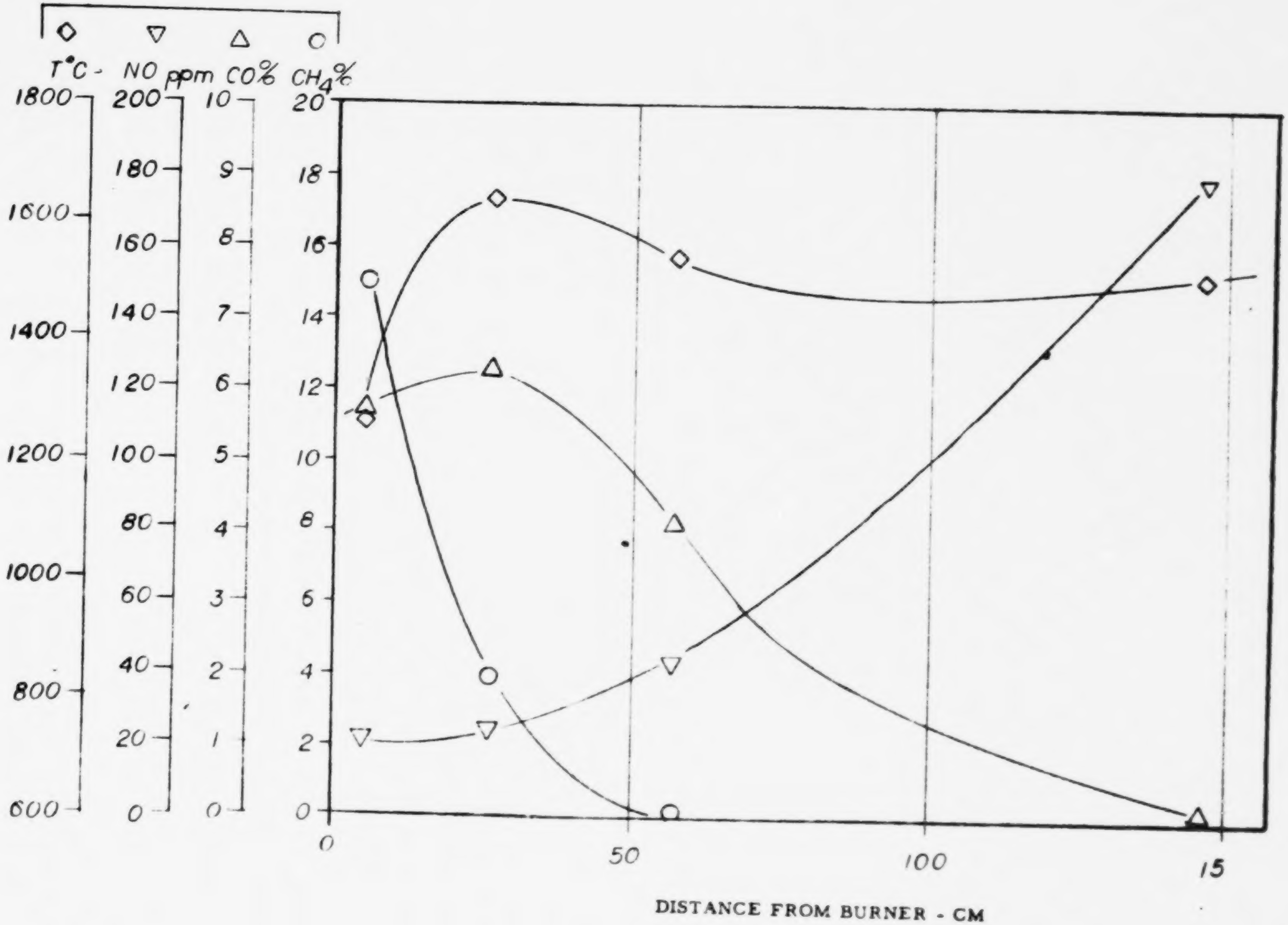

Figure 48. In-the-flame profiles for the axial fired baffle burner in the controlled operating condition

are not as desirable as the gases in the secondary recirculation zone because they contain both fuel and air. The angular difference between the IFLB (the air ports are angled at 15 degrees relative to the centerline of the baffle) and the burner block (air entry being an 8-degree divergent cone) is 7 degrees. Because the angle of the ports is greater than that of the burner block, the flow will not separate from the contour of the block. The IFLB was tested with the standard, divergent, and high-velocity axial gas nozzles with an air preheat temperature of approximately 460°C. The results are shown in Figure 49.

Table 4 compares the NO levels for integer values of the percentage of excess O_2 in the flue versus nozzle type between the 4 and 8-degree burner blocks. For the standard and divergent gas nozzles at low levels of excess O_2 (below 3%), the emission levels from the two burner blocks are comparable. However, as the excess air is increased, the emission levels from the 8-degree block become larger than those from the 4-degree block. Use of the high-velocity (611 ft/s) axial nozzle with the 8-degree block at normal operating levels of excess O_2 (below 3%) resulted in a 20% reduction in NO emissions. Thus the desired mass exchange among the primary jet, secondary jet, and the internal recirculation zones occurs only for the high-velocity axial nozzle. In this case of the standard nozzle (38 ft/s gas velocity) and the divergent nozzle (654 ft/s gas velocity), the increased burner volume resulted in high emissions. This increase occurred because a) the rate of heat release resulting from a high mass exchange between the primary and

Table 4. NORMALIZED NO AS A FUNCTION OF NOZZLE TYPE, BLOCK ANGLE, AND EXCESS O_2 FOR THE IFLB BURNER WITH AN AIR PREHEAT TEMPERATURE OF 460°C

		% O_2				
Nozzle Type	Block Angle, degrees	1	2	3	4	5
		ppm				
Standard	4	390	487	577	567	542
	8	408	492	564	612	636
Divergent	4	197	273	313	340	360
	8	204	272	360	428	480
Axial	4	227	255	280	300	313
	8	174	196	238	278	313

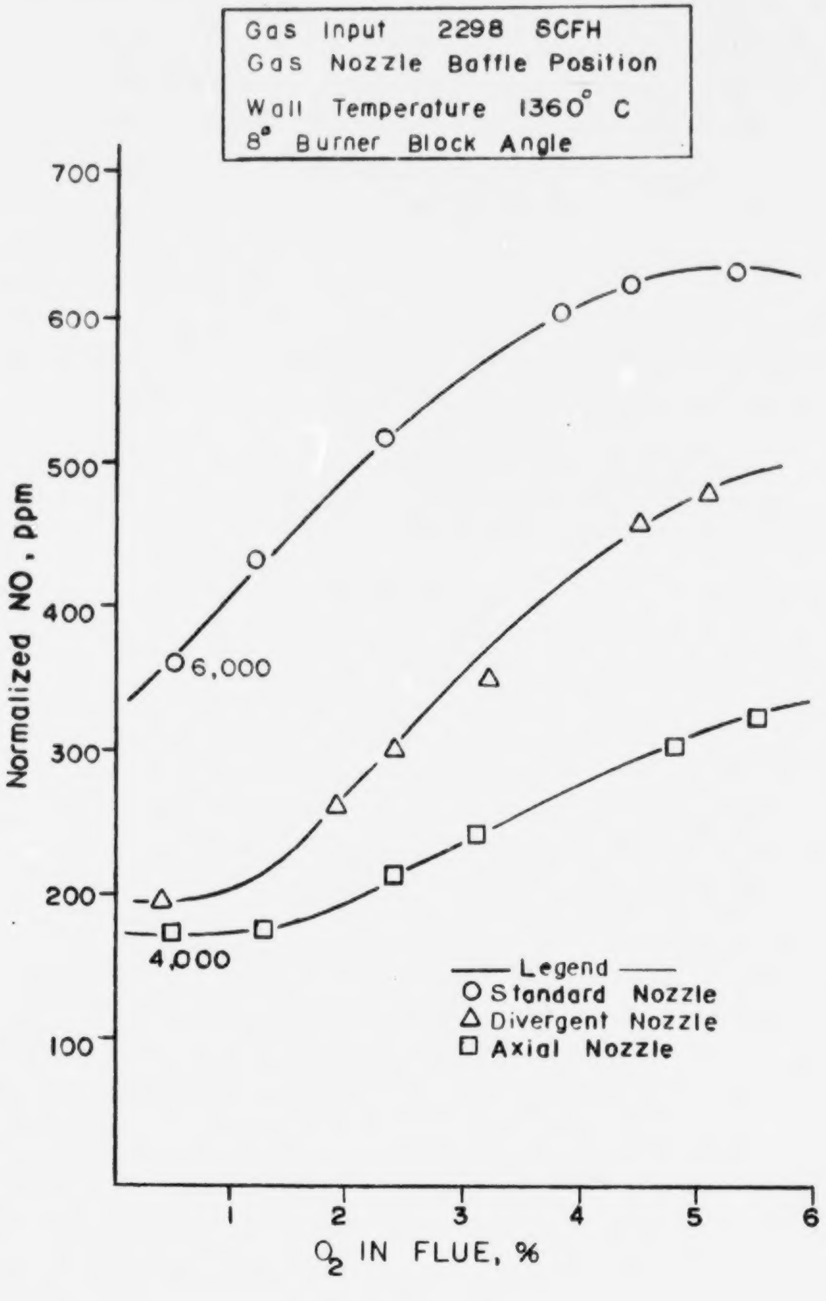

Figure 49. Normalized NO concentration as a function of flue O_2 for the IFLB burner with standard, divergent, and axial gas nozzles

secondary jets improved more than the mass exchange among the primary jet, the secondary jet, and the internal recirculation zones or b) the volume of the secondary recirculation zone was decreased.

SFLB BURNER

Air Velocity (SFLB)

Initial tests with the SFLB burner were conducted by using a high-velocity (126 ft/s) baffle and a low-velocity (80 ft/s) baffle. (Air injection ports are angled at 25 degrees relative to the centerline of the baffle.) Because of the extreme pressure drop associated with the high-velocity baffle (approximately 22 in. H_2O with an air flow rate of 38,000 SCFH at 450°C), the tests were conducted with a gas load of 2000 SCFH. The 8-degree burner-block angle used in these tests is the manufacturer's recommended angle for industrial applications.

Figure 50 presents the test results as normalized NO emissions plotted against the measured percentage of O_2 in the flue. The high-velocity baffle produced consistently lower emission levels than the low-velocity baffle as a result of the larger mass exchange between the secondary recirculation zone and the secondary jet due to the increased velocity gradient. Thus, the higher the velocity of the secondary jet, the lower the NO emission levels. The magnitude of the reduction in NO depends not only on the velocity gradient across the shear layer separating the secondary jet from the secondary recirculation zone, but also on the volume and temperature of the secondary recirculation zone. The cost involved for this method of NO reduction is additional fan horsepower required to overcome the increased pressure drop in the burner.

Wall Temperature (SFLB)

Figure 51 illustrates the effect of wall temperature on the NO emission levels of the SFLB as a function of secondary air preheat and excess air. Conclusions similar to those for the IFLB can be drawn for the SFLB: A wall temperature as low as possible must be maintained through increased wall cooling, lowered gas input, or furnace design.

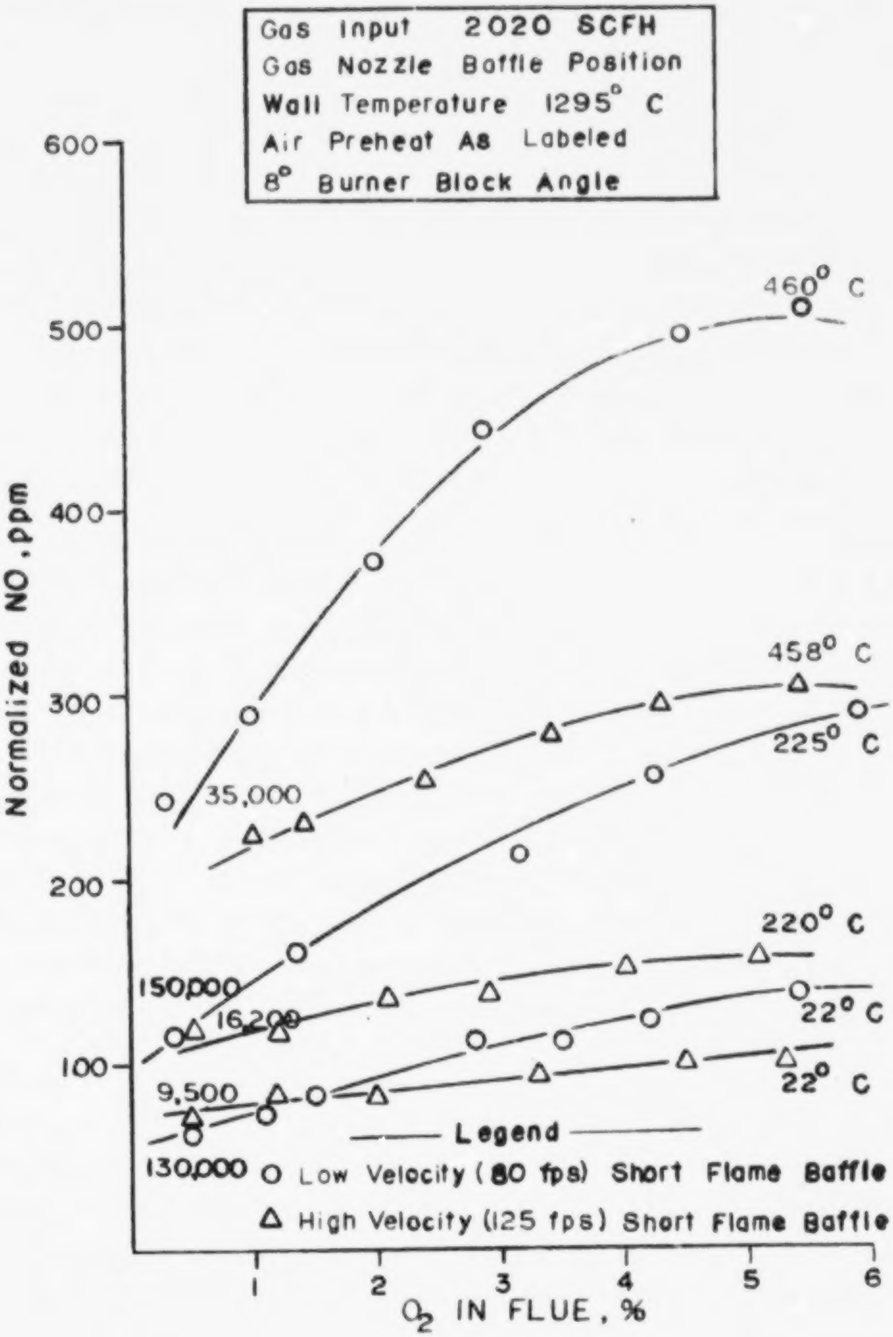

Figure 50. Normalized NO concentration as a function of flue O_2 for the SFLB burner with a standard gas nozzle

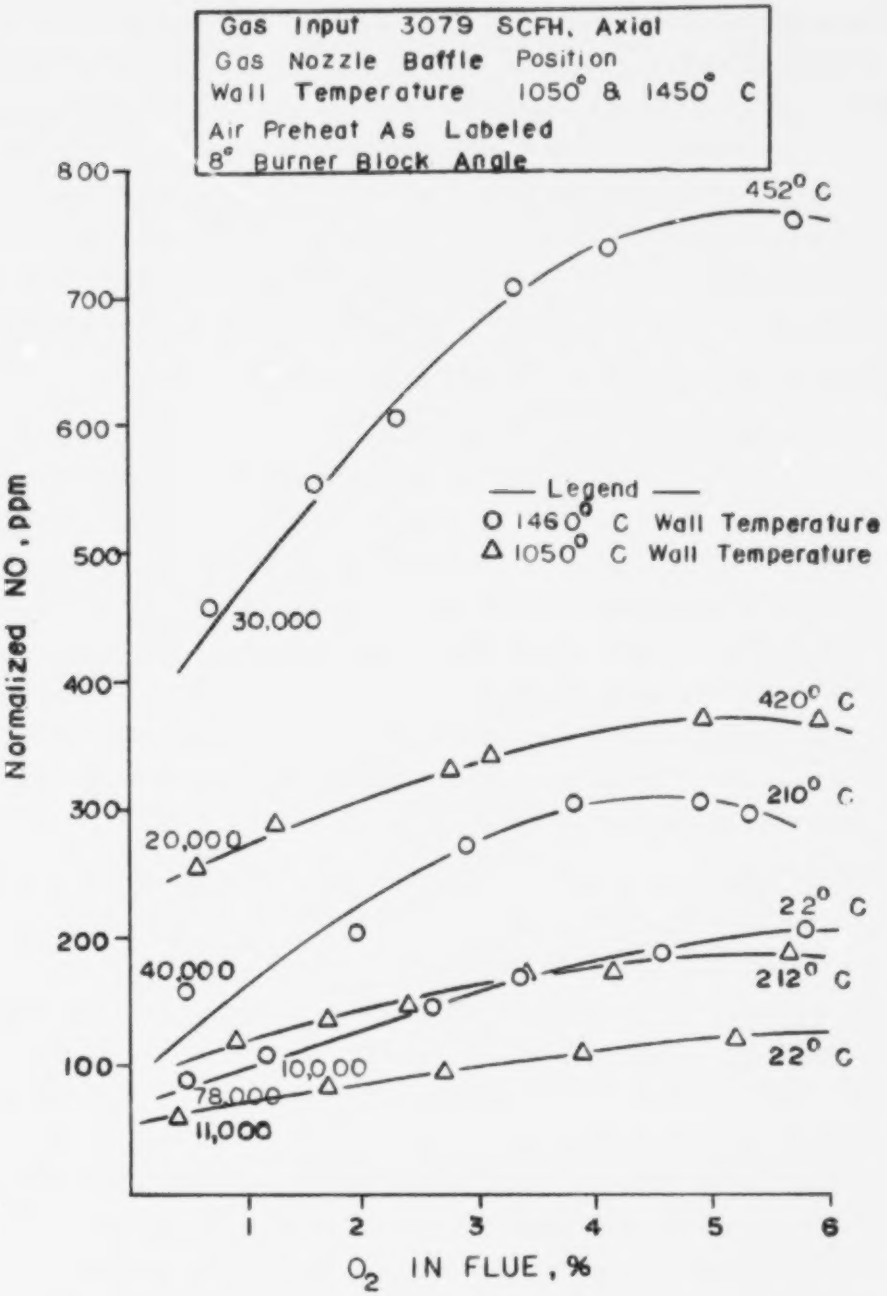

Figure 51. Normalized NO concentration as a function of flue O_2 for the SFLB burner with a standard gas nozzle at wall temperatures of 1450° and 1050°C

External FGR (SFLB)

To determine whether combustion aerodynamics can be used to recirculate combustion products to the base of the flame as an emission control technique, we simulated the idealized case (in which the combustion air and products are thoroughly mixed before ignition) by mixing flue gases with the combustion air outside the burner. Figure 52 compares the NO levels as a function of the percentage of O_2 in the flue for 0%, 15%, and 25% FGR. Again, as demonstrated for the kiln burner and the IFLB, external FGR is an extremely effective method of controlling NO emissions from the SFLB.

Nozzle Type (SFLB)

To determine the type of injector that would reduce NO emissions, a series of trials were conducted by using different methods of gas injection; the results are shown in Figure 53. The NO-versus-excess O_2 relationship for the standard nozzle (injection method recommended by manufacturer; 2-inch stainless-steel pipe with an inlet velocity of 38 ft/s and a gas input rate of 3000 SCFH)is shown as a reference, so that the effect of the gas injector type on the NO emission levels can be evaluated. Visual observations were made to determine the flame length for each gas nozzle tested. This allowed a first-order evaluation of alterations that can be made to obtain the flame shape desired by the manufacturer.

The visual flame length observed with the standard gas nozzle with the SFLB was 103 cm. The high-velocity (1043 ft/s) radial injector increased the NO emissions substantially above those measured for the standard nozzle. The shape of the emission curve closely resembled that of a premixed flame; peak emissions occurred at 1.5% excess O_2. The flame was invisible. Reducing the radial velocity to 532 ft/s resulted in a shift of the maximum NO emission to an excess O_2 level of 2.3%. Because of the reduction in the radial injection velocity, the magnitude of the peak NO concentration was reduced 20%. The visual flame length was 72 cm, still 31 cm shorter than that desired. The divergent nozzle, which was the first altered gas injector tested with the SFLB, yielded lower emission levels than the standard nozzle. The gas velocity from the divergent nozzle was 654 ft/s (at a 3000 SCFH gas load); however, a type III flame resulted because of the wake generated by

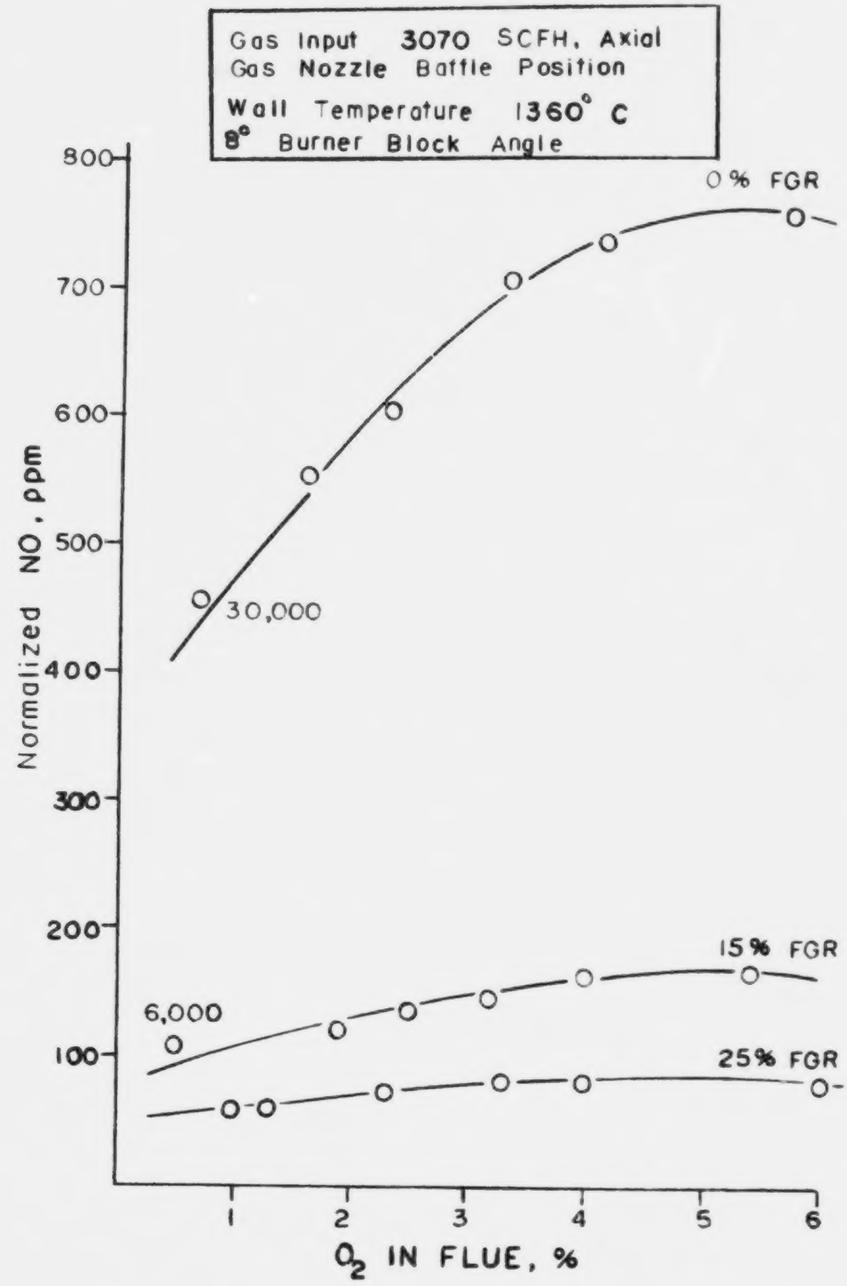

Figure 52. Normalized NO concentration as a function of flue O_2 for the SFLB burner with a standard gas nozzle and 15% and 25% FGR

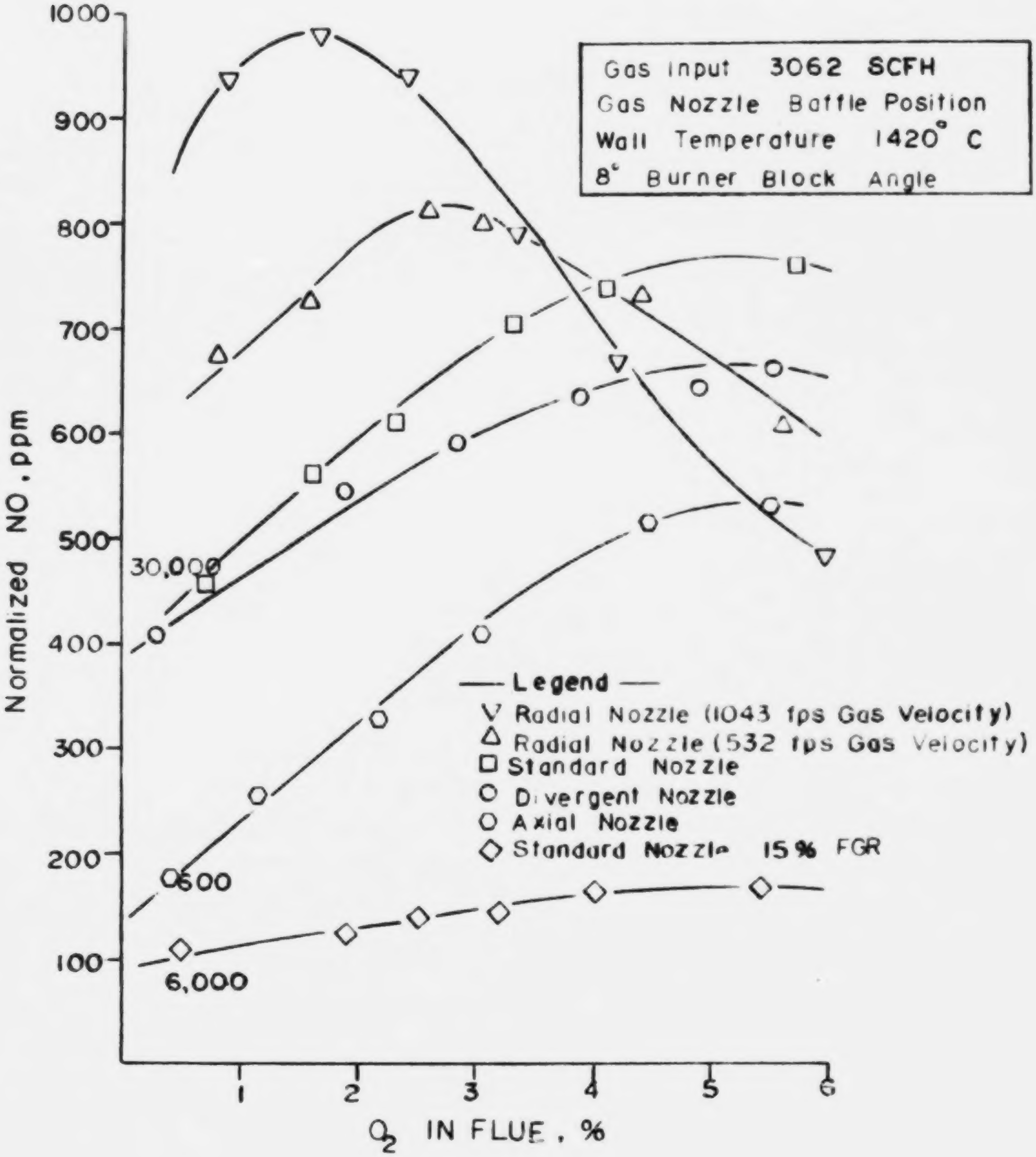

Figure 53. Normalized NO concentration as a function of flue O_2 for the SFLB burner with the various gas nozzles

the divergent cone in the nozzle. Despite the high inlet velocity, the flame length was 113 cm, which compares favorably with the desired length of 103 cm.

The injection method that resulted in the lowest emissions was the high-velocity axial nozzle (611 ft/s and a 3000 SCFH gas load). This nozzle produces a type II flame, even with the high-swirl SFLB, because the velocity of the gas is large enough to split the primary recirculation zone. Although the rate of entrainment per unit area between the primary jet and the surrounding flow zones increased because of the larger velocity gradient when compared with that from the standard nozzle, the flame length also increased, to 286 cm. The increased flame length was a result of a lower rate of mass exchange between the primary and secondary jets. This reduced mass exchange resulted from a decrease in the area of the shear layer caused by the smaller primary jet. Thus, by delaying the mixing between primary and secondary jets, not only was the heat release rate of the flame slowed, but it also approached the ideal of the EFGR by allowing more time for the secondary jet and the combustion products in the secondary recirculation zone to mix.

Burner-Block Angle (SFLB)

Figure 54 gives NO data from the SFLB trial with standard, divergent, and high-velocity axial nozzles and a 16-degree burner block. Obviously, the combustion aerodynamics were changed drastically as a function of excess air. There is no one general interaction theory that explains these curves in their entirety. Therefore, 1% level of excess O_2 was selected for analysis. This level was chosen because it consistently produced the lowest levels of NO, with concentrations below 50 ppm.

Table 5 lists the nozzle type as a function of burner-block angle for both the SFLB and the IFLB. The inlet gas velocity is listed in parenthesis beside the nozzle type. For 14% excess air (3% O_2), the velocity is 120 ft/s. Note that the air velocity increases with increasing excess air. The arrows indicate the direction of increasing NO concentration. It is known from flame-length observations that the standard and divergent nozzles have similar rates of mass exchange between flow zones, whereas the axial nozzle has a

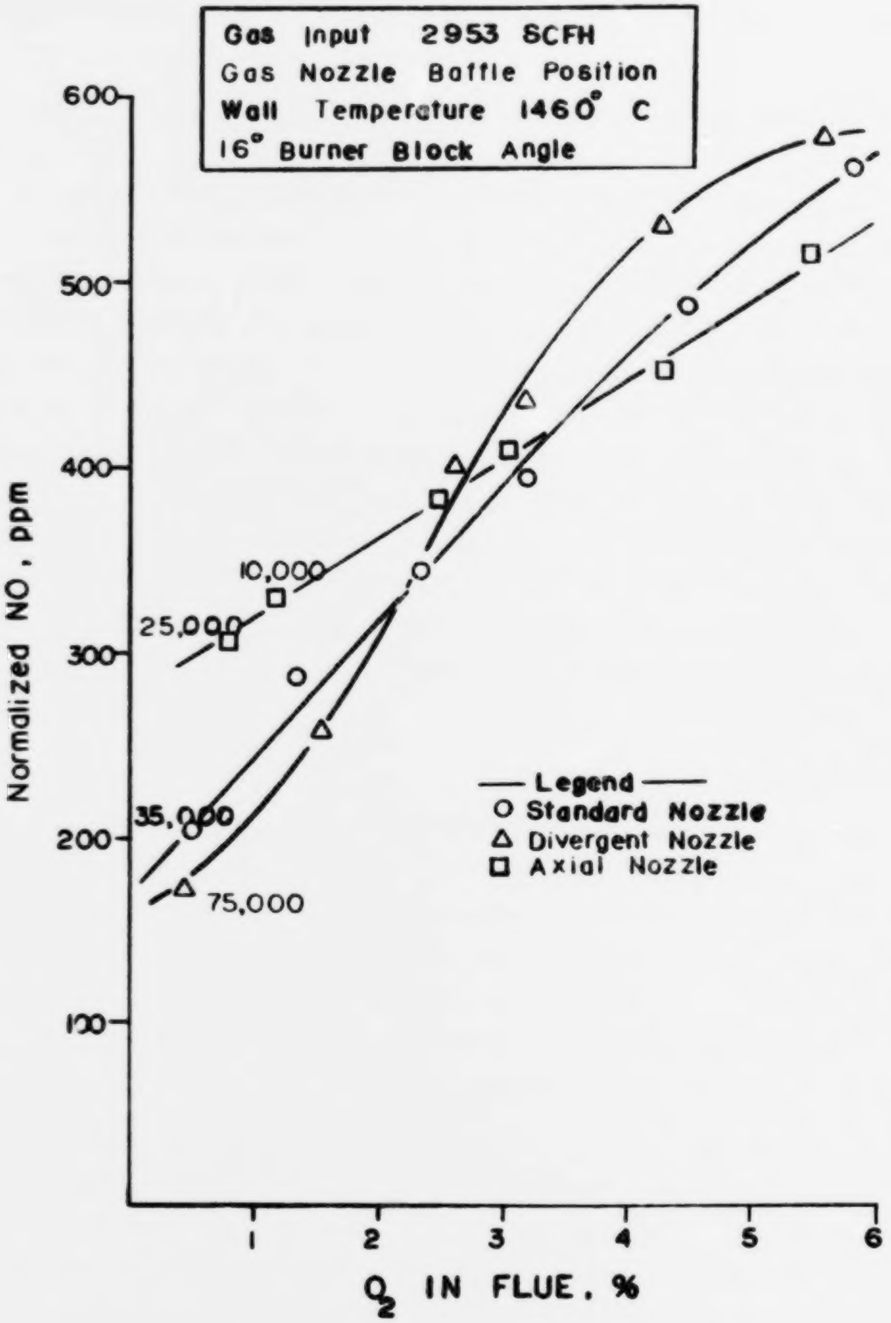

Figure 54. Normalized NO concentration as a function of flue O_2 for the SFLB burner with standard, divergent, and axial gas nozzles

Table 5. NORMALIZED NO CONCENTRATION AT 1% EXCESS O_2 WITH AN AIR PREHEAT TEMPERATURE OF 460°C AS A FUNCTION OF BAFFLE TYPE, GAS NOZZLE TYPE, AND BURNER-BLOCK ANGLE

	NO Concentrations				
	IFLB			SFLB	
	Block Angle, degrees				
	4	8	16	8	16
Nozzle Type	ppm				
Radial (1043 ft/s)	--	--	--	950	--
Radial (532 ft/s)	590	--	--	700	--
Standard (38 ft/s)	375→	400→	470	490←	240
Divergent (654 ft/s)	175→	200→	235	440←	210
Axial (611 ft/s)	215←	175→	200	230→	310
Standard, 15% FGR	120 (3% O_2)	--	--	110	--

slower exchange rate. It is not surprising that the standard and divergent nozzle show similar trends in NO formation as a function of burner-block angle. For the IFLB, the NO concentration increases with burner-block angle; for the SFLB, it decreases with an increasing angle.

For the IFLB, the mixing rate was increased between the primary and secondary jets more than the size, shape, and mixing rate of the primary recirculation zone with the primary and secondary jets. For the SFLB, the mass exchange between the primary recirculation zone and the primary and secondary jets was improved, which resulted in approximately a 55% reduction in NO emissions. The high-velocity axial nozzle showed almost the opposite effect. For the SFLB, there was a 30% increase in the emission level as the block angle was increased. Thus, for high swirl intensity and high axial velocity, increasing the burner-block angle resulted in a larger primary-secondary jet mass exchange. Investigations of the IFLB with the 16-degree block to study flow separation between the secondary jet and the block gave negative results. Therefore, it was assumed that it (flow separation) was also not present for the SFLB and the 16-degree block. The results for the IFLB and the high-velocity axial nozzle were somewhat mixed. There was a decrease in the NO level with a block angle increase from 4 to 8 degrees followed by an increase in the NO level with an angle increase from

8 to 16 degrees. The optimum burner-block angle for producing minimum NO emissions with the axial nozzle was approximately 10 degrees.

Wall Temperature (SFLB) Sensitivity

Because of the observed sensitivity of NO to wall temperature during these tests, NO data was taken during a warm-up cycle. The standard nozzle was fired with 3000 SCFH of gas at 3% excess O_2, 460°C air preheat, and the SFLB. The results are shown in Figure 55. The dramatic increase in the level of NO emissions above 1300°C indicates that an accurate control of wall temperature is required to produce a consistent set of experimental data. It also confirms that the furnace should be operated with as low a wall temperature as possible. It may not be possible to operate all industrial processes with a reduced wall temperature; however, because of its effectiveness as a control technique, operating wall temperature should be maintained as low as is practical.

FURNACE GEOMETRY

The IFLB burner was mounted on IGT's cylindrical (tunnel) test furnace, which has a cross-sectional area of 1.17 sq m (12.6 sq ft) and a volume of 6.4 cu m (226 cu ft). The following operating parameters were investigated: secondary combustion air preheat, method of gas injection, and position of gas injector.

Figure 56 shows the emissions data collected from the IFLB with the standard gas injector (2-inch stainless-steel tube), a 2000 SCFH gas input, and nonpreheated and preheated secondary combustion air. To determine the influence of furnace geometry on NO emissions, Figure 56 compares these data with similar data collected during a test on the larger-diameter furnace. The cross-sectional area of this rectangular furnace is 2.3 sq m (25 sq ft) and the volume is 10.6 cu m (375 sq ft). With the exception of secondary air preheat temperature (350°C for the cylindrical furnace, compared with 454°C for the rectangular furnace), all other burner and furnace operating conditions (gas input, gas nozzle position, burner-block angle, and wall temperature) were identical. For both conditions of secondary air preheat, the cylindrical furnace had the higher levels of emissions. The area ratio between the burner-block opening and the burner wall is 35.9 for the rectangular furnace and 18.2 for

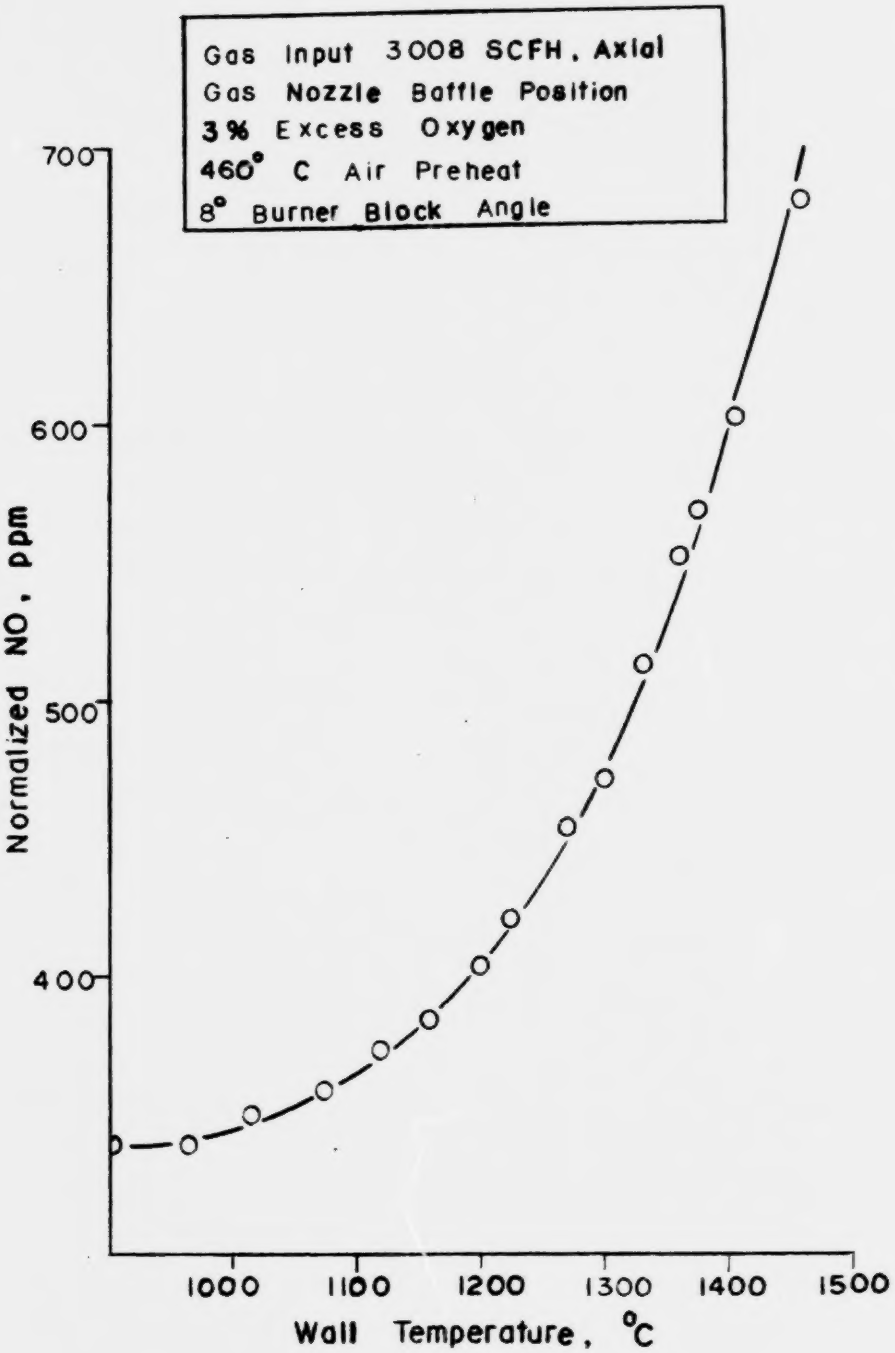

Figure 55. Normalized NO concentration as a function of wall temperature for the SFLB burner with a standard gas nozzle

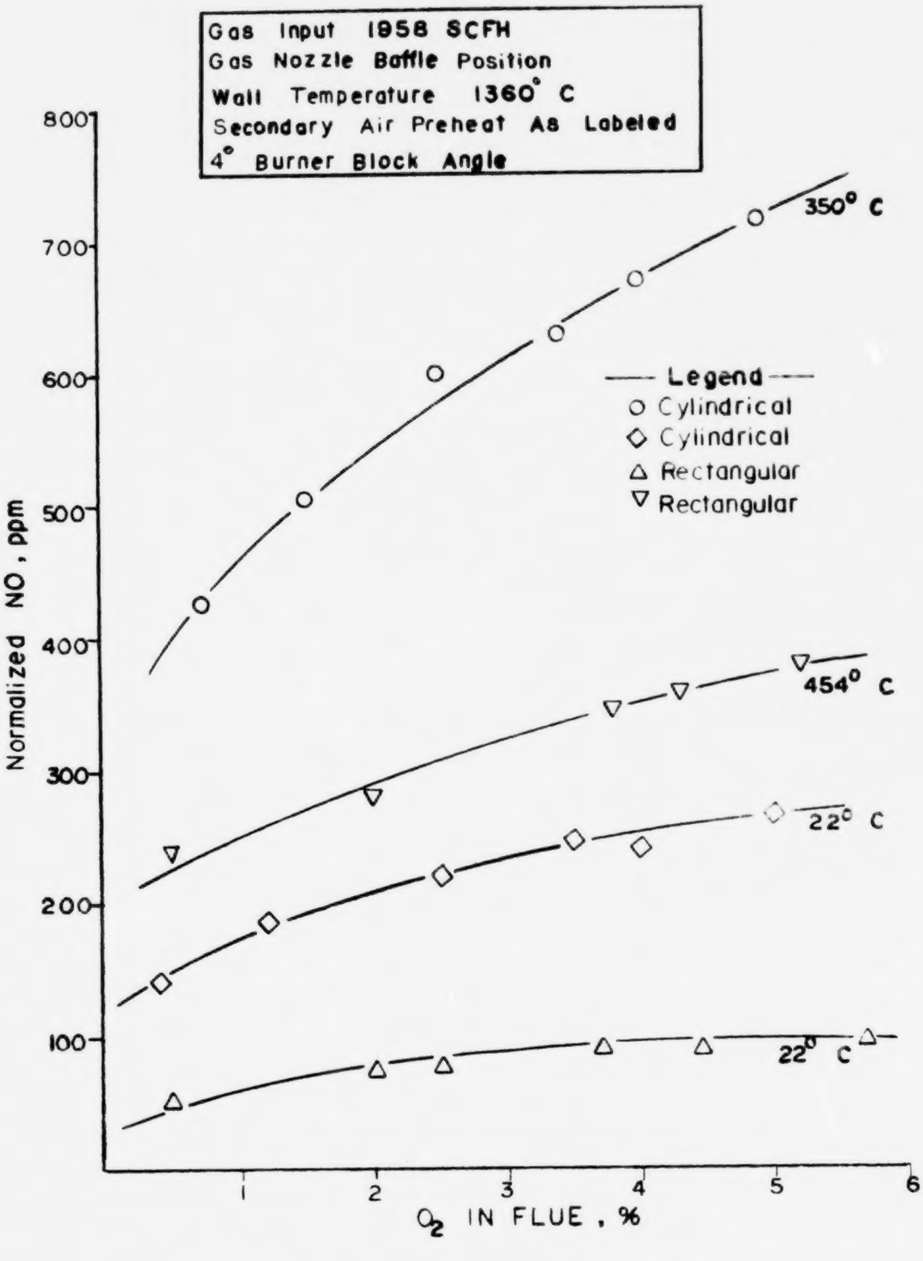

Figure 56. Normalized NO concentration as a function of flue O_2 for the IFLB burner with a low-velocity gas nozzle

the cylindrical furnace. These ratios reflect the relative sizes of the secondary recirculation zones. The primary reason for the difference in measured NO concentrations between the two combustion chambers is the unequal secondary recirculation zone volume.

Nozzle Type Variations

Additional tests were conducted to investigate the influence of gas injection on total NO emissions. In these trials, both a high-velocity (127 m/s, 407 ft/s) gas nozzle and a divergent gas nozzle (injection velocity 135 m/s, 436 ft/s) were used. Both injectors have only an axial velocity component. Figure 57 compares the normalized NO emissions as a function of excess O_2 from these gas nozzles. The low-velocity nozzle produces less NO, by a factor of 2, than the high-velocity nozzle. This result contradicts the data collected from the rectangular furnace, which are presented in Figure 58. Although the rectangular furnace has a higher gas input (2998 SCFH) and a higher secondary air temperature (450°C), the cylindrical furnace had the higher emission levels for a given gas nozzle. This occurs because NO production in gas flames is entirely thermal in origin. Thus, any change in the combustion chamber or fuel-air mixing that results in lower peak and average flame temperatures reduces the rate of NO production. Conditions that should reduce NO emissions include decreasing the rate of heat release, increasing the mass exchange between the flame zone and secondary recirculation zone, and reducing the wall temperature.

During previous trials with the rectangular furnace, the high-velocity gas nozzle always produced less NO emissions than nozzles with lower injection velocities. This result was explained by the different fuel-air mixing rates. An increase in injection velocity was achieved by decreasing the cross-sectional area of the injector, which caused a decrease in the fuel-air mixing rate and permitted an increase in recirculation and combustion zone mass exchange. The combustion zone is blended with combustion products, which result in lower flame temperatures. However, for the cylindrical furnace, the high-velocity gas nozzle causes higher NO emissions. This means that even though the same method of gas injection was used in each furnace, the thermal history of the two flames was different. The major reason for a higher flame temperature in the cylindrical furnace would be a smaller mass

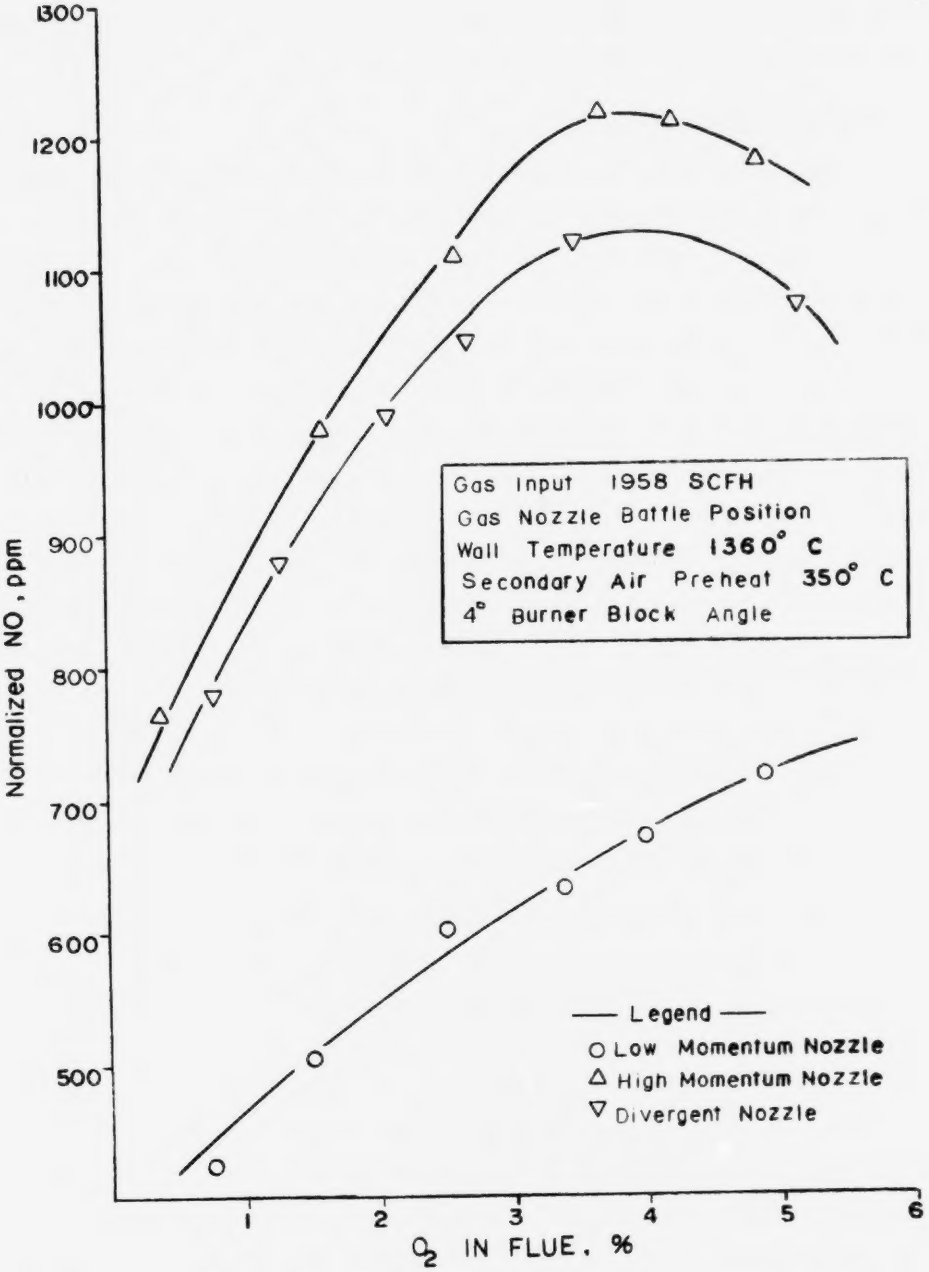

Figure 57. Normalized NO concentration as a function of flue O_2 for the IFLB burner with low-velocity, high-velocity, and divergent gas nozzles

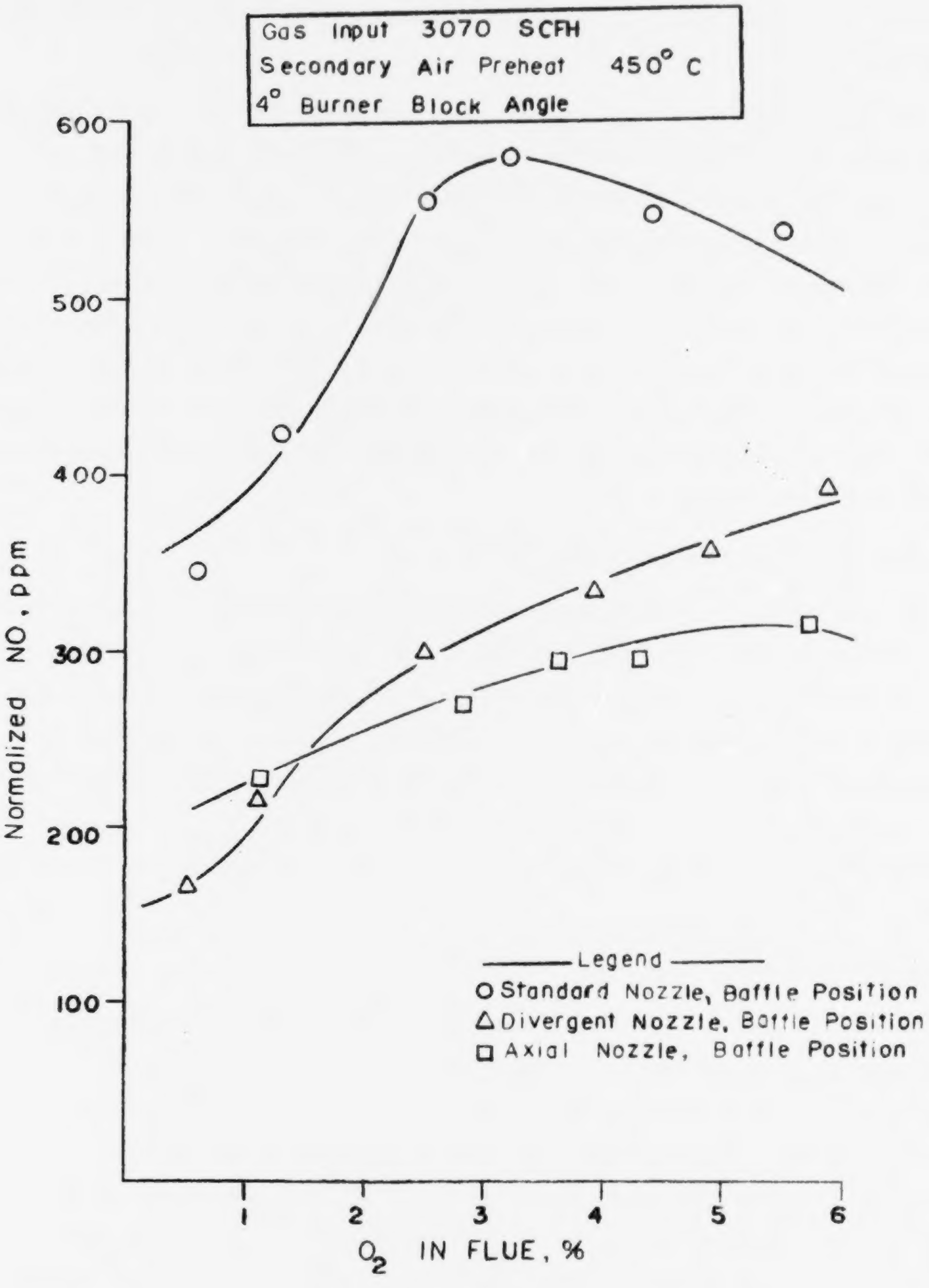

Figure 58. Normalized NO concentration as a function of flue O_2 for the IFLB burner with standard, divergent, and axial gas nozzles

exchange between the secondary recirculation and the combustion zones. The smaller mass exchange occurred because of a decrease in the size of the secondary recirculation zones, which, in turn, resulted from a smaller combustor cross-sectional area.

The divergent nozzle injects the gas radially at a 45-degree angle to the burner axis. Comparison of Figures 57 and 58 shows that the cylindrical furnace has the higher levels of emissions for the divergent nozzle. Arguments similar to those presented for high-velocity nozzle could also be made for the divergent nozzle. However, for both combustion chambers, the divergent nozzle has lower emissions than the high-velocity nozzle. The diverging gas injection causes a primary recirculation zone, which allows a larger dilution of the combustion zone with combustion products than an axial injector. This increased dilution leads to lower flame temperatures and reduced emissions.

NATURAL-GAS, LOW-NO$_x$ BURNER I

IGT has been commissioned by three gas utilities (Consumer's Gas Co., Consolidated Natural Gas Co., and Southern California Gas Co.) to develop a burner with low NO$_x$ emission levels relative to the industrial burner it was intended to replace and with a similar flame geometry and luminosity. The initial design guidelines for this burner development work were extracted from the data collected in this study. After fabrication, the low-NO$_x$ burner I (LNO-I) was mounted on the cylindrical furnace for NO$_x$ emission level testing.

Standard Operating Conditions

The initial set of trials was conducted by using 25% primary air. This percentage is determined by ratioing the volume of primary air to total air needed for stoichiometric combustion and multiplying it by 100. Figure 59 shows the results of these tests as normalized NO plotted against excess O_2. These data were collected by premixing the primary air and fuel, which gives rise to a clear flame. For comparison, Figure 59 also shows the emissions curve for the IFLB burner with a standard nozzle. The LNO-I burner was designed to replace burners in the IFLB burner category. Comparison of the emission levels of these burners at 350°C secondary air preheat shows that the LNO-I burner was extremely effective in reducing NO emissions. At

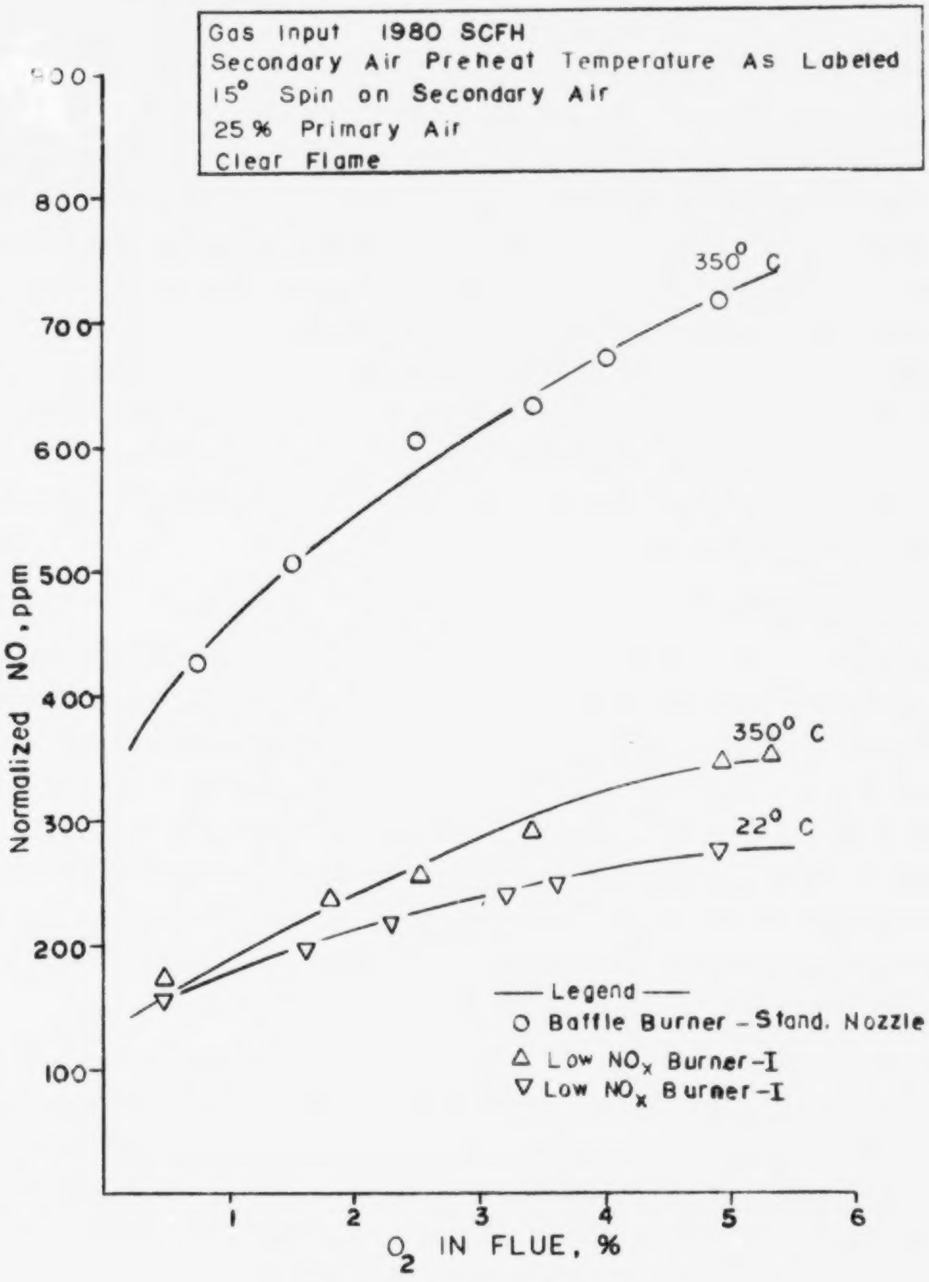

Figure 59. Normalized NO concentration as a function of flue O_2 with 25% primary air

a 2% level of excess O_2 (approximately 10% excess air), the LNO-I burner emitted 55% less normalized NO than the IFLB burner. This decrease in NO emissions dropped to 18% for NO secondary air preheat.

Flame Luminosity Adjustment

Adjusting the primary air and fuel so that no mechanically induced premixing occurred prior to ignition (luminous flame) did little to alter the LNO-I burner emissions without secondary air preheat. Figure 60 illustrates the normalized NO emissions versus excess O_2 for luminous flame operating conditions. With a 350°C secondary air temperature, the luminous flame had an NO level, at 2% excess O_2, 13% lower than that of the clear flame. Thus, the effect of the mixing rate of primary air and fuel on NO emissions is directly related to secondary air temperature. At ambient combustion air temperatures, the luminous and clear flames had nearly the same emission levels, but at the elevated (350°C) combustion air temperature, the clear flame had the higher emissions.

Variation in Primary Air

To determine the influence of primary air volume on NO formation, the amount of primary air was reduced to 15%. Figure 61 shows the normalized NO-versus-excess O_2 relationships determined for this primary air volume. The clear flame with 350°C secondary air preheat displayed little change in NO emissions between 15% and 25% primary air. The luminous flame was somewhat more sensitive to primary air volume, yielding a 10% increase in the NO emission levels at the lower primary air level. Thus, if a luminous flame is needed for the desired industrial application, the higher the percentage of primary air, the lower the NO emissions.

With an ambient secondary air temperature, both flame conditions produced the lowest levels of NO measured during the burner trial series, indicating that the percentage of primary air should be reduced as the secondary air preheat temperature is decreased. To completely generalize the dependence of NO emissions on primary air volume would require testing above 25% primary air; however, because of primary fan capacity, these trials were not possible.

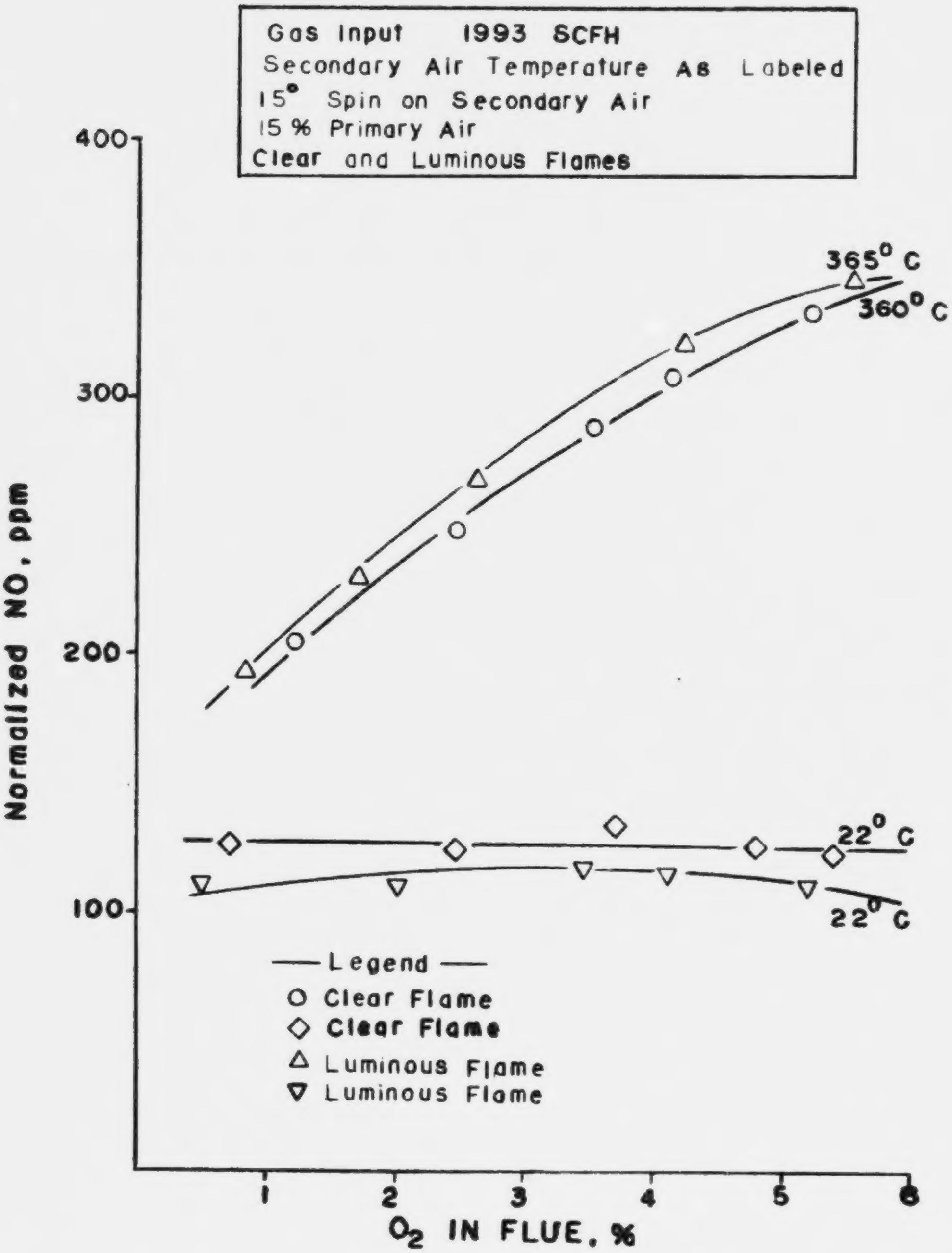

Figure 60. Normalized NO concentration as a function of flue O_2 for the LNO-I burner under luminous-flame operating conditions

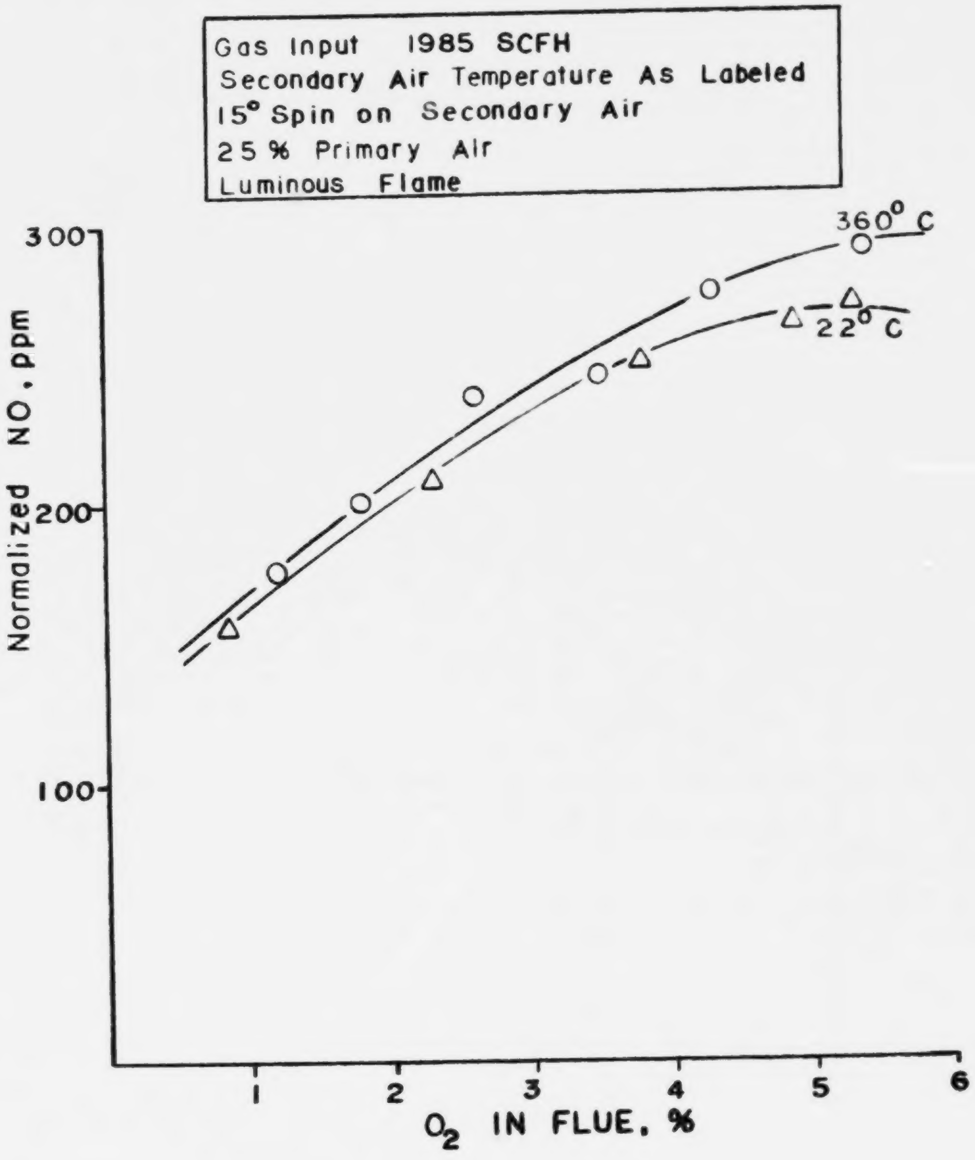

Figure 61. Normalized NO concentration as a function of flue O_2 for the LNO-I burner with 15% primary air

SUMMARY OF BAFFLE BURNER

A synopsis of the operational variables studied and their test results is presented in Table 6. The technique resulting in the most dramatic reductions of NO emission levels was external flue-gas recirculation. This verified the intimate relationship between flame temperature and NO emissions; thus, this program's efforts concentrated on reducing flame temperature either by reducing the rate of combustion or by diluting the flame with combustion products recirculated within the furnace using combustion aerodynamics.

Although large variations in NO emissions occur because of changes in the amount of excess air, reduction levels can be established in addition to their relative effectiveness by comparing the emission levels at several fixed levels of excess air. The conclusions reached below are based on an excess air level equivalent to 3% oxygen in the flue and a combustion air preheat temperature of 450°C.

For the intermediate flame length baffle burner (IFLB), which has a tangential-to-axial velocity component ratio of 0.27:

a. Reducing the firing rate from 3000 SCFH to 2000 SCFH resulted in a 47% reduction in NO emissions.

b. Reducing the combustion air preheat from 450°C to 225°C leads to a 59% reduction in NO emissions, and no preheat gives a 78% reduction.

c. By cooling the walls from 1400°C to 1100°C, the NO emissions diminished by 55%.

d. External flue-gas recirculation reduced NO emissions by 69% for 15% recirculation and 90% for 30% recirculation.

e. Several types of fuel injectors and positions were tested with a maximum reduction of 67% measured for the high-momentum axial nozzle in the throat position. The minimum changes in flame geometry and luminosity were observed for the divergent nozzle, which showed a 48% decrease in NO emissions.

f. The burner block angle was increased from 4-degrees to 8-degrees, leading to only a 4% reduction under standard burner operating conditions. However, by also changing the method of fuel injection a maximum reduction of 60% was measured with the high-momentum axial gas nozzle.

Table 6. SYNOPSIS OF DATA COLLECTED FOR THE BAFFLE BURNER

Excess Oxygen, %	1	3
Normalized NO, ppm		
IFLB Burner (Standard operating conditions: gas input, 3000 SCF/hr; 450°C, secondary air preheat; 2-inch-diameter axial fuel injector; baffle fuel injector; baffle position; and a 1400°C wall temperature, 4-degree burner block.)		
Standard Operation	390	580
Gas Input, 2000 SCF/hr	250	310
Secondary Air Temperature: 225°C	195	235
22°C	110	125
Wall Temperature, 1100°C	225	260
EFGR 15%	130	180
EFGR 30%	40	60
Radial Nozzle-Throat Position	200	260
Axial Nozzle-Throat Position	110	190
Throat Position	280	390
Divergent Nozzle	190	300
Axial Nozzle	210	250
8-Degree Burner Block (B. B.)	410	560
8-Degree B. B.-Axial Nozzle	200	230
8-Degree B. B.-Divergent Nozzle	220	350
SFLB Burner (Standard operating conditions: gas input, 3000 SCF/hr; 450°C, secondary air temperature; 2-inch-diameter axial fuel nozzle; baffle position; 8-degree burner block angle; and 1400°C average wall temperature.)		
Standard Operation	450	660
Gas Input, 2000 SCF/hr	270	430
Secondary Air Velocity, 125 ft/s	210	250
Secondary Air Temperature: 225°C	165	270
22°C	95	160
Wall Temperature, 1000°C	270	320
EFGR 15%	100	150
EFGR 30%	60	80
Radial Nozzle	660	800
Divergent Nozzle	440	580
Axial Nozzle	210	390
16-Degree Burner Block (B. B.)	210	380
16-Degree B. B.-Divergent Nozzle	180	400
16-Degree B. B.-Axial Nozzle	300	390
– Cylindrical Furnace –		
IFLB Burner (Standard operating conditions: gas input, 2000 SCF/hr, 350°C, secondary air temperature; 2-inch diameter axial fuel nozzle, baffle position, 4-degree burner block angle and 1100°C average wall temperature.)		
Standard Operation	460	610
Axial Nozzle	880	1170
Divergent Nozzle	825	1090
LNOX-I	180	280

For the short flame length baffle burner (SFLB), which has a tangential-to-axial velocity component ratio of 0.47:

a. Reducing the firing rate from 3000 SCFH to 2000 SCFH resulted in a 35% decrease in NO emissions.

b. With a 2000 SCFH gas input, the combustion air velocity was increased from 80 ft/s to 125 ft/s, which diminished the NO emissions by 42%

c. Reducing the combustion air temperature from 450°C to 225°C resulted in a 59% NO reduction and, with no preheat, a 76% reduction.

d. Decreasing the wall temperature from 1400°C to 1000°C reduced the NO emissions by 52%.

e. Externally recirculating flue gas and blending it with the combustion air produced a 77% decrease in emissions for 15% recirculation and 89% reduction for 30% recirculation.

f. Of the several types of fuel injectors tested, the high-momentum axial nozzle produced the minimum emissions with a 41% reduction.

g. The burner block angle was increased from 8-degrees to 16-degrees. This produced a 41% decrease in NO emissions for all gas nozzles tested.

The IFLB burner was tested on IGT's cylindrical test furnace, which has a volume of 226 ft^3 and an area ratio between the burner block opening and the burner wall of 18.2 compared with a 35.9 ratio for the rectangular furnace. During these trials the following observations were made:

a. At a 2000 SCFH firing ratio, the cylindrical furnace emissions were 97% greater than the emissions from the rectangular furnaces.

b. The high-momentum axial and the divergent nozzles produced increases in the NO emissions of 92% and 79%, respectively, although both produced reductions in NO emissions on the rectangular furnace.

This program has led to the design, development, and testing of a low-NO-emissions burner (LNOX-I), which, hopefully because of its versatile design, could be used in a large number of industrial applications. The following conclusion was drawn from the test data accumulated from LNOX-I:

- With 2000 SCFH firing rate on the cylindrical furnace, the LNOX-I burner resulted in a 54% reduction in NO emissions when compared with the IFLB burner under similar operating conditions.

UTILITY BOILER BURNER

An assembly drawing of the movable-vane boiler burner (MVBB) which was investigated during this program is shown in Figure 5. The combustion air enters perpendicular to the axis of the burner and passes through a register of guide vanes that impart a degree of spin to the air dependent on the vane orientation. Figure 6 illustrated how the angle of the movable vanes is measured. The ratio of the average tangential and radial velocity components at the exit of the movable-vane register depends only upon the geometric dimensions of the vanes on the axis perpendicular cross section (assuming a negligible Reynolds number influence). Leuckel has shown that this ratio equals —

$$\sigma = \frac{1}{1 - B} \cdot \frac{\tan \alpha}{1 + \tan \alpha \tan (\pi / n)} \qquad (1)$$

where —

$$B = \frac{nt}{2\pi R_1 \cos \alpha} \qquad (2)$$

is a blockage factor which accounts for the finite thickness t of the vanes, and n is the number of vanes in the register. The radial velocity component at the swirl exit (radius R_1 in Figure 6) is given by —

$$V = \frac{\dot{M}}{\rho 2\pi R_1 A} \qquad (3)$$

where $\dot{M}$ is the mass flow rate and A is the axial width of the channels. Knowing V and σ, the tangential velocity can be determined using the relationship —

$$W = \sigma V \qquad (4)$$

There are two fuel injectors commonly used with the MVBB — a "gun" (a pipe with a hemispherical cap) and a "ring" (two pipes, semicircular in shape with their ends capped). The gun injector is the least expensive and therefore was installed with many of the older burners. However, because of improved flame stability and lower NO_x emissions, the ring injector is being installed with most new burners. The total orifice area for an injector is 0.0491 sq in. for a 1762 SCFH natural gas throughput.

The ring injector (Figure 62) has the gas orifices clustered in eight groups with each group being separated by a 45-degree angle. The number of holes in a cluster can vary from three to nine. The orifices in a cluster are of different sizes, the largest hole being located in the center of the cluster and the smallest at the outside edge of the group. Thus, for the "No. 3" ring injector there are two different sizes of holes, while the "No. 5" ring injector has three different sizes of holes. The design criteria for determining the size of these holes for each injector was supplied by a utility boiler manufacturer. As an example: for the No. 3 ring injector with a normal input of 3000 SCFH of natural gas;

- The total orifice area of the ring will be 0.0836 sq in.
- The area of the center hole of a cluster will be (0.072)·(0.0836 sq in.) or 0.0059 sq in. (an approximate diameter of 3/32 inch).
- The area of each of the two smaller holes flanking the center hole will be (0.0268)·(0.0836 sq in.) or 0.0022 sq in. (an approximate diameter of 3/64 inch).
- Making the holes with 3/32 and 3/64-inch drill bits would make a total orifice area of 0.0828 sq in. (less than a 1% difference from the design area of 0.0836 sq in.).

The No. 5 ring injector would have the same total orifice area (0.0836 sq in.) as the No. 3 ring injector because it is also being designed for a 3000 SCFH throughput of natural gas. However, because there are five holes per cluster instead of three, the cross-sectional area of the holes will be different. For the No. 5 ring injector —

- The area for the center hole of the cluster will be (0.07)·(0.0836 sq in.) or 0.0058 sq in. (an approximate diameter of 5/64 inch).
- The area of the medium-size holes directly flanking the center hole will be (0.019)·(0.0836 sq in.) or 0.0016 sq in. (an approximate diameter of 3/64 inch).
- The two smallest holes, which are located at the outside edges of the cluster, have an area of (0.0094)·(0.0836 sq in.) or 0.0008 sq in. (an approximate diameter of 1/64 inch).

Thus, for the 3000 SCFH gas input, there is little difference between the orifices of the No. 3 and the No. 5 ring injectors. As a result, all the MVBB tests with a ring fuel injector were conducted using only a No. 3 ring. A drawing of the injection port arrangement for the No. 3 ring nozzle is presented in Figure 62.

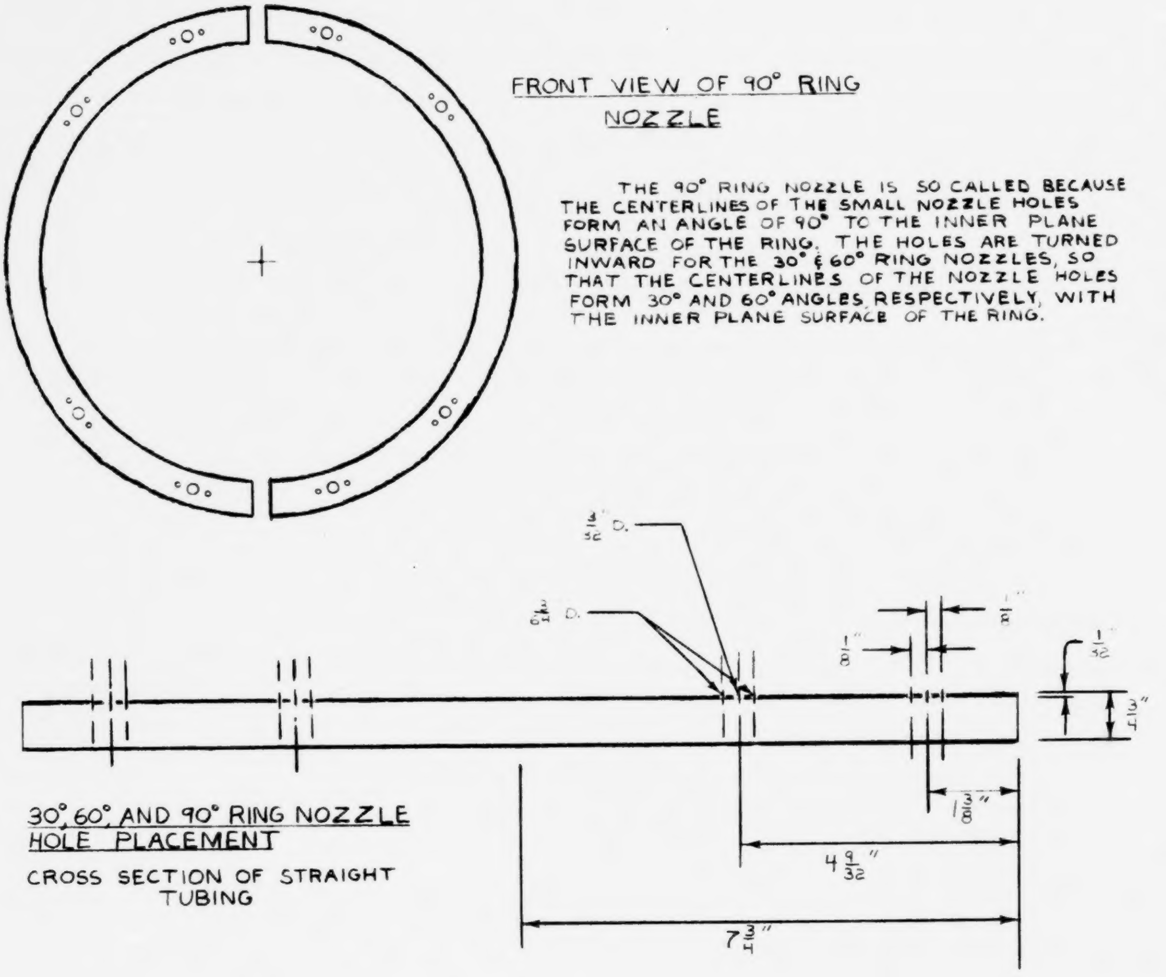
FRONT VIEW OF 90° RING NOZZLE
THE 90° RING NOZZLE IS SO CALLED BECAUSE THE CENTERLINES OF THE SMALL NOZZLE HOLES FORM AN ANGLE OF 90° TO THE INNER PLANE SURFACE OF THE RING. THE HOLES ARE TURNED INWARD FOR THE 30° & 60° RING NOZZLES, SO THAT THE CENTERLINES OF THE NOZZLE HOLES FORM 30° AND 60° ANGLES RESPECTIVELY, WITH THE INNER PLANE SURFACE OF THE RING.
3/32" D.
3/64 D.
1/8"
1/8"
1/32"
3/4"
1 3/8"
4 9/32"
7 3/4"
30°, 60°, AND 90° RING NOZZLE HOLE PLACEMENT
CROSS SECTION OF STRAIGHT TUBING

Figure 62. Ring fuel injector

The gas orifices on a ring injector can be rotated relative to a radial line passing from the centerline of the burner through the radial axis of the injector. The normal industrial rotation is 30 degrees toward the combustion chamber. In these trials tests were also conducted at 60-degree and 90-degree rotations.

The gun injector normally has six orifices. These are positioned symmetrically on a 60 degree conic section relative to the centerline of the injector. For industrial injectors, there are two different sizes of orifices, which are arranged in alternating order. The designed area ratio between the different-sized holes is 0.76, which, for the momentum-scaled injector to be used in our trials, would require orifice diameters of 8/64 inch and 9/64 inch. Because of the small size difference we decided to use only the 8/64-inch diameter hole. A drawing of the hemispherical caps used with the gun nozzle is presented in Figure 63.

A second criterion in fuel injector design is to design the nozzle so that the fuel will have the desired trajectory when leaving the orifice. For subsonic velocities and incompressible fluids, a path length of 5 to 10 orifice diameters is required to achieve the proper trajectory. A sonic fluid, however, will exit with its velocity component at the center of the orifice normal to the surface tangent. There is a directional velocity distribution about each orifice. For a sonic fluid, this directional velocity distribution is independent of wall thickness.

For a utility boiler burner, the fuel injector is designed for critical sonic flow. Thus, the manufacturer is able to achieve the desired initial fuel trajectory using thin-walled pipe or tubing at the expense of requiring a high gas-line pressure. A normal operating line pressure would be 30 psig.

The burner block used during the base-line characterization trials of the 30-degree ring nozzle had a 30-degree divergent angle with a 15.2-inch-diameter entrance and a 48.2-cm-diameter exit to the furnace. Three nozzle positions were investigated, as illustrated in Figure 64. When the nozzle is located 2.5 cm (1 in.) from the burner block exit and is within the 15.2-cm-diameter refractory duct connecting the burner with the block, the location is called the throat position. The exit position has the gas injector located 5.1 cm (2 in.) into the divergence of the burner block. When the nozzle is in the exit position and the deflector plate is positioned 2.5 cm from the tip of

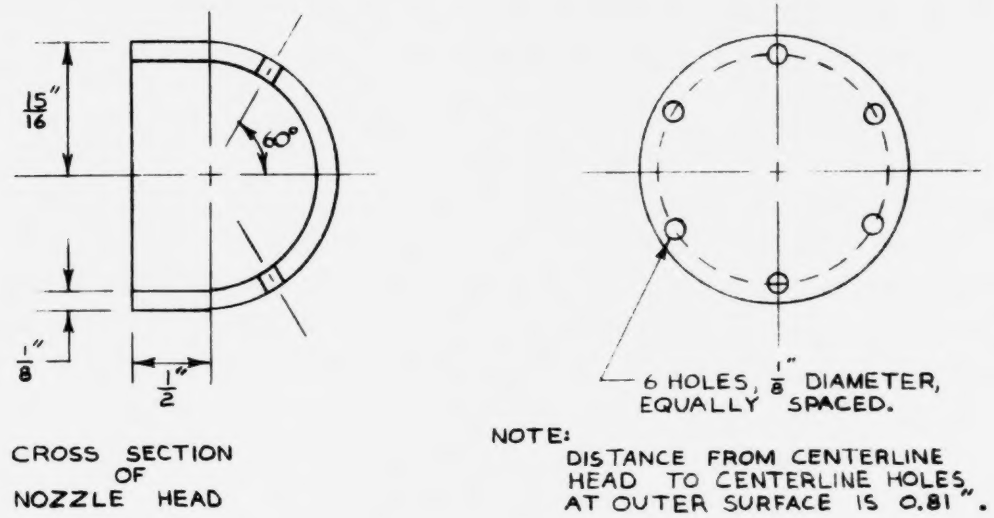
15/16"
60°
1/8"
1/2"
CROSS SECTION OF NOZZLE HEAD
6 HOLES, 1/8" DIAMETER, EQUALLY SPACED.
NOTE: DISTANCE FROM CENTERLINE HEAD TO CENTERLINE HOLES AT OUTER SURFACE IS 0.81".

60° NOZZLE HEAD

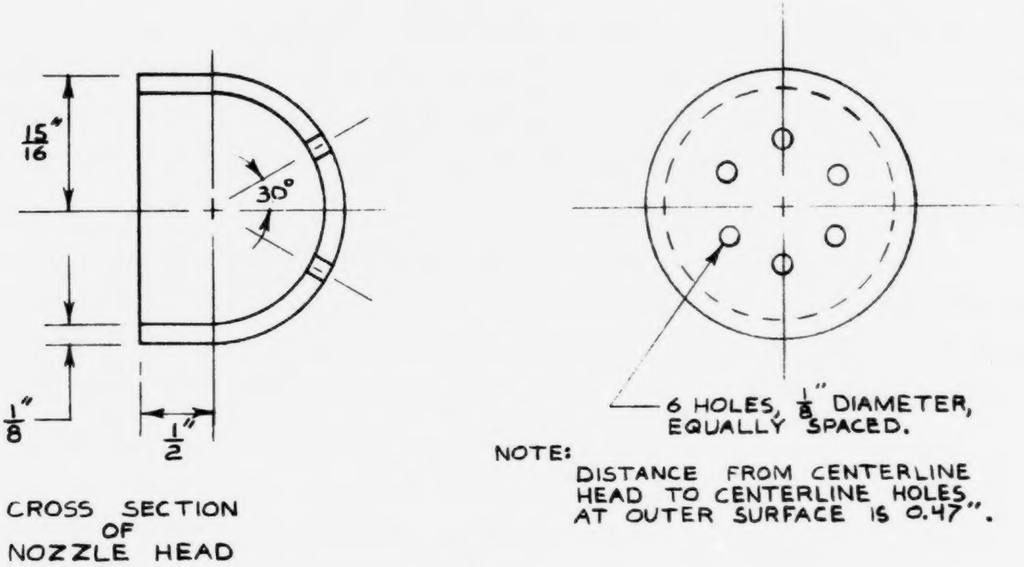
15/16"
30°
1/8"
1/2"
CROSS SECTION OF NOZZLE HEAD
6 HOLES, 1/8" DIAMETER, EQUALLY SPACED.
NOTE: DISTANCE FROM CENTERLINE HEAD TO CENTERLINE HOLES AT OUTER SURFACE IS 0.47".

30° NOZZLE HEAD

Figure 63. Nozzle heads for fuel gun injector

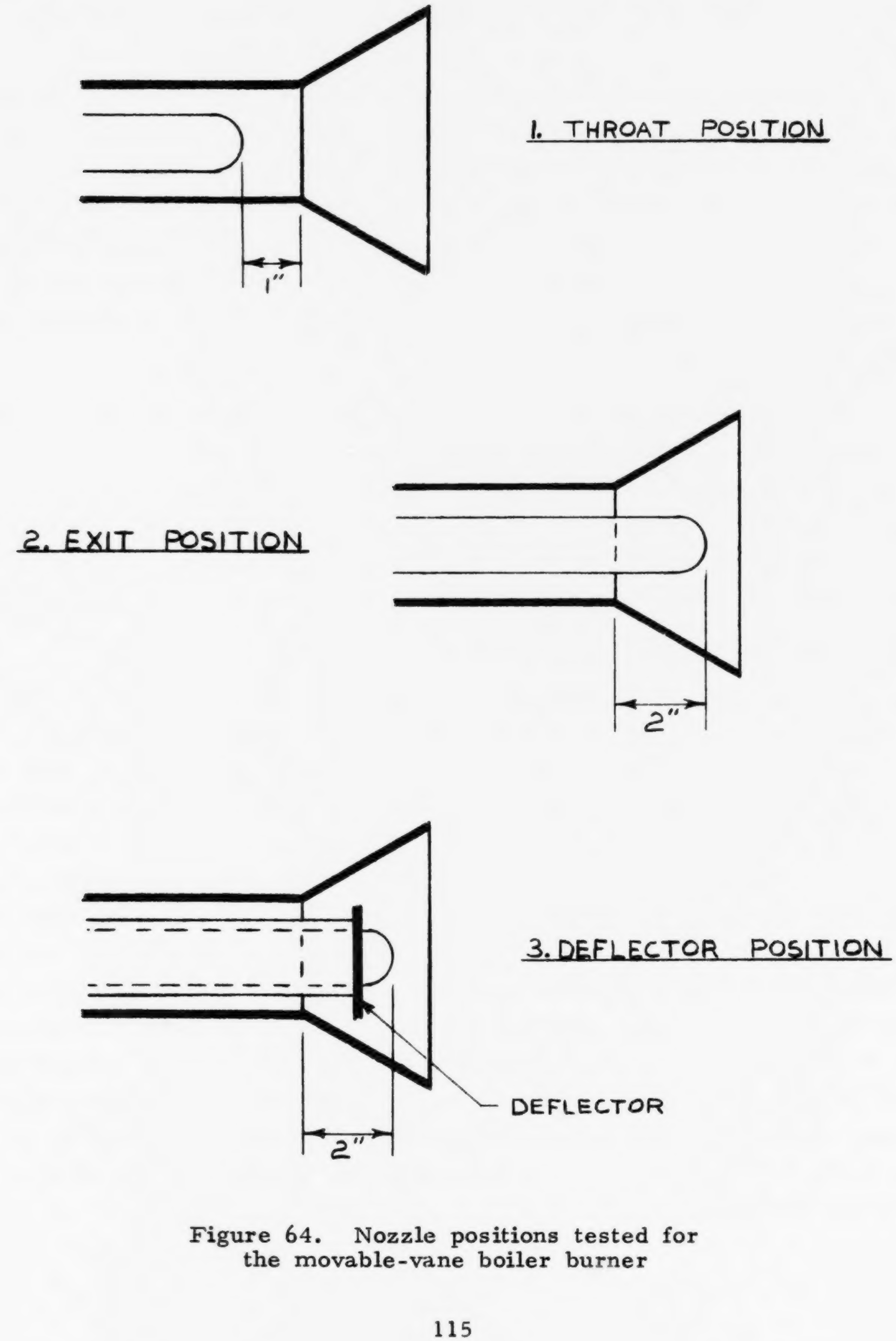
1. THROAT POSITION
1"
2. EXIT POSITION
2"
3. DEFLECTOR POSITION
DEFLECTOR
2"

Figure 64. Nozzle positions tested for the movable-vane boiler burner

the hemispherical cap, the location is called the deflector position. An illustration of the secondary combustion air deflector plate is given in Figure 65.

The base-line trials for the 60-degree gun and 30-degree ring nozzles were conducted with burner operating parameters similar to those found in industry. These operating conditions included a 470°C secondary combustion air temperature, a 30-degree vane setting, the exit nozzle position and a 3000 SCFH gas input. Measured CO levels greater than 500 ppm are listed by concentration next to their corresponding data point. Photographs of flames produced using these and other operating conditions are presented in Figures 65a and 65b.

Detailed flame surveys were conducted during the boiler burner trials. These surveys included flow direction, temperature and gas analysis. The details of this survey work along with complete in-the-flame data and a comprehensive listing of the input/output data are presented in Volume II. However, it is beneficial in understanding the interpretation of the input/output data to take a brief look at some in-the-flame data.

STANDARD CONDITIONS (60-Degree Gun Nozzle)

For the base-line operating conditions listed above with the 60-degree gun nozzle; Figure 66 presents the gas species and temperature data collected along the burner axis. The flow direction data reveals a flow profile of a type III. Thus the data in Figure 66 near the furnace front wall are reflecting properties of the primary recirculation zone. This is born out by the extremely high temperature measured at the burner block, 1660°C. The NO concentration is 187 ppm or 55% of the 340 ppm flue concentration. Unlike the kiln or baffle burner profiles there is no measurable amount of methane. The flame length was measured to be 33 cm compared to 186 cm for the kiln burner and 52 cm for the baffle burner. The NO emission test results for the 60-degree gun nozzle are plotted in Figure 67. Normalized NO is given as a function of excess oxygen in the flue and secondary air preheat. Unlike other burner-nozzle combinations at low and intermediate air preheats (22° and 244°C), the relationship of normalized NO versus flue oxygen has zero slope.

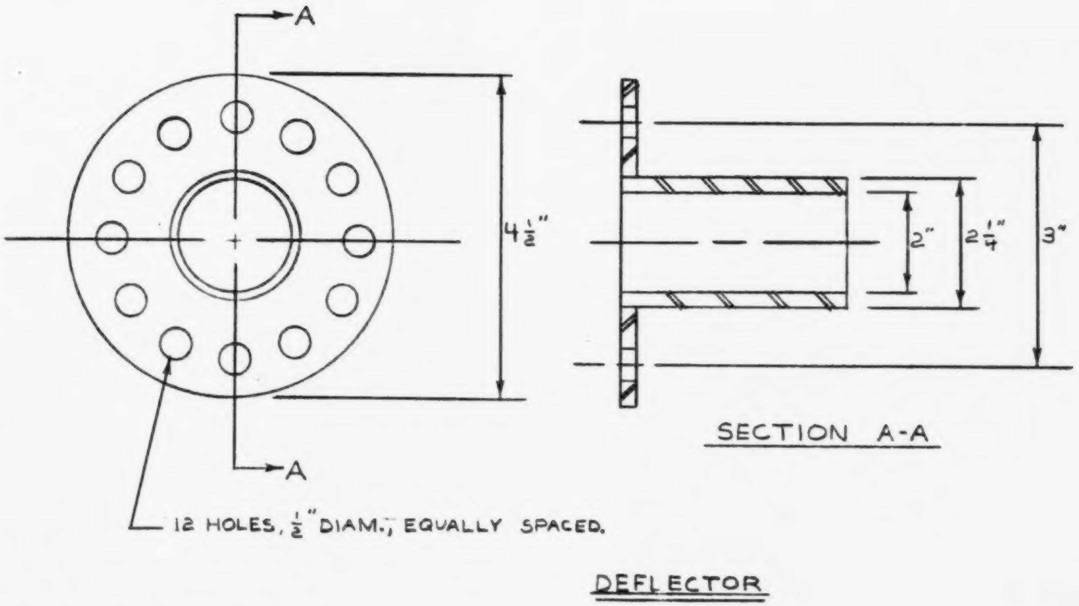
A
A
4½"
2"
2¼"
3"
SECTION A-A
12 HOLES, ½" DIAM., EQUALLY SPACED.
DEFLECTOR

Figure 65. Secondary combustion air deflector plate

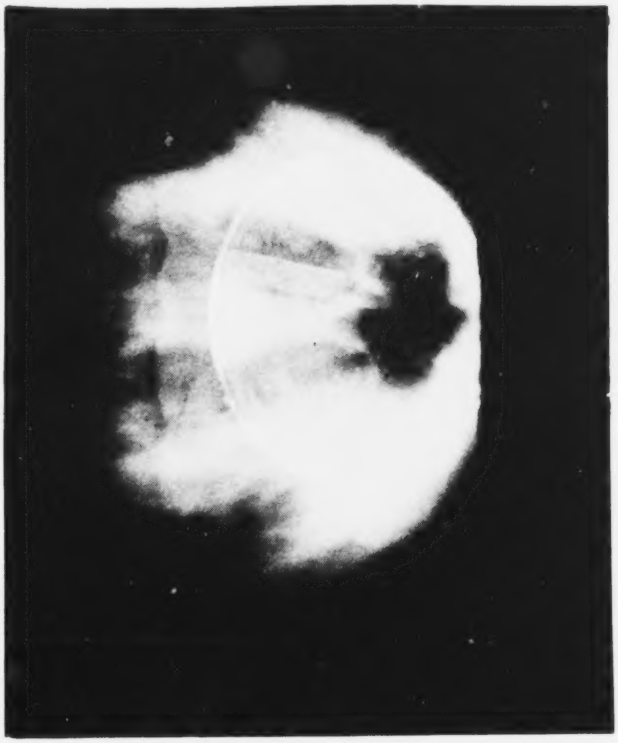

Figure 65a. 60-degree gun nozzle in exit position

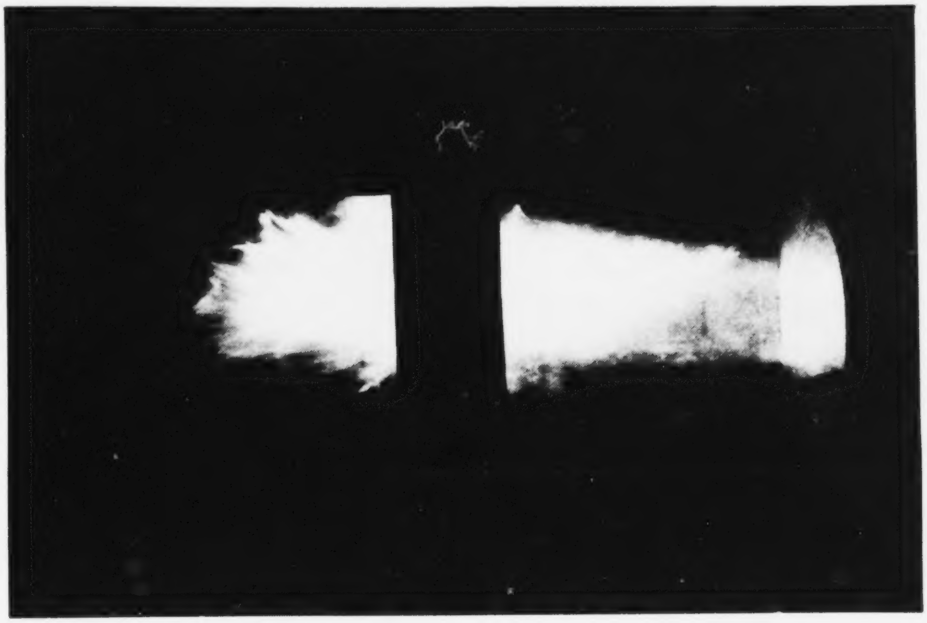

Figure 65b. 30-degree ring nozzle flame in deflector position

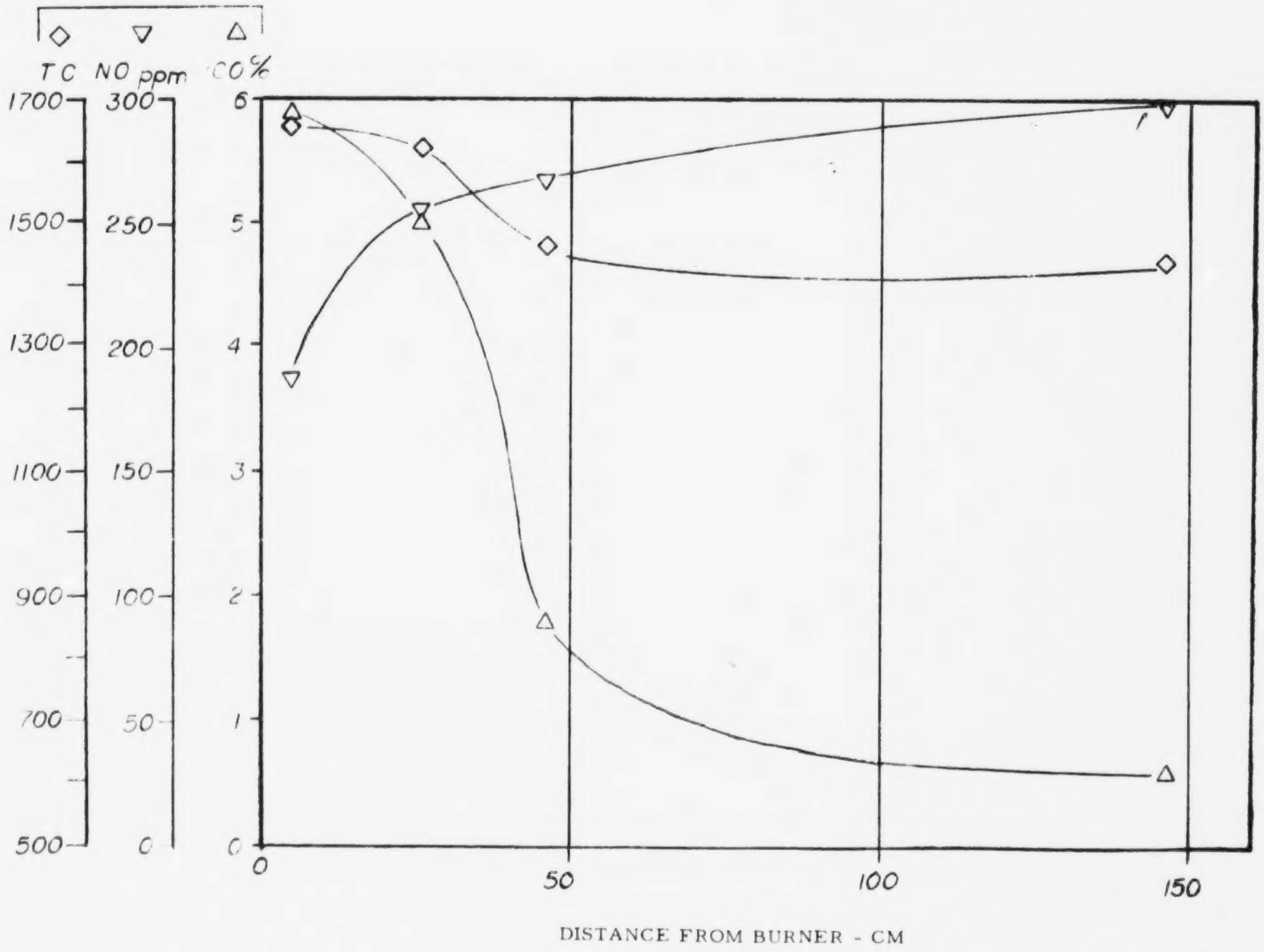

Figure 66. In-the-flame profiles of boiler burner operated under typical conditions

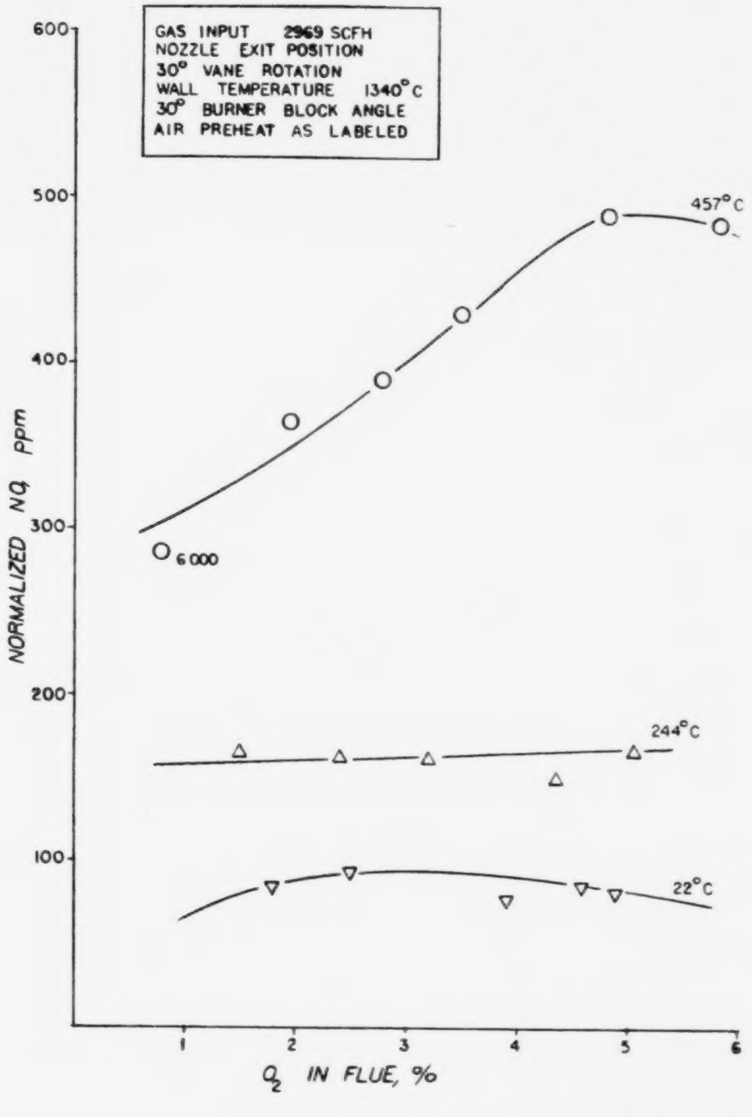

Figure 67. Normalized NO concentration as a function of flue O_2 for the movable-vane boiler burner with a 60-degree gun nozzle

EXTERNAL FLUE GAS RECIRCULATION (EFGR)
(60-Degree Gun Nozzle)

To determine how successful we can be applying combustion aerodynamics to recirculate combustion products to the base of the flame as an emission control technique, we simulated the idealized case (where the combustion air and products have been thoroughly mixed before ignition) by mixing flue gases with the combustion air outside the burner. Figure 68 compares the NO levels as a function of the percentage of oxygen in the flue for 0%, 15%, and 25% concentrations of flue-gas recirculation with the 60-degree gun gas nozzle. The percentage of flue-gas recirculation (FGR) is determined using the relationship —

$$\%\ \text{FGR} = \frac{\text{FGR (SCFH)}}{\text{Secondary air (SCFH)} + \text{Fuel (SCFH)}} \times 100$$

Again, as was demonstrated for the kiln and ported baffle burners, external flue-gas recirculation is an extremely effective method of controlling NO emissions from a natural gas flame. The cost of an external flue-gas system coupled with the additional fan horsepower needed to move the gas back into the plenum makes its adoption as an industrial emissions control device undesirable; therefore, it is prudent to use combustion aerodynamics to move the flue gas back close to the burner and to mix it as thoroughly as possible with the air and gas. Referring back to the Flow Analysis section and Figure 15, the zones containing combustion products, which for the most part are inert to the kinetics of NO_x formation, are the secondary recirculation zone and, to a lesser degree, the primary recirculation zone.

NOZZLE POSITION (60-Degree Gun Nozzle)

Our first attempts at altering the combustion aerodynamics to favor reduced NO_x emissions for the 60-degree gun nozzle were to use the three nozzle positions depicted in Figure 64. These NO emission test results are illustrated in Figure 69. From flame photographs, we were able to determine a visual flame length of 76.6 cm. Although the flame length was independent of the gas nozzle position, the luminosity of the flame was not. With the gas nozzle in the throat position, the flame was entirely blue (no luminosity). At the exit position, only the base of the flame was blue, with

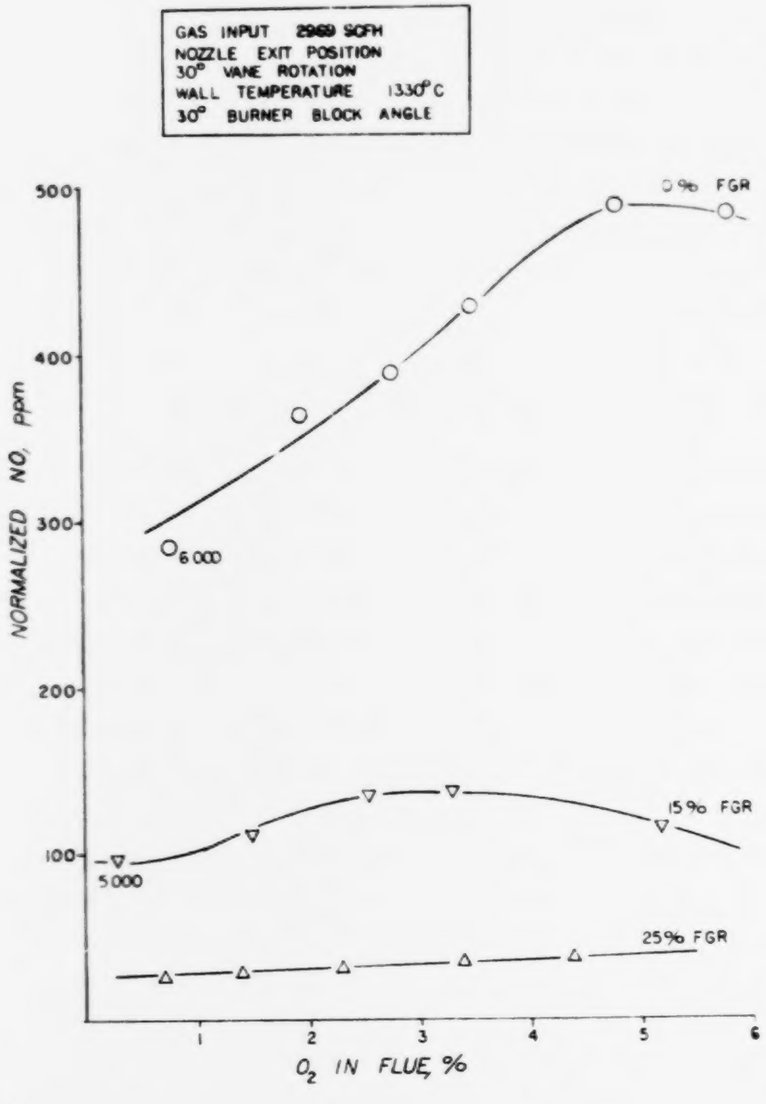

Figure 68. Normalized NO concentration as a function of flue O_2 for the movable-vane boiler burner with a 60-degree gun nozzle, 1.5% and 2.5% FGR

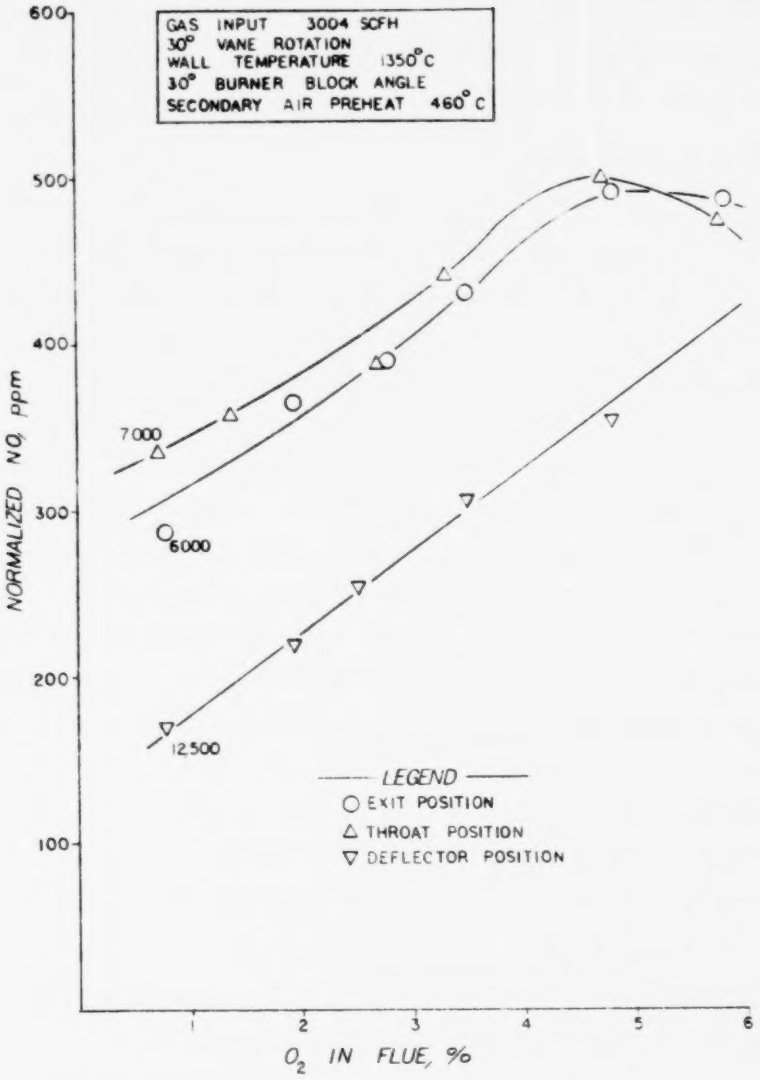

Figure 69. Normalized NO concentration as a function of flue O_2 for the movable-vane boiler burner with a 60-degree gun nozzle in different positions

80% of the flame displaying a high degree of luminosity. The deflector position displayed a central blue core, with luminosity occurring only at the flame boundaries. All three nozzle positions should exhibit a type III flow profile. The deflector plate position is obviously the most desirable as it shows a decrease in normalized NO of 132 ppm at 2% excess oxygen or 37% of the concentration measured in the exit position.

NOZZLE TYPE

A second technique for modifying the combustion aerodynamics is to vary the velocity components (both direction and magnitude) of the fuel. To this end, three modified fuel injectors were tested: a low-momentum axial nozzle (injection velocity of 12 m/s), a high-momentum axial nozzle (injection velocity of 186 m/s), and a divergent nozzle (injection velocity of 199 m/s). The results of these trials are plotted in Figure 70. All of these data were collected with the nozzles in the throat position. The low-momentum axial nozzle gave rise to the higher emission levels. This would imply that the low-momentum nozzle resulted in the highest flame temperatures, with minimum entrainment of recirculating combustion products. The circumference of the fuel jet was 2.5 cm upon injection, which should indicate the relative size of the mass-exchange boundary layer between the fuel and the air. A comparison of the fuel injection velocity (12 m/s, axial) and the velocity of the combustion air (23.4 m/s, axial; and 18.8 m/s, tangential) in the throat of the burner block indicates that the mixing is air-momentum controlled. Thus, the low-momentum nozzle should result in a rapidly mixing flame, with a very short length and a type III flow profile.

Except at low levels of excess air (below 1.5% excess oxygen and a 10.5:1 air/fuel ratio), the 60-degree gun and divergent nozzles have similar levels of NO emissions. Both nozzles inject the fuel with a diverging flow relative to the burner axis. The gun nozzle introduces the fuel as six jets, each with a 0.3-cm circumference and a sonic velocity. The divergent nozzle produces a single jet with a 199 m/s velocity and a 1.2-cm circumference. Because of the mechanically induced mixing created by a diverging injector and the resulting void of fuel created on the burner axis, both of these nozzles will give a type III flow profile.

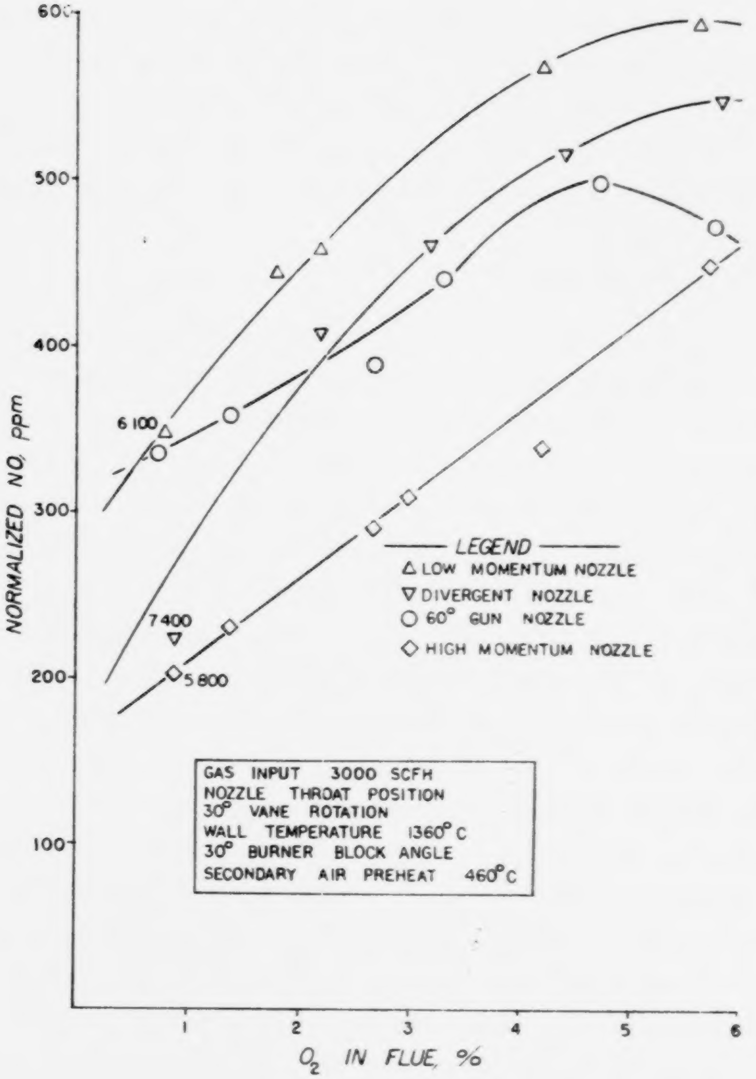

Figure 70. Normalized NO concentration as a function of flue O_2 for the movable-vane boiler burner with a composite plot of gas nozzles

The high-momentum nozzle should produce a type II flame because of the high axial velocity (186 m/s) of the fuel. The flame resulting from this nozzle is the longest studied, despite having a larger fuel/air velocity gradient than the low-momentum axial nozzle. This would indicate that the area of the mass-exchange boundary layer is the dominant factor in mixing control. This area is only 1.2 cm for the high-momentum nozzle compared with 2.5 cm for the low-momentum nozzle. The high-momentum nozzle yields slower mixing, lower flame temperatures, and lower emissions than the other injectors.

VANE ANGLE (SWIRL)
(60-Degree Gun Nozzle)

To investigate the effect of secondary combustion air swirl on the combustion aerodynamics and, more importantly, the influence it has on the formation of NO_x, trials similar to those discussed previously were conducted by varying the rotation of the vanes. The orientations studied were 15 degrees, 45 degrees, and 60 degrees. The results of the individual tests are plotted in Figures 71 through 75. We decided that the most effective way to compare the results of these tests would be to determine the relationship between the level of normalized NO emissions and the tangential/radial velocity ratio. First, a quantitative relationship between the vane orientation and the velocity ratio must be made. This is accomplished using Equations 1 and 2 of this section. The results of these calculations are shown in Figure 76. Table 7 lists the values calculated for σ. Note that the measured orientations of the vanes, listed as α_M, are different than the stated orientation, α. This is due to an error in fabrication. However, by using Equations 3 and 4, it is possible to calculate the magnitude of the radial and tangential velocity components, which are listed as V and W, respectively. Also listed in Table 7 are the normalized NO emissions for the 60-degree gun nozzle in the exit and deflector positions and the pressure drop in the plenum in inches of water. (Velocity, NO concentrations, and plenum pressure drops were all quantified at 2% excess oxygen.)

Figure 77 illustrates the relationship between normalized NO and the tangential/radial velocity ratio for the 60-degree gun in the exit and deflector positions. The exit position shows a maximum in NO emissions at a velocity ratio of 1.63 or a 57-degree vane rotation. This gives good agreement with

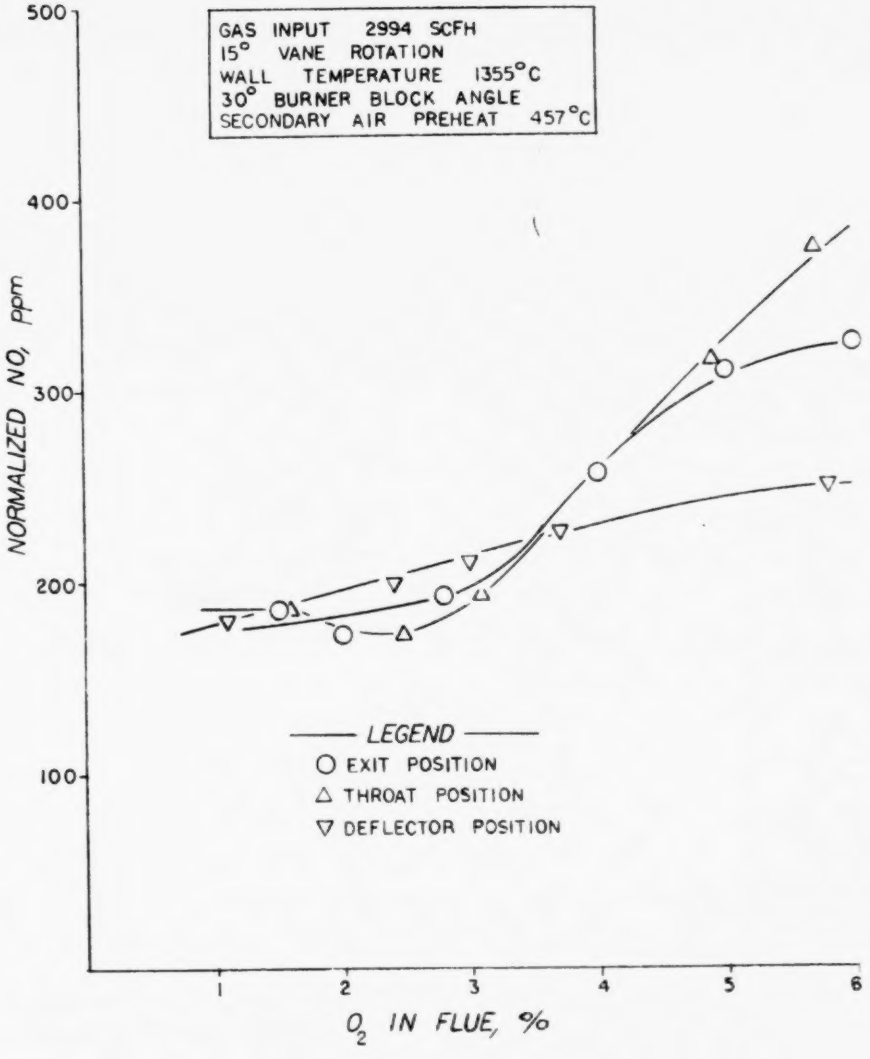

Figure 71. Normalized NO concentration as a function of flue O_2 for the movable-vane boiler burner with a 60-degree gun nozzle in different positions and a 15-degree vane angle

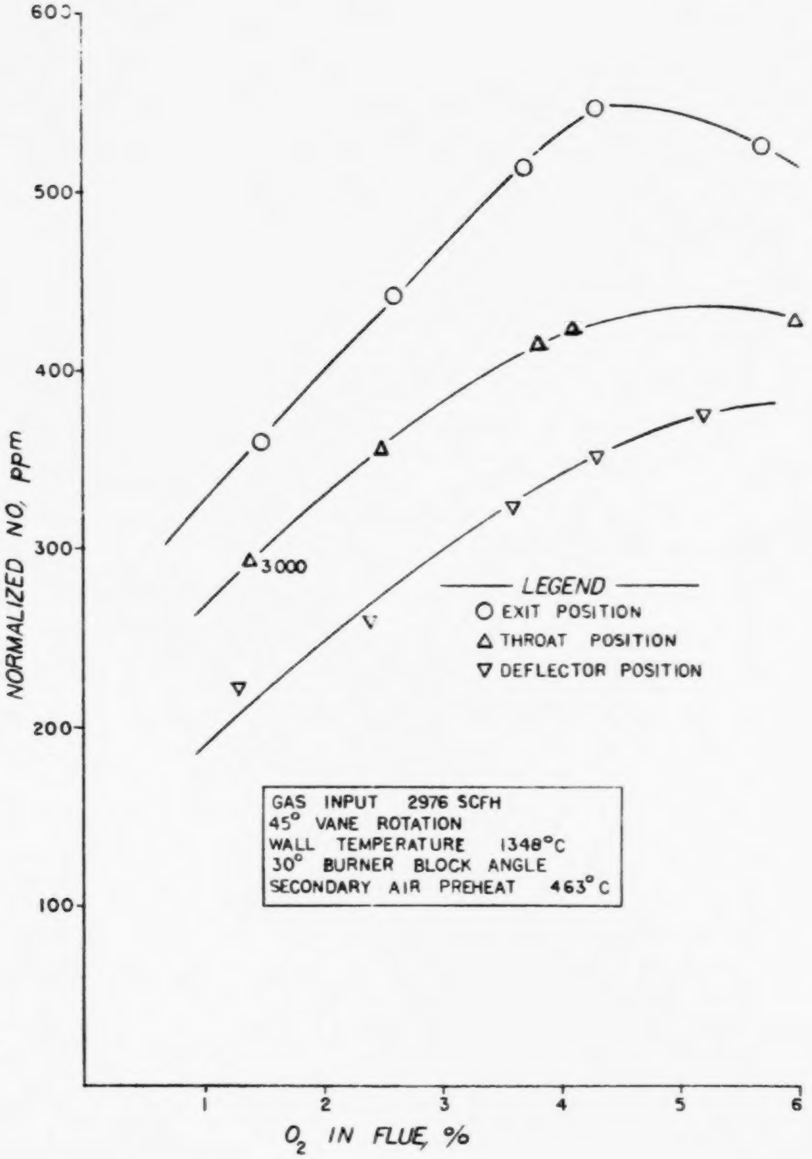

Figure 72. Normalized NO concentration as a function of flue O_2 for the movable-vane boiler burner with a 60-degree gun nozzle in different positions and a 45-degree vane angle

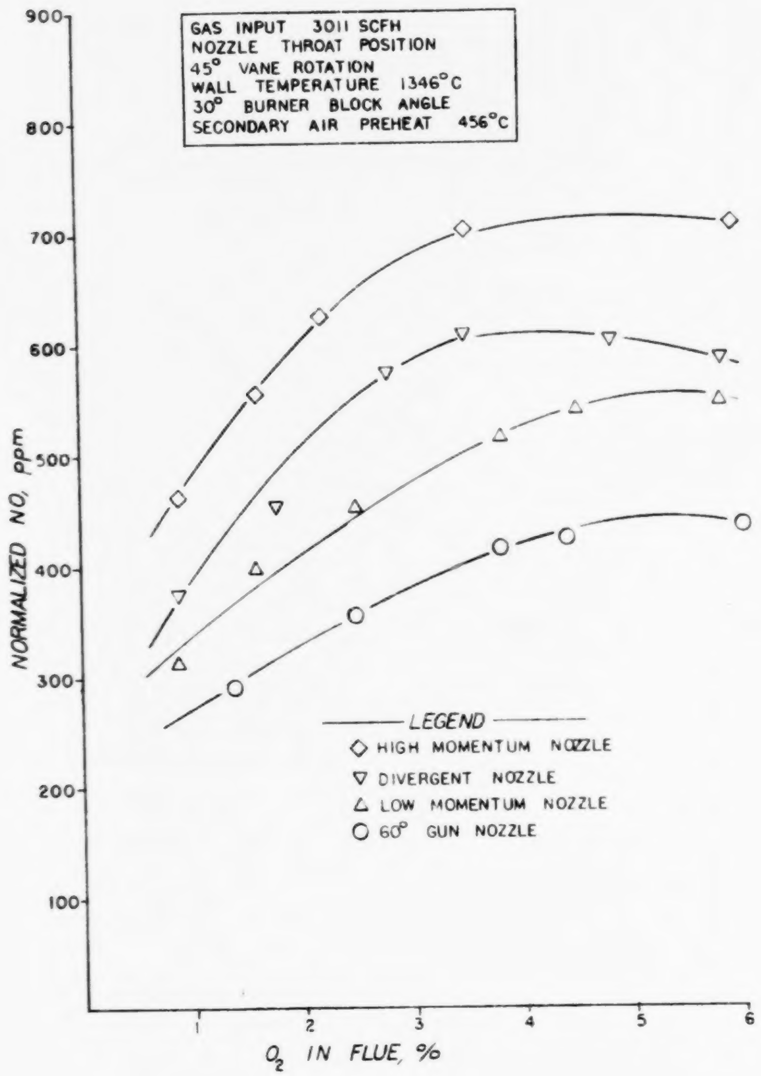

Figure 73. Normalized NO concentration as a function of flue O_2 for the movable-vane boiler burner with a composite plot of gas nozzles at a 45-degree vane angle

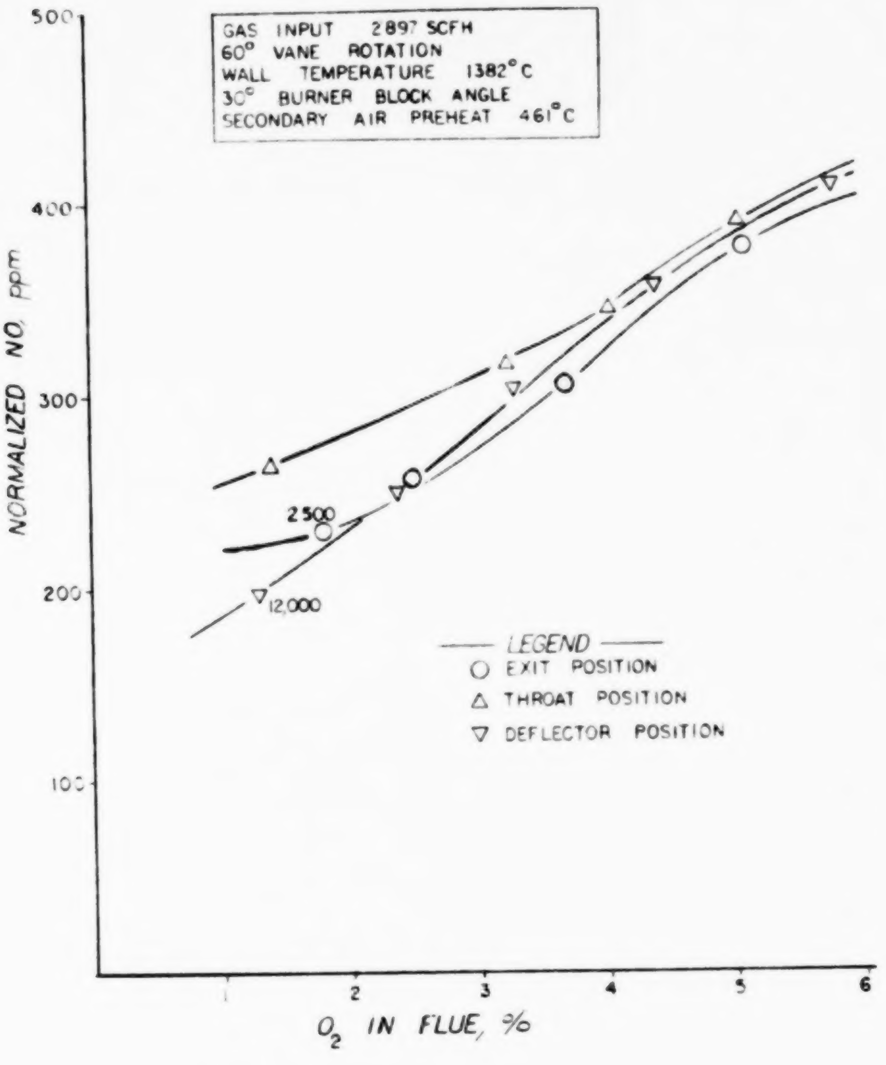

Figure 74. Normalized NO concentration as a function of flue O_2 for the movable-vane boiler burner with a 60-degree gun nozzle in different positions and a 60-degree vane angle

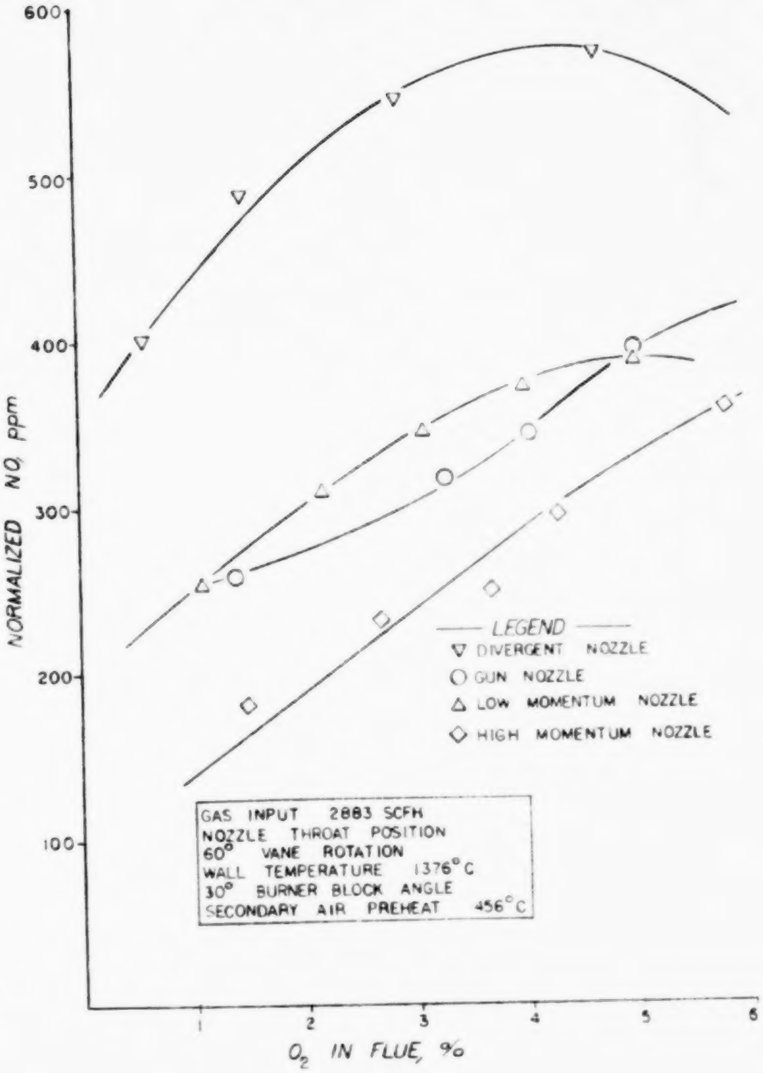

Figure 75. Normalized NO concentration as a function of flue O_2 for the movable-vane boiler burner with a composite plot of gas nozzles at a 60-degree vane angle

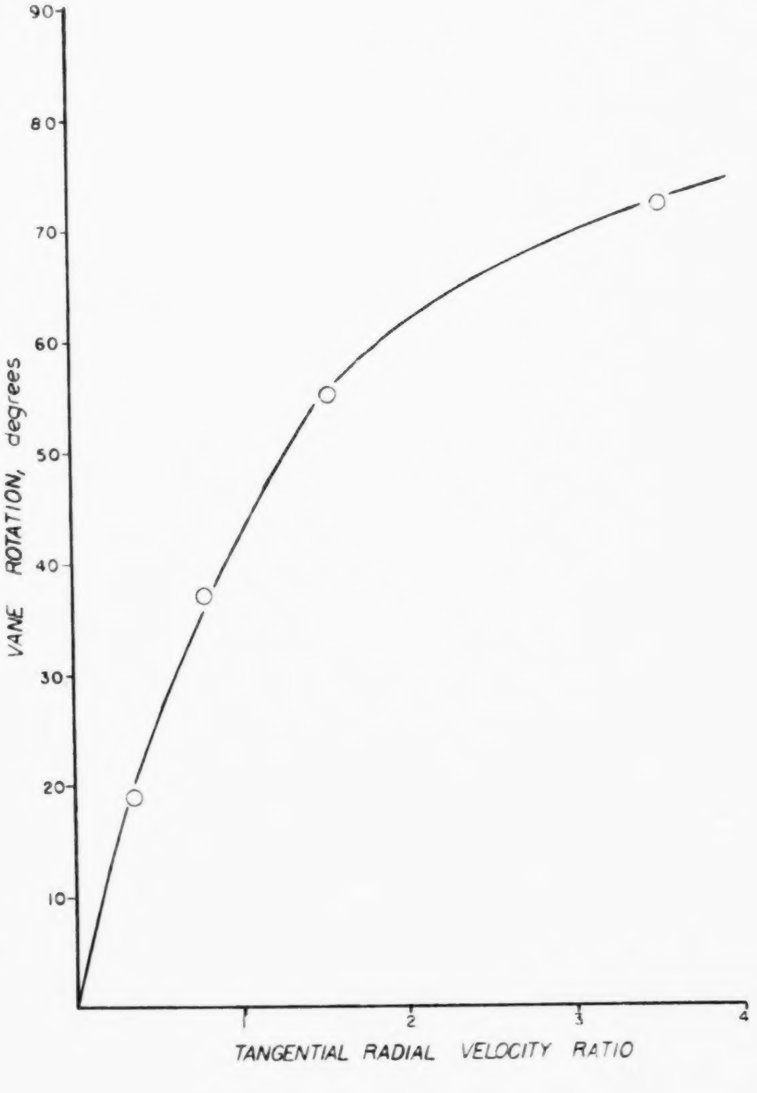

Figure 76. Tangential/radial velocity ratio as a function of vane angle

Table 7. LISTING OF BURNER OPERATING CONDITIONS AS A FUNCTION OF VANE ANGLE FOR THE 60-DEGREE GUN NOZZLE (Gas Input, 2996 SCFH; Exit and Deflector Positions; 1340°C Wall Temperature; 30-Degree Burner-Block Angle; 460°C Secondary Air Preheat Temperature)

α	α_M	σ	V	W	Normalized NO, ppm		Burner ΔP_1, in H_2O
			ft/s	ft/s	Exit	Deflector	
15	19	0.37	33.8	12.4	183	197	1.3
30	37	0.81	31.9	25.7	357	225	1.9
45	55	1.55	29.6	46.0	398	247	2.6
60	72	3.54	26.3	93.0	233	227	3.3

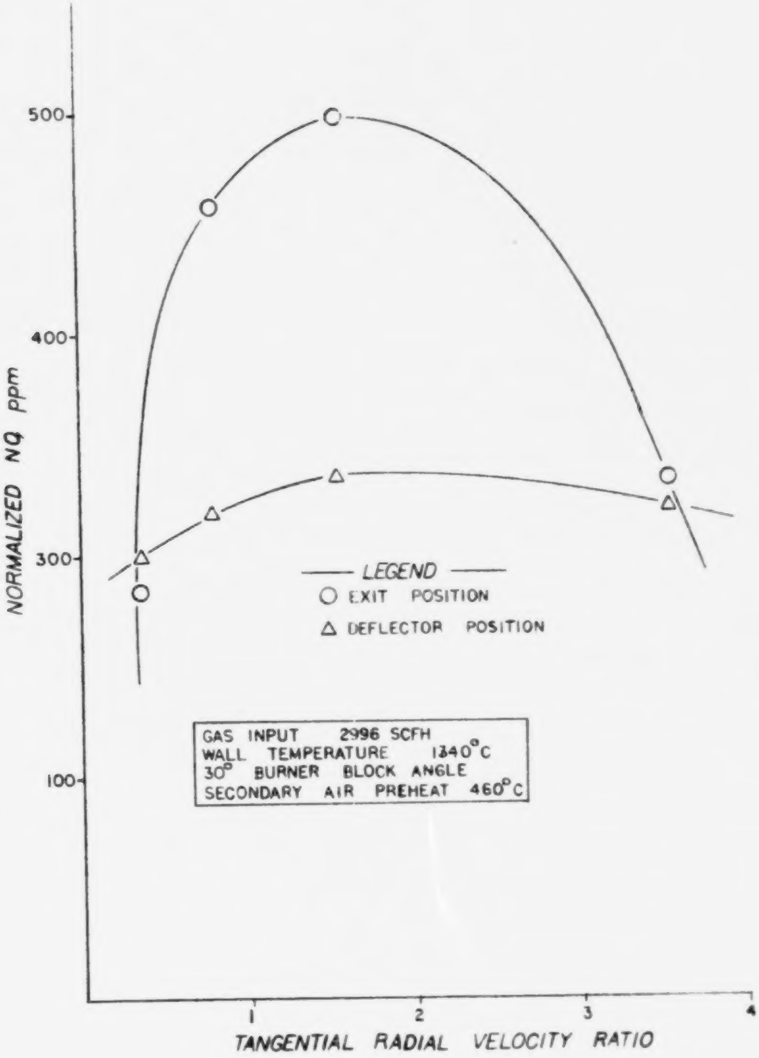

Figure 77. Normalized NO concentration as a function of tangential/ radial velocity ratio for the movable-vane boiler burner with a 60-degree gun nozzle

the MVBB 53-degree vane rotation determined during the trials previously conducted under EPA Contract No. 68-02-0216 with air preheats of 22°, 132°, and 277°C. From this graph, it is obvious that the vane rotation should be set as low as possible while maintaining an acceptable flame profile. It is possible to decrease emissions by going to vane positions above 57 degrees; however, the plenum pressure drop will make the fan horsepower and electrical consumption prohibitive.

In-the-flame data for NO emission controlled operating conditions were collected with the 60-degree gun nozzle in the exit position and a 15-degree vane angle. Figure 78 gives some of the gas species and temperature data collected along the burner axis. The flow direction data showed a type II profile. The primary jet, however, was combustion air and the secondary jets were fuel. Because of the low tangential velocity the air did not spread to the edges of the 30-degree burner block but remained on the burner axis. The 60-degree gun nozzle injected high velocity divergent fuel jets which penetrated the primary recirculation zones. Despite the primary jet being mainly combustion air, the temperature at the burner block exit was 1365°C. The NO concentration at the burner block exit was 20 ppm compared to a flue concentration of 196 ppm. This flue level of NO emission is a 42% reduction when compared to the emission level from standard operating conditions with the 60-degree gun.

The gas nozzle position that consistently produced the lowest NO was the deflector position. The data for this nozzle position are also plotted in Figure 77. The plot shows little variation in NO as a function of velocity, with only a 40-ppm difference between minimum and maximum emission levels. At the 30-degree vane rotation, which is normally used in industry, there is a 218-ppm normalized emission for the deflector position versus a 357-ppm emission for the exit position. Thus, by using the deflector, it is possible to reduce the NO by 37% while maintaining all other furnace and burner operating parameters unchanged. Photographically, the flame length, geometry, and luminosity showed little change between these nozzle positions. However, the photos were taken with a low wall temperature (less than 800°C) and a negative furnace pressure. Under normal operating conditions, the flame cannot be defined with either nozzle position.

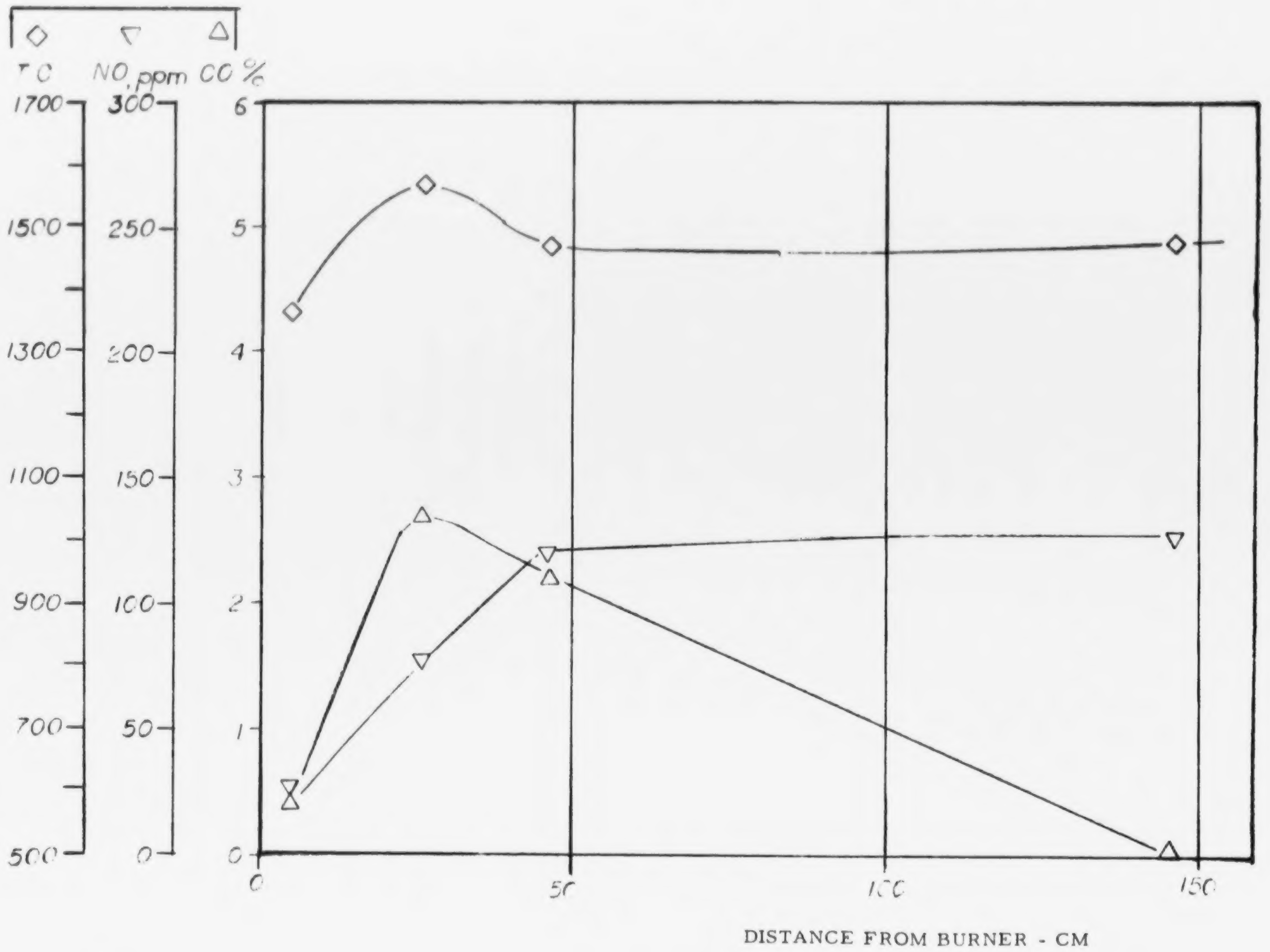

Figure 78. In-the-flame profiles of boiler burner using 60-degree gun nozzle

Note that the vane rotation producing the maximum NO will be linked to the cross-sectional exit area and divergent angle of the burner block.

WALL TEMPERATURE (60-Degree Gun Nozzle)

Because of the observed sensitivity of the wall temperature on the flue concentrations of NO during these tests, we decided to gather data relating NO to wall temperature during a warm-up cycle. The 60-degree gun nozzle in the exit position was fired with 3000 SCFH of gas at 3.5% excess oxygen and 460°C air preheat. The results are plotted in Figure 79. There is a dramatic increase in the level of NO emissions above 1300°C. This indicates that accurate control of the wall temperature is required to produce a consistent set of experimental data. It also confirms that the furnace should be opened with as low a wall temperature as possible. Although it is not possible to operate with reduced wall temperature (below 1200°C) in all industrial applications, these data demonstrates its effectiveness as an NO control technique.

SECONDARY AIR PREHEAT TEMPERATURE (60-Degree Gun Nozzle)

A similar study was made to determine the sensitivity of NO emissions to changes in secondary air preheat temperature. This trial was made with a 3000 SCFH gas input, 2% excess air, and a 1340°C wall temperature that was maintained constant throughout the trial by varying the air cooling to the furnace walls. These test results are plotted in Figure 80. A comparison of Figures 69 and 80 indicates that reducing the secondary air preheat to 325°C produces the same emission level as using the deflector position with 450°C preheat. Also, by inference from Figure 79, since these data were collected at 3.5% excess oxygen, a 1200°C wall temperature with a 450°C air preheat will produce concentrations of NO similar to those using a 1340°C wall temperature and a 325°C air preheat.

By use of the data presented in Figures 77, 79, and 80, the level of NO emissions can even be minimized from a furnace that has certain operating constraints. However, the one operating parameter that seems to override the amount of secondary air swirl, the furnace wall temperature, and the secondary air preheat temperature, is the nozzle position. By placing the injector in the deflector position, the level of emissions becomes independent

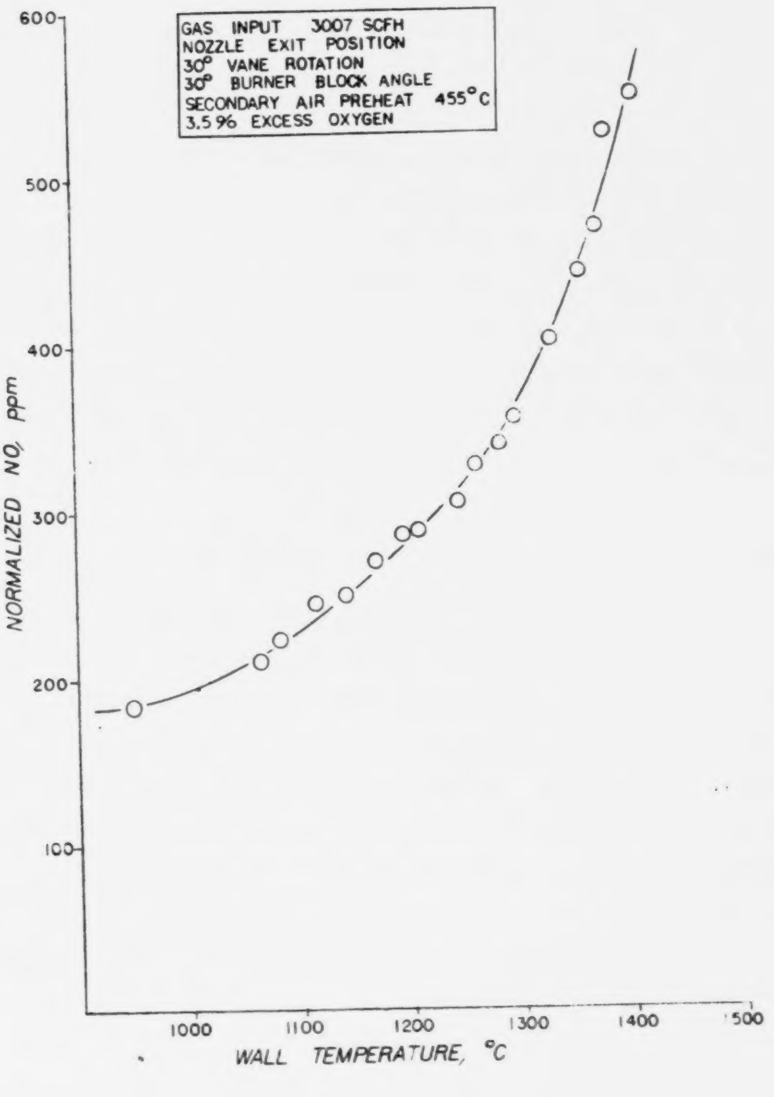

Figure 79. Normalized NO concentration as a function of wall temperature for the movable-vane boiler burner with a 60-degree gun nozzle

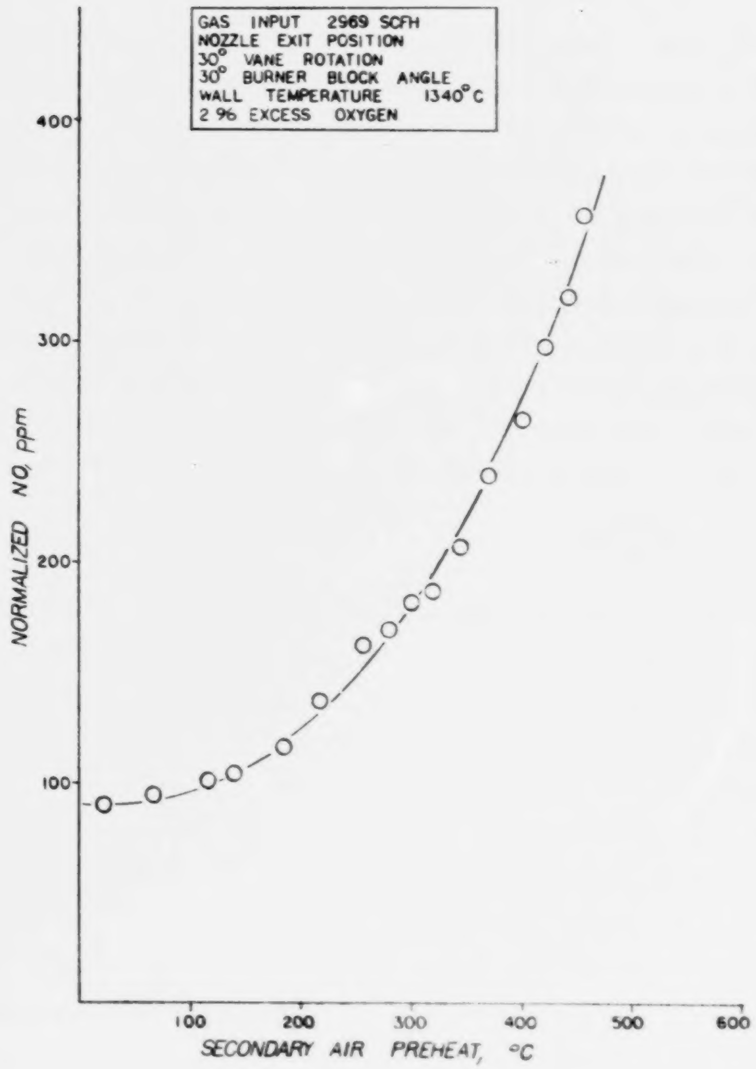

Figure 80. Normalized NO concentration as a function of secondary air temperature for the movable-vane boiler burner with a 60-degree gun nozzle

of swirl. The 60-degree gun nozzle in the exit position can only achieve an equivalent emission level by a 29% reduction in secondary air preheat temperature or a decrease in wall temperature of 12%.

STANDARD CONDITIONS (30-Degree Ring Nozzle)

The NO_x test results for the base-line trials of the 30-degree ring nozzle are plotted in Figure 81. Data were collected at each of the three nozzle positions depicted in Figure 64. The throat position had the highest level of NO emissions. This nozzle position allows for a higher rate of mass exchange between the fuel and air jets, which results in a higher flame temperature than the other two nozzle positions. The exit position results in a 40% reduction in the normalized NO at 2% excess oxygen as compared with the throat position. This position should minimize the rate of mass exchange between the fuel and air jets, causing the lowest flame temperature. At 2% excess oxygen, there is a 54% reduction in normalized NO as compared with the throat position and a 24% reduction as compared with the exit position.

VANE ANGLE (SWIRL) (30-Degree Ring Nozzle)

Trials were conducted varying the rotation of the vanes to investigate the effect of secondary combustion air swirl on the combustion aerodynamics associated with the 30-degree ring nozzle and the influence it has on the formation of NO_x. The orientations studied were 15-degrees, 45-degrees, and 60-degrees. The results of the individual tests are plotted in Figures 82 through 84. Table 8 lists the values calculated for the tangential/radial velocity ratios in addition to the normalized NO emissions for the 30-degree ring nozzle in the exit and deflector positions and the pressure drop in the plenum in inches of water.

Figure 85 illustrates the relationship between normalized NO and the tangential/radial velocity ratio for the 30-degree ring nozzle in the exit and deflector positions. The exit position shows a decrease in NO emissions as the vane rotation is increased. Assuming a linear relationship between NO emissions and vane rotation with the nozzle in the exit position, there is approximately a 1.4 ppm decrease in NO emissions per degree increase in vane rotation. On the other hand, for every degree increase in vane rotation there is an additional 0.01-inch H_2O pressure drop in the burner plenum.

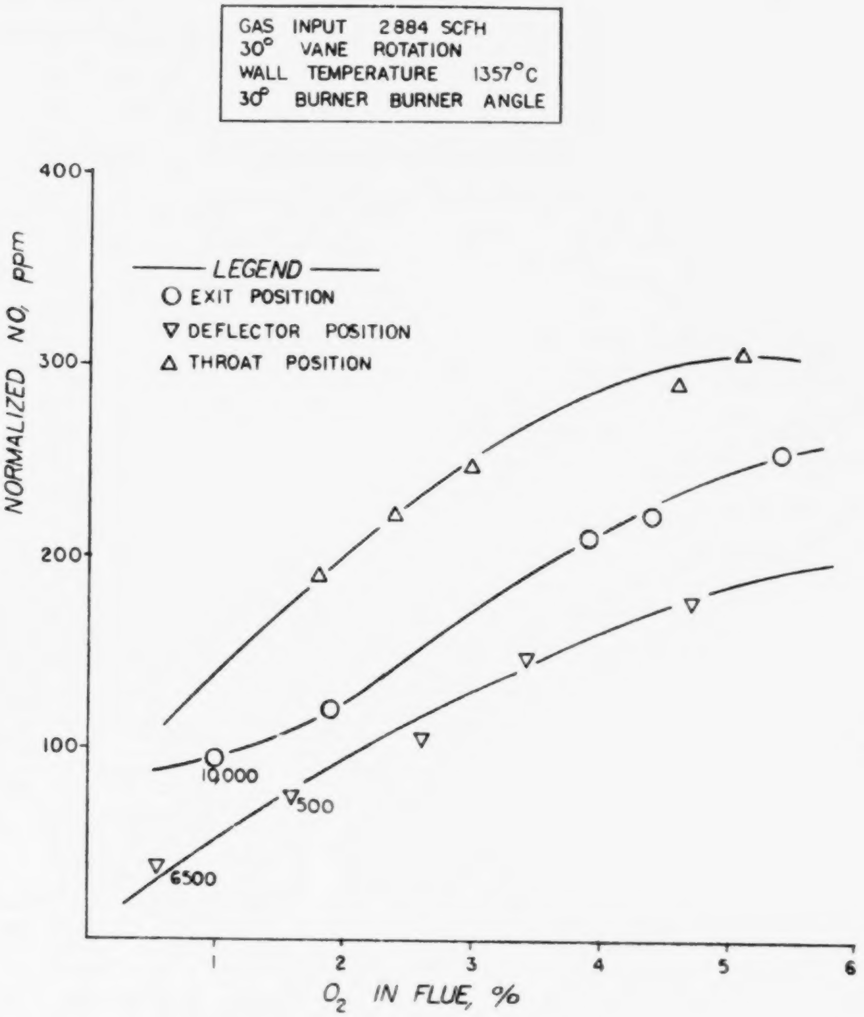

Figure 81. Normalized NO concentration as a function of flue O_2 for the movable-vane boiler burner with a 30-degree ring nozzle in different positions

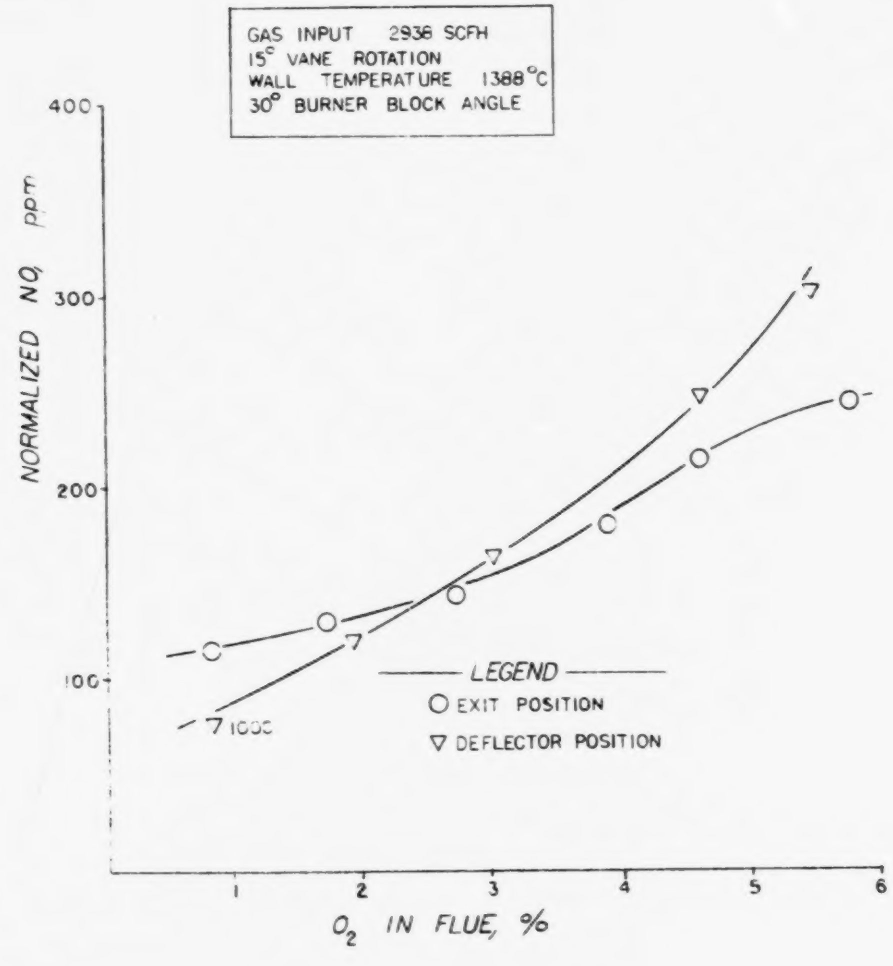

Figure 82. Normalized NO concentration as a function of flue O_2 for the movable-vane boiler burner with a 30-degree ring nozzle in different positions and a 15-degree vane angle

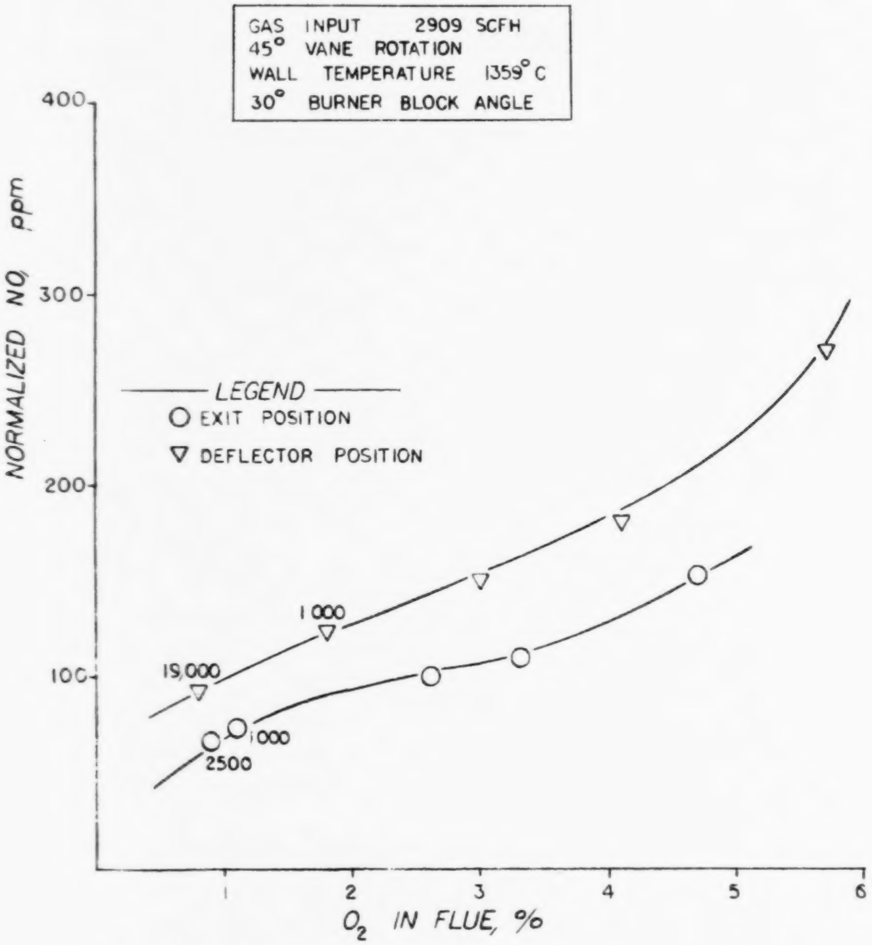

Figure 83. Normalized NO concentration as a function of flue O_2 for the movable-vane boiler burner with a 30-degree ring nozzle in different positions and a 45-degree vane angle

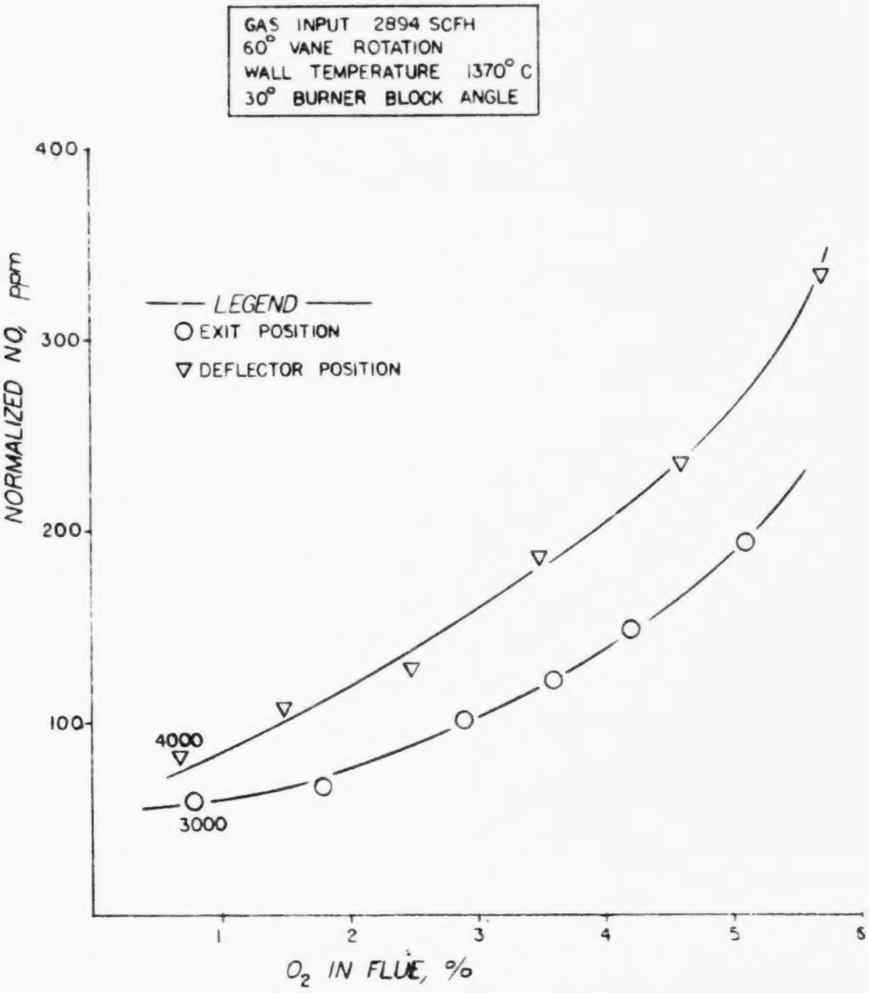

Figure 84. Normalized NO concentration as a function of flue O_2 for the movable-vane boiler burner with a 30-degree ring nozzle in different positions and a 60-degree vane angle

Table 8. LISTING OF BURNER OPERATING CONDITIONS AS A FUNCTION OF VANE ANGLE FOR THE 30-DEGREE RING NOZZLE WITH A 30-DEGREE BURNER BLOCK
(Gas Input, 2907 SCFH; Exit and Deflector Nozzle Positions; 1369°C Wall Temperature; 460°C Secondary Air Preheat; 2% Excess Oxygen)

					Normalized NO, ppm		
α	α_M	σ	V, ft/s	W, ft/s	Exit	Deflector	Burner ΔP_1, in H_2O
15	19	0.37	33.8	12.4	133	123	0.7
30	37	0.81	31.9	25.7	122	92	0.9
45	55	1.55	29.6	46.0	92	126	1.1
60	72	3.54	26.3	93.0	75	117	1.3

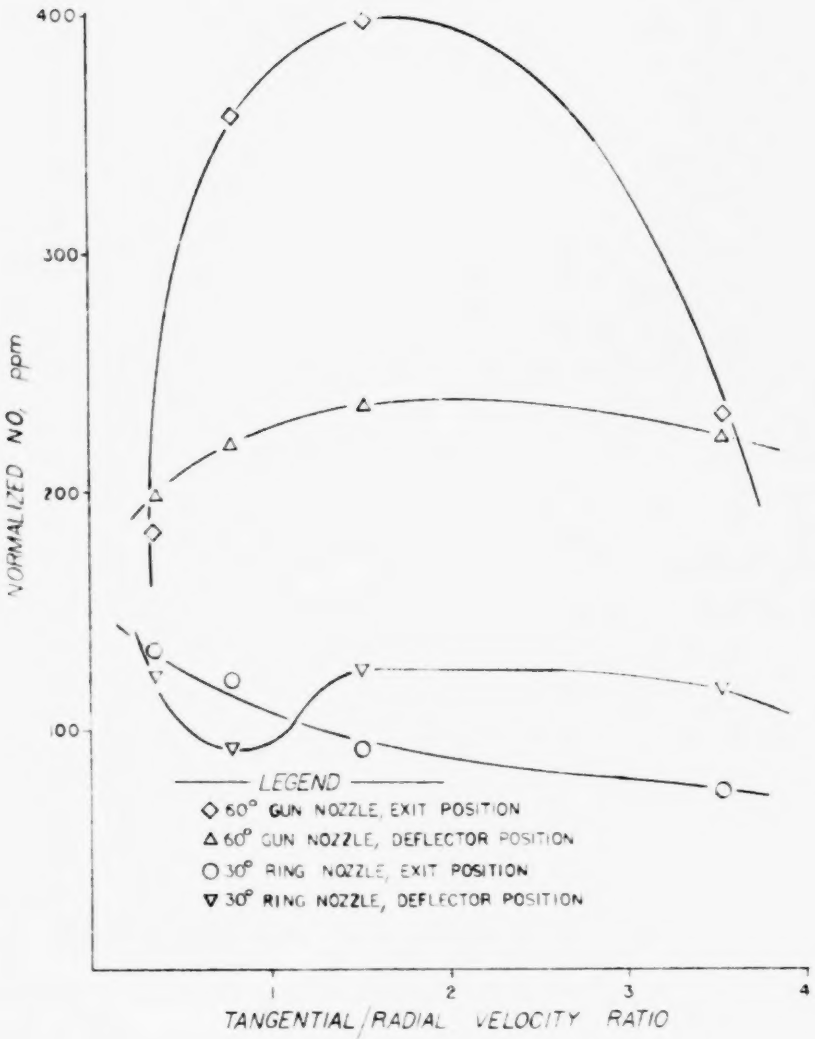

Figure 85. Normalized NO concentration as a function of tangential/radial velocity ratio for the movable-vane boiler burner with a composite plot of nozzles

The deflector position shows minimum emissions for the 30-degree ring nozzle at a 30-degree vane rotation. A comparable emission level is not achieved with the exit position until a 58-degree measured vane rotation is reached. This would result in an additional 0.28-inch H_2O pressure drop. Included in Figure 85 are data collected under identical operating conditions except that a 60-degree gun fuel injector was used. The optimum conditions were the 30-degree ring, the deflector position, and a 30-degree vane rotation. This results in a reduction of 74% in NO_x emissions when compared with the 60-degree gun in the exit position, 58% when compared with the 60-degree gun in the deflector position, and 25% when compared with the 30-degree ring in the exit position.

WALL TEMPERATURE (30-Degree Ring Nozzle)

In order to investigate the effect of the temperature on the flue concentrations of NO, data was gathered relating NO to wall temperature during a warm-up cycle. The 30-degree ring nozzle in the exit position was fired with 2856 SCFH of gas at 3% excess oxygen and 450°C air prehat. The results are plotted in Figure 86. There is a dramatic increase in the level of NO emissions above 1300°C. This indicates that accurate control of wall temperature is required to produce a consistent set of experimental data. It also confirms that the furnace should be operated with as low a wall temperature as possible. It is not possible to operate all industrial processes with reduced wall temperatures (below 1200°C). These data demonstrate the effectiveness of wall temperature as an NO emission control technique.

SECONDARY AIR PREHEAT TEMPERATURE (30-Degree Ring Nozzle)

A similar study was made to determine the sensitivity of NO emissions to changes in secondary air preheat temperature. This trial was made with a 2872 SCFH gas input, 3% excess air, and a 1358°C wall temperature that was maintained constant by varying the cooling air to the furnace walls. These trial results are plotted in Figure 87. A comparison of Figures 81 and 87 indicates that reducing the secondary air preheat to 290°C produces the same emission level as using the deflector position with a 466°C preheat. Also, a 1200°C wall temperature with a 450°C air preheat will produce concentrations of NO similar to those using a 1358°C wall temperature and a 290°C air preheat.

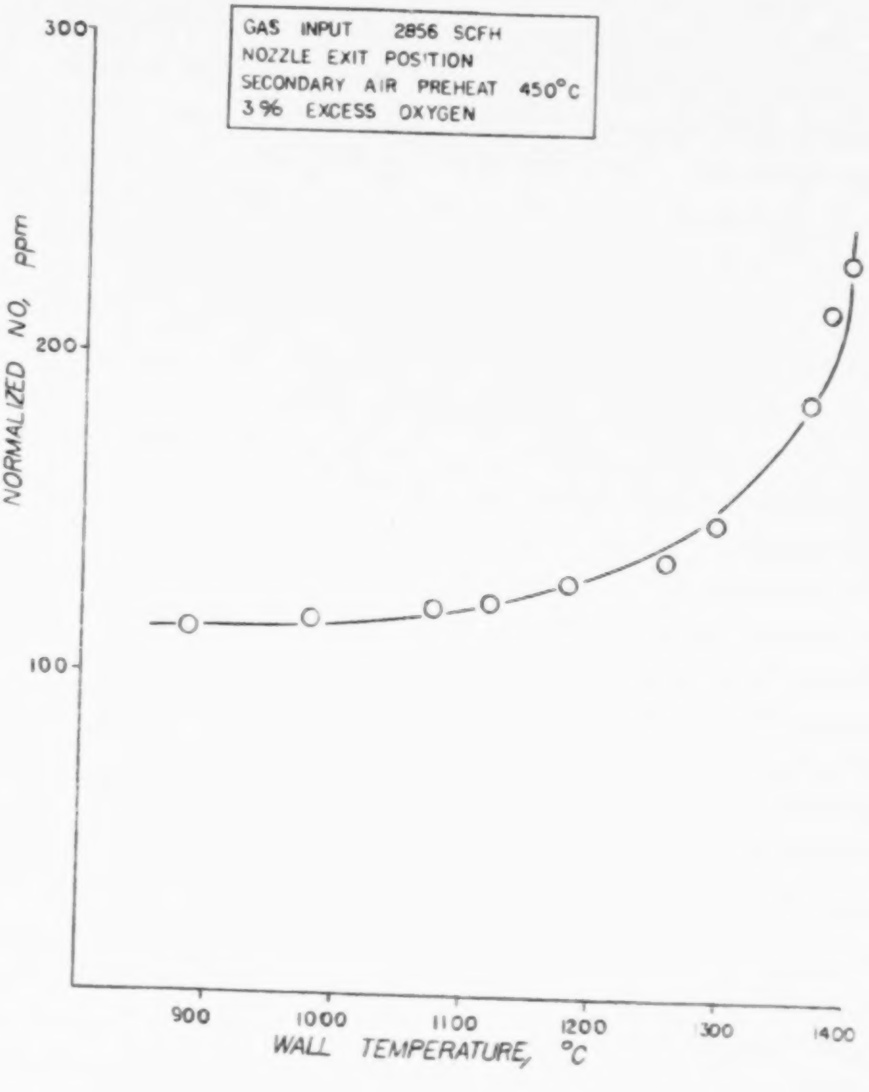

Figure 86. Normalized NO concentration as a function of wall temperature for the movable-vane boiler burner with a 30-degree ring nozzle

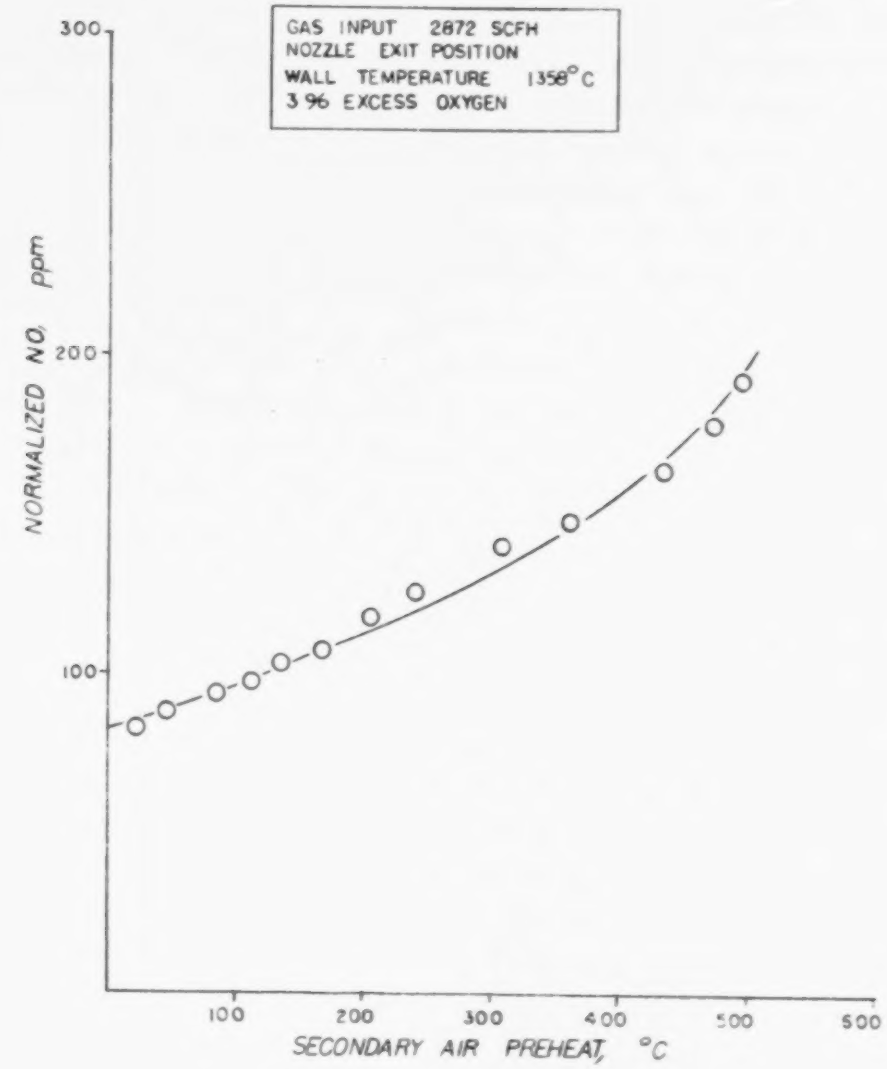

Figure 87. Normalized NO concentration as a function of secondary air temperature for the movable-vane boiler burner with a 30-degree ring nozzle

EXTERNAL FLUE GAS RECIRCULATION (30-Degree Ring Nozzle)

A similar study was also made to determine the sensitivity of NO emissions to changes in external flue-gas recirculation percentage. This trial was made with a 2942 SCFH gas input, 3% excess oxygen, a 455°C secondary air preheat, and a 1365°C wall temperature that was maintained constant throughout the trial by varying the air cooling to the furnace walls. These test results are plotted in Figure 88. A comparison of Figures 81 and 88 indicates that having a 9.8% flue-gas recirculation produces the same emission level as using the deflector position with a 466°C preheat. Also, a 1200°C wall temperature with a 450°C air preheat will produce concentrations of NO similar to those using a 1315°C wall temperature, 455°C air preheat, and 9.8% flue-gas recirculation.

By use of the data presented in Figures 85, 86, 87, and 88, the level of NO emissions can even be minimized for a furnace that has certain operating constraints. With the ring nozzle, the level of emissions has become practically independent of swirl. This level of emissions can be reduced by lowering the operating wall temperature and/or the level of secondary air preheat or by externally recirculating flue gases into the secondary combustion air.

30-DEGREE GUN NOZZLE

A 30-degree gun nozzle was next tested. By decreasing the divergent angle of the fuel jets from 60 degrees to 30 degrees, it was hoped that this would delay the fuel/air mixing and allow a larger mass exchange between the secondary air jet and the secondary recirculation zone. This would result in a lower peak flame temperature and therefore lower levels of NO emissions. The experimental data are plotted in Figure 89. Again, as with most previous input/output data, the deflector nozzle position produced lower levels of NO emissions than the exit position. The 30-degree gun in the exit position gave a normalized NO-to-excess oxygen relationship similar to the 60-degree gun in the deflector position. The minimum emissions for a gun-style nozzle occurred with the 30-degree gun in the deflector position. At 2% excess oxygen, it produced a 48% reduction when compared with the 30-degree gun in the exit position, a 48% reduction when compared with the 60-degree gun

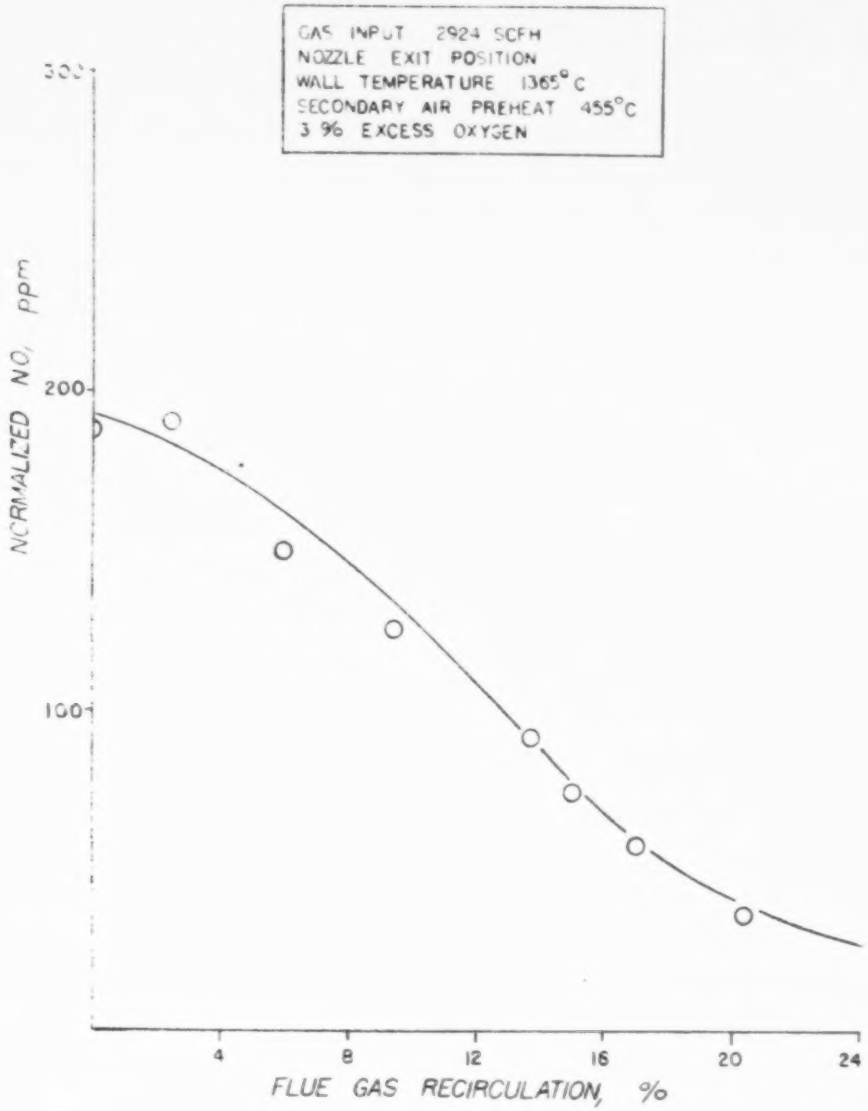

Figure 88. Normalized NO concentration as a function of flue gas recirculation percentage for the movable-vane boiler burner with a 30-degree ring nozzle

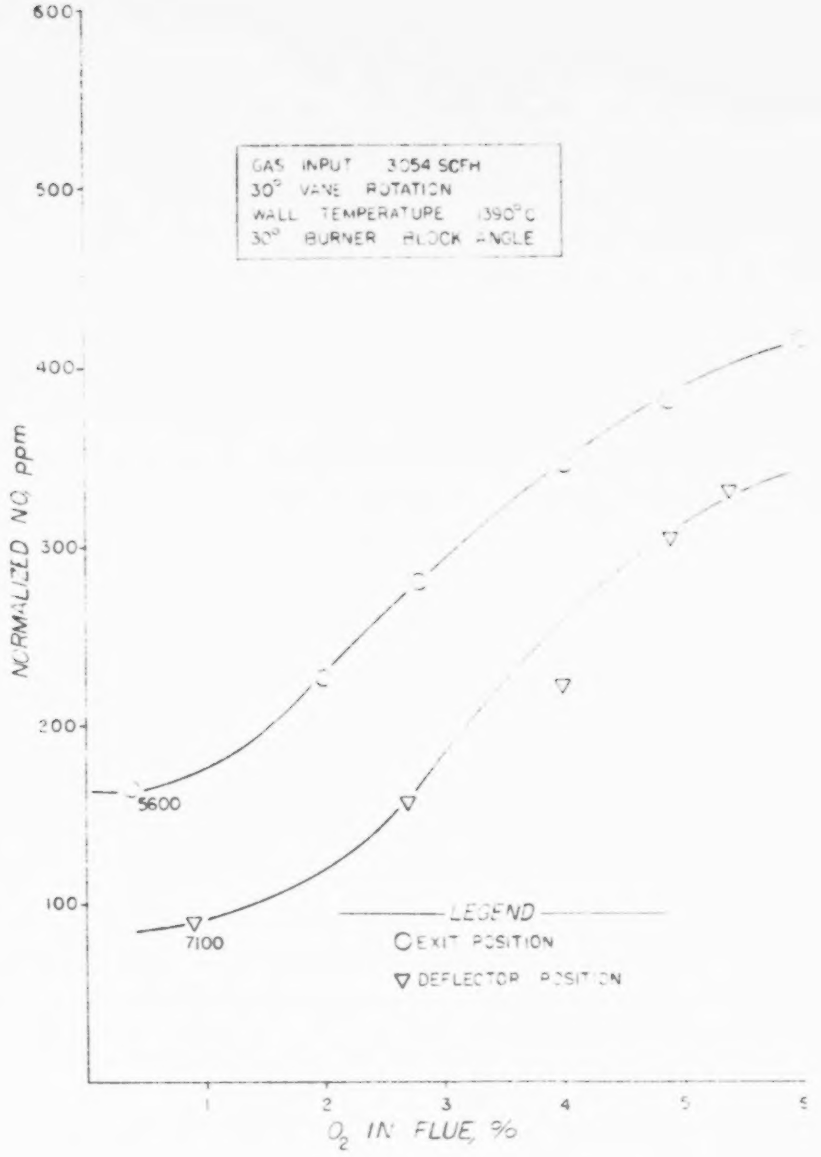

Figure 89. Normalized NO concentration as a function of flue O_2 for the movable-vane boiler burner with a 30-degree gun nozzle

in the exit position, and a 26% increase when compared to the 30-degree ring in the deflector position.

BURNER BLOCK ANGLE

As part of the combustion aerodynamic investigation, a 15-degree and a 45-degree burner block were tested. Figure 90 illustrates the data collected with a 30-degree vane, a 3044 SCFH gas input, a 1347°C wall temperature, a 460°C secondary air preheat, and a 15-degree burner-block angle. As with the 30-degree block, the ring nozzle produced lower NO emission levels than the 60-degree gun in the deflector position. However, unlike the previous data, the 60-degree gun in the deflector position produced higher emissions than the 60-degree gun in the exit position. At 2% excess oxygen, the 30-degree ring nozzle produces a 69% reduction compared with the 60-degree gun in the exit position and an 81% reduction when compared with the 60-degree gun in the deflector position.

To investigate the effect of secondary combustion air swirl on the combustion aerodynamics and the influence it has on the formation of NO_x, trials were conducted with a 15-degree burner block and varying the rotation of the vanes. The orientations studied were 15-degrees, 45-degrees, and 60-degrees. The results of these individual trials are plotted in Figures 91 through 93.

Figure 94 illustrates the relationship between normalized NO and the tangential/radial velocity ratio for the 30-degree ring in the exit position, the 60-degree gun nozzle in the exit position, and the 60-degree gun nozzle in the deflector position. All three operating conditions showed a minimum in NO emissions with a 30-degree vane angle. A comparison of Figures 85 and 94 will show the dependence of NO emissions on burner-block angle. The optimum operating conditions would be a 15-degree burner block with a 30-degree ring nozzle in the exit position and a 30-degree vane rotation.

The NO emission levels produced by a 45-degree burner block were tested using a 30-degree ring nozzle. These data are plotted in Figure 95. Minimum emissions were measured for a 15-degree vane rotation, with maximum emission being produced by a 45-degree vane rotation.

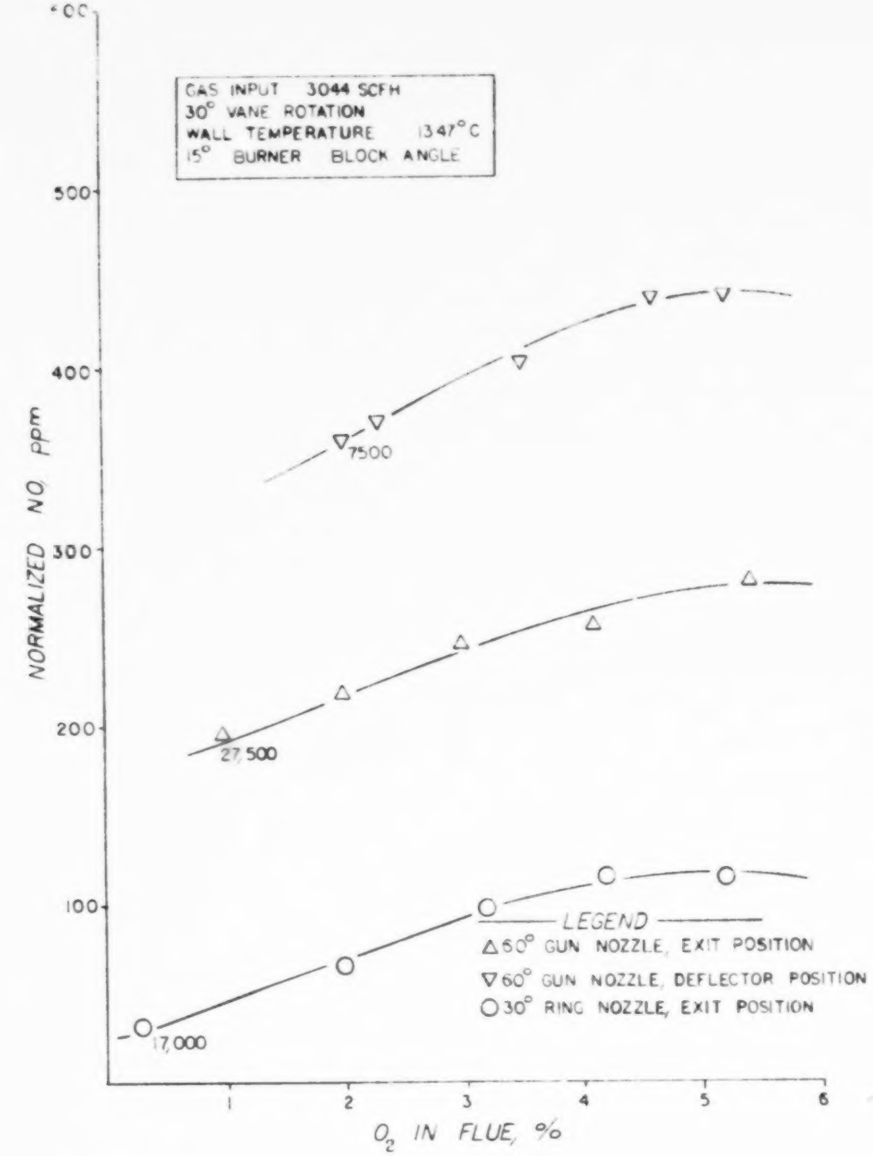

Figure 90. Normalized NO concentration as a function of flue O_2 for the movable-vane boiler burner with a composite nozzle plot and a 15-degree burner block angle

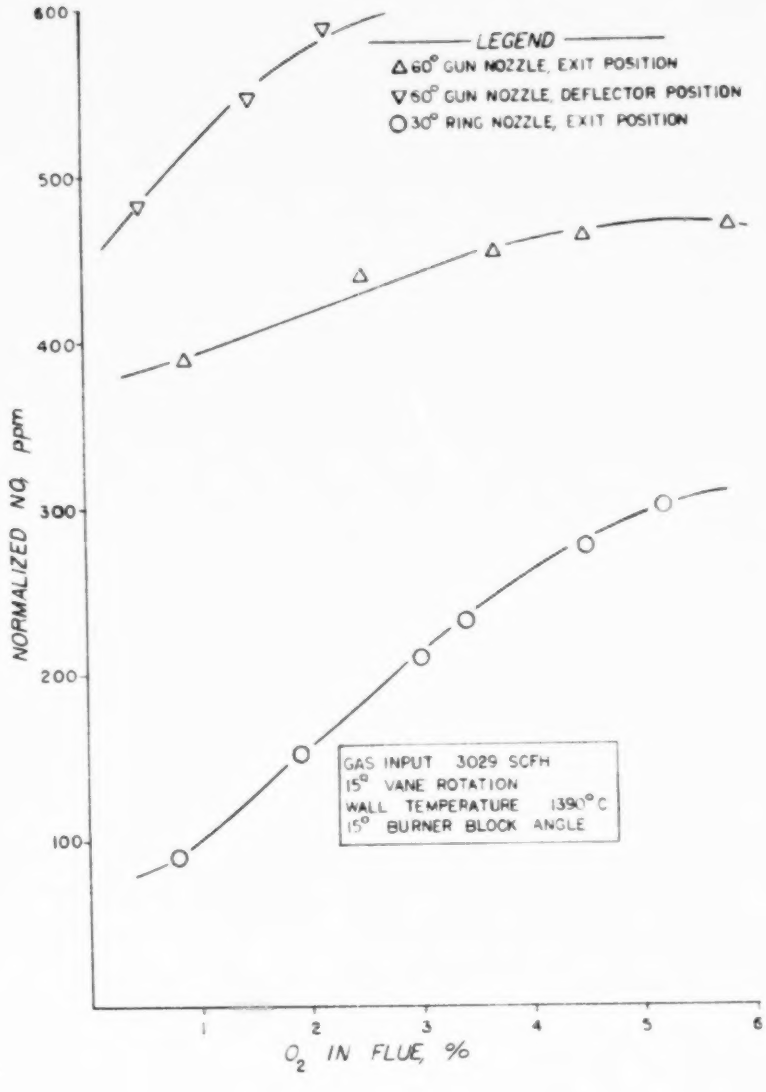

Figure 91. Normalized NO concentration as a function of flue O_2 for the movable-vane boiler burner with a composite nozzle plot, a 15-degree burner block angle and a 15-degree vane angle

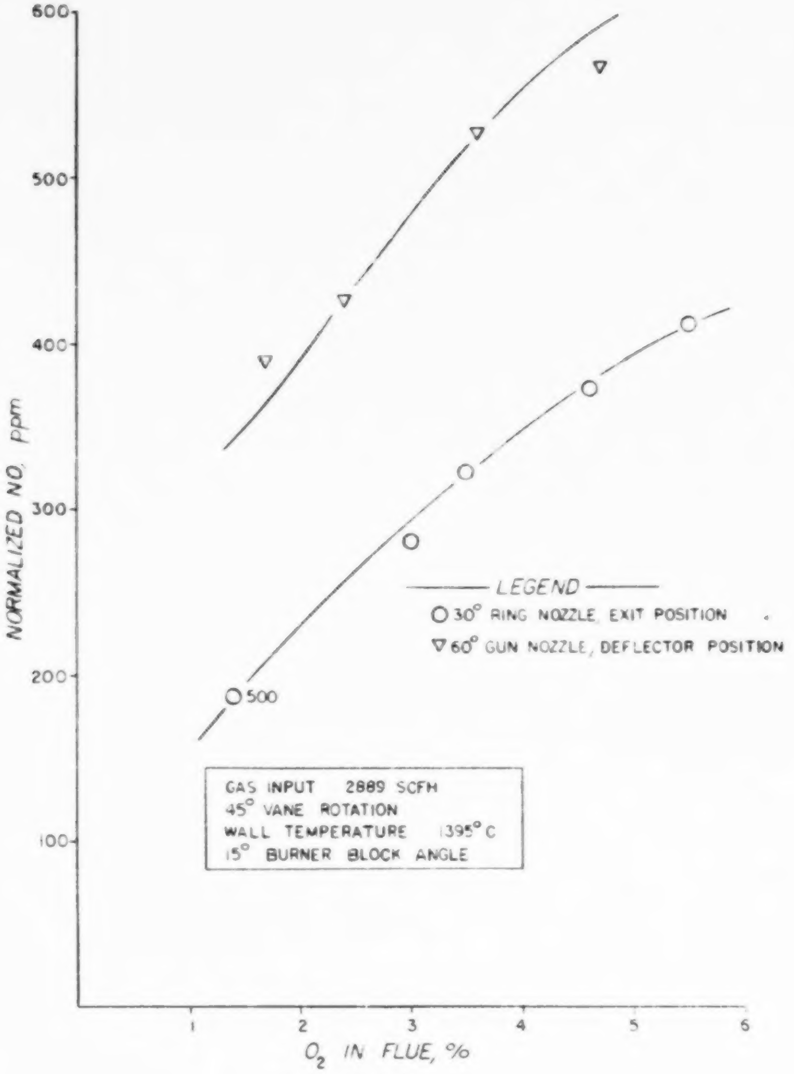

Figure 92. Normalized NO concentration as a function of flue O_2 for the movable-vane boiler burner with a composite nozzle plot, a 15-degree burner block angle and a 45-degree vane angle

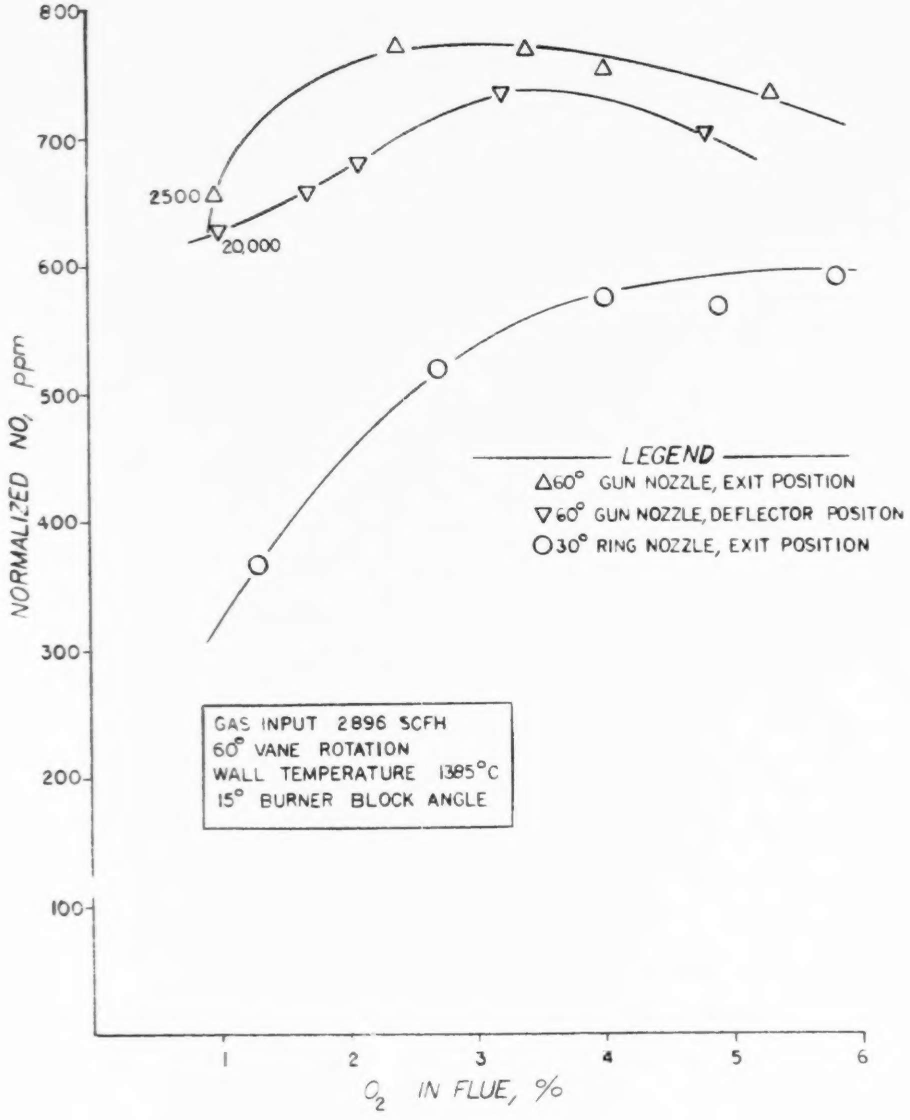

Figure 93. Normalized NO concentration as a function of flue O_2 for the movable-vane boiler burner with a composite nozzle plot, a 15-degree burner block angle and a 60-degree vane angle

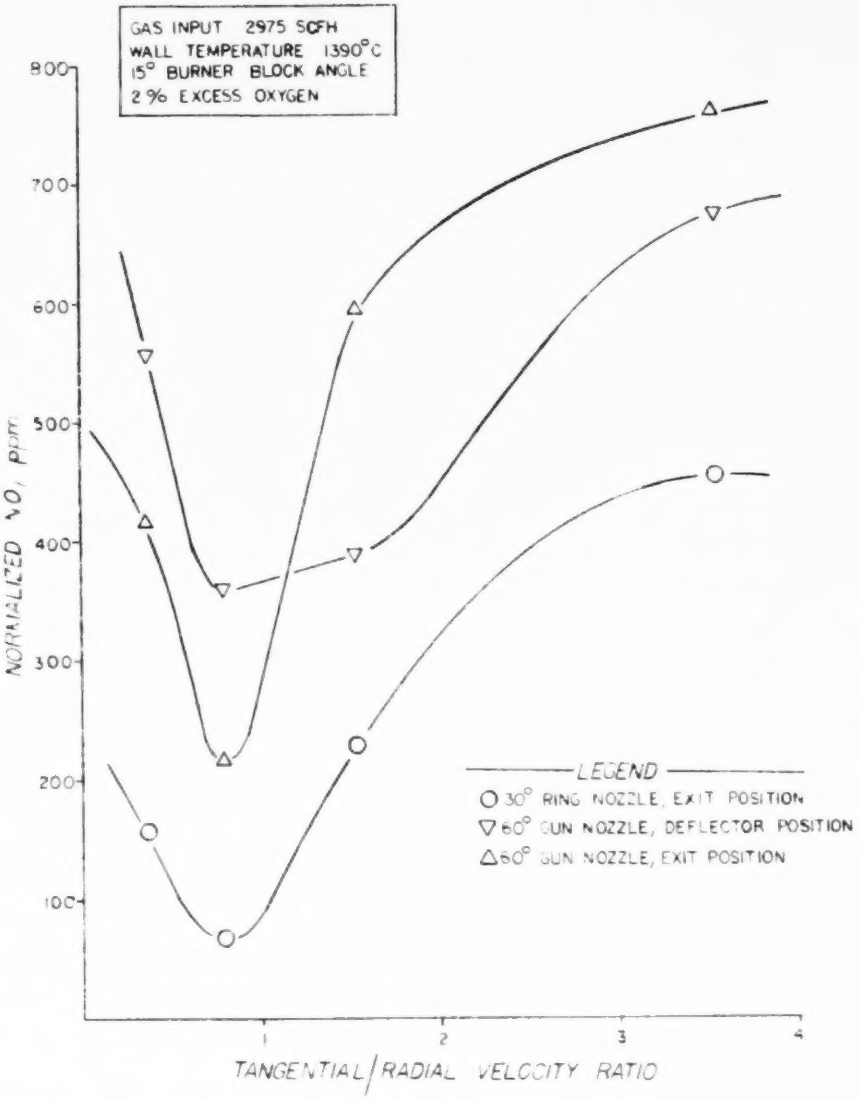

Figure 94. Normalized NO concentration as a function of tangential/radial velocity ratio for the movable-vane boiler burner with a composite nozzle plot

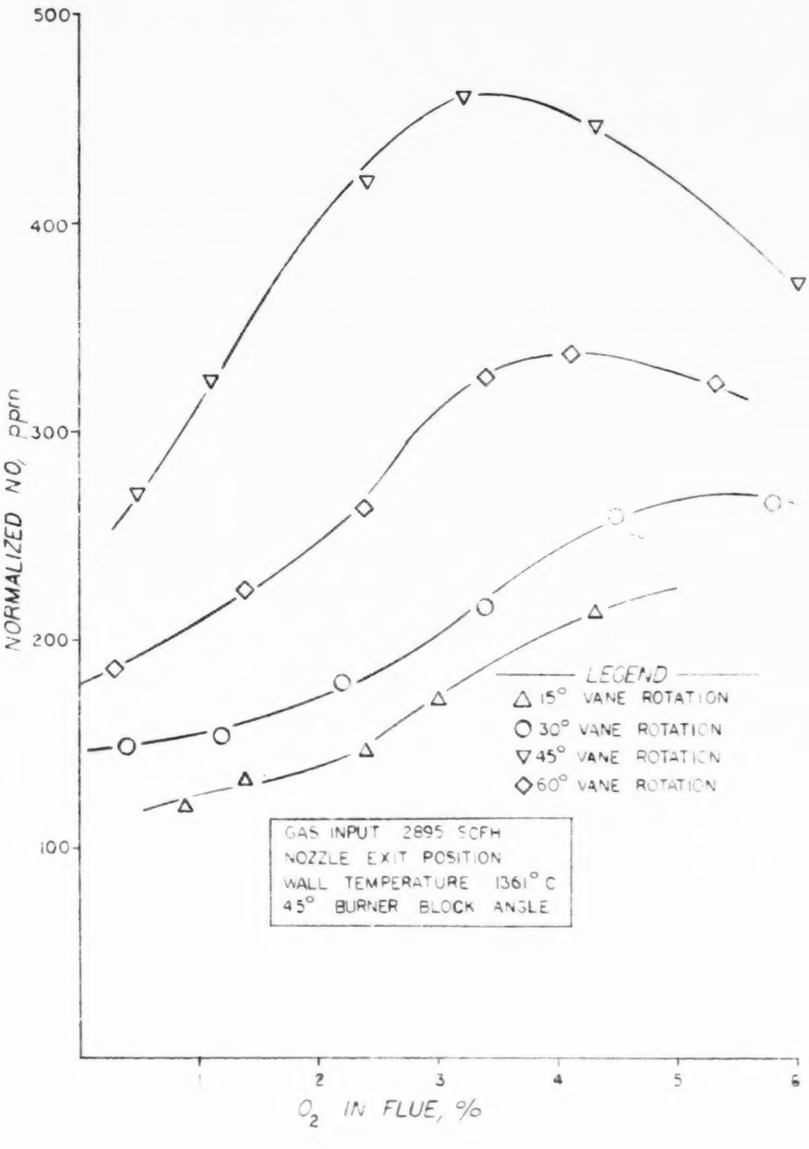

Figure 95. Normalized NO concentration as a function of flue O_2 and vane angle for the movable-vane boiler burner with a 30-degree ring nozzle

Figure 96 presents plots of normalized NO as a function of burner-block angle for the four vane rotations investigated. All other vane rotations produced their minimum emissions with a 30-degree burner block. An extrapolation of the 30-degree-vane-rotation curve would indicate that the minimum emissions would be produced with a 0-degree burner-block angle. An attempt was made at testing the 60-degree gun nozzle with the 45-degree burner block; however, the flame produced was extremely damaging to the front wall of the furnace. Flame edges protruded from the observation ports and the probing doors. Because of these unacceptable combustion characteristics, the 60-degree gun nozzle was not tested during the 45-degree burner-block trial sequence.

Figure 97 presents plots of the normalized NO versus tangential/radial velocity ratio for the three burner-block angles investigated. The 15-degree burner block shows a minimum emission level of 67 ppm for a 30-degree vane rotation. The 30-degree burner block produced a decrease in emissions as a function of vane rotation for all the angles tested. The minimum level measured was 75 ppm with a 60-degree vane rotation. The 45-degree burner block has a peak emission level of 400 ppm at a 45-degree vane rotation. Its minimum measured level of emissions was 142 ppm at a 15-degree vane rotation.

Several gas nozzles were tested with the 45-degree burner block. These included the 30-degree ring, 30-degree gun, and the low-momentum axial nozzles. Data for these tests are plotted in Figure 98. All the test data presented were collected for a 60-degree vane rotation. At excess oxygen levels below 4.5%, the 30-degree ring and the low-momentum axial nozzles had comparable levels of emissions. The low-momentum nozzle would be preferred because it operates at 4-psig line pressure compared with 30 psig for the 30-degree ring nozzle. The 30-degree gun produced NO levels approximately 74% higher than the other two nozzles.

SUMMARY OF BOILER BURNER RESULTS

A synopsis of the operational variables studied and their test results is presented in Table 9. Although large variations in NO emissions occur because of changes in the amount of excess air, reduction levels can be established in addition to their relative effectiveness by comparing the

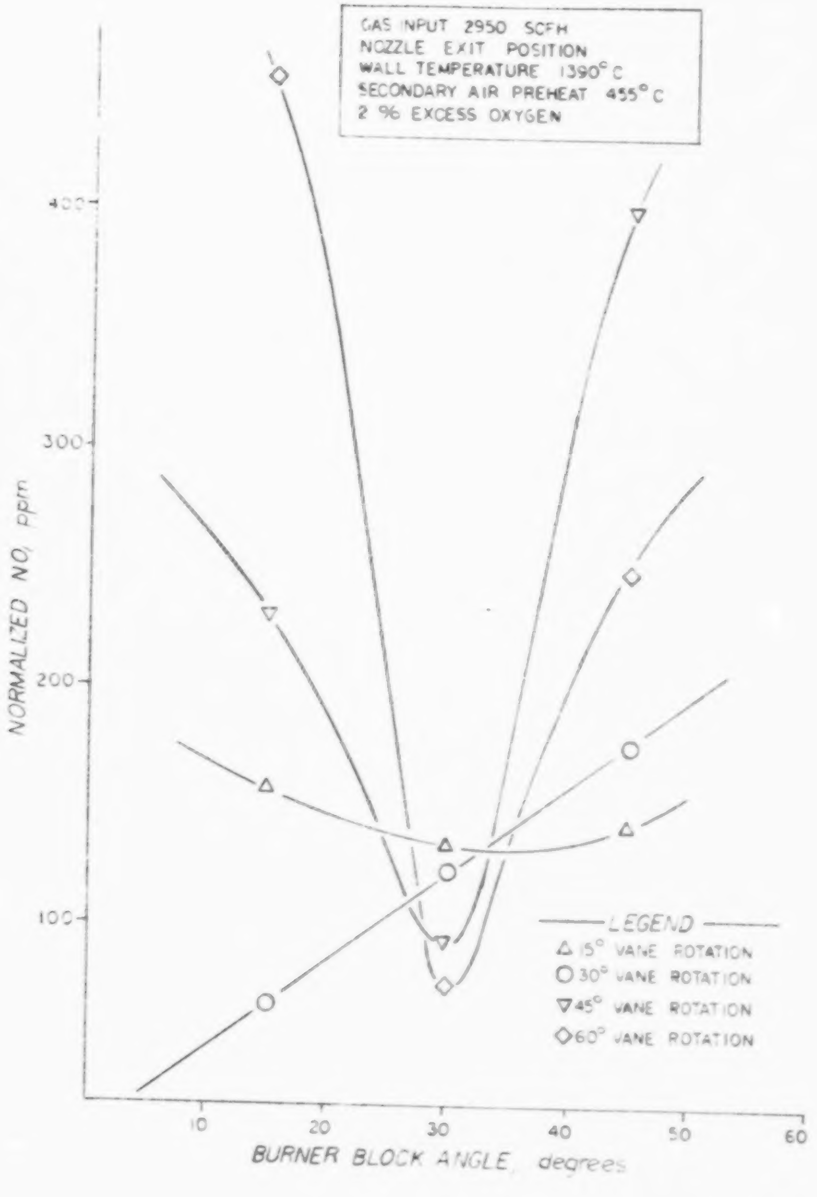

Figure 96. Normalized NO concentration as a function of burner block angle for the movable-vane boiler burner with a 30-degree ring nozzle

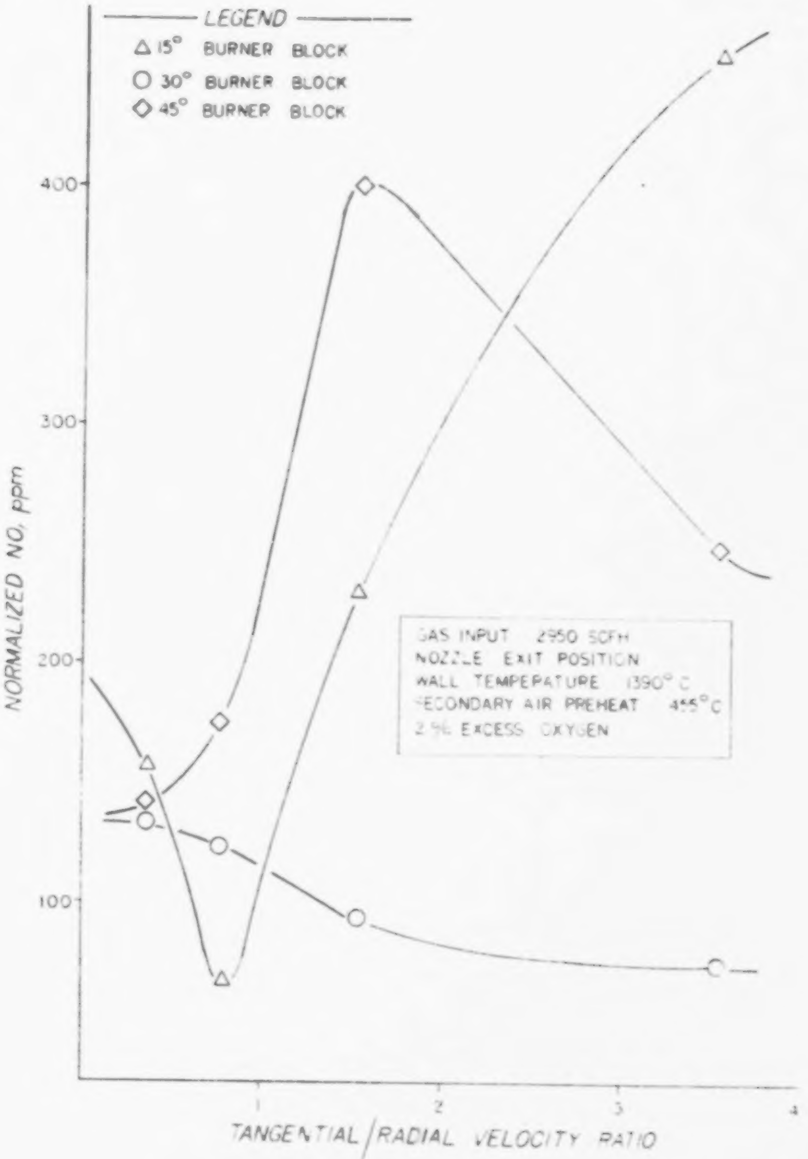

Figure 97. Normalized NO concentration as a function of tangential/ radial velocity ratio and burner block angle for the movable-vane boiler burner with a 30-degree ring nozzle

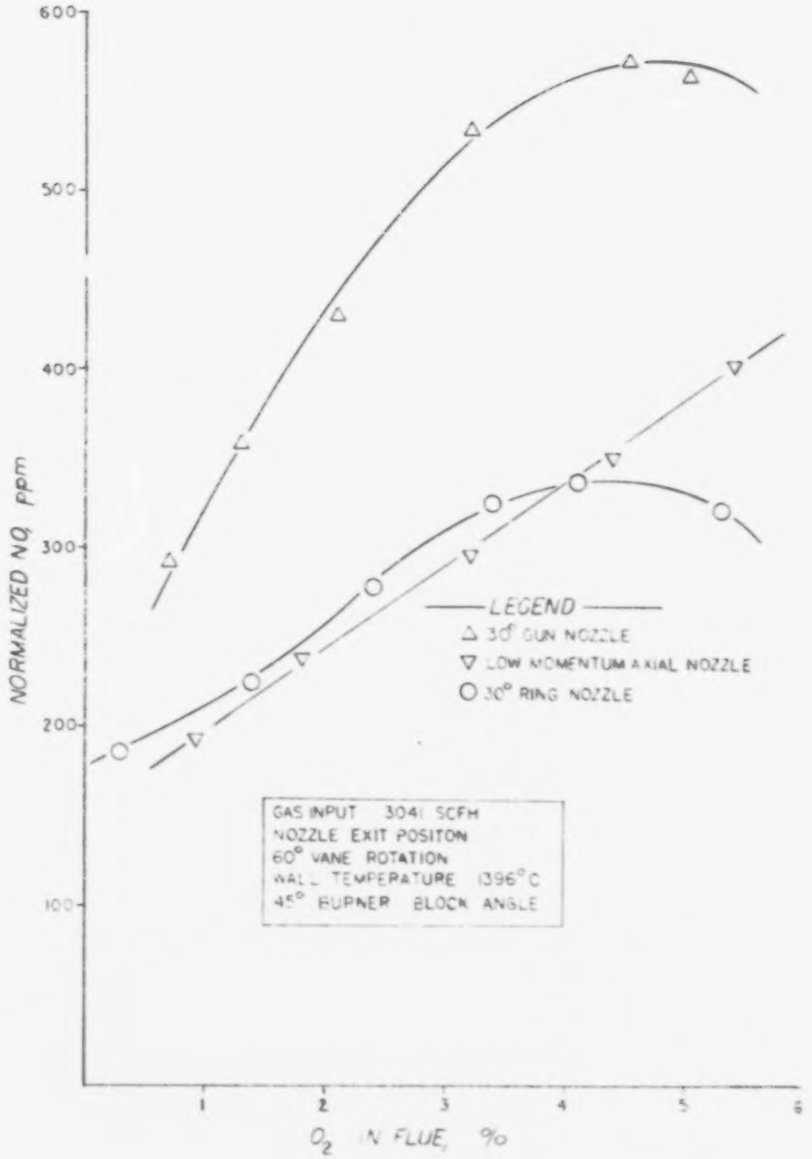

Figure 98. Normalized NO concentration as a function of flue O_2 for the movable-vane boiler burner with a composite nozzle plot, 60-degree vane angle and 45-degree burner block

Table 9. SYNOPSIS OF DATA COLLECTED FOR THE BOILER BURNER

Excess Oxygen, %	1	3
Normalized NO, ppm		
(Standard operating conditions: gas input 2960 SCFH; secondary air preheat 450°C; 60-degree gun nozzle; vane angle 30-degrees; exit nozzle position; wall temperature 1340°C and 30-degree burner block angle)		
Standard Operation	310	400
Secondary Air Temperature		
244°C	160	163
22°C	63	93
EFGR, 15%	100	137
EFGR, 25%	27	33
Throat Position	343	423
Deflector Position	173	277
Throat Position		
Low Axial Momentum Nozzle	370	512
Divergent Nozzle	280	450
Axial Nozzle	210	315
15-Degree Vane Angle		
Exit Position	173	197
Throat Position	187	188
Deflector Position	180	213
45-Degree Vane Angle		
Exit Position	328	465
Throat Position	267	283
Deflector Position	223	300
Throat Position, 45-Degree Vane Angle		
Low Axial Momentum Nozzle	335	470
Divergent Nozzle	385	580
Axial Nozzle	475	685
60-Degree Vane Angle		
Exit Position	220	270
Throat Position	253	310
Deflector Position	187	280
Throat Position, 60-Degree Vane Angle		
Low Axial Momentum Nozzle	250	343
Divergent Nozzle	437	555
Axial Nozzle	163	237
30-Degree Gun Nozzle		
Exit Position	175	293
Deflector Position	90	183
15-Degree Burner Block, Deflector Position		
15-Degree Vane Angle	520	610
30-Degree Vane Angle	327	393
45-Degree Vane Angle	317	477
60-Degree Vane Angle	625	730

Table 9, Cont. SYNOPSIS OF DATA COLLECTED FOR THE BOILER BURNER

(Standard operating conditions: gas input 2938 SCFH; secondary air preheat 450°C; 30-degree ring nozzle; exit nozzle position; wall temperature 1380°C; 30-degree vane angle and 30-degree burner block)

Standard Operation	93	173
Throat Position	137	247
Deflector Position	53	128
15-Degree Vane Angle		
Exit Position	118	153
Deflector Position	90	164
45-Degree Vane Angle		
Exit Position	68	107
Deflector Position	100	153
60-Degree Vane Angle		
Exit Position	58	102
Deflector Position	85	160
EFGR, 12%	--	108
EFGR, 24%	--	28
15-Degree Burner Block Angle		
15-Degree Vane Angle	100	210
30-Degree Vane Angle	45	92
45-Degree Vane Angle	150	293
60-Degree Vane Angle	325	537
45-Degree Burner Block Angle		
15-Degree Vane Angle	129	171
30-Degree Vane Angle	154	200
45-Degree Vane Angle	311	456
60-Degree Vane Angle	209	311

emission levels at several fixed levels of excess air. The conclusions reached below are based on an excess air equivalent to 3% oxygen in the flue and a combustion preheat temperature of 450°C.

For the 60-degree gun nozzle and a 30-degree vane angle, the following conclusions can be drawn:

a. Reducing the combustion air preheat from 450°C to 244°C leads to a 59% reduction in NO emissions, and no preheat gives a 77% reduction.

b. External flue-gas recirculation reduced NO emissions by a 66% for 15% recirculation and 91% for 25% recirculation.

c. Several nozzle positions were tested with a maximum reduction measured for the deflector position of 31%. The nozzle type which produced the lowest level of emissions for the throat position was the axial nozzle with a 21% reduction.

d. NO emissions showed a maximum for a 57-degree vane rotation. The test results show that the vane rotation should be set as low as possible while maintaining an acceptable flame profile.

For the 30-degree ring nozzle and a 30-degree vane angle, the following conclusions can be drawn:

a. At standard operating conditions, the 30-degree ring produced 57% fewer NO molecules than the 60-degree gun.

b. The deflector nozzle position results in a 26% reduction in NO emissions.

c. External flue-gas recirculation reduced NO emissions by 38% for 12% recirculation and 84% for 24% recirculation.

d. The combination of burner block angle and vane rotation which resulted in minimum emissions were: a 15-degree burner block and a 30-degree vane rotation producing a 56% reduction in NO emissions; or a 30-degree burner block and a 60-degree vane rotation which resulted in a 48% reduction.

In conclusion, the 30-ring nozzle consistently produced lower levels of NO emissions than the 60-degree gun nozzle. Additional reductions are possible by adapting the deflector or nozzle position or by using a 15-degree burner block and a 30-degree vane angle. The emissions from the 15-degree burner block and the 30-degree vane angle are even lower than those measured using 12% EFGR.

APPENDIX. Data Correlation

SUMMARY

This project generated a large quantity of data on the effect of numerous operating variables on pollution characteristics of three different burner types. Many conclusions can be drawn on the basis of the data alone. It is useful, however, to attempt to derive some more general conclusions on the effects of burner parameters on pollutant emissions. This can best be accomplished, at this time, by analyzing and correlating some of the data, in the light of specific theories or questions. In this work the focus was on correlating the influence of flue gas recirculation and air preheat on NO emissions as a function of the adiabatic flame temperature. Additionally, attempts were made to correlate the effects of excess air levels.

Results indicated that the data could be correlated to a remarkable extent. Indeed, it appears that (provided the restriction of unchanged fluid dynamics is maintained) the effects of three variables — air preheat, flue gas recirculation and excess air — for a given burner, can be (roughly) predicted from a single data point. These results are intriguing, and should provide impetus for further interpretation in the light of fundamental phenomena. The practical implications are important too, since our results indicate that given experimental emission measurements on a particular natural gas-fired system at different air preheat temperatures, it is possible to conservatively estimate the amount of flue gas recirculation needed to meet specific NO emission requirements. This, in turn, allows a reasonable cost/effectiveness analysis prior to system procurement and installation.

INTRODUCTION

Pollutant emissions from the diverse furnace flames investigated in this project arise through the interaction of many complex physical and chemical phenomena. Ideally, one would like to interpret the experimental data obtained in the light of these physical or chemical phenomena. However, a rigorous theoretical analysis is difficult and outside the scope of this project. It was felt, therefore, that interpretation of the results could best be achieved, through attempts to correlate the data in a rational but empirical way.

Because of the complexity of the process involved, and the volume of the data acquired, it is first necessary that the scope of this analysis portion of the project be narrowed. The focus, therefore, is on a single, limited aspect of the problem; namely, the relationship between air preheat and flue gas recirculation (FGR). The objective is to show that for a given piece of burner hardware, secondary air preheat and flue gas recirculation both affect NO_x emissions, primarily by changing the local flame temperature which is assumed to be directly related to (but probably not equal to) the theoretical adiabatic temperature of the flame.

Inherent in this analysis is the assumption that the temperature of the reaction zone in which NO is being formed in the flame, can have some "average" value which is directly proportional to the adiabatic flame temperature.

APPROACH

In this section the general approach used throughout the analysis is described. Discussion of specific experimental results is deferred to the next section. The following burner types were examined:

- Kiln burner — combination nozzle
- Intermediate flame length ported baffle burner — standard nozzle
- Short flame length ported baffle burner — standard nozzle
- Movable-vane boiler burner — gun nozzle.

Data sets included various secondary air preheats and flue gas recirculation levels for each burner. All the data in a particular set, however, were for the same fuel injector types and position, quarl angle, excess air, firing rate, etc. so that the fluid dynamics would be approximately the same.

Three types of plots were made for each burner:

1.0. NO vs. T_{ADB}

The NO emissions (in ppm, dry, normalized to stoichiometric) were plotted against the adiabatic flame temperature based on the particular air preheat, FGR level and excess air of the test point. In this manner, data at various preheats and FGR levels could be superimposed on the same graph, parametric with excess air. If flue gas recirculation and decreased air preheat both reduce NO_x via a purely thermal mechanism, and if the local flame temperatures are directly related to the adiabatic flame temperature, then all the data for a particular burner at a given excess air should fall on a smooth curve.

2.0. Ln(NO) vs. $1/T_{ADB}$

Secondly, the NO emissions (in ppm, dry, normalized) were plotted vs. the reciprocal adiabatic flame temperature on a semi-log basis in an attempt to obtain simple semilogarithmic correlations. Such a correlation would indicate that the rate determining mechanism has an Arrhenius dependence on temperature. Originally the theoretical flame temperature was calculated allowing for the high temperature disassociation of both CO_2 and water vapor according to the following equilibrium relations:

$$1/2\ O_2 + CO = CO_2$$

$$1/2\ O_2 + H_2 = H_2O$$

The correlation was improved; however, when this partial equilibrium was not taken into account; i.e., when the fuel was assumed to burn completely to CO_2 and H_2O. In retrospect, perhaps this is not surprising. Clearly the actual, local flame temperatures are below the adiabatic temperature and at these lower temperatures the equilibrium would heavily favor CO_2 and H_2O. For this reason, all of the adiabatic temperatures shown in the following sections assume complete combustion to CO_2 and H_2O.

3.0. Ln(NO/[O_2]) vs. $1/T_{ADB}$

Finally, the NO emissions (wet, as measured) divided by the percent oxygen (wet) in the flue gas were plotted vs. the reciprocal flame temperature on a semi-log basis.

If one assumes that NO formation is via the Zeldovich mechanism —

$$N_2 + O = NO + N$$

$$O_2 + N = NO + O$$

and that oxygen atoms are equilibrated –

$$M + O_2 = O + O + M$$

then it can be shown that –

$$d[NO]/dt \propto \exp[-A/T] * [O_2]^{1/2}$$

If one further makes the gross (unsupported) assumption that the residence time/temperature history allows direct integration, then a plot of –

$$\ln\{NO/[O_2]^{1/2}\} \text{ vs. } 1/T$$

should be linear. The data considered herein do not support this; however, they correlated remarkably well when plotted as –

$$\ln\{NO/[O_2]\} \text{ vs. } 1/T_{ADB}$$

This suggests that a simple equilibrium relationship between oxygen atoms and molecules is invalid for the reaction zone in which NO is being formed. It should be noted that for diffusion flames, at any instant, the midpoint of the reaction zone is determined by that point at which the overall stoichiometric ratio is equal to one. Furthermore, the linear dependence on excess oxygen is intriguing, and suggests that the thickness of the reaction zone (or apparent volume in which NO is formed) is controlled by diffusion of oxygen. Further work is necessary to fully interpret these results.

DETAILED RESULTS

Table 10 gives the specific details of each of the burners considered. These cases were selected because there was both air preheat and flue gas recirculation data available. Three excess oxygen levels were used throughout the analysis: 1.5, 3.0, and 4.5% O_2. Where necessary, data were obtained at exactly these levels by interpolating between actual experimental points.

In all of the plots presented in this section, the parametric lines represent the different levels of excess oxygen. The circled points are data with no flue gas recirculation while the diamonds represents points with flue gas recirculation.

Table 10. BURNER OPERATING CONDITIONS
USED IN DATA CORRELATION

BURNER NO.	DESCRIPTION
1	Kiln burner - Combination nozzle 810 SCFH axial gas 1890 SCFH radial gas 3.5% primary air 1130°C wall temperature 22°C primary air temperature (Table 43, Volume II)
2	Intermediate flame length ported baffle burner - Standard gas nozzle 3070 SCFH gas baffle gas nozzle position 1435°C wall temperature 4° burner block angle (Table 57, Volume II)
3	Short flame ported baffle burner - Standard gas nozzle 3070 SCFH gas baffle nozzle position 1360°C wall temperature 8° burner block angle (Table 74, Volume II)
4	Movable-vane boiler burner 60° gun nozzle 2969 SCFH gas exit gas nozzle position 30° vane angle 1340°C wall temperature 30° burner block angle (Table 82, Volume II)

Figures 99 to 101 show the results for the kiln burner. Figure 99 indicates that the FGR data tend to fall slightly above the normal curve. This is not typical of the other burners and may be related to the fact that the kiln burner has a primary air stream which is not supposedly preheated. One possible explanation for FGR being "less effective" than reduced air preheat is that since the FGR data are at a high preheat, there may have been some "artificial heating" of the primary air stream prior to combustion. Figure 100 again shows the FGR data to be slightly higher. Figure 101 shows all the data for the kiln burner plotted as $NO/[O_2]$ vs. $1/T_{ADB}$ and considering the data are for different levels of –

- Excess air
- Flue gas recirculation
- Secondary air preheat

the linearity is quite remarkable.

Figures 102 through 104 show the results for the intermediate flame length ported baffle burner. As Figure 102 shows, the preheat and FGR data generally fall on the same curve for a particular excess air. Figure 104 again shows good linearity with respect to first order oxygen dependence and reciprocal adiabatic temperature.

Figures 105 through 107 show the results for the short flame length ported baffle burner. As Figure 105 indicates, the FGR data for this burner fall far below the 0% FGR line. This type of burner produces a very short, rapidly mixed, intense flame. Perhaps in this case the FGR is being more beneficial than expected because in addition to reducing local flame temperatures directly, it is spreading the entire flame out. It should be recalled that the secondary air injection velocity is different by almost a factor of two between the circle and diamond points at the same flame temperature. For example, the point labeled A in Figure 105 is at 210°C preheat, 0% FGR; while the point labeled A' is at 455°C preheat and 15% FGR. Thus, it is not surprising that a difference in fluid dynamics might exist. This is further substantiated by the original plot of the data (Figure 51) where the high preheat data exhibit a different dependence on excess air than the no preheat data). Figure 107 shows the composite plot and the agreement is not particularly good. Again, the FGR data are lower than would be predicted.

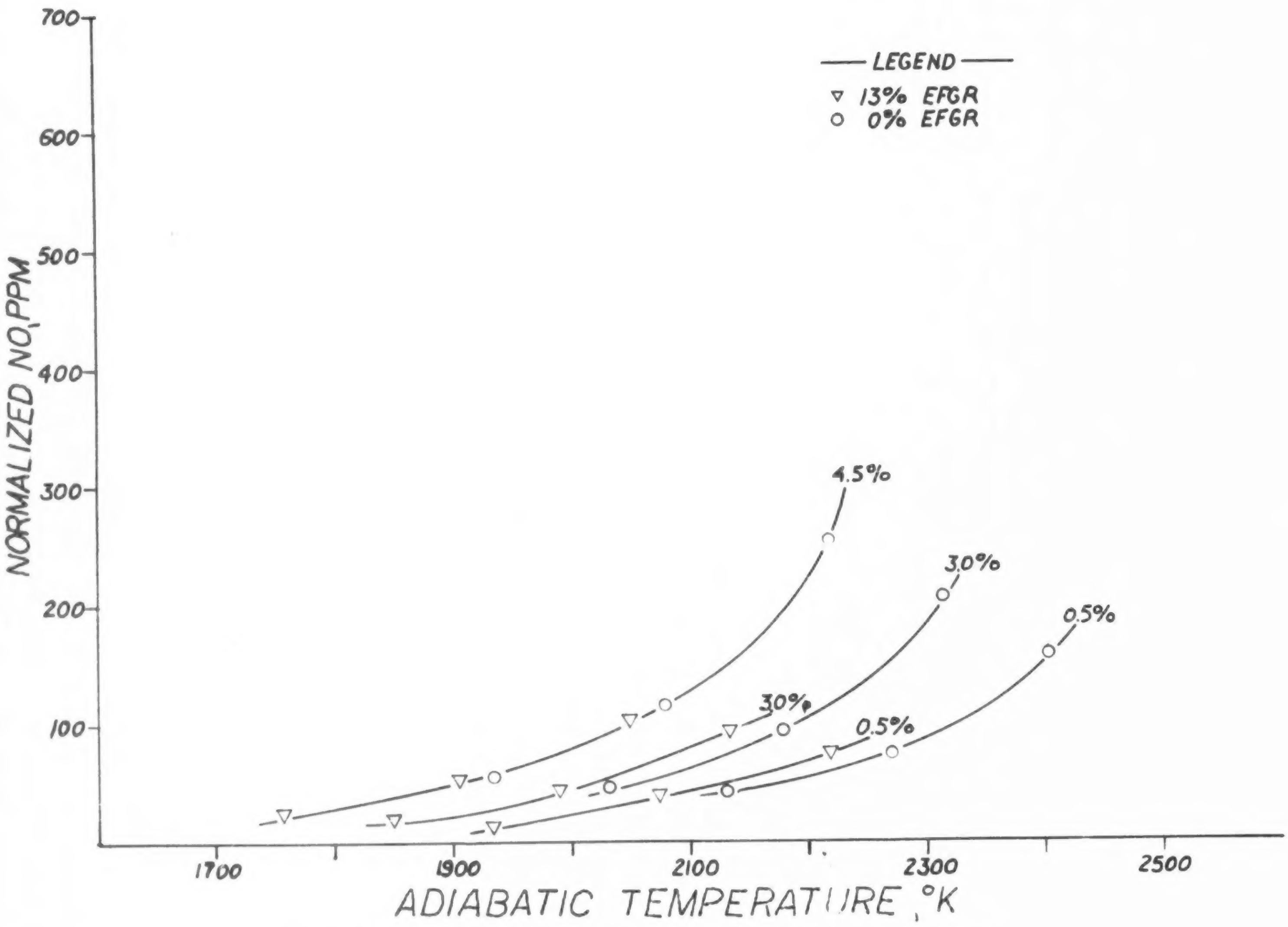

Figure 99. Normalized NO concentration as a function of adiabatic flame temperature for the kiln burner

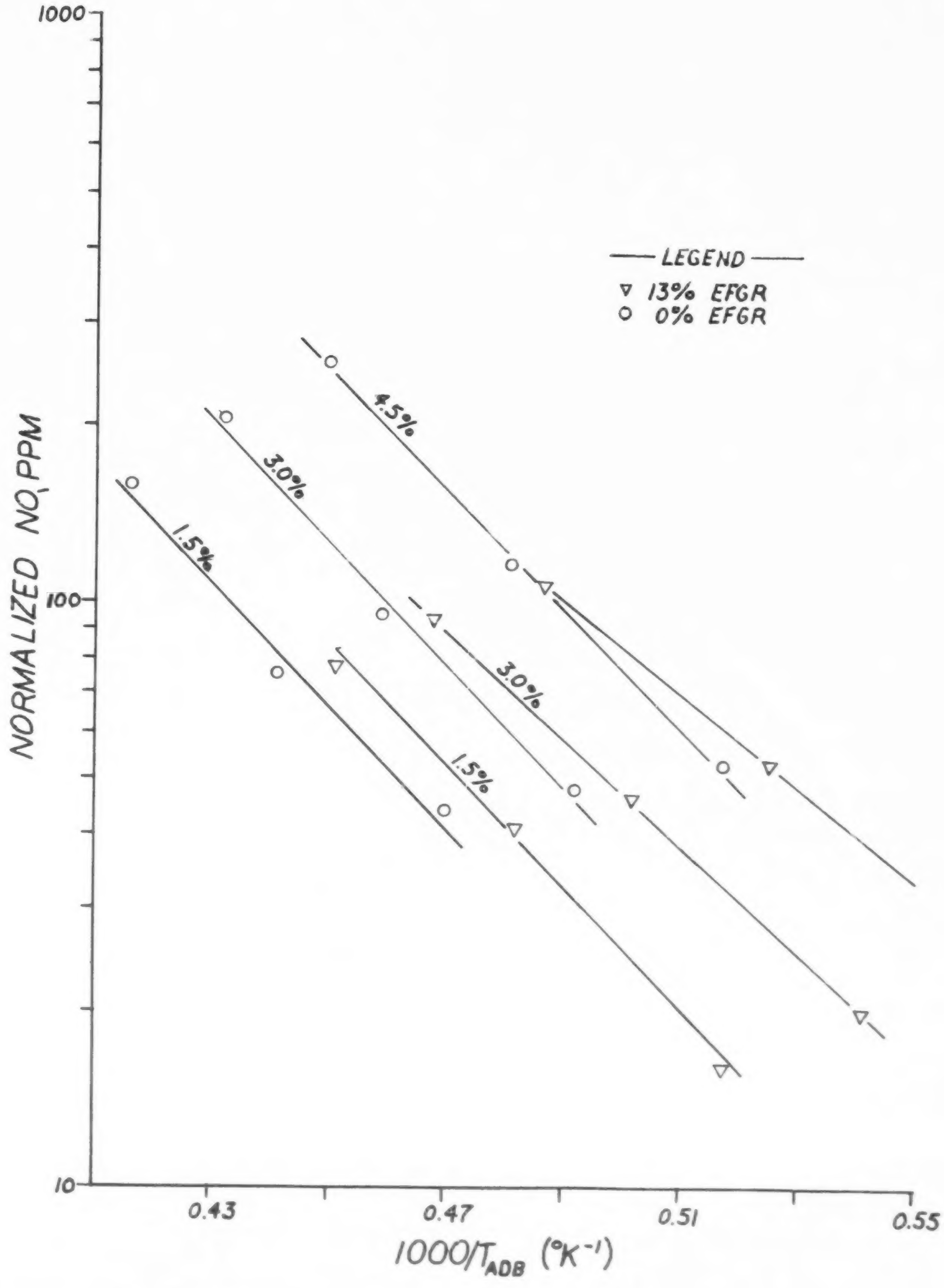

Figure 100. Normalized NO concentration as a function of [1000/T_{ADB}(°K)] for the kiln burner

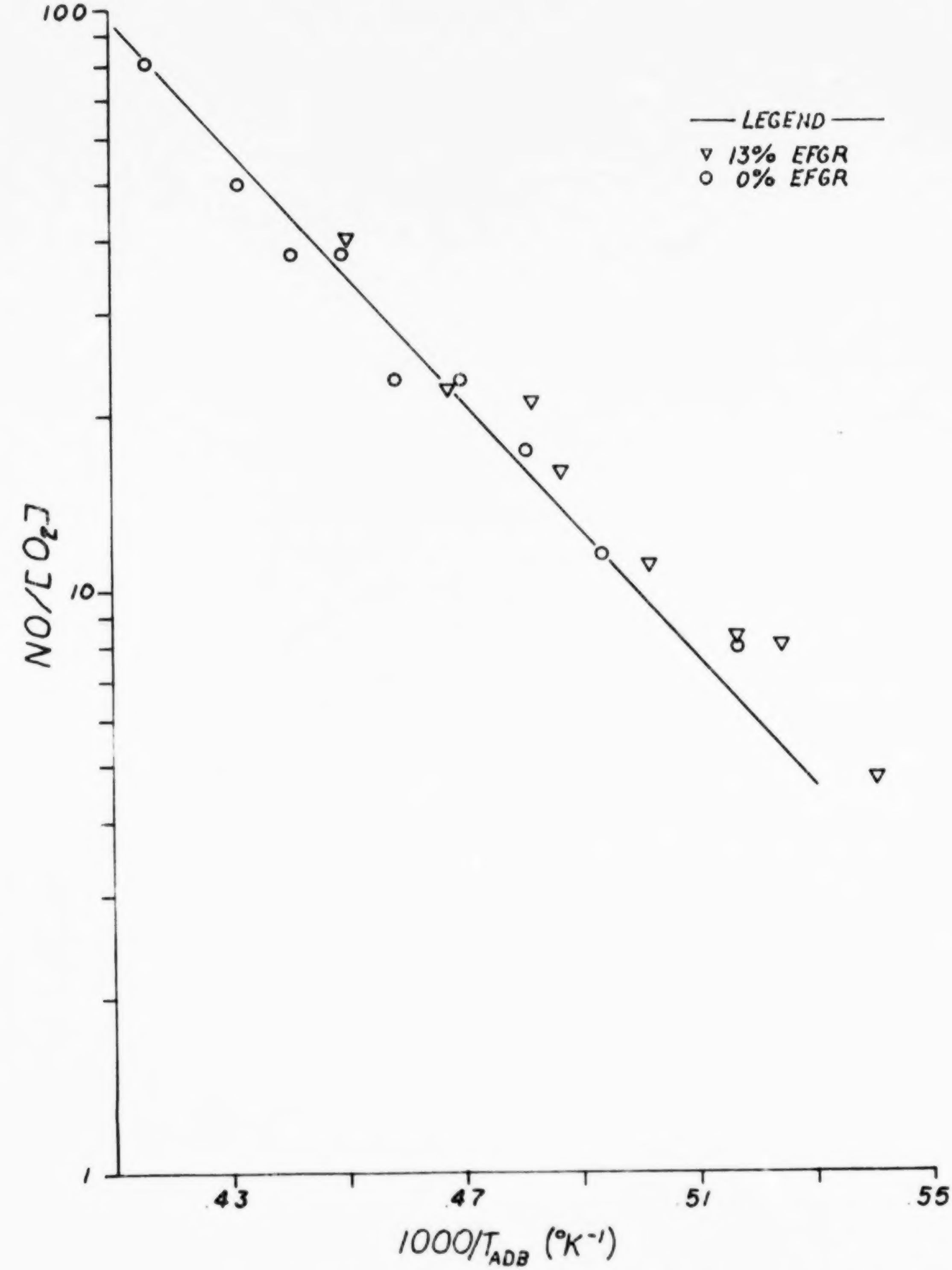

Figure 101. Logarithmic ratio of NO/[O_2] as a function of [1000/T_{ADB}(°K)] for the kiln burner

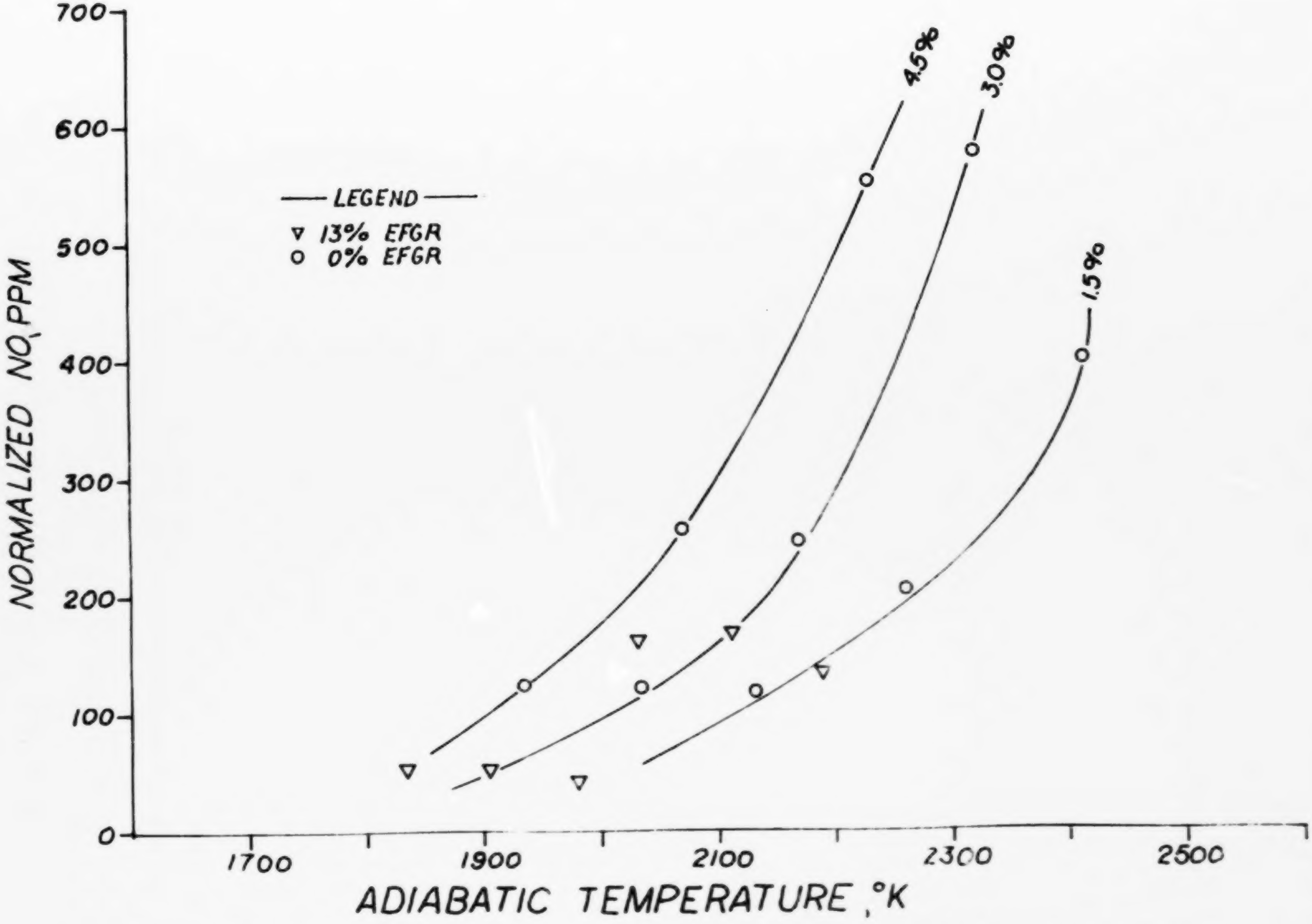

Figure 102. Normalized NO concentration as a function of adiabatic flame temperature for the intermediate flame length ported baffle burner

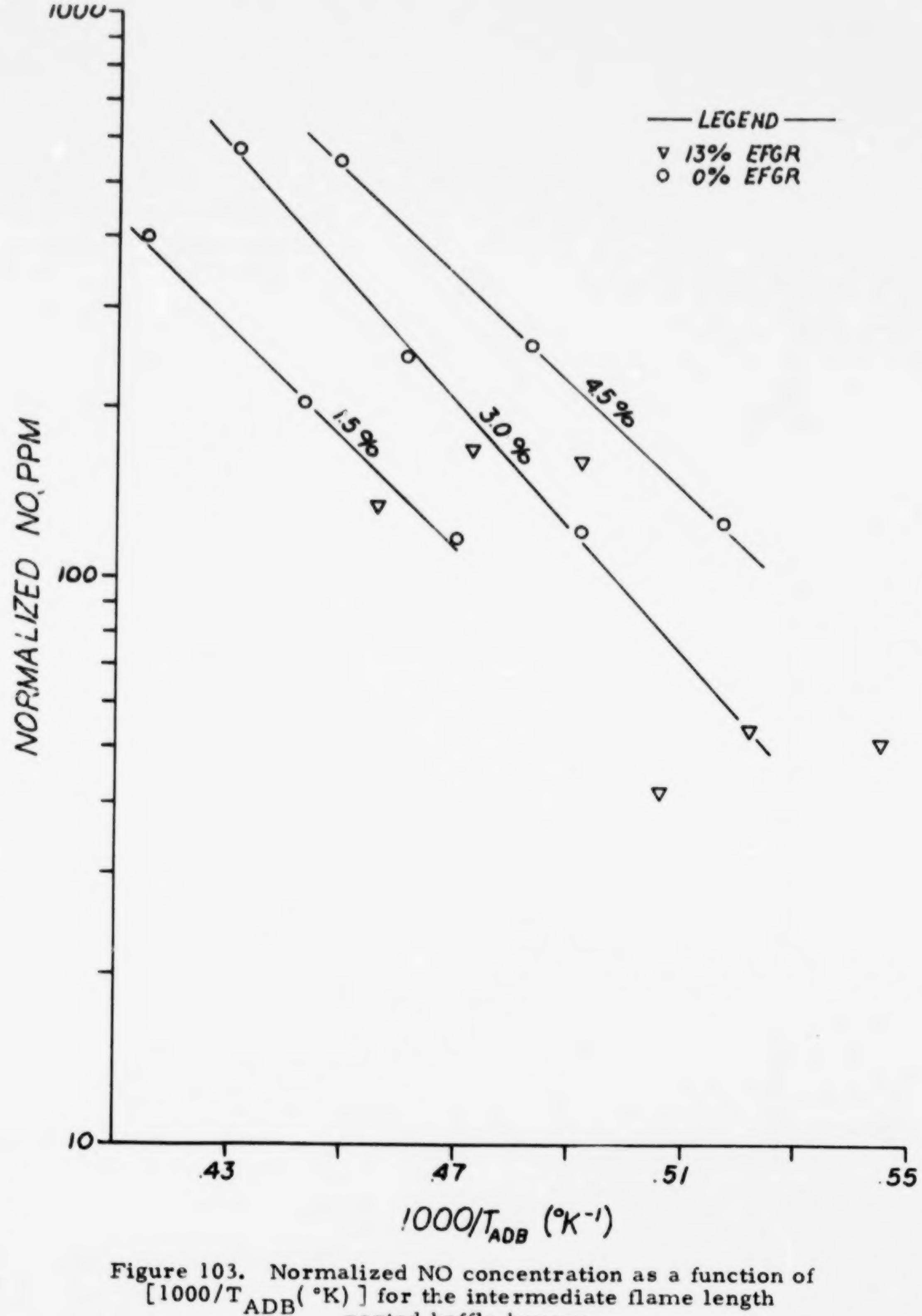

Figure 103. Normalized NO concentration as a function of [1000/T$_{ADB}$(°K)] for the intermediate flame length ported baffle burner

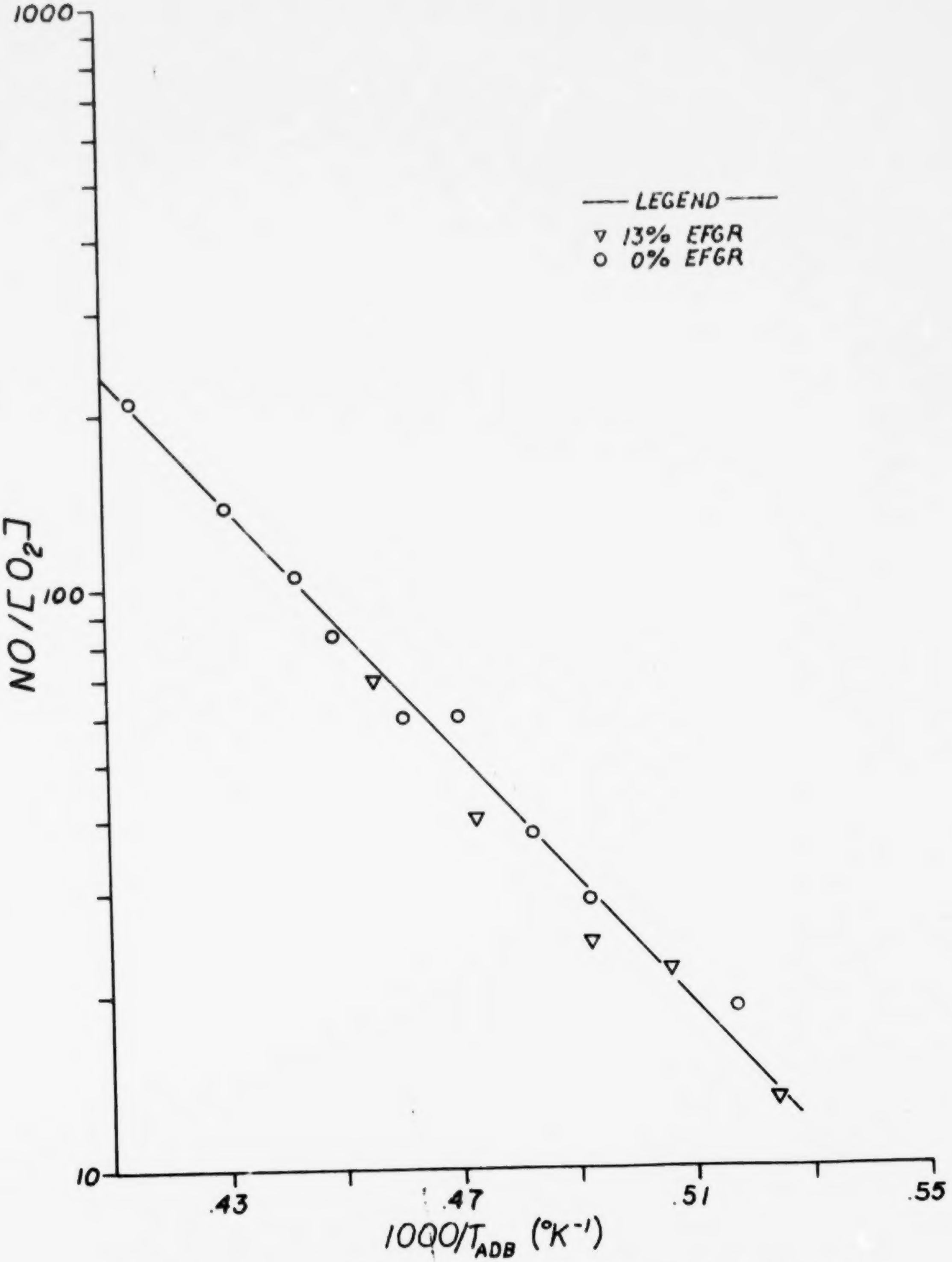

Figure 104. Logarithmic ratio of NO/[O_2] as a function of [1000/T_{ADB}(°K)] for the intermediate flame length ported baffle burner

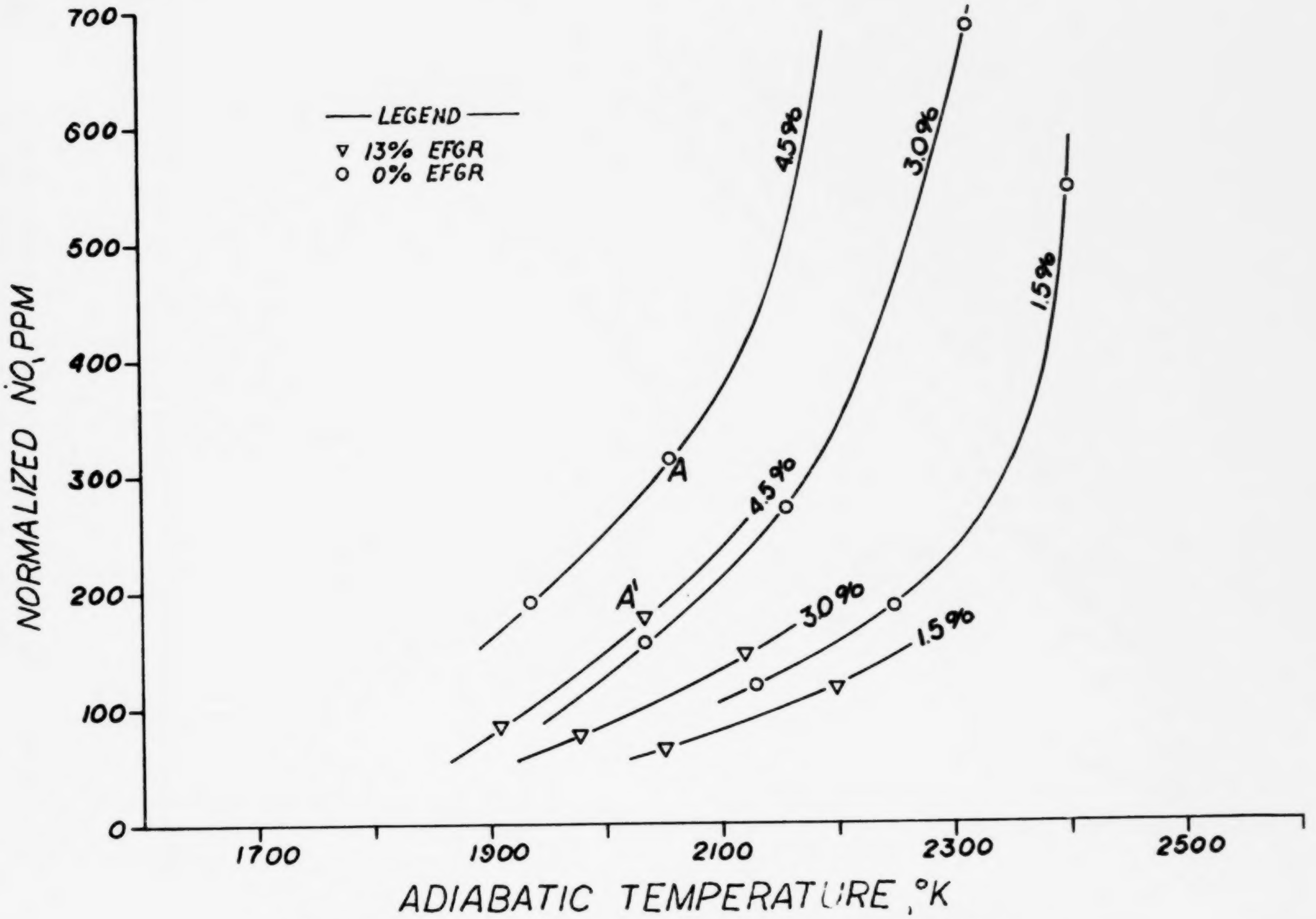

Figure 105. Normalized NO concentration as a function of adiabatic flame temperature for the short flame ported baffle burner

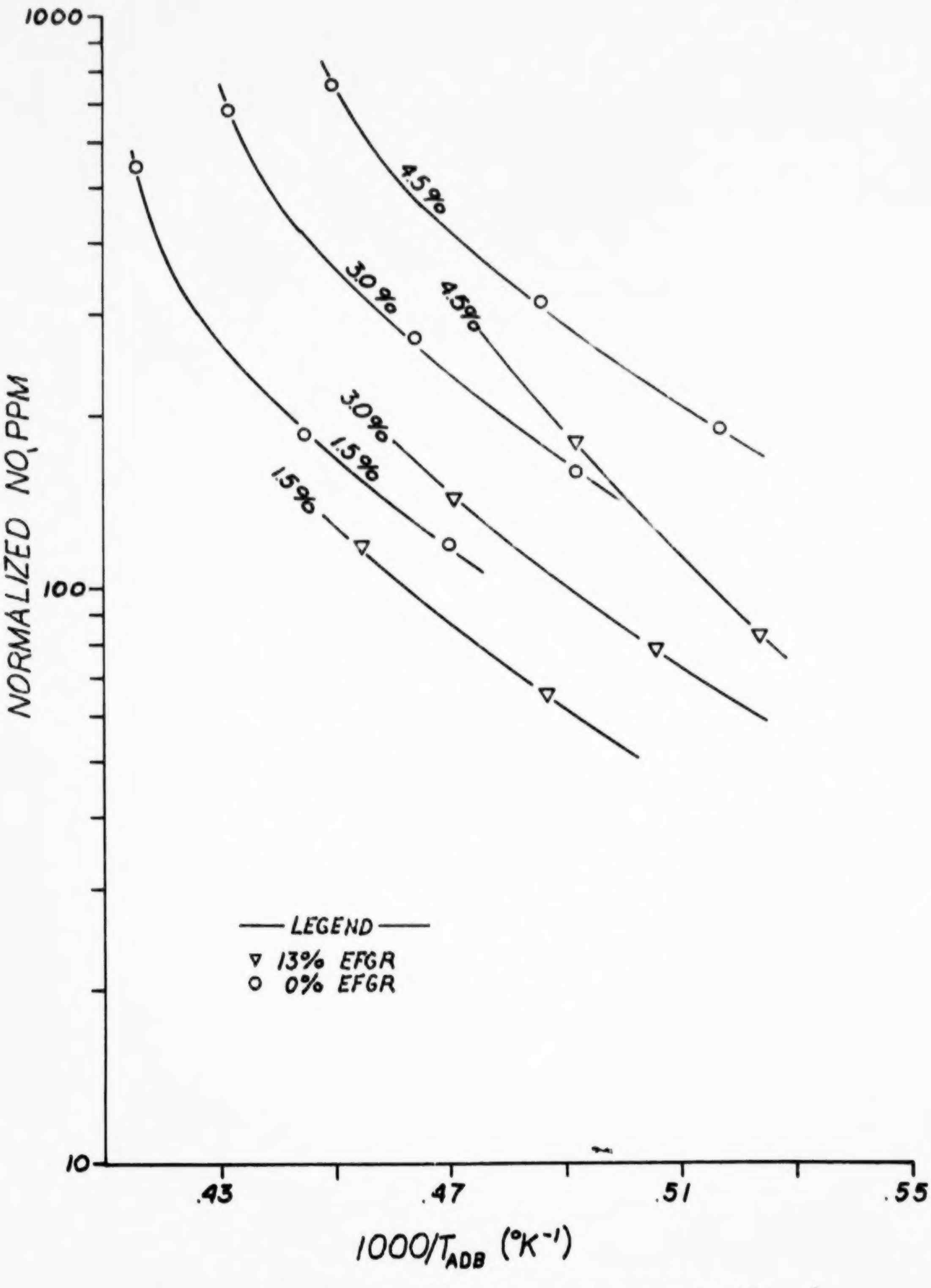

Figure 106. Normalized NO concentration as a function of $[1000/T_{ADB}(°K)]$ for the short flame ported baffle burner

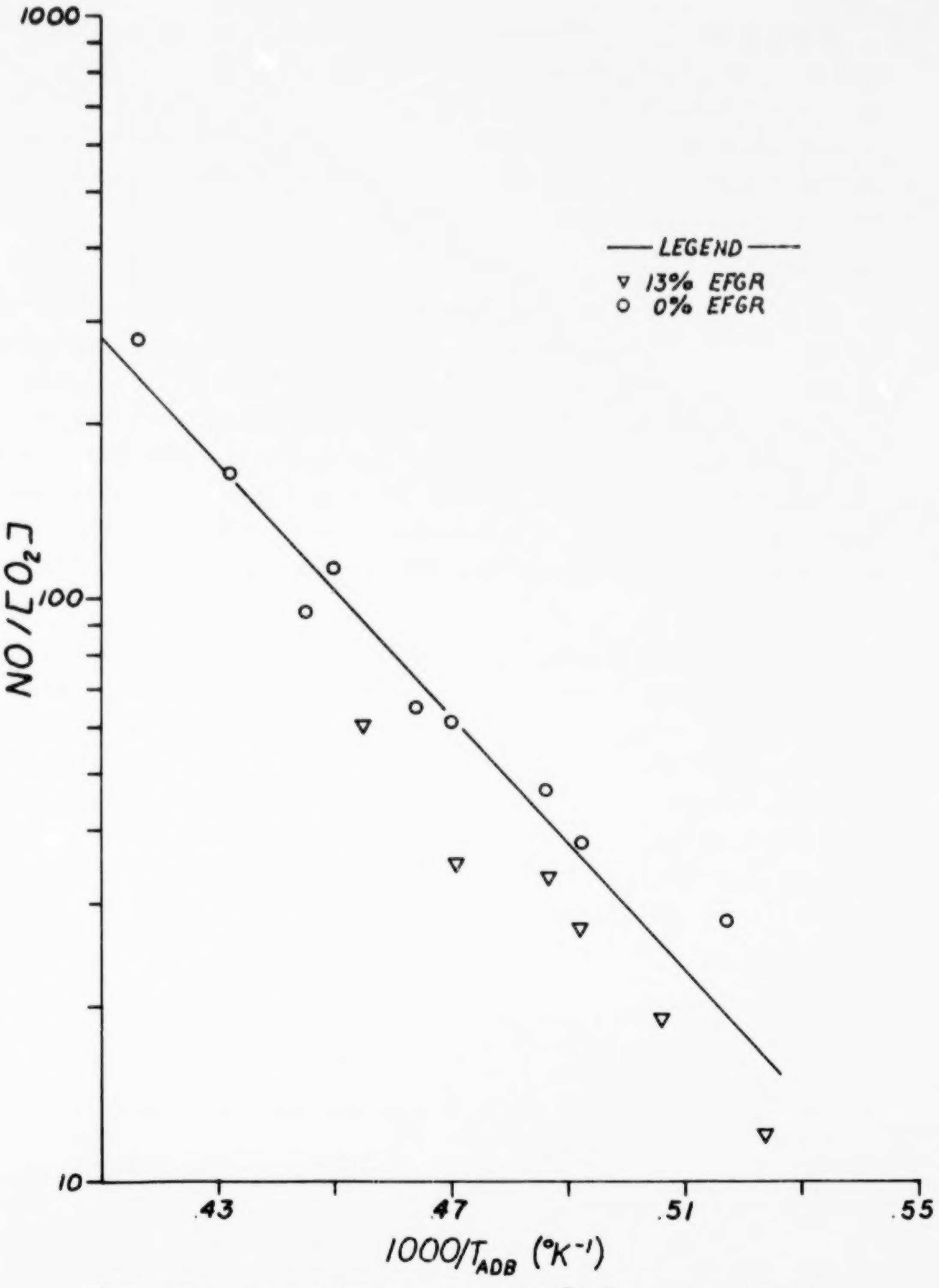

Figure 107. Logarithmic ratio of NO/[O_2] as a function of [1000/T_{ADB}(°K)] for the short flame ported baffle burner

Figures 108 through 110 show the results for the movable-vane boiler burner. As Figures 108 and 109 indicate, the low FGR level (15%) falls very nicely on the solid curves. The higher FGR data (25%) are below the curves, again possibly due to some type of fluid dynamic effects. The composite plot, Figure 110, shows reasonable agreement except at the very high levels of flue gas recirculation.

DISCUSSION

As the previous section has shown, in many cases, emission data for various levels of air preheat and FGR fall on a smooth curve when plotted against adiabatic flame temperature. In no case did the FGR emissions exceed the smooth curve through the no-preheat data by more than 20 ppm. Thus, given experimental emission measurements on a particular natural-gas-fired system at different air preheat temperatures, it is possible to conservatively estimate the effect of installing a certain size FGR system. This allows a reasonable cost/effectiveness analysis prior to system installation.

By far the most unusual and unexpected result of the analysis is the finding that the vast majority of the data can be linearized in the form $\ln\{NO/[O_2]\}$ vs. $1/T_{ADB}$. Further, while each plot has a different intercept, they have identically the same slope for all of the burners examined. This is particularly surprising since the kiln burner gives a fifteen-foot-long, very thin flame and relatively low NO (always below 300 ppm) while the short flame ported baffle burner gives a flame less than 2 feet long and emissions over 700 ppm in some cases.

CONCLUSIONS

- The effect of flue gas recirculation on NO_x emissions can generally be correlated (or estimated) to within 20% for a wide variety of burners if one has data at various preheat levels and no FGR.
- Adiabatic flame temperature is a reasonable parameter to correlate preheat and FGR data against.
- Further study should be given to the significance of the high degree of correlation obtained between $\ln(NO/O_2)$ vs. $1/T_{ADB}$.

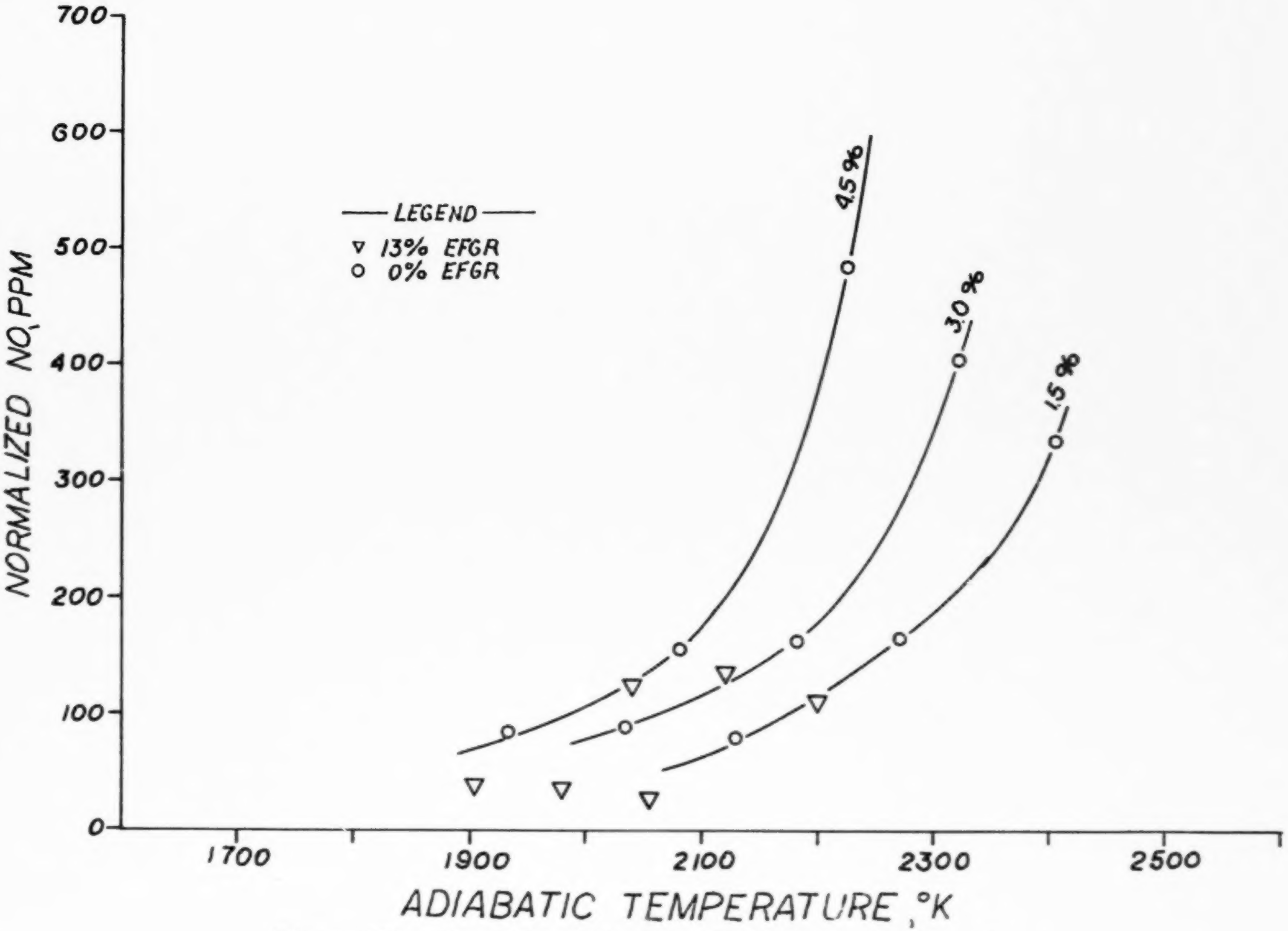

Figure 108. Normalized NO concentration as a function of adiabatic flame temperature for the movable-vane boiler burner

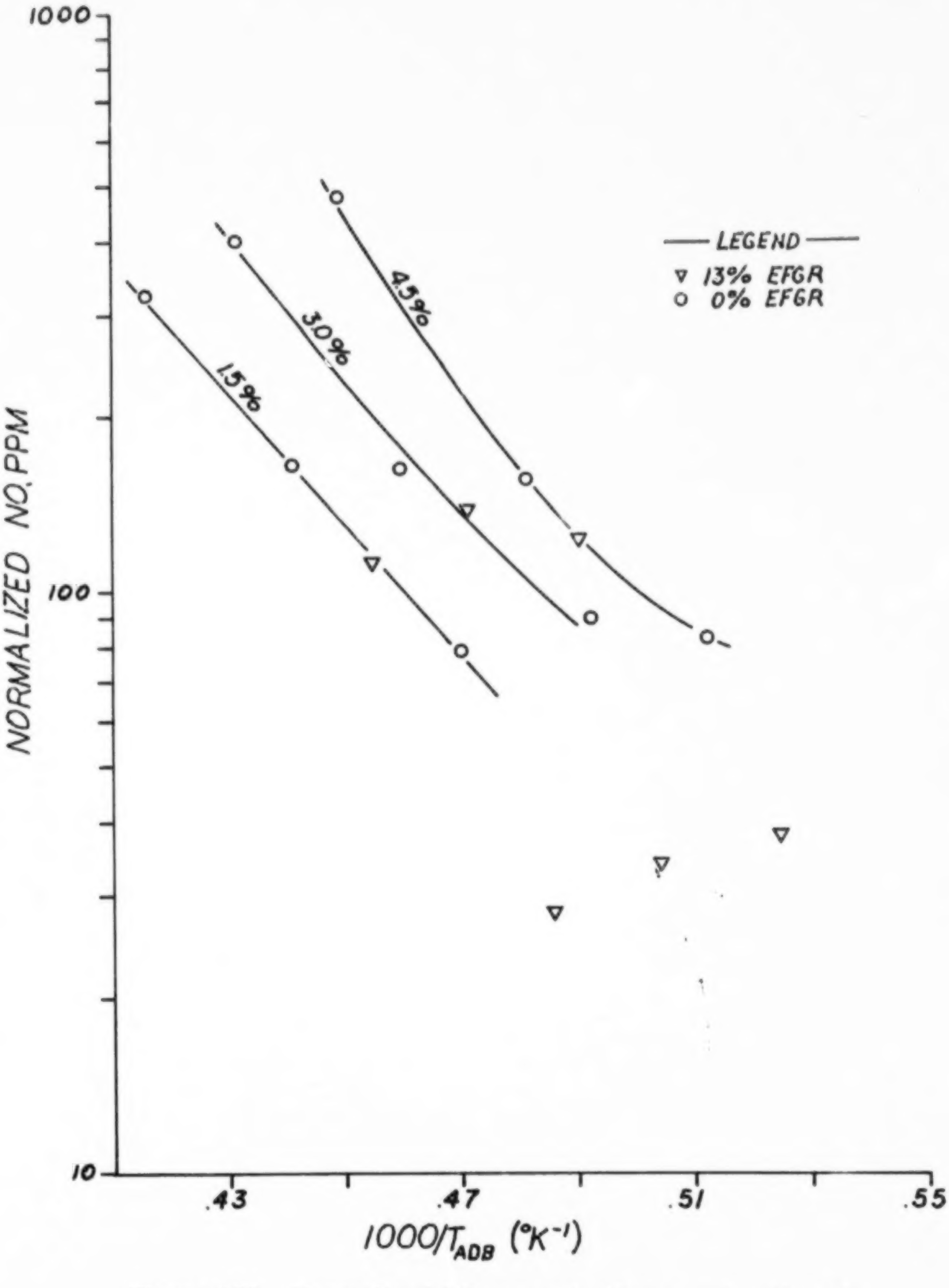

Figure 109. Normalized NO concentration as a function of $[1000/T_{ADB}(°K)]$ for the movable-vane boiler burner

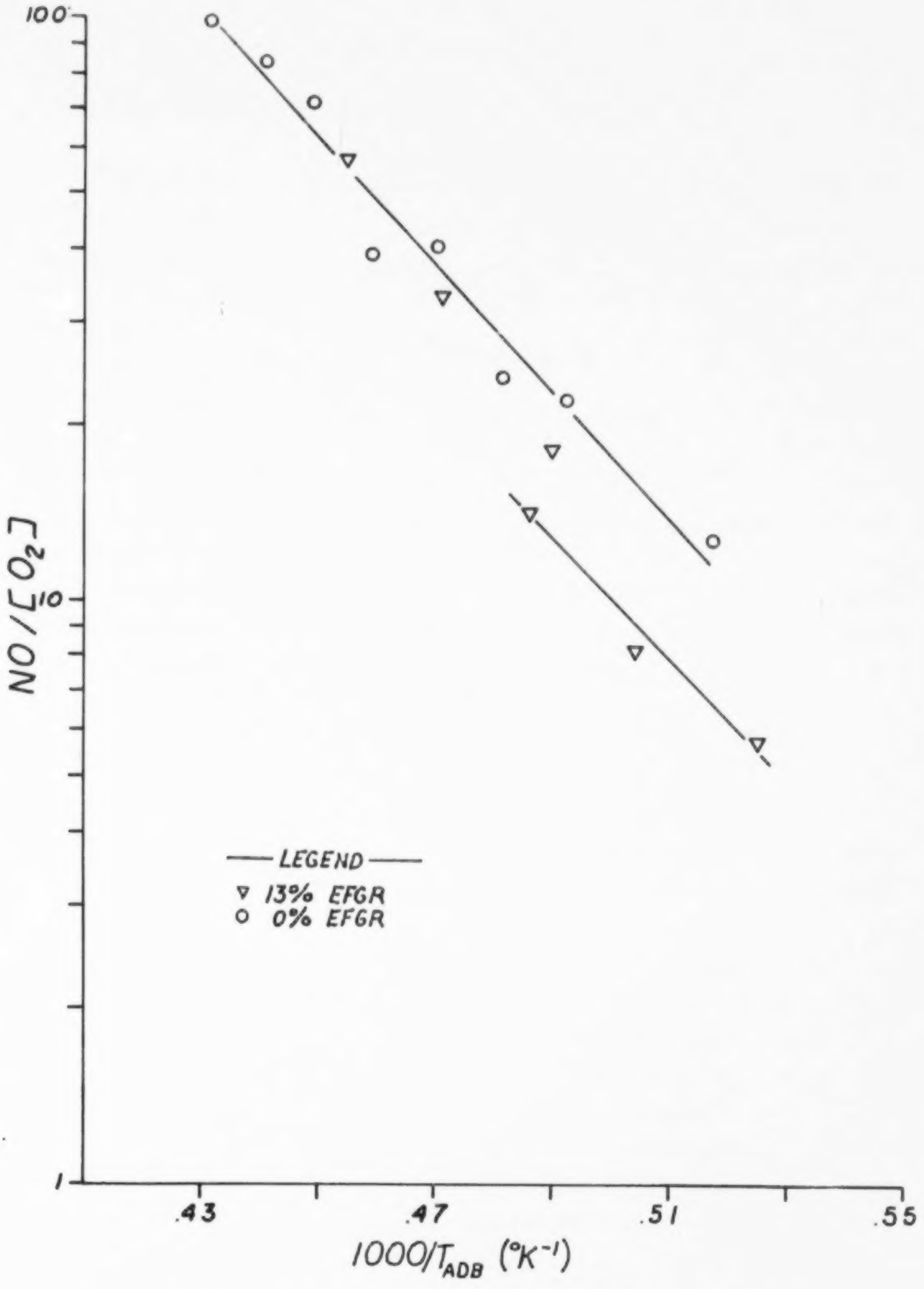

Figure 110. Logarithmic ratio of NO/[O_2] as a function of [1000/T_{ADB}(°K)] for the movable-vane boiler burner

CONVERSION TABLE

ENGLISH TO SI METRIC CONVERSION FACTORS

To Convert From	To	Multiply By
Lb/10^6 Btu	ng/J	4.299 E +02
10^6 Btu/hr	MWt	2.928751 E − 01
PSI	Pa	6.894757 E +03
SCFH	m^3/s	7.865790 E − 06
Ft/s	m/s	3.048000 E − 01
Inch	m	2.540000 E − 02
Feet	m	3.048000 E − 01
$Feet^2$	m^2	9.290304 E − 02
Inches of water (pressure)	Pa	2.4884 E +01
Lb/ft^3	kg/m^3	1.601846 E +01
GPM	m^3/s	6.309020 E − 05
$Inch^2$	m^2	6.451600 E − 04
°F	°C	t°c=(t°F − 32) /1.8

J = Joule
g = gram
s = second
MWt = Megawatts thermal
GPM = Gallons (U.S. liquid) /minute
Pa = Pascal
m = metre
k = kilo (10^3)
n = nano (10^{-9})
M = mega (10^6)
C = Celsius
F = Fahrenheit
PSI = pounds per square inch
SCFH = standard cubic feet per hour